TITLE PAGE

BASALT ALTERATION AND AUTHIGENIC MINERALIZATION NEAR THE EFFECTIVE BASE OF THE SNAKE RIVER PLAIN AQUIFER AT THE IDAHO NATIONAL ENGINEERING AND ENVIRONMENTAL LABORATORY, IDAHO

by

Lee H. Morse

A thesis

submitted in partial fulfillment

of the requirements for the degree of

Master of Science in the Department of Geology

Idaho State University

December 2002

PHOTOCOPY AND USE AUTHORIZATION

In presenting this thesis in partial fulfillment of the requirements for an advanced degree at Idaho State University, I agree that the Library shall make it freely available for inspection. I further state that permission for extensive copying of my thesis for scholarly purposes may be granted by the Dean of Graduate Studies, Dean of my academic division, or by the University Librarian. It is understood that any copying or publication of this thesis for financial gain shall not be allowed without my written permission.

Signature _____

Date _____

COMMITTEE APPROVAL PAGE

To the Graduate Faculty:

The members of the committee appointed to examine the thesis of Lee H. Morse find it satisfactory and recommend that it be accepted.

_____
Dr. Michael McCurry, Major Advisor

_____
Dr. John Welhan, Committee Member

_____
Dr. John H. Kalivas, Graduate Faculty Representative

ACKNOWLEDGEMENTS

I am very grateful to David Blackwell for permitting me to use his temperature log data. Linda Davis provided valuable assistance in my logging of drill core. Ray Lambert assisted in the operation of the electron microprobe and SEM equipment. Steve Anderson provided his insights into correlations of basalt flows and sedimentary interbeds. Scott Hughes provided assistance in INAA analyses. Chris Martin was instrumental in my work on core from well ANL-OBS-AQ-014.

I would also like to thank my advisor, Dr. Michael McCurry, for his patience and his assistance in completing this research. The faculty and staff of the Geology Department provided guidance and support that made this thesis possible. This research is supported by Department of Energy Remediation Technologies at the INEEL Grant No. DE-FG07-96ID13420, through the Idaho Water Resources Research Institute - Idaho Universities Consortium.

TABLE OF CONTENTS

PHOTOCOPY AND USE AUTHORIZATION i

TITLE PAGE ii

COMMITTEE APPROVAL PAGE iii

ACKNOWLEDGEMENTS iv

TABLE OF CONTENTS v

LIST OF FIGURES vii

LIST OF TABLES viii

ABSTRACT 1

1.0 INTRODUCTION 3

1.1 PROBLEM STATEMENT 3

1.2 SCOPE 4

1.3 GEOLOGIC SETTING 8

1.4 PREVIOUS WORK 9

1.4.1 Basalts and Basalt Alteration 9

1.4.2 Base of the Aquifer 11

1.4.3 Groundwater 13

1.5 METHODOLOGY 13

1.5.1 Core Logging 13

1.5.2 Petrography 14

1.5.3 SEM Analysis 14

1.5.4 Chemical Analysis 15

1.5.5 X-ray Powder Diffraction 15

2.0 DESCRIPTION OF CORES 16

2.1 WELL 2-2A 17

2.2 WELL WO2 19

2.3 WELL C1A 21

2.4 WELL ANL-1 22
2.5 WELL CH-1 22
2.6 SUMMARY 23
3.0 PETROGRAPHY 24
3.1 WELL 2-2A 24
3.2 WELL WO2 25
3.3 WELL C1A 27
3.4 WELL ANL-1 29
3.5 WELL CH1 29
3.6 SUMMARY 30
4.0 ANALYSIS OF CORE SAMPLES AND MINERAL SEPARATES 31
4.1 BULK ROCK ANALYSES 31
4.2 SEM, MICROPROBE, AND X-RAY POWDER DIFFRACTION ANALYSES 39
4.3 SUMMARY 42
5.0 DISCUSSION 46
6.0 CONCLUSIONS 53
7.0 SUGGESTIONS FOR FURTHER WORK 54
8.0 REFERENCES 55
APPENDIX A: CORE LOGS 60
APPENDIX B: PETROGRAPHIC DESCRIPTIONS 105
APPENDIX C: ANALYTICAL DATA 126

LIST OF FIGURES

Figure 1. Location of wells at the INEEL discussed in this study 5

Figure 2. Temperature gradients of deep wells.....6

Figure 3. Conceptual model of the ESRP aquifer system 7

Figure 4. Idealized cross-section through a pahoehoe flow.....18

Figure 5. Photograph of drusy chabazite crystals in core from well 2-2A.....20

Figure 6. Photograph of core from well WO2.....20

Figure 7. Photomicrograph of calcite and chabazite in a vesicle.....26

Figure 8. Photomicrograph of three minerals in a diktytaxitic cavity.....26

Figure 9. Photomicrograph of spherulitic clays in a vesicle 28

Figure 10. Photomicrograph of clays with a "caterpillar" texture.....28

Figure 11. Analytical data plotted on a total alkali-silica diagram.....35

Figure 12. Spider diagrams of trace element abundances.....37

Figure 13. Plot of Na_2O/FeO^* vs. CaO/FeO^* 38

Figure 14. Ternary diagram of Sr, Ba, and Zr abundances.....38

Figure 15. SEM photograph of chabazite crystals 40

Figure 16. X-ray powder diffraction pattern of chabazite from well 2-2A.....40

Figure 17. Chabazite and zeolite-like mineral ternary diagram.....43

Figure 18. X-ray powder diffraction pattern of typical clay.....43

Figure 19. SEM photograph of smectite clay.....44

Figure 20. Smectite clay ternary diagram.....44

Figure 21. Graphs depicting authigenic mineralization and alteration in wells 48

Figure 22. Sketch of proposed geothermal input to aquifer 52

Figure 23. Graphs depicting results of thermodynamic modeling.....52

LIST OF TABLES

Table 1. Basalt bulk rock analytical data 32

Table 2. Average microprobe analyses of authigenic minerals 45

ABSTRACT

This study characterizes and interprets three-dimensional spatial patterns of altered basalts, ranging in age from about 0.5 to 2.5 Ma, in the eastern Snake River Plain aquifer near the northern border of the eastern Snake River Plain based upon detailed examinations of basalt core from five deep boreholes located across the Idaho National Engineering and Environmental Laboratory.

Consistent patterns of alteration occur. Basalts in the upper parts of wells, including the vadose zone and most active part of the aquifer, are remarkably fresh, aside from minor caliche (vadose zone) or drusy calcite (aquifer) deposits in vesicles, mostly near upper flow margins. At depths ranging from 320 to 508 meters below land surface in the five deep wells there are pronounced increases in the intensity of authigenic pore-mineralization and glass alteration. Changes from largely unaltered to moderately to strongly altered basalt occur over narrow vertical intervals in at least two of the wells. In four wells the occurrence of authigenic minerals increases substantially over narrow vertical intervals. These transitions in the four wells correlate closely with sharp inflections in the temperature gradients in these wells. In the fifth well the temperature gradient inflection occurs near the bottom of the well. Many pores and fractures are partially or completely filled by nontronite ± saponite ± calcite; intersertal glass and olivine are partially to completely altered to nontronite ± saponite. Spotty occurrences of additional authigenic minerals occur in some cores. Alteration of the basalts increases in intensity downward from the temperature-gradient inflections and appears to have been largely isochemical. At depths below ~500 meters plagioclase is also partially altered to smectite clay. Pyroxenes are distinguished by their lack of any apparent alteration.

Pronounced downward transitions from unaltered to altered basalts do not correlate systematically with depth, age of the basalts, prevailing temperatures, or stratigraphic features (e.g., sediment interbeds) within the boreholes. Modeling of thermodynamic relations for pertinent authigenic minerals suggests that an increase in water temperature

alone could produce important authigenic mineral components of some of the most altered basalts observed. This study proposes that the alteration is produced by transient thermal inputs into the base of the aquifer from a deep-seated geothermal source and that the coincidence of alteration and the temperature-gradient inflections can be used to identify the effective base of the aquifer in this part of the eastern Snake River Plain aquifer with a high degree of confidence.

1.0 INTRODUCTION

1.1 PROBLEM STATEMENT

Studies of vertical temperature profiles (Brott et al., 1981; Blackwell et al., 1992; Smith et al., 1994) within five deep (548 to 3,160 meters) wells at the Idaho National Engineering and Environmental Laboratory (INEEL) (Fig. 1) document sharp inflections in the temperature gradients in these wells. The temperature gradients for these five wells and a sixth deep well at the INEEL are illustrated in Figure 2. Temperature gradients above the inflections are steep (~1.1 to 22° C/km); below the inflections, the gradients are shallower (~39 to 80° C/km). These changes in temperature gradient suggest a rapid upward transition from conductive to convective heat flow within the eastern Snake River Plain (ESRP) aquifer system.

Brott et al. (1981), Blackwell et al. (1992), and Smith et al. (1994) suggest that the temperature gradient inflections define the "base" of the active portion of the aquifer system. A conceptual model of the ESRP aquifer system is shown in Figure 3. Blackwell et al. (1992) suggest that the base of the aquifer is generally associated with an increase in basalt alteration and that the transition from unaltered to altered basalt correlates with age or depth of burial of the basalts. Their suggestions are based solely on the results of indirect geophysical logging techniques.

Alteration and authigenic mineralization of basalts of the ESRP would affect the hydraulic characteristics of the aquifer by reducing porosity and permeability, and would substantially affect the bulk K_d's of the rocks by producing highly sorbtive minerals such as smectite clays. These characteristics are important limitations for ongoing development of models of contaminant fate and transport in this sensitive aquifer system.

The principle purpose of my research is to test the hypothesis of Blackwell et al. (1992) that the temperature gradient inflection correlates with basalt alteration by direct petrologic and geochemical analyses of basalt cores, and to propose a mechanism for the rock alteration. I will also test the related hypotheses that: (2) basalt alteration and

authigenic mineralization correlate to the depth of burial of the basalts, as suggested by Blackwell et al. (1992), and (3) basalt alteration and authigenic mineralization correlate to the age of the basalts (Anderson and Bowers, 1995; Blackwell et al., 1992). Specific objectives are to document the vertical distributions, types, and magnitudes of basalt alteration and authigenic mineralization in drill core as a function of depth from five deep wells (2-2A, WO2, C1A, ANL-OBS-AQ-014 [hereafter referred to as well ANL-1], and CH-1) at the INEEL.

1.2 SCOPE

To achieve the objectives of my study, selected sections of available cores from the five deep wells were examined at the USGS Core Library at the INEEL. Core from a sixth deep well, INEL-1, was not examined because very little of the well was cored. Available core is all from below the temperature gradient inflection and mostly composed of rhyolite. Doherty et al. (1979) reported hydrothermal alteration of basalts below a depth of approximately 488 meters in INEL-1 based on their examination of drill cuttings. Few cuttings were collected from above 488 meters due to the loss of circulation of drilling fluids.

The primary emphasis of this work was on core from well 2-2A. Core from this well is readily available and penetrates the entire section of basalts below the base of the aquifer. The other four wells were used to compare and contrast alteration features and authigenic mineralization present in the cores with that found in well 2-2A.

Core intervals were selected from both above and below the temperature-gradient inflection in each well in an effort to observe spatial variations in alteration and authigenic mineralization and possible correlations to the temperature gradient inflections. A total of 817 meters of core were logged. From this core, 52 samples were collected for petrographic, scanning electron microscope (SEM), electron microprobe, X-ray powder

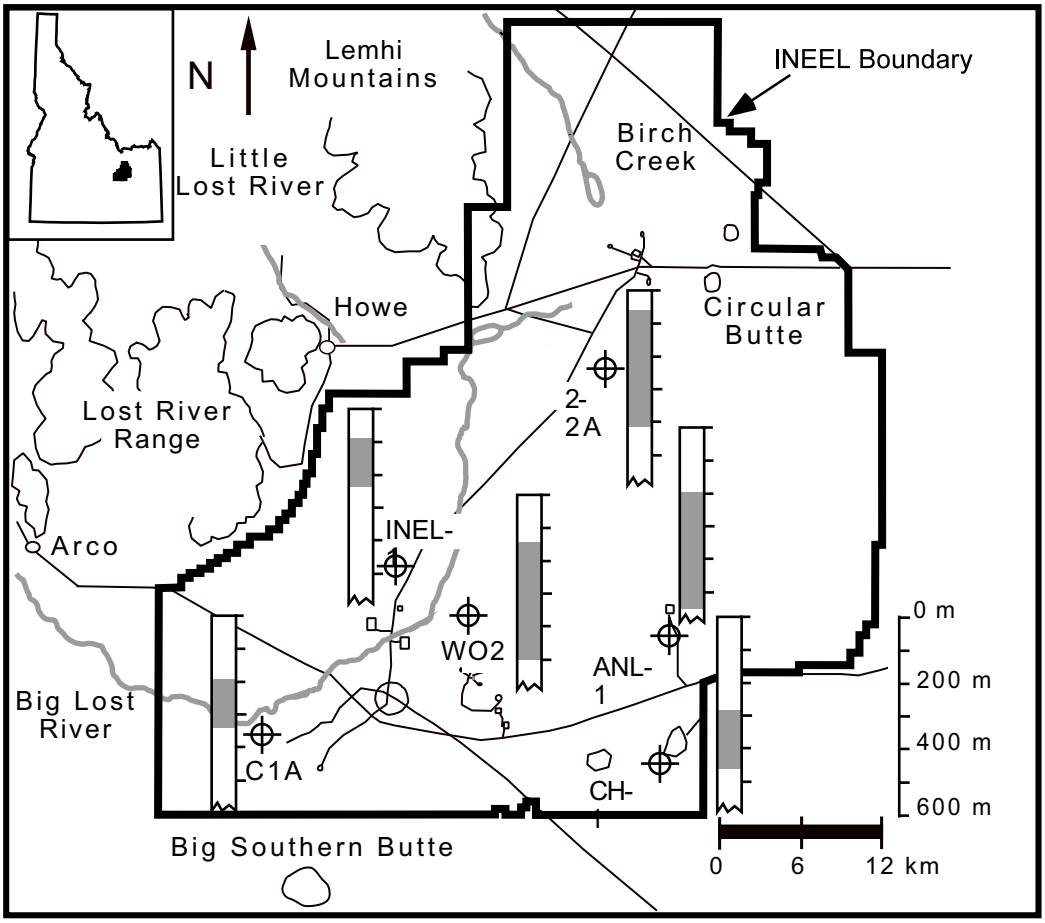

Figure 1. Location of deep wells discussed in this study. The wells are all located within the boundaries of the INEEL. The location of the INEEL is indicated in black on the inset map of Idaho in the upper left corner. Well locations are indicated by circles with crosses. Vertical bar graphs represent wells; shaded portions of the bar graphs represent the portion of the aquifer above the temperature gradient inflection in each well (Smith et al., 1994).

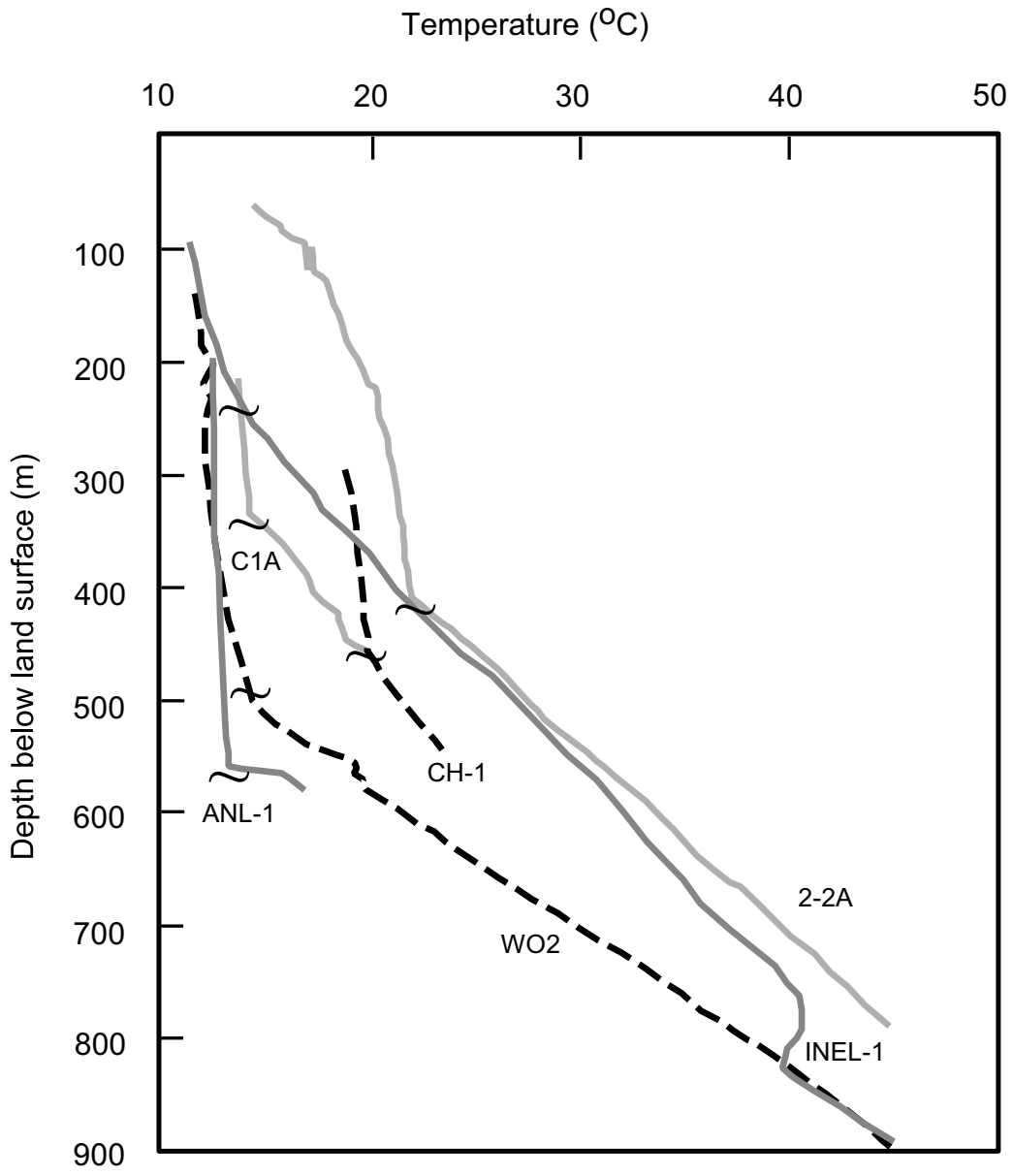

Figure 2. Temperature gradients of six deep wells discussed in this study. The inflection in the temperature gradient for each well is indicated by a tilde. Modified from Blackwell et al. (1992) and Smith et al. (1994).

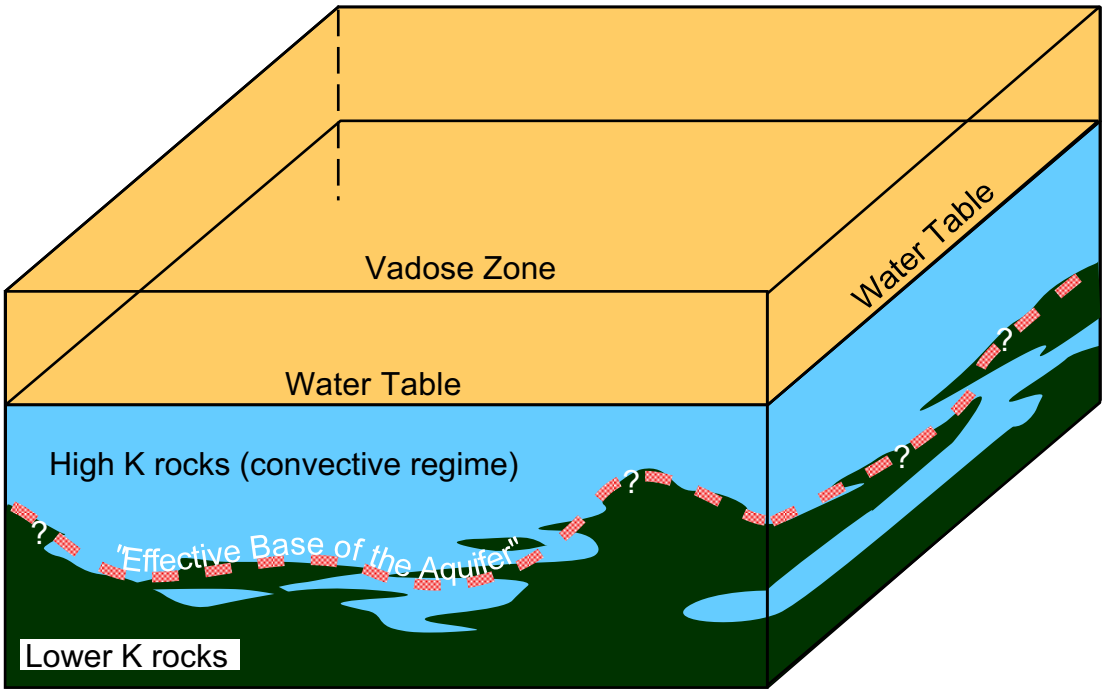

Figure 3. Conceptual model of the ESRP aquifer. The boundary between the lower hydraulic conductivity (lower K) rocks and the high hydraulic conductivity (high K) rocks is inferred to be the effective base of the aquifer [Brott et al. (1981); Blackwell et al. (1992); Smith et al. (1994)]. The three-dimensional nature of this boundary is not known. However, the varying depths of the temperature gradient inflections suggest that the boundary has a very irregular shape and is not a flat planar feature, and that the conductive portion of the aquifer varies in thickness across the study area. The dark green area represents the conductive regime within altered basalts and the blue area represents the convective regime within unaltered basalts.

diffraction, bulk chemical, and trace element analyses from both unaltered and altered sections of the core.

1.3 GEOLOGIC SETTING

The INEEL is a Department of Energy facility that covers an area of approximately 2,300 km^2 on the ESRP (Fig.1). It is the site of nuclear reactor testing, nuclear fuel reprocessing, and nuclear waste storage. Numerous wells have been drilled into the basalts and the upper portion of the ESRP aquifer at the INEEL. The majority of these wells were drilled into the upper portion of the aquifer for monitoring purposes. Six deep (548 to 3,160 meters) wells (2-2A, WO2, C1A, ANL-1, CH-1, and INEL-1) penetrate the effective base of the aquifer as inferred from sharp inflections in the temperature gradient. These deep wells were designed in part to penetrate the effective base of the aquifer and to characterize the regional stratigraphy. The locations of these six wells are shown in Figure 1.

The ESRP is a northeast trending depression 50 to 100 km wide and 300 km long that cuts across the northern Basin and Range province (Leeman, 1982). The plain rises from an average elevation of 600 meters in the southwest to an average elevation of 1,800 meters in the northeast. Mountains bordering the northern and southern margins of the plain consist largely of Paleozoic and Mesozoic carbonate and siliciclastic sedimentary rocks that have been uplifted by northwest trending normal faults.

The surface of the plain is underlain primarily by thin, nearly flat-lying, Quaternary olivine tholeiite basalts (Leeman, 1982; Kuntz et al., 1992; Lanphere et al., 1994) with intercalated sedimentary interbeds of lacustrine, eolian, and alluvial origin (Olmsted, 1962; Wood and Low, 1986; Anderson and Bowers, 1995; Bartholomay, 1990; Bestland et al., 2002; Mark and Thackary, 2002). This basalt-sediment sequence has accumulated to thicknesses of 1 to 2 kilometers (Kuntz et al., 1992; Hackett and Smith, 1992; Smith et al.,

1994) and overlies thick Pliocene to upper Miocene silicic lava flows and pyroclastic deposits.

The ESRP aquifer, one of the largest aquifer systems in North America (Heath, 1984), is located within the basalt-sediment sequence (Barraclough and Jensen, 1976). The aquifer is largely unconfined (Wood and Low, 1986) except where local, interbedded clays and dense, unfractured basalt flows create semiconfined conditions (Whitehead, 1992). Groundwater flow in the ESRP aquifer moves from the northeast to the southwest (Nace, 1953; Olmsted, 1962), primarily along rubble zones between basalt flows, and discharges to the Snake River as a series of springs between Twin Falls and King Hill. Hydraulic conductivities within the convective portion of the aquifer vary with depth due to vertical changes in permeability within individual flows and changes in the structures of the different basalt flows (Barrash et al., 1994; Johnson et al., 1994).

Most of the waters from the convective portion of the aquifer are of a calcium and magnesium carbonate type, with bicarbonate the principal anion (Olmsted, 1962). Waters from the conductive portion of the aquifer tend to be of a sodium bicarbonate type (Mann, 1986). Groundwaters from the convective portion of the aquifer are slightly alkaline, with an average pH of ~8, and have an average temperature of ~13° C (Olmsted, 1962; McLing, 1994). Groundwaters from the conductive portion of the aquifer are also slightly alkaline, with a pH of ~8, and have temperatures ranging from ~34 to 146° C (Mann, 1986).

1.4 PREVIOUS WORK

1.4.1 Basalts and Basalt Alteration

Pahoehoe lavas, emplaced as multiple flow units, are the prevailing type of basaltic lava flow on the Snake River Plain (Greeley, 1982). Most of the ESRP developed by the accumulation of multiple low shield volcanoes. Basalts of the ESRP display subtle geochemical variations between sequences of flows (Knutson et al., 1990; Lanphere et al., 1994; Geist et al., 2002; Hughes et al., 2002); however, nearly all have similar bulk

chemistries, textures, and mineralogical assemblages. The basalts are typically porphyritic, consisting of phenocrysts of olivine and plagioclase in a fine-grained matrix of interlocking plagioclase, augite, Fe-Ti oxide minerals, and intersertal tachylitic glass (Bates, 1999; Knutson et al., 1990; Lanphere et al., 1993, 1994). Flow margins are generally highly vesicular, and large parts of flows are characterized by abundant diktytaxitic cavities (Knutson et al., 1990). Upper and lower flow contacts often contain coarse basalt rubble with high hydraulic conductivity.

Previous studies of alteration of basalt flows in wells in the convective portion of the aquifer indicate that it is generally minor, and consists of reddish oxidation of olivine (Olmsted, 1962; Lanphere et al., 1993). Olivine is locally altered to chrysotile (?) and intersertal glass to opaque minerals (Lanphere et al., 1994).

Studies of more intensely altered basalts in the ESRP have been of a reconnaissance nature. In a well-log report, Doherty et al. (1979) document alteration and zeolite mineralization of basalts below 488 meters depth in well INEL-1; alteration was most intense between 610 and 658 meters. In an abstract, Fromm et al. (1994) describe aspects of alteration in well WO2. Basalts above 468 meters are little altered, and deeper basalts contain authigenic smectite, calcite, and phillipsite; they observed that alteration is more predominant in flow tops and bottoms than in mid-flow intervals.

There are few other pertinent published studies of low-temperature alteration of Quaternary basalts in the northwest U.S.A. Keith and Bargar (1988) document low temperature isochemical alteration of Quaternary basalt in a 932 meter deep drill core near Newberry Caldera, Oregon. Benson and Teague (1982) describe aspects of alteration of Miocene basalts of the Columbia River Basalt Province. Other unpublished studies of altered Columbia River Basalts have documented the presence of a wide variety of alteration phases including green, yellow-green, and greenish-brown smectite, mordenite, heulandite, chalcedony, black manganese oxide, opal, quartz, and pyrite (Staff, Basalt Waste Isolation Project, 1979).

1.4.2 Base of the Aquifer

Studies of vertical temperature profiles in six deep wells, which include the five deep wells of this study, located at the INEEL document changes in the temperature gradient suggestive of rapid upward transitions from conductive to convective heat flow (Smith et al., 1994; Brott et al., 1981; Blackwell et al., 1992). These researchers suggest that sharp temperature-gradient inflections (Fig. 2) in these wells may correlate with the effective base of the aquifer.

Temperature gradients above the inflections suggest the water in this convective regime mixes with cold recharge waters and moves through the aquifer system quickly. The temperature gradients below the inflections suggest the water in this conductive regime has been in contact with the host rock for a long time and has not experienced much, if any, mixing with cold recharge waters. The sharp temperature gradient inflections suggest the boundary between the conductive and convective regimes occurs over a narrow interval in each well. The three-dimensional nature of this boundary is not known. The varying depths of the inflections suggest that the boundary has a very irregular shape, as shown in Figure 3, and is not a flat planar surface. While the boundary appears to be continuous in the vicinity of these wells, it may not be continuous across the INEEL or be present in other areas of the ESRP.

The term “base of the aquifer” may be misleading (Welhan, 2002, personal communication) as it suggests there is no vertical movement of water across the boundary between the domains of higher and lower thermal conductivity. An aquifer is a geological formation that can store and produce useful quantities of water to a well and may be part of an aquifer system. The terms “base of the aquifer” and “effective base of the aquifer” are used in this study to identify with the concept of a boundary between the conductive and convective regimes that is defined by the temperature gradient inflections, as suggested by

Brott et al. (1981), Blackwell et al. (1992), and Smith et al. (1994), but not to suggest that waters below the temperature gradient inflections are not a part of the aquifer system.

High water-rock ratios and short residence times for the ESRP aquifer were demonstrated by Wood and Low (1986, 1988). They proposed that ~20% of the aquifer solute load is derived from reaction of groundwater with sediments and Quaternary basaltic host rocks. However, they did not define the specific spatial distribution of rock alteration within the aquifer. If, as Blackwell et al. (1992) suggest, alteration occurs primarily at and below the effective base of the aquifer, alteration would have little effect on the solute balance of the aquifer.

Anderson and Bowers (1995) correlate the base of the aquifer in wells 2-2A and WO2 with ~1.8 Ma basalts correlative with the Glenns Ferry Formation of the Idaho Group (cf. Armstrong et al., 1975). In well 2-2A the ~1.8 Ma basalts are at a depth of ~259 meters and the temperature-gradient inflection occurs at a depth of 408 meters, while in well WO2 the ~1.8 Ma basalts are at a depth of ~505 meters and the temperature-gradient inflection occurs at a depth of 508 meters.

Welhan and Wylie (1997) interpret C. Knutson's unpublished permeameter data obtained from C1A core to indicate a rapid downward decrease in porosity and permeability at the same depth (~335 meters) as the temperature-gradient inflection in well C1A.

Mann (1986) found the hydraulic conductivities of basalt in the aquifer in the upper 60 to 245 meters of well INEL-1 were two to five orders of magnitude greater than in the rocks below 460 meters. He indicated the base of the aquifer may be coincident with one of two sedimentary interbeds between 260 and 470 meters depth in this well, and that these interbeds are likely to be continuous over a large area. The temperature-gradient inflection in this well occurs at a depth of 230 meters.

1.4.3 Groundwater

Robertson et al. (1974) relate variations in groundwater composition to variations in lithology of recharge source areas and discount significant water-basalt reactions within the aquifer. McLing (1994) concludes that groundwater compositions are the product of extensive mixing of water from multiple sources rather than extensive diagenesis due to water-rock interactions. Wood and Low (1986, 1988) demonstrate high water-rock ratios and short residence times for the ESRP aquifer. They proposed that ~20% of the aquifer solute load is derived from reaction of groundwater with sediments and Quaternary basaltic host rocks.

In hydrogeologic studies of well INEL-1, Mann (1986) demonstrated that waters beneath the effective base of the aquifer have a strong upward potential for flow. The paucity of hot springs within the ESRP suggests that any geothermal waters that are upwelling from depth are mixing with, and diluted by, the cooler waters of the effective portion of the aquifer (Robertson et al., 1974; Wood and Low, 1988; McLing, 1994; McLing et al., 1997; McLing et al., 2002). Previous thermodynamic modeling of ESRP aquifer waters suggests the calcium-bicarbonate waters are saturated with respect to calcite and calcium-montmorillonite, and that the aquifer system is currently undergoing open-system precipitation of calcite (McLing, 1994; Knobel et al., 1997).

1.5 METHODOLOGY

1.5.1 Core Logging

Selected sections of available cores from wells 2-2A, WO2, C1A, ANL-1, and CH-1 were examined at the USGS Core Library at the INEEL. Core intervals were selected from both above and below the temperature-gradient inflection in each well. A total of 817 meters of core were examined. Field logs describing characteristics of the core were prepared at a scale of 1:48. Fifty-two samples of core were collected for petrographic, SEM, electron microprobe, X-ray powder diffraction, bulk chemical, and trace element analyses from both

unaltered and altered sections of the core as determined by the presence of authigenic minerals and by variations in color of the core from the typical gray of fresh basalts to green for altered basalts.

1.5.2 Petrography

Billets were cut from core samples and delivered to Spectrum Petrographics in Winston, Oregon for mounting and final preparation as thin sections. Fifty-three thin sections were prepared from 50 core samples. The thin sections were examined using a Nikon petrographic microscope at Idaho State University. In addition, six sample mounts prepared by Spectrum Petrographics for electron microprobe analysis were also examined using the petrographic microscope. The goals of the petrographic analysis were to identify the primary, authigenic, and alteration mineral phases present in each thin section; to estimate the relative abundance of the minerals; and to determine the paragenesis of the authigenic and alteration minerals.

1.5.3 SEM Analysis

Six samples were cut from core samples collected from well 2-2A for SEM analysis. All SEM samples were cleaned in an ultrasonic cleaner with a very weak solution of soap in warm deionized water for four to six minutes. The samples were rinsed with warm tap water, and then rinsed in deionized water. SEM analyses were performed at the University of Utah using a Hitachi S-500 scanning electron microscope with a Kevex 5500 X-ray energy spectrometer. The goals of the SEM analyses were to observe the morphology of primary, authigenic, and alteration mineral phases, and to obtain qualitative data on mineral compositions.

1.5.4 Chemical Analysis

Analyses of bulk rock major, minor, and some trace elements (SiO_2, TiO_2, Al_2O_3, FeO, MnO, MgO, CaO, Na_2O, K_2O, P_2O_5, Ba, Sr, and Zr) were performed for 52 core samples at the Idaho State University Laboratory for Environmental Geochemistry (LEG) using a JY70C Inductively Coupled Plasma – Atomic Emission Spectrometer (ICP-AES). Relative standard deviations (RSDs) are ≤ 2% for Si, Ti, Al, Fe, Mn, Mg, Ca, and Sr; ≤ 5% for Na, P, Zr, and Ba; and ≤ 10% for K (Wright, 1998).

Analyses to determine the concentrations of other trace elements (Sc, Cr, Co, Ni, Rb, Cs, La, Ce, Nd, Sm, Eu, Tb, Yb, Lu, Hf, Ta, Th, U, and Zn) were performed for 48 core samples at LEG using Instrumental Neutron Activation Analysis (INAA). RSDs are 0.1% to 1% for Sc, Cr, Co, Ce, Sm, and Eu; 2% to 4% for La, Yb, Lu, Hf, Ta, and Th; 5% to 10% for Tb; 10% to 15% for Rb, Cs, and Nd; and 20% to 30% for Ni and U (Reed et al., 1997). Sample preparation and analytical procedures for ICP-AES and INAA are described by Wright (1998).

Billets were cut from core samples and delivered to Spectrum Petrographics for mounting and preparation as samples for electron microprobe analysis. Six samples of well 2-2A core, one sample of well C1A core, and six samples of well CH-1 core were selected for electron microprobe analysis. An additional seven samples were selected for analysis from well 2-2A core samples collected by Dr. Scott Hughes (Idaho State University) and Jason Casper (a graduate student at Idaho State University). Primary, authigenic, and alteration mineral phase compositions were determined using a SX-50 Electron Microprobe at the University of Utah. The goal of the electron microprobe analyses was to determine the composition of primary, authigenic, and alteration mineral phases.

1.5.5 X-ray Powder Diffraction

One sample of a zeolite mineral from well 2-2A was analyzed by X-ray powder diffraction at LEG using a Phillips X-ray Powder Diffractometer with a CuKα target. The

sample was prepared by plucking a large crystal from the vug of a core sample. The crystal was crushed using a metal anvil, powdered in a ceramic crucible using ethanol as a coolant/lubricant, and deposited on a frosted microscope slide using a pipette. The sample was allowed to dry overnight before it was analyzed.

Eighteen samples of clays (five from well 2-2A, eight from well WO2, three from well C1A, and two from well CH-1) were analyzed by X-ray powder diffraction at LEG. Eight samples were prepared from clays scraped from fractures in the core samples. The remaining 10 samples were prepared from clays removed from the rock matrix of the core samples. An ultrasonic cleaner was used to disaggregate the clays and to remove the clays from the rock matrix. Oriented samples were produced on porcelain slides using a peel technique described by Drever (1973). The goal of the clay X-ray powder diffraction analyses was to identify the clays present in the core samples.

Each clay sample was analyzed after it was air dried. All samples were then placed on a wire rack in a Pyrex dish with approximately 5 mm of ethylene glycol in the bottom of the dish. The dish was covered with foil and allowed to sit for approximately 45 hours, at which time the samples were removed from the dish and placed in a desiccator. The samples remained in the desiccator until they were placed in the sample holder and analyzed with the diffractometer.

Following the analysis of the glycolated samples, all the samples were heated in a muffle furnace at 300° C for one hour. The samples were removed from the muffle furnace and placed in a desiccator to cool until they were placed in the sample holder and analyzed with the diffractometer. Following analysis of the samples heated at 300° C, the samples were heated at 550° C for one hour and placed in a desiccator to cool until they were placed in the sample holder and analyzed with the diffractometer.

2.0 DESCRIPTION OF CORES

Available cores from wells 2-2A, WO2, C1A, ANL-1, and CH-1 were examined at the USGS Core Library at the INEEL. Core intervals were selected for examination from both

above and below the depth of the temperature gradient inflection in each well in an effort to observe spatial variations in alteration and authigenic mineralization and possible correlations to the inflections. In describing unaltered and altered basalts, the term "authigenic" refers to minerals that have precipitated in preexisting pore spaces (i.e., vesicles, diktytaxitic cavities, voids, fractures) and the term "alteration" refers to replacement of preexisting mineral phases. All of the basalts examined are fine to medium-grained, aphyric to porphyritic, olivine bearing, and have a diktytaxitic texture.

Self et al. (1998) describe emplacement of pahoehoe lavas as inflated lobes. They describe a typical pahoehoe flow as having a vesicular upper crust, a core with very few vesicles, and a lower crust that is nearly as vesicular as the upper crust, as shown in Figure 4. The flow cores tend to have a greater crystallinity than the upper or lower crust. The upper crust, flow core, and lower crust of Self et al. (1998) are used here in the description of basalt cores that were examined. Logs of the examined cores are in Appendix A.

Samples of core were selected from both unaltered and altered basalts to compare the bulk-rock, minor, and trace element compositions, mineral textures, and authigenic mineral assemblages of the unaltered and altered basalts. Altered core samples were also collected for examination of distinctive authigenic minerals.

2.1 WELL 2-2A

The temperature gradient inflection occurs at a depth of 408 meters in well 2-2A. The following intervals of core from well 2-2A were examined and logged: 174 – 192 meters, 349 – 408 meters, 477 – 495 meters, and 671 – 711 meters.

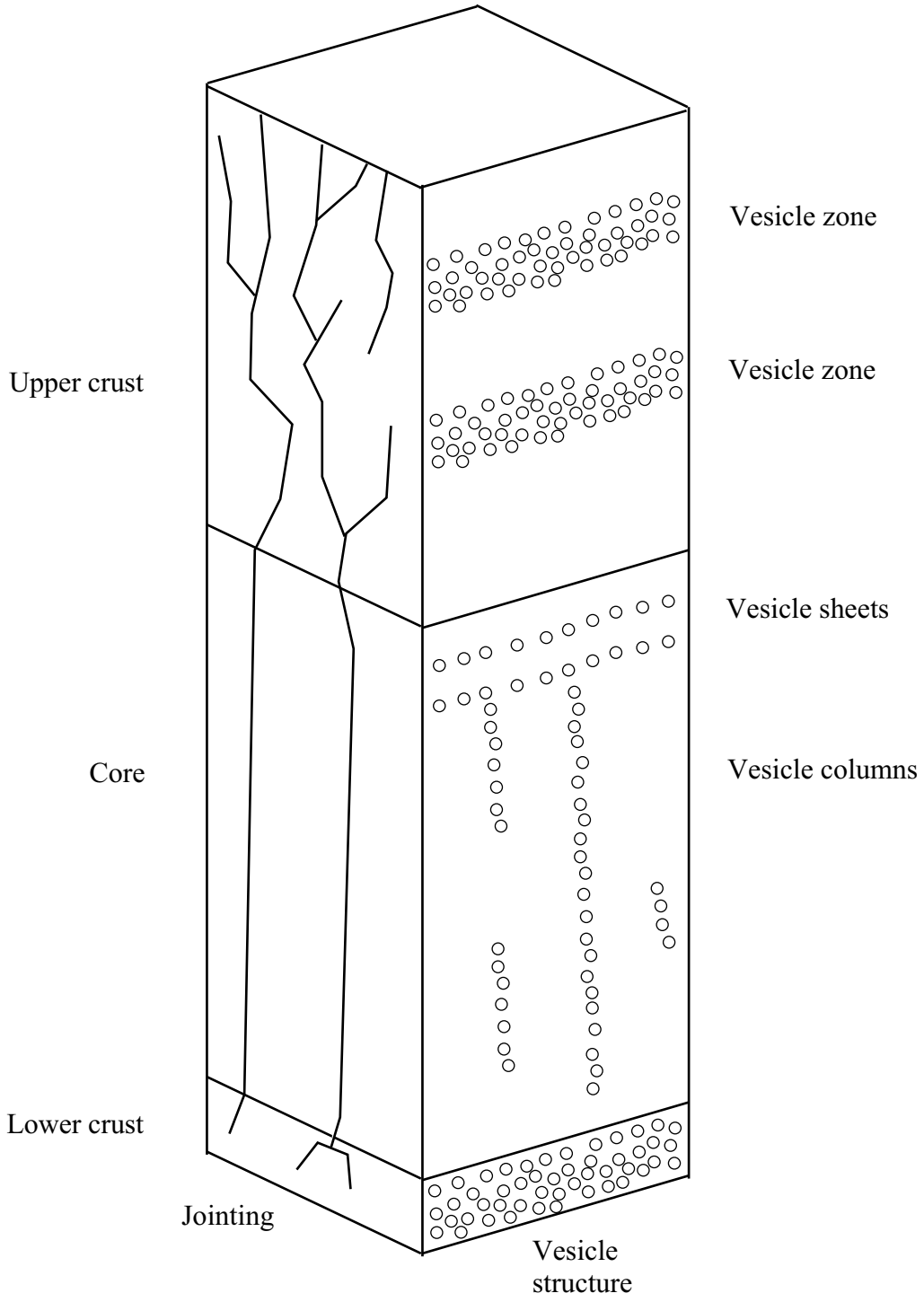

Figure 4. Idealized cartoon of a cross-section through an inflated pahoehoe flow. The upper crust is vesicular, often with discrete vesicular zones. The core has very few vesicles. Vesicles in the core are present mostly in vesicle sheets and vesicle cylinders. The lower crust is nearly as vesicular as the upper crust. After Self et al. (1998).

Core from above the temperature gradient inflection at 408 meters is mostly unaltered. Minor alteration, as indicated by a green tint to the core, is present from 184 – 188 meters, from 363 – 367 meters, at 371 meters, and at 386 meters. Fine-grained sand and silt in fractures and vesicles of unaltered core are probably from overlying sedimentary interbeds. Minor amounts of calcite are present on fracture surfaces and in vesicles and diktytaxitic cavities of unaltered basalts. Green clay coats fractures and fills diktytaxitic cavities of altered basalts above 408 meters.

Little core was recovered between 408 meters and 477 meters. All of the basalt core examined from below 477 meters is moderately to intensely altered. Green clay and calcite are common. The clay coats or fills fractures and fills most vesicles and diktytaxitic cavities. Calcite is less abundant than clay, but is also present on fractures and fills vesicles and diktytaxitic cavities.

Fine-grained chabazite crystals fill vesicles or coat vesicle walls between 478 and 488 meters. Drusy chabazite crystals are present in a vug at 485 meters (Fig. 5). Chabazite is the only zeolite observed in the core from well 2-2A, and is present only between 478 and 488 meters. Acicular radiating aragonite crystals are present on a fracture surface at 691 meters. Calcite increases in abundance with depth.

2.2 WELL WO2

The temperature gradient inflection occurs at a depth of 508 meters in well WO2. The following intervals of core from well WO2 were examined and logged: 396 – 456 meters, 518 – 529 meters, 573 – 610 meters, and 1,033 – 1,069 meters.

Basalts from above the temperature gradient inflection at 508 meters are mostly unaltered. Weak alteration of basalt is present at 424 meters as indicated by a light green tint to the basalt. Silt, probably from overlying sedimentary interbeds, coats or fills most fractures. Occurrences of calcite on fractures or in vesicles and diktytaxitic cavities are minor and sporadic.

Figure 5. Photograph of drusy chabazite crystals in a vug. Core sample is from well 2-2A from a depth of 485.0 meters. Green clay fills diktytaxitic cavities. Bar scale above core is 3 cm long.

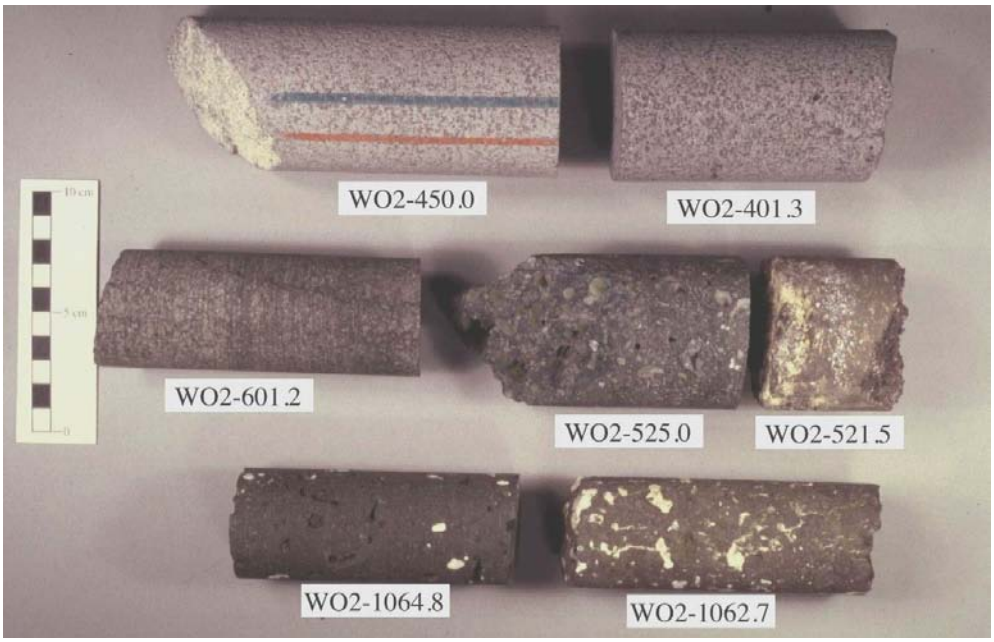

Figure 6. Photograph of core from well WO2. Core is placed in order by depth, with core from the most shallow depth in the upper right and core from the greatest depth in the lower left. Note change in the color of the core and the increase in cavity filling with authigenic minerals with depth. Core changes from gray to dark green with depth due to alteration of primary phase mineral phases to clays and filling of cavities with clays. Bar scale at left is 10 cm long.

Alteration, as indicated by the change in color of the core from the typical gray of unaltered basalt to green of altered basalts, increases with depth below the temperature gradient inflection (Fig. 6). The abundance of authigenic minerals on fractures and filling vesicles and diktytaxitic cavities also increases with depth. Alternating zones of altered and unaltered basalts are present between 518 and 529 meters, and between 573 and 595 meters. All basalts that were examined from below 595 meters are moderately to intensely altered.

Sediments in interbeds below 1,033 meters are green to dark green in color. Calcite increases in abundance with depth. Dogtooth calcite crystals are present in a vesicle at a depth of 1,042 meters.

2.3 WELL C1A

The temperature gradient inflection occurs at a depth of 337 meters in well C1A. The following intervals of core from well C1A were examined and logged: 296 – 326 meters, 354 – 402 meters, and 474 – 550 meters. The bottom of the well is at 550 meters.

Basalts from above the temperature gradient inflection at 337 meters are unaltered. Silt, probably from overlying sedimentary interbeds, coats or fills many fractures. Minor calcite is present in vesicles at a depth of 321 meters.

Intervals of weakly altered basalt occur at 360 meters, at 363 meters, from 385 to 386 meters, at 479 meters, at 480 meters, and from 508 to 510 meters. Light green clay fills vesicles and diktytaxitic cavities in these intervals. Intervals of moderately to intensely altered basalt occur at 475 meters, from 490 to 499 meters, and from 512 to 516 meters. Dogtooth calcite is present on fractures at depths of 484 and 514 meters. Most fractures in altered basalts are coated with green clay and occasional minor calcite, while most fractures in unaltered basalts are coated with tan silt with occurrences of calcite. The abundance of calcite increases with depth below 500 meters. Core between 540 and 550 meters is black and fine-grained. An iridescent green opal-like material coats vesicle walls at a depth of 540 meters. Some fractures are coated with green clay. The thickest single basalt flow

examined in this study occurs in this well between 475 and 518 meters, a thickness of 43 meters. Intervals of altered basalts alternate with intervals of unaltered basalts within this flow. Basalts below this flow are unaltered.

2.4 WELL ANL-1

The temperature gradient inflection occurs at a depth of 560 meters in well ANL-1. The following intervals of core from well ANL-1 were examined and logged: 122 – 190 meters, 279 – 309 meters, and 464 – 582 meters. The bottom of the well is at 582 meters.

All of the basalt core examined is fresh appearing with no evidence of alteration. Fine-grained sand, silt, and clay on fractures and in vesicles are probably from overlying sedimentary interbeds. Authigenic mineralization is limited to calcite and, possibly, clay. Clay coexists with calcite in some vesicles, but it is difficult in these instances to distinguish authigenic clay from clay infiltrated from overlying sediment interbeds. There is very little calcite or clay above 309 meters. Minor calcite is present in vesicles and on fractures at depths of 122 meters, 172 meters, and 177 meters, and in the interval from 279 to 281 meters. Calcite increases in abundance below 465 meters.

Core from 565 to 573 meters is dark gray and fine-grained. There are thick (three to four meters) sedimentary interbeds above and below this interval, with a thin (~0.5 meter) interbed at 570 meters. Fresh basalt is present below the lower sedimentary interbed.

2.5 WELL CH-1

The temperature gradient inflection occurs at a depth of 455 meters in well CH-1. The following intervals of core from well CH-1 were examined and logged: 358 – 370 meters and 454 – 610 meters. The bottom of the well is at 610 meters.

None of the core examined from well CH-1 is basalt in composition. All of the core appeared fresh with no evidence of alteration. Vapor phase cavities occur at a depth of 360

meters in a rhyolite flow. Flow banding is present in several intervals. Flow contacts are difficult to identify in some parts of the core, possibly due to core loss.

Authigenic mineralization is spotty in the upper parts of the core. Pale green clay and chalcedony are present in vesicles and on fractures at a depth of 458 meters. Authigenic mineralization increases below 484 meters, and consists of spotty occurrences of calcite, chalcedony, siderite, and clay on fractures and in vesicles. Dendritic minerals, possibly pyrolusite, are present on some fracture surfaces below 484 meters. There are spotty occurrences of a pale blue coating on some vesicles.

2.6 SUMMARY

Alteration and authigenic mineralization is most pervasive below the temperature gradient inflection in wells 2-2A and WO2. Alteration above the temperature gradient inflection in these wells is minor. Alteration occurs only below the temperature gradient inflection in well C1A. Alteration in C1A is much less pervasive than in wells 2-2A and WO2. No alteration is evident in the examined cores from wells ANL-1 and CH-1.

Authigenic minerals in all the wells are primarily clays and calcite. Chabazite, found in core from well 2-2A, is the only zeolite identified in any of the cores. Siderite occurs only in core from well CH-1. Authigenic mineralization tends to increase with depth below the temperature gradient inflection in each of the wells, except for well ANL-1. The bottom of this well is only 22 meters below the temperature gradient inflection. The 43 meter thick basalt flow observed in the core from well C1A occurs below the temperature gradient inflection in this well. Basalts below this flow are unaltered, while intervals of altered basalts alternate with intervals of unaltered basalts in this flow.

3.0 PETROGRAPHY

Fifty-two thin sections and six microprobe mounts were examined to identify the primary, authigenic, and alteration mineral phases present in each sample. They were also used to estimate the relative abundance of the minerals and to determine the paragenesis of the authigenic and alteration minerals. Modal percentages of minerals are based on point counts (1,000 counts per thin section) for three samples from well 2-2A; all others are based on estimating the percentages by eye using the binocular microscope. Grain size is defined as follows: fine-grained indicates most crystals < 0.5 mm; medium-grained indicates most crystals ≥ 0.5 mm and ≤ 2 mm; and coarse-grained indicates most crystals > 2 mm. Olivine composition was determined using Figure 11.2 of Nesse (1986). Opaques are identified by their shape. Elongate opaques are probably mostly ilmenite (solid solution) and equant opaques are probably mostly magnetite (solid solution). Detailed petrographic descriptions are in Appendix B.

3.1 WELL 2-2A

Six thin sections and four microprobe mounts from well 2-2A were examined. All samples are basalts with plagioclase, olivine, and augite. Red-brown staining along rims and fractures of olivines is common. Olivine compositions range from ~Fo_{78} to ~Fo_{84} in those samples for which the composition could be determined. Three samples from above the depth of the temperature gradient inflection were examined. Minor alteration of tachylite to clay was observed in the sample from a depth of 185.3 meters. Diktytaxitic cavities of this sample are filled with clay. No alteration was observed in the samples from depths of 351.6 and 388.8 meters.

All samples from below the temperature gradient inflection exhibit some degree of alteration and authigenic mineralization. Olivines exhibit a greater degree of alteration than plagioclase. Alteration and authigenic mineralization increased with depth below the temperature gradient inflection. The sample from a depth of 484.3 meters contains a vesicle

~6mm in diameter that is partially filled with calcite and chabazite (Fig. 7). The calcite adheres to the vesicle wall. Clay forms a thin coating over the calcite and the remainder of the vesicle walls. Chabazite forms a coating over the clay. Most of the diktytaxitic cavities are filled with one or more of the following authigenic minerals: clay, chabazite, fluorapophyllite, calcite, and an unidentified zeolite-like silicate mineral. The zeolite-like mineral has a moderate negative relief relative to fluorapophyllite, is colorless, and has a birefringence of ~0.001. It may be isotropic. The mineral has a radiating habit and is found with fluorapophyllite or chabazite; most frequently it is found with fluorapophyllite. A few cavities contain fluorapophyllite, chabazite, and the zeolite-like mineral (Fig. 8).

The sample from a depth of 485.0 meters contains chabazite, but no fluorapophyllite or zeolite-like minerals. No chabazite was observed in the samples from greater depths. Chabazite was observed only in well 2-2A.

Alteration of olivine, plagioclase, and tachylite to clays increases in intensity with depth. Olivine is more frequently and more intensely altered than plagioclase. Two types of clay are commonly intergrown with each other (Fig. 9). Some of the clay exhibits a spherulitic habit. Augite does not exhibit alteration in any sample.

3.2 WELL WO2

Nine thin sections (from seven depths with duplicates for two samples) from well WO2 were examined. All samples except one are basalts with plagioclase and olivine. The sample from a depth of 521.5 meters is a picrobasalt with olivine and plagioclase in a tachylite groundmass. Red-brown staining along rims and fractures of olivines is common. Olivine compositions range from ~Fo_{78} to ~Fo_{84} in those samples for which the composition could be determined. Two samples from above the depth of the temperature

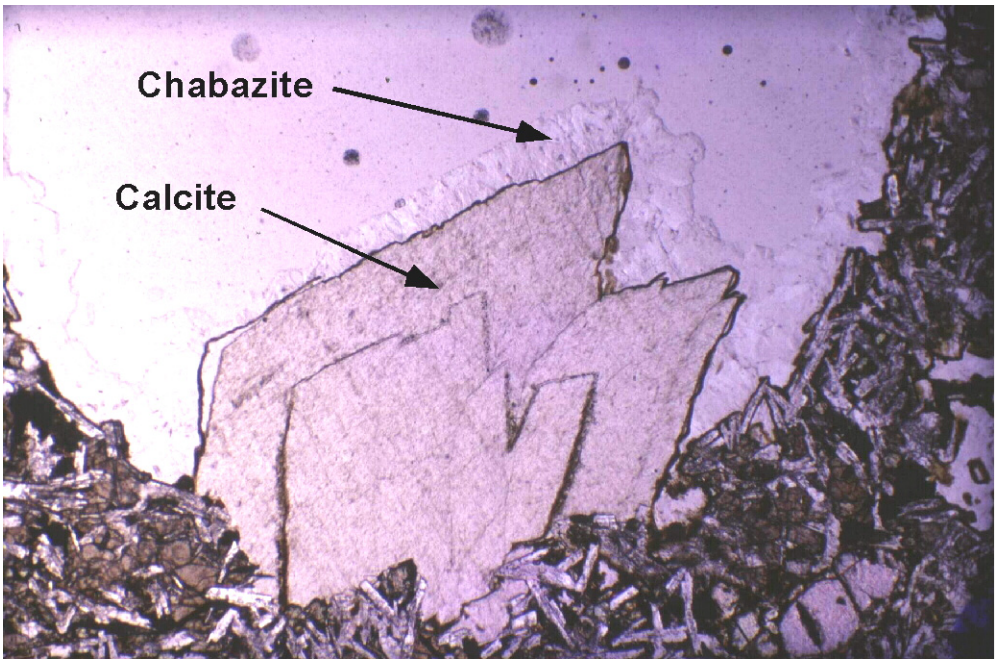

Figure 7. Photomicrograph of calcite and chabazite in a vesicle of sample 2-2A-484.3. Calcite adheres to the vesicle wall. Clay coats the calcite and the remainder of the vesicle wall. Chabazite forms a coating over the clay. Horizontal field of view is 5.4 mm.

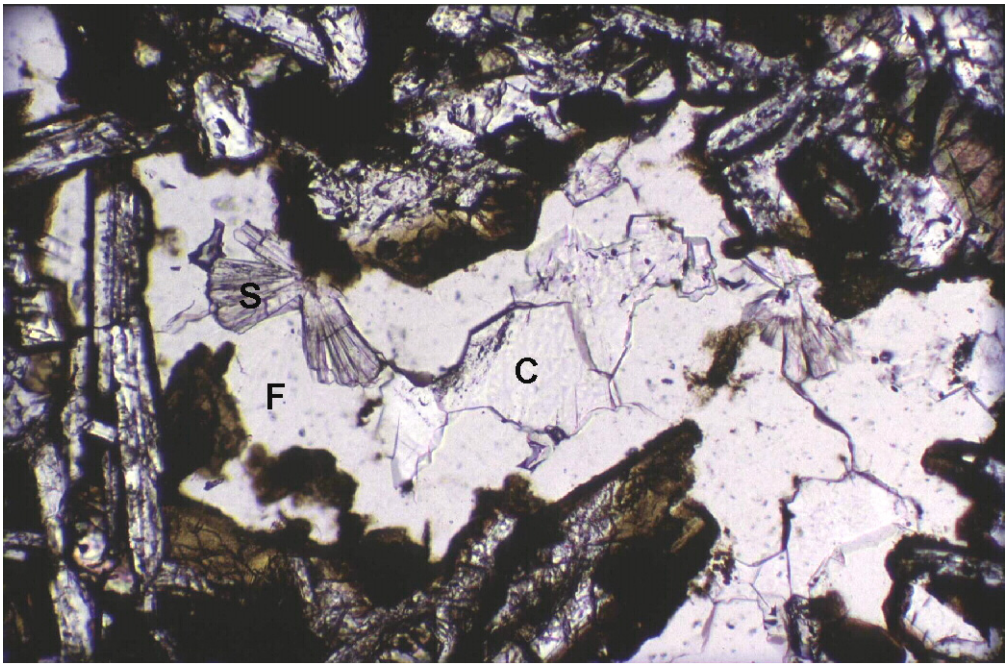

Figure 8. Photomicrograph of chabazite (C), fluorapophyllite (F), and an unidentified zeolite-like silicate mineral (S) in a diktytaxitic cavity of sample 2-2A-484.3. The cavity walls are coated with clay. The zeolite-like mineral has a moderate negative relief relative to fluorapophyllite and has a radiating habit. Horizontal field of view is 1.3 mm.

gradient inflection were examined. No alteration or authigenic mineralization was observed in either sample.

All samples of basalts from below the temperature gradient inflection exhibit some degree of alteration and authigenic mineralization. Olivines exhibit a greater degree of alteration than plagioclase, and alteration of olivine is more pervasive than in well 2-2A. Alteration of tachylite to clay is less pervasive than in well 2-2A. Alteration and authigenic mineralization increases with depth below the temperature gradient inflection. Calcite and/or clay fill most vesicles, diktytaxitic cavities, and fractures. No alteration of augite was observed in any sample.

The picrobasalt from a depth of 521.5 meters does not exhibit alteration, but calcite and clay were observed in vesicles and fractures. An unidentified, biaxial positive mineral (possibly a zeolite) was observed as a minor constituent of fracture filling minerals.

3.3 WELL C1A

Five thin sections and one microprobe mount from well C1A were examined. Four samples are basalts with plagioclase, olivine, and augite. Two samples are basaltic trachyandesites with plagioclase and olivine in a tachylite groundmass. Red-brown staining along rims and fractures of olivines is common. Olivine compositions are ~Fo_{84} in those samples of basalt for which the composition could be determined. Olivine compositions are ~Fo_{65} in the two basaltic trachyandesite samples. One sample from above the depth of the temperature gradient inflection was examined. No alteration or authigenic mineralization was observed in the sample.

Alteration and authigenic mineralization in samples from below the temperature gradient inflection is not as intense or as pervasive as in wells 2-2A and WO2. Clays in diktytaxitic cavities of a sample from a depth of 363.0 meters have a “caterpillar” texture (Fig. 10). Olivines in this sample are partially to completely altered to clays. Some

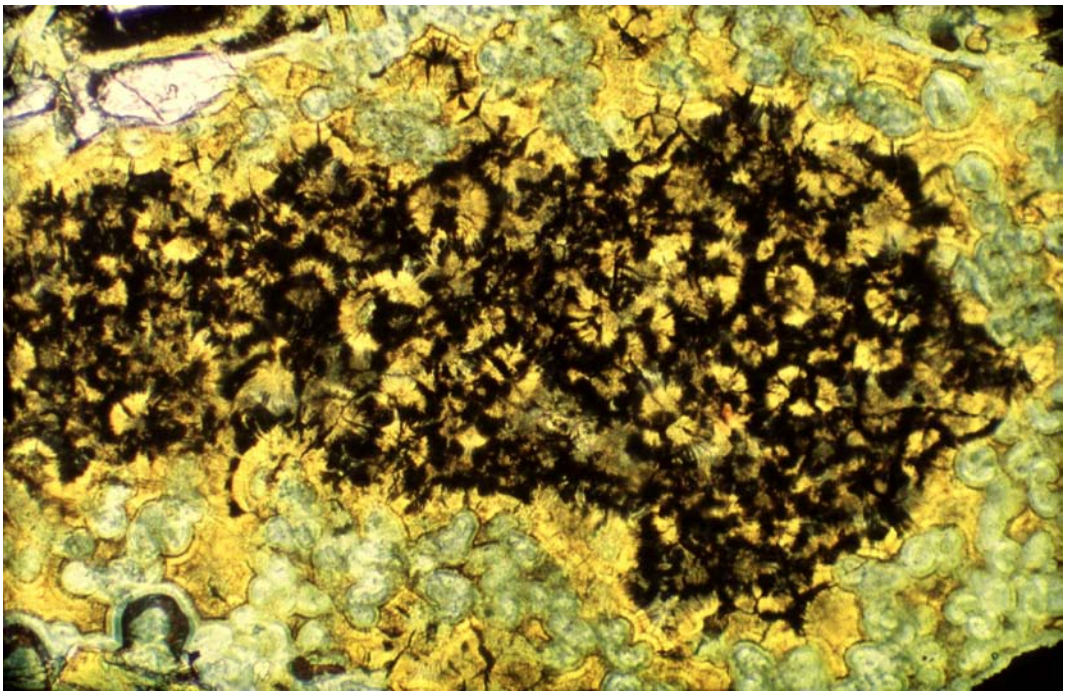

Figure 9. Photomicrograph of spherulitic clays in a vesicle of sample 2-2A-691.1. Horizontal field of view is 1.3 mm.

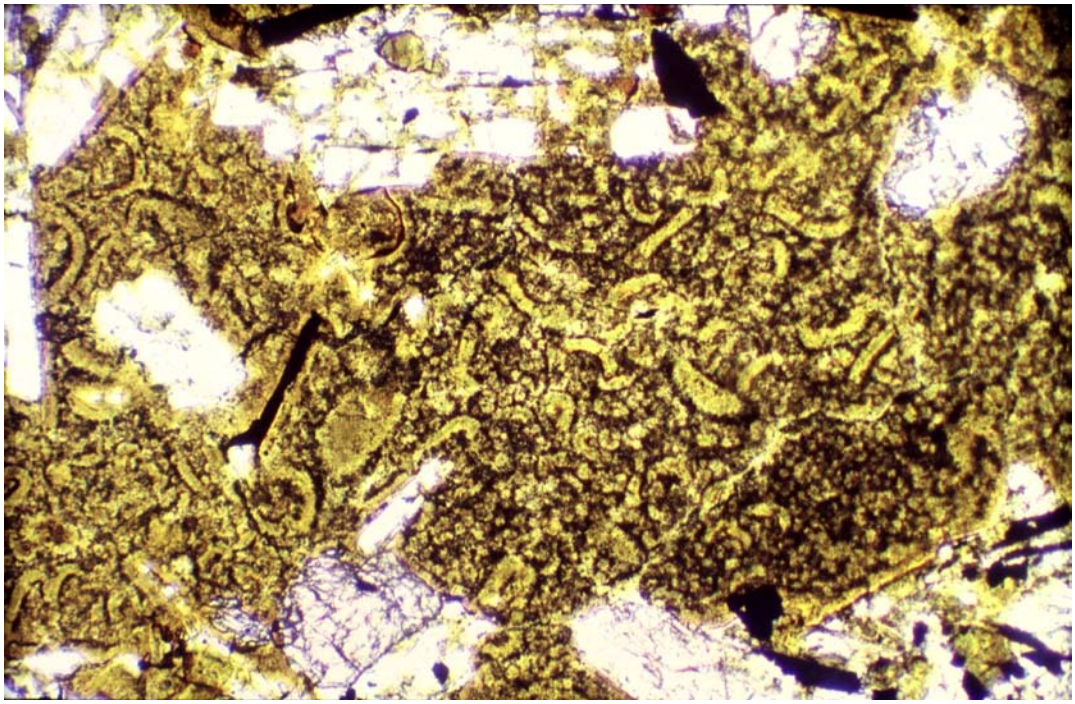

Figure 10. Photomicrograph of clays with a “caterpillar” texture in diktytaxitic cavities of sample C1A-363.0. Horizontal field of view is 1.3 mm.

tachylite is altered to clay, and all diktytaxitic cavities are filled with clays. A sample from a depth of 494.3 meters exhibits only minor alteration of olivines to clay, though all diktytaxitic cavities are filled with clays.

A large vesicle ~20mm long in the sample from a depth of 540.8 meters is coated with a clear opal-like material. Most diktytaxitic cavities are filled with a light brown opal-like material. Vesicles and diktytaxitic cavities in the sample from a depth of 541.7 meters are filled with the light brown opal-like material or with clay. Neither of these samples exhibits any alteration of primary phase minerals.

3.4 WELL ANL-1

Eleven thin sections of ten samples from well ANL-1 were examined. Nine samples are basalts with plagioclase and olivine. One sample is a trachyandesite with plagioclase, olivine, and augite in a felty fine-grained groundmass. Red-brown staining along rims and fractures of olivines is common. Olivine compositions range from ~Fo_{78} to ~Fo_{84} in those samples of basalt for which the composition could be determined. Olivine compositions are ~Fo_{65} in the trachyandesite sample. Nine samples are from above the depth of the temperature gradient inflection and one sample is from below the inflection. No alteration was observed in any of the samples. There are spotty occurrences of calcite filling diktytaxitic cavities.

3.5 WELL CH1

Twenty-one thin sections and one microprobe mount of samples from well CH-1 were examined. All of the samples range in composition from basaltic andesite to rhyolite. One sample is from above the temperature gradient inflection; the remaining samples are from below the inflection. Minor alteration of tachylite to clay in the sample from a depth of 507.0 meters is the only alteration observed in any of the samples. Authigenic mineralization is limited to precipitation of minor quantities of clay in twelve samples, and

precipitation of minor to moderate quantities of siderite in eight samples, calcite in four samples, and an unidentified golden-brown mineral in four samples. The samples are all fine-grained with fewer cavities or voids than the basalts of the other wells.

3.6 SUMMARY

Basalts above the temperature gradient inflection in the wells exhibit minor alteration only in well 2-2A. Alteration and authigenic mineralization increases with depth below the temperature gradient inflection in wells 2-2A and WO2, and to a lesser degree in well C1A. Olivines are more pervasively altered in well WO2 than in well 2-2A, but tachylite is less pervasively altered in well WO2. Chabazite is observed in two samples from well 2-2A that are 0.7 meters apart. Fluorapophyllite and an unidentified zeolite-like silicate mineral are observed in only the upper of these two samples. Chabazite, fluorapophyllite, and the zeolite-like mineral are not observed in samples from any of the other wells. None of the basalts of well ANL-1 is altered. The temperature gradient inflection occurs near the bottom of this well. Only one of the samples from well CH-1 exhibits minor alteration. Siderite is observed as an authigenic mineral only in well CH-1.

4.0 ANALYSIS OF CORE SAMPLES AND MINERAL SEPARATES

Bulk rock major, minor, and trace element analyses were performed on core samples from all wells to compare the compositions of unaltered and altered basalts and to classify the rock type for each sample. Scanning electron microscope analyses of selected samples from well 2-2A were used to examine the habit of individual minerals and to obtain qualitative compositional data for the minerals. The composition of unaltered primary phase minerals, alteration products, and authigenic minerals were determined for selected samples from wells 2-2A, C1A, and CH-1 with the electron microprobe. One zeolite sample from well 2-2A and clays from wells 2-2A, WO2, C1A, and CH-1 were examined using X-ray powder diffraction techniques to aid in identifying the minerals.

4.1 BULK ROCK ANALYSES

Bulk major, minor, and trace element analyses were performed in the LEG at Idaho State University using ICP-AES and INAA techniques. Analytical data for all core samples are in Appendix C. Data for basalt samples only are presented in Table 1. Analytical results were plotted on the total alkali-silica (TAS) diagram of Le Bas et al., (1986) in Figure 11. The results indicate that all the samples from well 2-2A are basalts, all but one sample (a picrobasalt) from well WO2 are basalts, all but one sample (a basaltic trachyandesite) from well C1A are basalts, and all but one sample (a trachyandesite) from well ANL-1 are basalts. All of the samples from well CH-1 range in composition from basaltic andesite to rhyolite.

The basalts of wells 2-2A and WO2 plot over a slightly larger area on the TAS diagram than the basalts of wells C1A and ANL-1. Comparison of the data for the unaltered and altered basalts in Table 1 provides no obvious correlation between silica and alkali abundances and whether a basalt is unaltered or altered. It is not possible to distinguish between unaltered and altered basalts on the TAS diagram.

a le 1. asalt ulk rock analytical data

ell	2-2A	2-2A	2-2A	2-2A	2-2A	2-2A	2-2A	02	2	2	2
ample epth meters	18 .3	3 1.6	388.8	8 .3	8 .0	681.9	691.1	01.3	0.0	21.	2 .0
naltered altered				A	A	A	A			A	A
xides wt											
i 2	8.0	.11	.38	6. 1	.21	8.60	6. 6	.2	6.8	3.86	6. 9
i 2	2.66	3.29	2.9	2.29	2.30	2.20	2.26	2.01	2.68	3.39	3.3
Al2 3	1 .11	13.9	1 . 8	1 .91	1 .10	1 . 9	1 . 9	1 .1	1 .1	1 .11	1 .2
Fe	13.33	1 . 8	1 .3	12.93	12.80	12.83	13.13	12.	13.	1 . 3	1 .12
n	0.20	0.22	0.21	0.20	0.20	0.16	0.20	0.19	0.20	0.2	0.18
g	.38	.1	.22	9.2	9.31	.6	9.00	9. 0	.88	6.12	8.
Ca	9.39	9.8	9.62	10. 8	10.20	11.63	10.12	10.0	9. 8	13. 0	8.92
a2	2.61	2. 3	2.	2. 0	2.28	2. 2	2.3	2. 1	2.6	2.2	1.98
2	0.61	0.6	0. 0	0. 1	0.20	0. 2	0.31	0.	0. 2	0.26	0. 0
P2	0.6	0. 6	0.	0.39	0. 1	0. 1	0.39	0. 3	0.	0.82	0.6
riginal total	98. 6	98.9	9 .09	9 .23	98.18	9 . 6	9 . 2	98.3	9 . 3	9 . 9	96.80
race elements ppm											
c	28.6	31.3	30.0	29.9	29.0	31.3	33.3	31.2	29.	31.	31.3
Cr	216	21	22	281	2 9	1 8	161	3 8	209	23	2 2
Co	.0	6 .9	.2	.8	.8	60.	.	68.	.	.1	.0
i	90	120	110	1 0	90	30	110	110	100	80	90
n	138	19	1	109	110	106	96	1 9	1 2	18	18
		8			6	22		10	6		
r	3 0	3 0	30	38	28	280	2 0	2 3	2 8	26	223
Cs	0.1	0.39	0.2	0.30	0.08	30.2	1. 1	0.11	0.10	0.11	0.1
a	31	0	39	226	16	229	1	33	308	0	369
a	31.	30.	21.	1 .6	1 .0	1 .1	1 .1	18.	18.6	2 .0	20.6
Ce	1.1	69.9	1.9	33.0	3 .	36.8	3 .1	2.	2.6	2.3	0.2
d	28	39	30	19	19	19	19	2	31	3	2
m	.	8.86	.09	.90	. 2	. 3	.86	.0	.91	.29	.00
u	2. 1	3.3	2.6	1.8	1. 6	1.82	1.90	1.9	2.2	2. 6	2. 6
	1.26	1.66	1.31	0.8	0.	0.9	0.9	0.91	1.20	1.26	1.13
	3. 6	.12	3. 0	2.6	2. 0	2.8	2.	2. 2	2.98	.28	3.
u	0.	0.	0.	0.38	0.3	0.38	0.36	0. 0	0. 8	0.62	0. 8
r	2 0	29	2 1	1	1 9	1	1 8	191	201	266	260
Hf	.9	. 2	6.21	3.	3.68	3. 2	3.8	.66	.06	6. 6	6.68
a	1. 0	1. 3	1.00	0. 2	0.82	0.83	0.	0.92	0.99	1.1	1.10
h	1.22	0.93	0. 2	0.66	0. 9	0. 9	na	1.0	0.93	1.22	0. 8
	0.8	1.0	0.9	0.2	0.	1.2	0.	0.2	0.	0.	0.3

enotes all Fe as Fe
xides normalized to 100
unaltered asalt A altered asalt na not analyzed for this constituent

a le 1. asalt ulk rock analytical data

ell	2	2	2	C1A	C1A	C1A	C1A	A -1	A -1	A -1
ample epth meters	601.2	1062.	106 .8	318.2	363.0	00.	93.3	132.	1 .1	182.9
naltered altered	A	A	A		A		A			
xides wt										
i 2	.30	9.0	9.6	.	.1	.30	6. 0	6.8	6.88	6.9
i 2	2. 3	1. 6	1.32	2.0	2.	2.38	2.6	3. 0	3.	3.00
Al2 3	1 .96	1 .32	1 .12	1 .16	1 .18	1 .99	1 .9	1 .66	1 . 1	1 .26
Fe	13.09	11.80	11.2	12.26	13.69	12.83	13.	1 .	1 .81	13.
n	0.19	0.1	0.21	0.19	0.19	0.19	0.20	0.22	0.23	0.21
g	8.31	. 9	.89	9.09	.86	8.6	8.6	6.90	6.32	.1
Ca	10.20	10.99	9. 0	10. 2	9.38	9.9	10.23	9.31	9.29	9.
a2	2. 9	2. 6	2.6	2.	2. 8	2.	2. 0	2.	2.	2.69
2	0.	0.3	0.29	0. 0	0.	0. 9	0.38	0.	1.02	0.86
P2	0. 6	0.29	0.19	0. 3	0.63	0. 6	0. 1	0.69	0.8	0.68
riginal total	9 .63	9 .62	98.6	99.93	96. 3	96.8	9 . 9	99.20	98.83	99.01
race elements ppm										
c	33.0	29.9	26.9	3 .	28.1	33.3	3 .0	30.3	na	28.9
Cr	29	212	196	1	190	19	3 3	16	na	1 9
Co	8.0	3.	.	68.0	1.3	63.6	66.	1.	na	0.8
i	90	na	na	na	90	na	na	30	na	0
n	1 2	0	102	112	1 8	1 0	13	1 1	na	1 3
	8	8	9	19		1	11	1	na	18
r	230	238	230	238	2	2	26	329	329	323
Cs	0.03	0.21	0.16	0.1	0.13	0.21	0.1	0.20	na	0. 6
a	30	21	21	2	3 0	322	26	8	02	82
a	18.3	1 .9	1 .1	1 .6	2 .2	2 .3	1 .1	29.	na	29.
Ce	3.9	38.3	31.1	0.1	61.	3.1	3 .9	6 .8	na	66.
d	28	21	19	2	3	29	2	3	na	33
m	. 8	. 0	.11	. 1	6.90	6.28	. 8	8.31	na	8.0
u	2.2	1.36	1.3	2.0	2.3	2.22	2.0	3.1	na	2.89
	1.10	0.89	0.	0.61	1.22	1.2	0.9	1.	na	1.28
	2.9	3.10	2.3	2.88	3.2	3.08	2.8	3.90	na	3.62
u	0. 8	0. 2	0.3	0.39	0. 6	0.	0.39	0. 1	na	0. 9
r	20	1 3	133	1 9	2 1	213	1 8	320		291
Hf	.3	.	3.63	.81	. 1	.36	. 8	.80	na	.12
a	0.96	0. 6	0. 6	1.23	1.39	1.3	0. 9	1. 0	na	1. 1
h	0.3	2.0	1. 6	0.98	0. 1	1.09	0. 0	1.21	na	1.31
	na	1.2	1.	0.	0.2	1.2	0.9	0.	na	1.0

enotes all Fe as Fe
xides normalized to 100
unaltered asalt A altered asalt na not analyzed for this constituent

a le 1. asalt ulk rock analytical data

ell	A -1	A -1	A -1	A -1	A -1	A -1	A -1
ample epth meters	189.	306.6	8.2	30.	1.0	0.2	82.2
naltered altered							
xides wt							
i 2	.	6.83	6.10	6.66	6.93	6.21	.10
i 2	3.19	3.0	3.08	2.	2.30	3.1	2. 1
Al2 3	1 . 2	1 .8	1 .61	1 . 8	1 . 6	1 . 8	1 .38
Fe	1 .00	13.98	1 .23	12. 6	12.26	1 .8	12.98
n	0.21	0.21	0.22	0.19	0.19	0.21	0.21
g	6.6	.29	.80	8. 8	8.82	. 6	.6
Ca	9.	9. 3	10.23	10.36	10. 0	9.90	10.3
a2	2. 6	2.69	2.	2.	2. 1	2.	2. 3
2	0.83	0.6	0. 6	0.	0.	0.	0.61
P2	0.9	0. 1	0. 3	0.	0.36	0. 2	0.69
riginal total	98.28	98. 6	98.36	98.12	9 .96	100.39	9 .6
race elements ppm							
c	30.0	30.1	31.	32.2	32.	29.2	32.1
Cr	1 2	196	209	286	33	198	23
Co	.	2.	6.	0.	2.0	66.	0.6
i	60	60	80	30	0	120	90
n	1 1	162	1 3	88	122	23 .	138
	21	23	11	11	13	2	1
r	313	306	300	266	2 3	32	22
Cs	0.20	0.2	0.16	0.22	0.28	0.23	0.2
a	0	38	32	2 3	2 0	39	2
a	.0	28.	28.	18.6	1 .8	2 .2	30.3
Ce	96.0	63.1	60.	2.2	3 .6	62.3	6 .3
d		3	29	22	19	3	0
m	10.30	8.00	. 3	.	.9	8.0	.81
u	3. 2	2.8	2.6	2.13	1.81	2.90	2.61
	1. 2	1.3	1.09	0.86	0.96	1.29	1. 0
	.1	3. 8	3.3	2.90	2. 8	3.3	.02
u	0. 1	0. 1	0. 2	0. 3	0.36	0. 8	0. 6
r	3 0	2	2 0	181	1 9	2	332
Hf	8.0	6.3	.80	. 3	.01	6.2	. 2
a	2.06	1.60	1.29	0.99	0.9	1.31	1.29
h	2.61	1. 9	0.62	0.91	1.0	0.3	1.31
	1.	0.6	1.3	0.8	0.6	0.	na

enotes all Fe as Fe
xides normalized to 100
unaltered asalt A altered asalt na not analyzed for this constituent

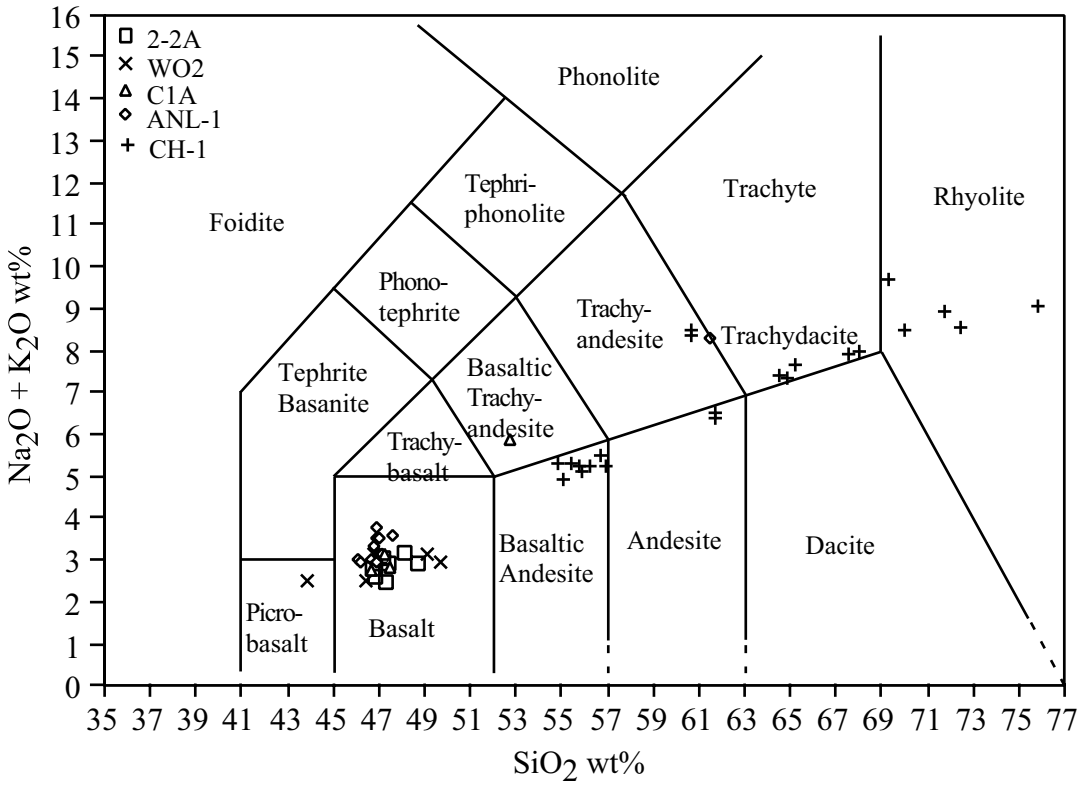

Figure 11. Analytical data for SiO_2 vs. $Na_2O + K_2O$ plotted on the Total Alkali Silica (TAS) diagram of Le Bas and Streckeisen (1986) used to classify volcanic rocks. Most analyses of core from wells 2-2A, WO2, C1A, and ANL-1 fall within the basalt field. None of the analyses of core from well CH-1 fall within the basalt field. Altered and unaltered basalts are not distinguishable in this diagram.

Trace element abundances of samples from each well are plotted on spider diagrams in Figure 12. Abundances were normalized to a "primitive" ESRP tholeiite from well ICPP 123 from a depth of 126 meters (Reed et al., 1997). Both unaltered and altered basalts from all of the wells exhibit a similar pattern on the spider diagrams, except for Cs abundances for altered basalt samples from well 2-2A at depths of 681.9 and 691.1 meters. The plots of the trace element abundances of the basaltic trachyandesite from well C1A and the trachyandesite from well ANL-1 are similar.

The Na_2O/FeO* versus CaO/FeO* data are plotted for altered and unaltered basalts (Fig. 13) to examine the mobility of dissolved constituents. Na and Ca are considered to be mobile in typical groundwater environments, while Fe is considered immobile. Fields for what are considered high-P series (> 1.4 wt% P_2O_5) and low-P series (<1.4 wt% P_2O_5) basalts are also plotted. Most of the analyses are within the low-P series field, except for two altered basalt analyses that are below this field. No unusual alteration features were observed in either of these samples, although the sample with higher CaO/FeO* had an unidentified zeolite-like mineral filling fractures and may have undergone minor migration of some Na due to dissolution of matrix minerals. Other altered basalts plot in the same region as unaltered basalts.

The Sr, Ba, and Zr data are plotted on the ternary diagram in Figure 14 to examine the mobility of dissolved trace elements. Sr and Ba are considered to be mobile in typical groundwater environments, while Zr is considered immobile. Fields for what are considered high-P series and low-P series basalts are also plotted. Most basalts plot within the low-P series field.

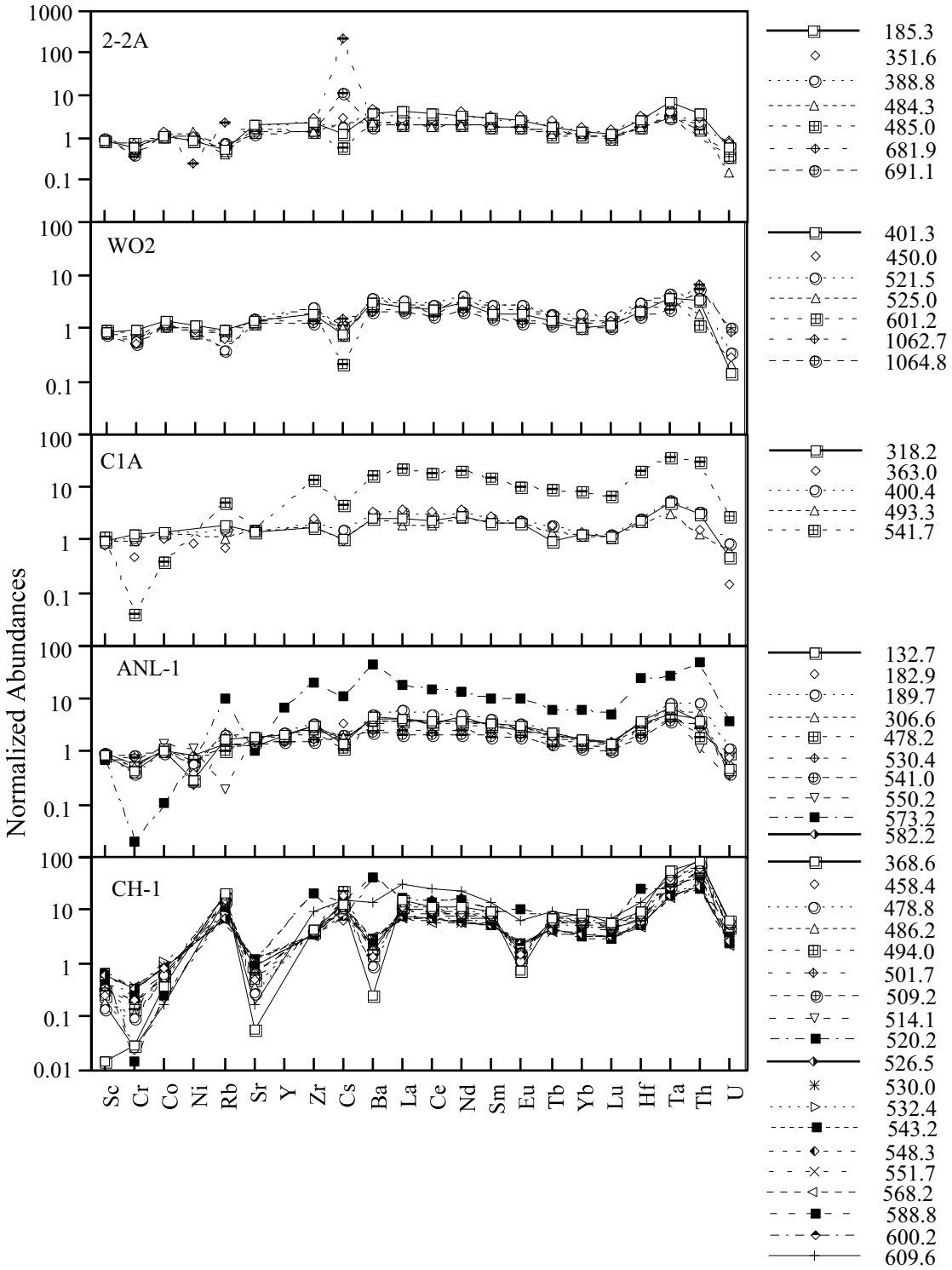

Figure 12. Trace element abundances plotted on spider diagrams. Abundances are normalized to a "primitive" ESRP basalt (Reed et al., 1997). Unaltered and altered basalts from all wells exhibit similar patterns and are not distinguishable on this diagram. Analytical data for the "primitive" basalt are in Appendix C.

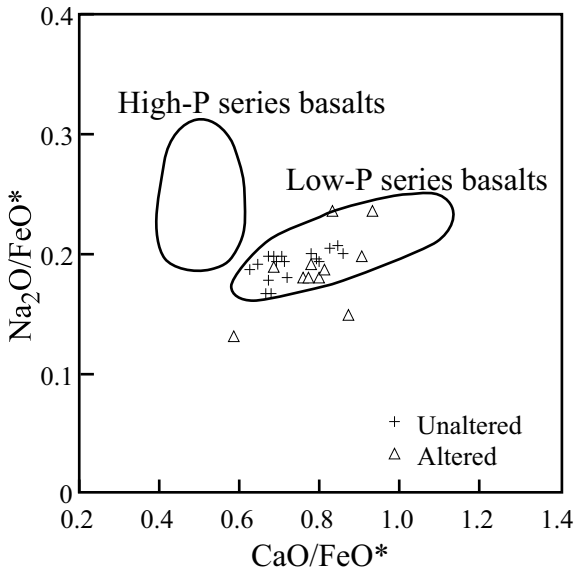

Figure 13. Na_2O/FeO^* vs. CaO/FeO^* data for unaltered and altered basalt samples from wells 2-2A, WO2, C1A, and ANL-1 are plotted. FeO* denotes all Fe calculated as FeO. Ca and Na are considered mobile in typical groundwater environments, while Fe is considered immobile. High-P series basalt and low-P series basalt fields are based on analyses of Snake River Plain basalts that are either high in P (>1.4 wt% P_2O_5) or low in P (<1.4 wt% P_2O_5). Most samples plot within the low-P series basalt field.

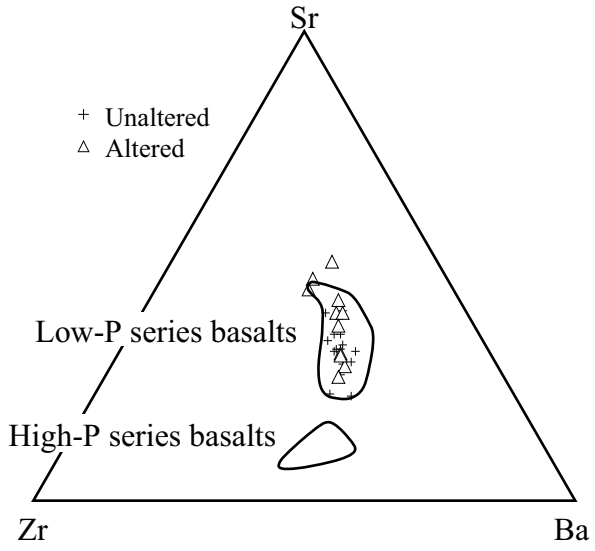

Figure 14. Ternary diagram showing the relation of Sr and Ba to Zr. Sr and Ba are considered mobile in typical groundwater environments, while Zr is considered immobile. High-P series basalt and low-P series basalt fields are based on analyses of Snake River Plain basalts that are either high in P (>1.4 wt% P_2O_5) or low in P (<1.4 wt% P_2O_5). Most basalts plot within the low-P series basalt field. Geochemical analyses for unaltered and altered basalt samples from wells 2-2A, WO2, C1A, and ANL-1 are plotted.

4.2 SEM, MICROPROBE, AND X-RAY POWDER DIFFRACTION ANALYSES

Six samples from well 2-2A were analyzed using the SEM at the University of Utah to examine the habit of primary and authigenic minerals. Six samples from well 2-2A, one sample from well C1A, and six samples from well CH-1 were analyzed by electron microprobe at the University of Utah. An additional seven samples from well 2-2A that were collected by Dr. Scott Hughes (Idaho State University) and Jason Casper (a graduate student at Idaho State University) were also selected for microprobe analysis. Primary phase minerals, authigenic minerals, and alteration phase minerals were examined to determine their chemical compositions. Mineral structural data were calculated using the computer software MinTab, version 1.1 (Carroll, 1991). All microprobe data is in Appendix C.

One sample of a zeolite from well 2-2A and eighteen samples of clays (five from well 2-2A, eight from well WO2, three from well C1A, and two from well CH-1) were analyzed by X-ray powder diffraction in the LEG at Idaho State University. Oriented clay samples produced on porcelain slides using a peel technique described by Drever (1973) were analyzed after air drying, after glycolation, after heating at 300° C, and after heating at 550° C. X-ray powder diffraction data for the zeolite and clay samples are in Appendix C.

Large chabazite crystals in a vesicle of a sample from 485.0 meters have a rhombohedral habit (Fig. 15); globular clusters of prismatic chabazite crystals were also observed in this section of core. Analysis of a large crystal from this vesicle by X-ray powder diffraction (Fig. 16), the observation of the rhombohedral habit, and the results of microprobe analysis of individual crystals were all used to identify the mineral as chabazite.

As described in chapter 3, fluorapophyllite and a zeolite-like silicate mineral were identified in vesicles and diktytaxitic cavities from 484.3 and 485.0 meters in well 2-2A (Fig. 8). The zeolite-like mineral has a radiating habit and coexists with chabazite and/or fluorapophyllite. A ternary diagram of microprobe analyses for chabazite and the zeolite-like mineral is presented in Figure 17.

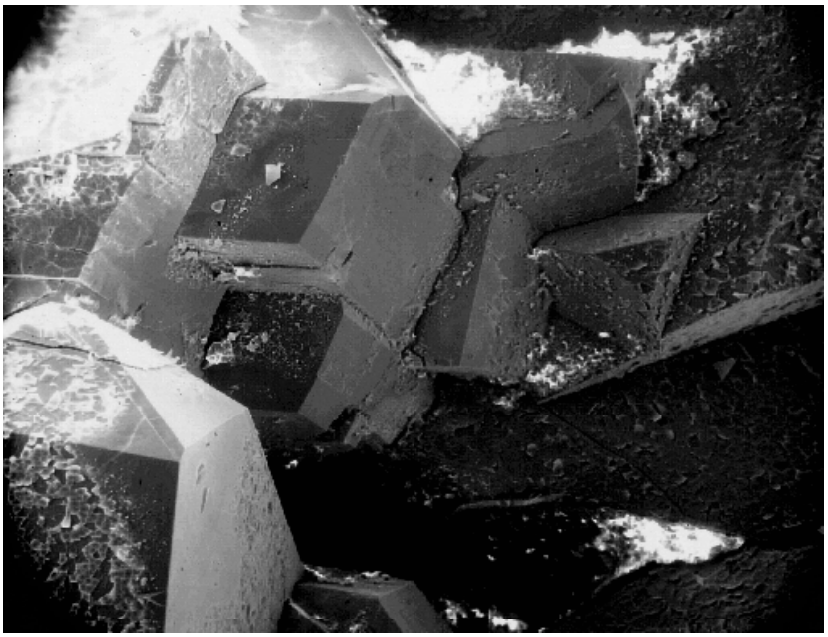

Figure 15. Scanning electron microscope photograph of drusy rhombohedral chabazite crystals in a vug of well 2-2A from a depth of 485.0 meters. Horizontal field of view is approximately 1.7 mm.

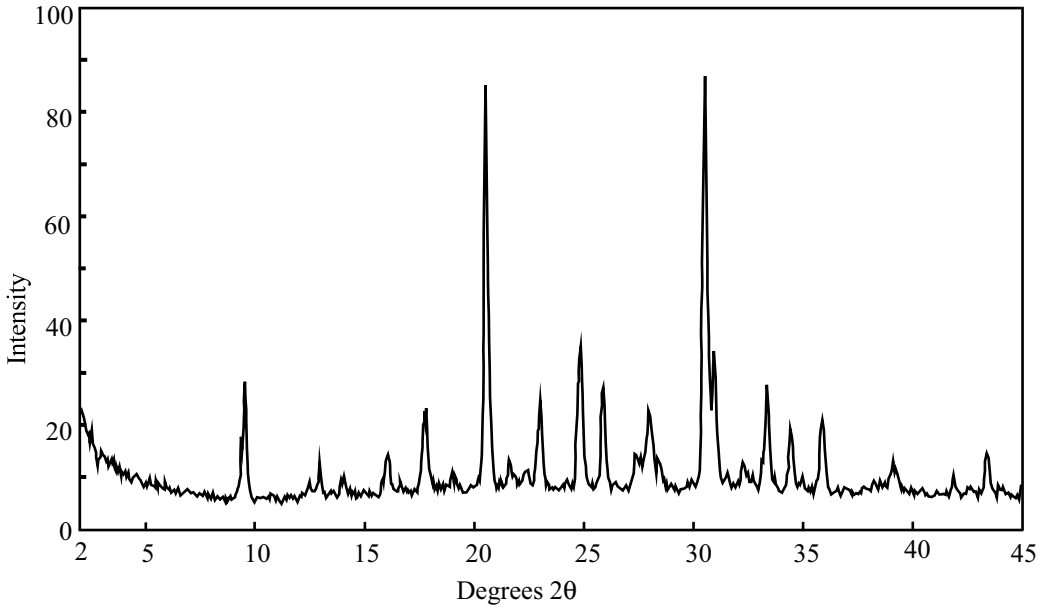

Figure 16. X-ray powder diffraction pattern for a chabazite crystal from well 2-2A from a depth of 484.3 meters.

A Sr-rich chabazite crystal was observed in the sample from 485.0 meters. Sr-rich and Sr-poor chabazites are similar in appearance, are distinguished only by their compositions, and are present, in places, side-by-side, suggesting they are coexisting phases or, texturally speaking, exhibit an unusual growth sequence. Compositions of these phases based on microprobe analyses are as follows:

Chabazite, Sr-poor: $(Na_{0.70}K_{1.01}Ca_{1.08})(Si_{7.88}Al_{4.20})O_{24}\bullet 12H_2O$

Chabazite, Sr-rich: $(Na_{0.74}K_{0.36}Ca_{1.40}Sr_{0.16})(Si_{7.95}Al_{3.99})O_{24}\bullet 12H_2O$

Zeolite-like Mineral: $(Na_{1.05}K_{0.61}Ca_{0.40})(Si_{9.10}Al_{3.04})O_{24}$

Smectite clays were identified by X-ray powder diffraction in 17 of 18 clay samples from wells 2-2A, WO2, C1A, and CH-1. Kaolinite may have been present in a sample from well 2-2A. A typical smectite clay diffraction pattern is shown in Figure 18. The 001 peak shifted to a smaller 2θ after glycolation and to a larger 2θ after heating at 550° C. The shift in the 001 peak is consistent with smectite group minerals. Typical diffraction patterns for clays from a vug, a fracture, and the rock matrix are in Appendix C.

SEM analysis of a light green clay from a sample from 351.6 meters in well 2-2A showed a botryoidal habit. Caterpillar-like aggregates of clays are present with a globular shaped clay (Fig. 19) lining the vesicle of the sample from 485.0 meters that contained the drusy chabazite crystals. The clay morphologies observed are consistent with smectite group minerals.

In thin section, two types of clays are commonly observed intergrown with each other, indicating they are in textural equilibrium. Electron microprobe analyses of clays from well 2-2A span a range of compositions suggesting that the smectite clays identified by X-ray powder diffraction methods are probably mixtures of dioctahedral and trioctahedral types. Structural formulas inferred from representative analyses from opposing parts of the compositional spectrum are shown on the next page, and most closely resemble Fe^{3+}-rich nontronite and Mg-rich saponite:

Nontronite: $(Ca_{0.36}Na_{0.05}K_{0.06})(Fe^{3+}_{2.53}Mg_{1.91}Al_{0.22})(Si_{7.11}Al_{0.89})O_{20}(OH)_4 \bullet nH_2O$

Saponite: $(Ca_{0.09}Na_{0.02}K_{0.01})(Fe^{3+}_{2.19}Mg_{4.01})(Si_{5.08}Al_{2.12}Fe^{3+}_{0.80})O_{20}(OH)_4 \bullet nH_2O$

However, since very fine Fe-Ti minerals may be present within the clays, the mineral compositions proposed are only estimates. Based upon the similar appearance of clays, and similar alteration features of matrix glass and minerals, the smectite clays identified in all the wells are probably similar in composition to the clays in well 2-2A. Figure 20 shows the composition of clays as determined by microprobe analyses plotted on a ternary diagram. Shaded fields on the diagram represent the microprobe analyses of primary phase minerals from wells 2-2A and CH-1, except for the intersertal glass data that is from Bates (1999). Clay data plot primarily in the middle of the diagram, near the pyroxene and intersertal glass fields. No alteration of pyroxenes was observed in any sample, so the clay compositions observed on the diagram probably represent the alteration primarily of olivines and intersertal glass.

Averages of microprobe analyses for chabazite, fluorapophyllite, and the unidentified zeolite-like mineral and for selected smectite samples are presented in Table 2. The H_2O^+ data were calculated by allocating measured oxygen to each of the cation proportions, and then allocating all remaining oxygen to H_2O^+ . Due to an apparent problem with measured oxygen for some suites of analyses, not all average analyses have H_2O^+ data listed.

4.3 SUMMARY

Analyses of samples of altered and unaltered rocks exhibit little to no systematic differences in bulk rock major, minor, or trace element compositions that could be attributed to open-system chemical alteration. This suggests the authigenic minerals observed were precipitated from solutions produced by the alteration and incongruent dissolution of minerals in the aquifer rocks.

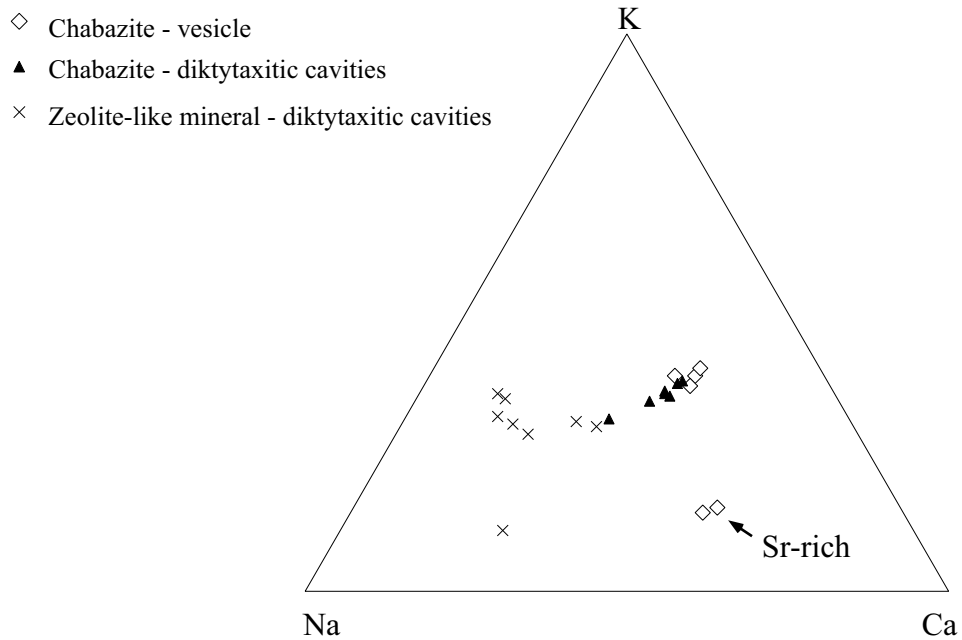

Figure 17. Ternary diagram of microprobe analyses for chabazite and a zeolite-like mineral that has not been identified. Samples are from well 2-2A from depths of 484.3 meters and 485.0 meters. Multiple analyses were performed on three crystals in diktytaxitic cavities of the sample from 484.3 meters and four crystals in vesicles of the sample from 485.0 meters.

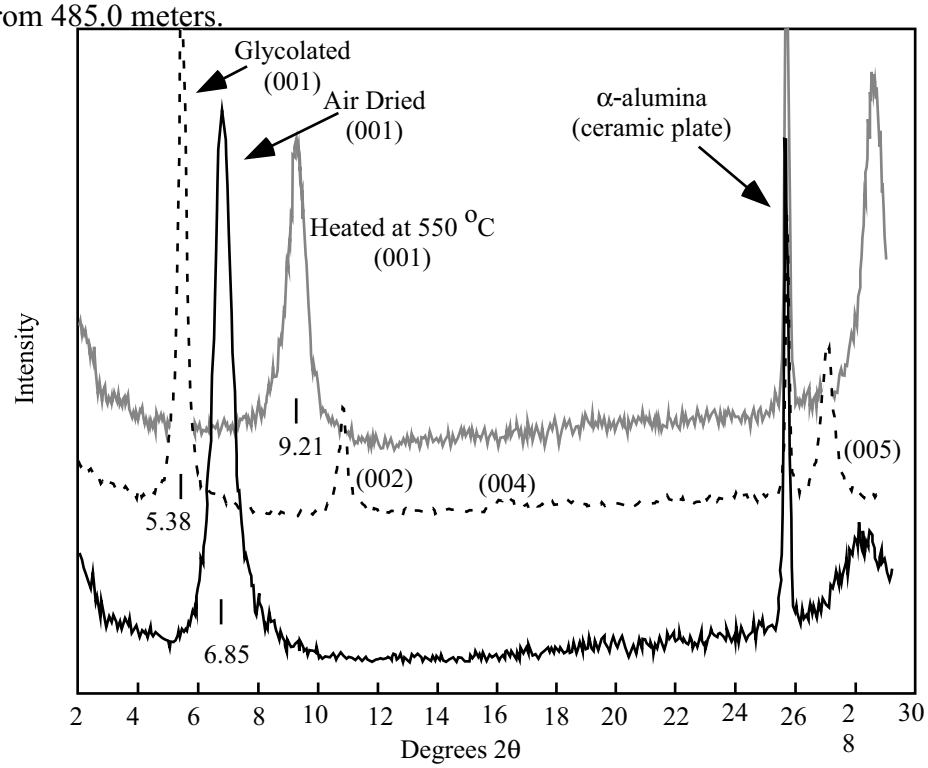

Figure 18. Typical X-ray powder diffraction pattern for smectite clays from the wells examined in this study. Note the shift of the 001 peak to a smaller 2θ after glycolation of the clay, and the shift of the 001 peak to a larger 2θ after heating of the clay. This clay is from a fracture surface in well WO2 from a depth of 1034.8 meters.

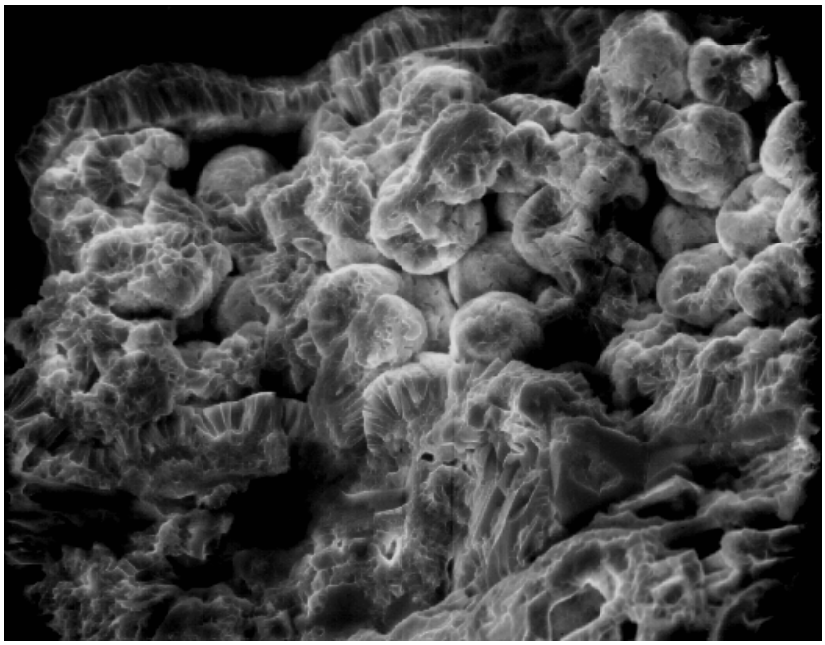

Figure 19. Scanning electron microscope photograph of spherulitic aggregates of smectite clay on the edge of a vug of well 2-2A from a depth of 485.0 meters. Horizontal field of view is approximately 240 µm.

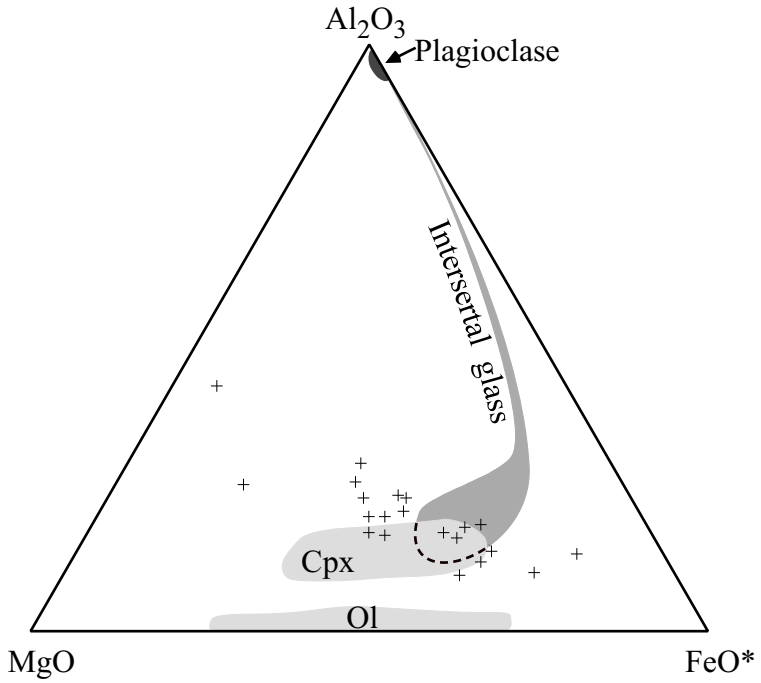

Figure 20. Ternary diagram of microprobe analyses for clays. Samples are from wells 2-2A, C1A, and CH-1. Shaded fields represent results of microprobe analyses of primary phase minerals from wells 2-2A and CH-1, except for intersertal glass data from Bates (1999).

a le 2. Average micropro e analyses of authigenic minerals

	Cha azite 1 r-rich	Cha azite 2 r-poor	aponite 3	ontronite	Fluorapophyllite	nidentified ineral 6
i 2	1. 1	2.6	33. 2	0.	2.39	6 . 2
Al2 3	22.01	23.	11.80	6. 1	1.08	19.16
i 2	na	na	0.01	0.01	na	na
Fe2 3	nd	0.0	26.16	23.98	0.1	0.10
Cr2 3	na	na	0.01	0.00	na	na
g	nd	nd	1 .69	9.13	nd	0.01
n	na	na	0.3	0.0	na	na
Ca	8. 0	6. 0	0.	2.38	23. 8	2.80
a2	2. 0	2. 0	0.08	0.19	0.28	.01
2	1.86	.31	0.03	0.3	.02	3. 2
r	1.8	0.01	na	na	0.01	0.01
a	0.06	0.32	na	na	0.0	0.0
F	na	na	na	na	2.06	na
H2		. 0			1 .93	2.91
otal	88. 8	98. 8	90.10	93. 3	99. 3	100.29
xygens in structural formula	2	2	22	22	21 H F	2
i	.9	.88	.08	.11	.96	9.10
Al	3.99	.20	2.12	1.11	0.19	3.0
i	na	na	0.00	0.00	na	na
Fe3	nd	0.00	2.99	2. 3	0.02	0.01
Cr	na	na	0.00	0.00	na	na
g	nd	nd	.01	1.91	0	0.00
n	na	na	0.0	0.01	na	na
Ca	1. 0	1.08	0.09	0.36	3.83	0. 0
a	0.	0. 0	0.02	0.0	0.08	1.0
	0.36	1.01	0.01	0.06	0. 8	0.61
r	0.16	0.00	na	na	0.00	0.00
a	0.00	0.02	na	na	0.00	0.00
F	na	na	na	na	0.99	na
otal Cations	1 .61	1 .88	1 .3	13.13	12.8	1 .21

H20 calculated from oxygen analyses y allocating re uired oxygens to oxides and assigning remaining oxygens to H2

H2 data not used in calculating structural formulas

na not analyzed for this constituent nd not detected

1 average of 2 analyses

2 average of 11 analyses

3 analysis of one selected clay that represents the saponite end-mem er of the smectite clays

analysis of one selected clay that represents the nontronite end-mem er of the smectite clays

average of analyses

6 average of 8 analyses

5.0 DISCUSSION

Textures of the authigenic minerals indicate that calcite and smectite-group clays coprecipitated at depths above the temperature gradient inflection in wells 2-2A, WO2, and ANL-1. Although the possibility that the calcite originally precipitated within the vadose zone cannot be ruled out, the coarse grain size and euhedral form of many of the calcite grains suggests that some of the calcite was in equilibrium with ground water. The botryoidal and spherulitic habits of clays mantling some apparently unaltered vesicle walls suggest they precipitated congruently from aqueous solution.

Below the temperature-gradient inflections clays are much more abundant and are accompanied by a range of other authigenic mineral phases. In well 2-2A, several samples exhibit a time-growth sequence of calcite $\pm$ clay followed by chabazite $\pm$ fluorapophyllite $\pm$ zeolite-like mineral. Chabazite and fluorapophyllite that completely fill vesicles appear to have been the last authigenic minerals to form. When chabazite occurs in combination with other authigenic minerals, it typically occurs as overgrowths. In other wells the paragenitic sequence is not as clear. Clay and calcite often occur alone in vesicles and diktytaxitic cavities. Where they occur together, either may have precipitated before the other or they may be intimately intergrown.

Figure 21 depicts alteration and authigenic mineralization and shows basalt ages based on an interpolation of paleomagnetic ages of basalt flows and sedimentary interbeds (Anderson and Bowers, 1995; Anderson and Bartholomay, 1995; Anderson et al., 1997; Champion and Lanphere, 1997; Bestland et al., 2002; Geslin et al., 2002; Anderson, 1999, personal communication). Paleomagnetic reversals in basalts and sediments are used to delineate the Brunhes/Matuyama boundary (0.78 Ma) and the Olduvai normal polarity subchron (1.77 Ma) (Berggren et al., 1995). The Brunhes/Matuyama boundary and the upper limit of the Olduvai subchron are indicated in Figure 21 for four of the wells.

Alteration and authigenic mineralization of basalts correlate well with the temperature-gradient inflection in four of the five wells examined. The temperature gradient inflection

for each well occurs at the following depth below land surface (BLS): 2-2A, 408 meters; WO2, 508 meters; C1A, 337 meters; ANL-1, 560 meters; CH-1, 455 meters. In well ANL-1 the inflection occurs 22 meters above the bottom of the well; no alteration or increase in authigenic mineralization was observed in the core below the inflection. In wells 2-2A and WO2 both the degree of alteration and authigenic mineralization increase with depth below the inflections. The CH-1 core that was examined, all from below 118 meters, consisted entirely of rocks ranging in composition from basaltic andesite to rhyolite. Authigenic mineralization in this well correlates well with the inflection, but no alteration was observed, perhaps due to the silicic composition and lower apparent permeability of the rocks in this well. Only minor alteration was observed in well C1A. However, as in other wells, authigenic mineralization increases with depth below the inflections.

Basalt alteration and authigenic mineralization do not correlate to the depth of burial of the basalts, as is apparent in Figure 21. In well 2-2A precipitation of clays and alteration of mineral phases is observed first at depths of ~360 to ~460 meters. In well WO2 this occurs at a depth of ~510 meters, while in well ANL-1 it is not observed at all, even at a depth of 582 meters.

Basalt alteration and authigenic mineralization do not correlate to the age of the basalts. Anderson and Bowers (1995) suggest that the base of the aquifer is associated with alteration and is primarily constrained to ≥ ~1.8 Ma basalts. At well WO2 Anderson and Bowers pick the ~1.8 Ma basalts at a depth of ~500 meters, which is approximately the depth at which alteration and most authigenic mineralization are first observed. However, there is no apparent correlation between alteration and the age of basalts in well 2-2A. At that well Anderson and Bowers pick the ~1.8 Ma basalts at a depth of ~259 meters. Geslin et al. (2002) and Bestland et al. (2002) place the top of Olduvai age sediments (~1.8 Ma) at a depth of ~280 meters in well 2-2A. However, no alteration of the basalts above a depth

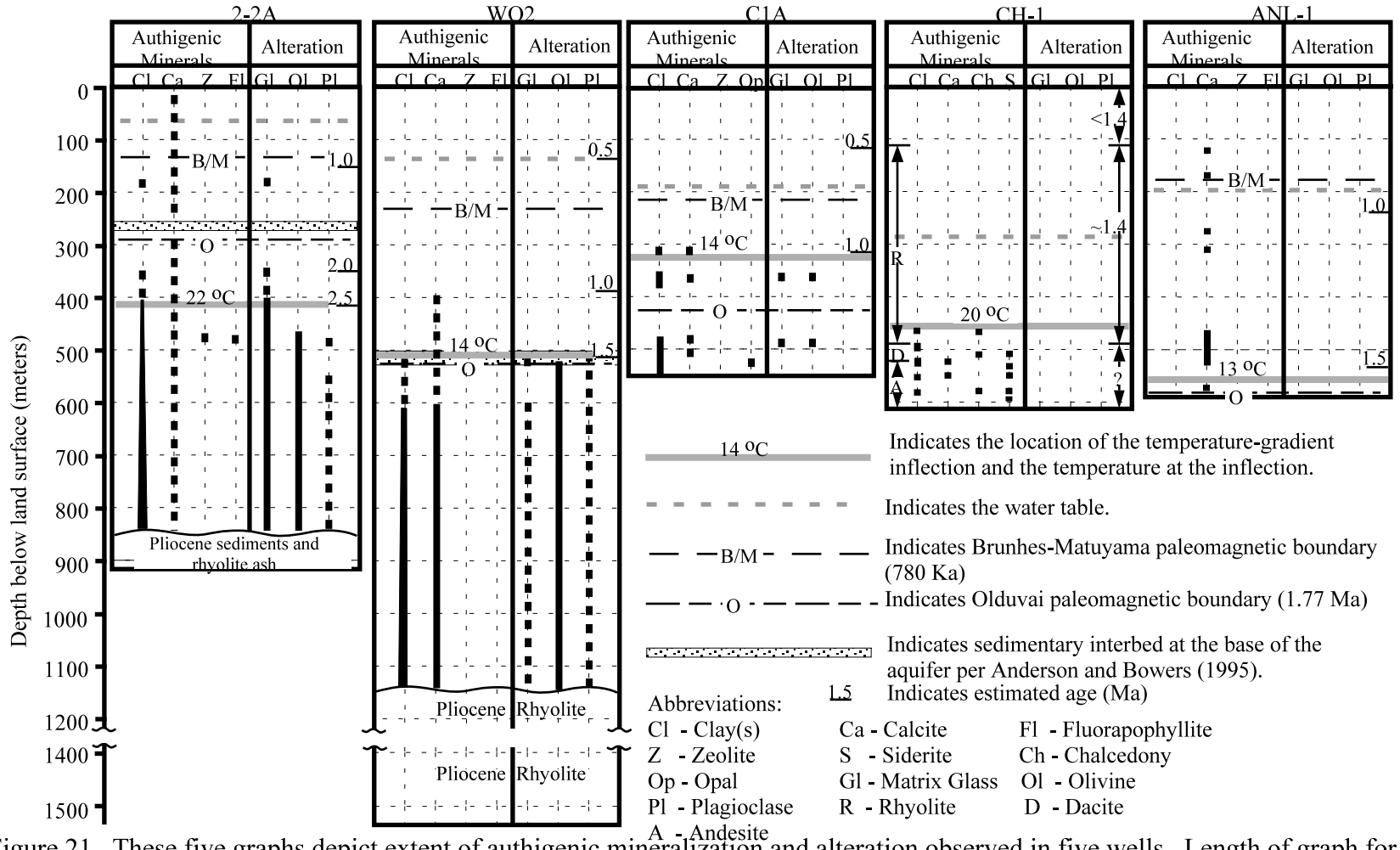

Figure 21. These five graphs depict extent of authigenic mineralization and alteration observed in five wells. Length of graph for each well is proportional to depth of well. Vertical lines on graphs depict vertical ranges of respective authigenic minerals and alteration and widths of lines depict relative abundance. Dashed lines indicate lower abundance than solid lines. An age of ca. 1.42 ma has been assigned to rhyolitic unnamed dome penetrated by well CH-1 (Kuntz and Dalrymple, 1979), but ages have not been determined for rocks above and below the rhyolites. Basalts overlie sequence of rhyolite, dacite, and andesite indicated for well CH-1.

of 351 meters was observed. Substantial alteration was only observed at depths greater than 477 meters, which corresponds to an estimated age of ~2.6 Ma.

The high degree of correlation between alteration and authigenic mineralization with the temperature-gradient inflections in the wells studied suggests that the coincidence of these three properties characterize the base of the aquifer in this part of the ESRP aquifer. The temperature-gradient inflections represent the change from a conductive regime deeper in the aquifer to a convective regime in the shallower parts of the aquifer. Average residence times in the convective regime are 200 to 250 years (Wood and Low, 1986, 1988). The rapid movement of water cooled by recharge in the convective regime relative to the slow movement of water at depth most likely produces the sharp temperature-gradient inflection observed in the wells studied. The slower moving waters in the conductive regime have time to equilibrate with the temperature of the host rocks, while the cooler waters of the convective regime carry away and subdue the heat of the host rocks.

Robertson et al. (1974) and Mann (1986) suggest the base of the aquifer correlates to sedimentary interbeds. While the temperature gradient inflections for wells 2-2A and WO2 occur within thick (10 to 70 meters) sedimentary interbeds and the temperature gradient inflection for well ANL-1 occurs about one meter above a four meter thick sedimentary interbed, there are no similar interbeds near the temperature gradient inflections in wells C1A and CH1. Therefore, the base of the aquifer doesn't correlate well with sedimentary interbeds.

It thus appears that there is no systematic correlation between the depth at which basalt alteration becomes pronounced and prevailing characteristics of the basalts or sediment interbeds. Therefore, this study evaluates the possibility that a transient event, specifically the inputs of warmer and chemically distinct waters from greater depths into the base of the active portion of the aquifer as depicted in the sketch in Figure 22, may play a role in the alteration of the basalts. The plausibility of this idea is supported by the occurrence of hot

springs in areas marginal to the ESRP (Robertson et al., 1974; McLing et al., 1997), and continuing volcanism in the area (Kuntz et al., 1992; Hackett and Smith, 1992).

The computer program MINTEQA2 (Allison et al., 1991) was used to calculate solute activities over a range of plausible compositions (Mann, 1986; McLing, 1994; Fromm, 1995) and temperatures ranging from 12 to 99° C. Thermodynamic relations for pertinent authigenic mineral phases were modeled using The Geochemist's Workbench® (Bethke, 1998). Thermodynamic data for chabazite is not available, so laumontite was used as a surrogate. Calcium-beidellite, a calcium-smectite clay, was used as a surrogate for saponite and nontronite. Results are shown in Figure 23. Twelve degrees C corresponds to typical water temperatures in the convective regime of the aquifer, while 150° C corresponds to warm water (146° C) from a depth of 3,043 meters in well INEL-1 (Mann, 1986). The water compositions plotted on diagrams are for waters from the convective regime (McLing, 1994; Fromm, 1995) and for geothermal waters from depths ranging from 461 to 3,159 meters (Mann, 1986). The temperatures at which the temperature gradient inflections occur range from 13° C to 22° C, so the plot for 12° C water corresponds to mineral stabilities within the convective regime. The other three plots correspond to mineral stabilities within the conductive regime. Note that water chemistry does not significantly influence the mineral stability relationships, but that they are significantly dependent upon temperature. An increase of about 50° C shifts the water chemistry in the direction of laumontite stability. Thus an increase in water temperature alone could produce important authigenic mineral components of some of the most altered basalts observed. However, the region of stability between chabazite and nontronite or saponite could vary from that shown for laumontite and calcium-beidellite, allowing for stability of the minerals under ambient conditions.

An additional hypothesis is that the alteration and authigenic mineralization occurs under ambient conditions, and that alteration is focused into a narrow vertical interval as a result of positive geochemical feedback. For example, as pore spaces are plugged with the products of alteration and authigenic mineralization, water flow through that portion of the

aquifer is slowed. This would allow the water temperature to increase and pore water residence time to increase. The increased water temperatures would enhance alteration of primary mineral phases and the precipitation of authigenic minerals, resulting in a positive feedback loop. Also, closed system calcite precipitation would result in a reduction in pH, driving more vigorous alteration of the primary mineral phases. Both processes seem plausible. However, I do not have sufficient information regarding calcite precipitation rates or the pH and temperature dependence of silicate weathering to quantitatively evaluate their respective plausibilities.

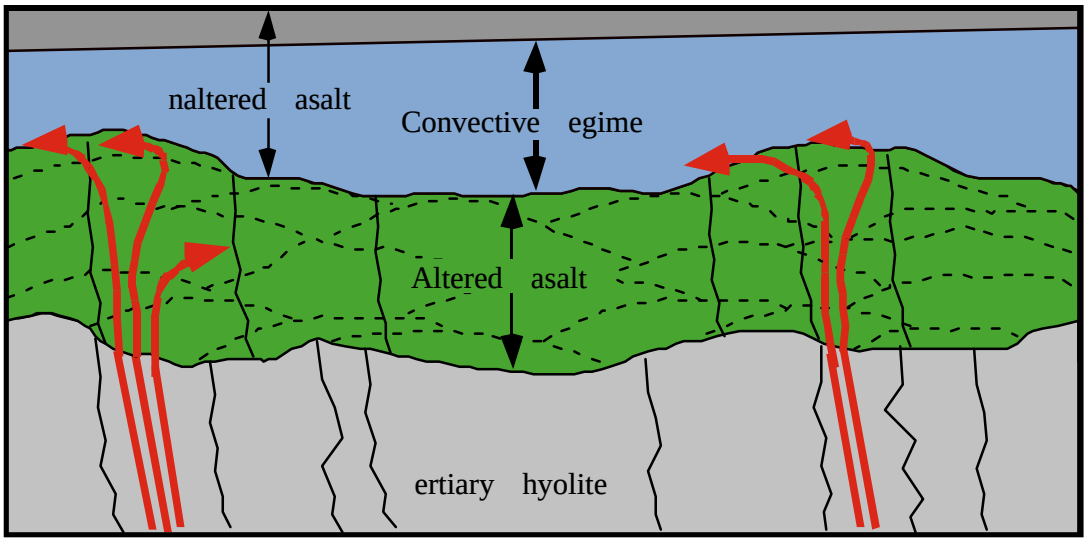

Figure 22. ketch of conceptual model of transient inputs into the ase of the a uifer. eep waters arrows move upward along fractures or other structures and mix with the water of the convective regime of the nake iver Plain a uifer. elow the effective ase of the a uifer warm waters move slowly through the asalts resulting in alteration of primary mineral phases and precipitation of authigenic minerals. ashed lines represent overlapping areas of alteration and authigenic mineralization produced y this process over time. here is no scale applied to this sketch.

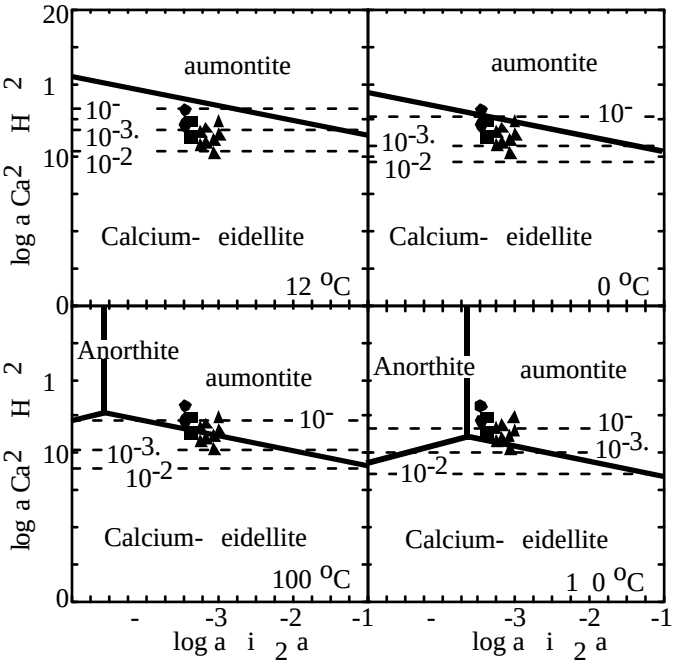

Figure 23. eolite-smectite clay e uili ria for waters from the P a uifer. Closed circles and s uares represent water chemistries for waters from the convective region of the a uifer c ing 199 Fromm 199 . riangles represent analyses of waters from deep in the a uifer ann 1986 . Horizontal dashed lines represent calcite solu ility at the fugacity of C 2 listed for each line. ater chemistry data is in Appendix C.

6.0 CONCLUSIONS

Petrographic, mineralogical, and geochemical analyses of basalts from deep boreholes from a part of the ESRP indicate that there is a regionally significant pronounced and rather sudden downward change from largely unaltered to moderately to strongly altered basalts. These observations are in agreement with assertions by McLing (1994) and Robertson et al. (1974) that very little diagenesis is occurring in the convective regime of the aquifer sysem. Wood and Low (1986, 1988) concluded that diagenesis is a significant process within the convective regime. Their conclusions were based on changes in the water chemistry as the groundwater flowed through the aquifer system from the northeast to the southwest. Since very little diagenesis appears to be occurring within the convective regime, the results of Wood and Low may represent the mixing of geothermal waters from depth with the waters of the convective regime.

Dominant alteration phases include smectite clays (nontronite and saponite) and calcite ± chabazite. The change from the convective regime to the conductive regime occurs over a narrow depth interval, defining a spatially highly irregular surface having the form of an alteration front. It is spatially correlated with pronounced changes in temperature gradient profiles and rock permeability. However, it does not correlate systematically with any other obvious prevailing aspects of the rocks (e.g., host rock depth of burial or age , or the ratio of basalt to sediment interbeds).

Authigenic mineralization and alteration associated with the transient upward influx and mixing of geothermal waters with the Snake River Plain aquifer may best account for the assemblages and space-time patterns of alteration observed in the deep wells investigated. Variations in the degree of authigenic mineralization and alteration may be due to varying amounts of geothermal water that enters the system at different locations and moves vertically and laterally along fractures or other structural control features.

7.0 SUGGESTIONS FOR FURTHER WORK

Further investigation of basalt alteration and the relation of alteration and authigenic mineralization to the base of the aquifer in other parts of the ESRP aquifer should be conducted where possible. Drill core from other deep boreholes, if available for sampling and analysis, should be examined to determine the nature of alteration and authigenic mineralization. Drill core from shallow wells that has been reported by other researchers to exhibit alteration should be examined to compare the reported alteration to that observed in the five deep boreholes examined in this study. Examination of core from deep wells outside the boundaries of the INEEL may shed light on the regional extent of basalt alteration and authigenic mineralization within the aquifer, and may be used to help define the effective base of the ESRP aquifer in other areas of the plain.

The hypothesis that a positive feedback mechanism operating at temperatures typical of the convective regime may have started alteration or authigenic mineralization that eventually resulted in the observed alteration and authigenic mineralization should be investigated. Another possible area of study is the relationship of alteration and authigenic mineralization to hydraulic conductivity of the rocks. Additional work might include quantitative estimates of water-rock ratio variations in basalts and silicic volcanic rocks and the relationship of those variations to the degree and type of alteration.

8.0 REFERENCES

Allison, J. D., Brown, D. S., and Novo-Gradac, K. J., 1991, MINTEQA2/PRODEFA2, A geochemical assessment model for environmental systems 3.0: Athens, GA, U.S. Environmental Protection Agency, EPA-/600/3-91/021.

Anderson, S. R., and Bartholomay, R. C., 1995, Use of natural-gamma logs and cores for determining stratigraphic relations of basalt and sediment at the Radioactive Waste Management Complex, Idaho National Engineering Laboratory, Idaho: Journal of the Idaho Academy of Science, v. 31, 10 p.

Anderson, S. R., and Bowers, B., 1995, Stratigraphy of the unsaturated zone and uppermost part of the Snake River Plain aquifer at Test Area North, Idaho National Engineering Laboratory, Idaho: U. S. Geological Survey Water-Resources Investigations Report 95-4130, 47 p.

Anderson, S. R., Liszewski, M. J., and Cecil, L. D., 1997, Geologic ages and accumulation rates of basalt-flow groups and sedimentary interbeds in selected wells at the Idaho National Engineering Laboratory, Idaho: U. S. Geological Survey Water-Resources Report 97-4010, 39 p.

Armstrong, R. L., Leeman, W. P., and Malde, H. E., 1975, K-Ar dating, Quaternary and Neogene volcanic rocks of the Snake River Plain, Idaho: American Journal of Science, v. 275, no.3, p. 225-251.

Barraclough, J. T., and Jensen, R. G., 1976, Hydrologic data for the Idaho National Engineering Laboratory site, Idaho, 1971 to 1973: U. S. Geological Survey Open-File Report 75-318, 52 p.

Barrash, W., Morin, R. H., Wood, S. H., and Bennecke, W., 1994, Hydrostratigraphic interpretation of the upper portion of the Snake River Plain aquifer near the Idaho Chemical Processing Plant at the INEL, *in* Link, P. K., ed., Hydrogeology, Waste Disposal, Science and Politics, Proceedings of the 30th Symposium on Engineering Geology and Geotechnical Engineering: College of Engineering, Idaho State University, Pocatello, Idaho, p. 181-193.

Bartholomay, R. C., 1990, Mineralogical correlation of surficial sediment from area drainages with selected sedimentary interbeds at the Idaho National Engineering Laboratory, Idaho: U.S. Geological Survey Water-Resources Investigations Report 90-4147, 18 p.

Bates, D. L., 1999, The-in situ chemical fractionation of an eastern Snake River Plain basalt flow: Implications for heterogeneous chemical interaction with groundwater contaminants [M.S. thesis]: Pocatello, Idaho, Idaho State University, 146 p.

Benson, L. V., and Teague, L. S., 1982, Diagenesis of basalts from the Pasco Basin, Washington. 1. Distribution and composition of secondary mineral phases: Journal of Sedimentary Petrology, v. 52, no. 2, p. 595-613.

Berggren, W. A., Hilgren, F. J., Langereis, C. G., Kent, D. V., Obradovich, J. D., Raffi, I., Raymo, M. E., and Shackleton, N. J., 1995, Late Neogene chronology: New perspectives in high-resolution stratigraphy: Geological Society of America Bulletin, v. 107, no. 11, p. 1272-1287.

Bestland, E. A., Link, P. K., Lanphere, M. A., and Champion, D. E., 2002, Paleoenvironments of sedimentary interbeds in the Pliocene and Quaternary Big Lost Trough, eastern Snake River Plain, Idaho, *in* Link, P. K., and Mink, L. L., eds., Geology, Hydrogeology, and Environmental Remediation: Idaho National Engineering and Environmental Laboratory, Eastern Snake River Plain, Idaho: Boulder, Colorado, Geological Society of America Special Paper 353, p. 27-44.

Bethke, C. M., 1998, The geochemist's workbench: Urbana, Illinois, University of Illinois, 184 p.

Blackwell, D. D., Kelley, S., and Steele, J. L., 1992, Heat flow modeling of the Snake River Plain, Idaho: EG&G Idaho Report EGG-C91-103450, 109 p.

Brott, C. A., Blackwell, D. D., and Ziagos, J. P., 1981, Thermal and tectonic implications of heat flow in the eastern Snake River Plain, Idaho: Journal of Geophysical Research, v. 86, no. B12, p. 11,709-11,734.

Carroll, G., 1991, MinTab, University of Western Australia.

Champion, D. E., and Lanphere, M. A., 1997, Age and paleomagnetism of basaltic lava flows in corehole ANL-OBS-AQ-014 at Argonne National Laboratory-West, Idaho National Engineering and Environmental Laboratory: U.S. Geological Survey Open-File Report 97-700, 34 p.

Doherty, D. J., McBroome, L. A., and Kuntz, M. A., 1979, Preliminary geological interpretation and lithologic log of the exploratory geothermal test well (INEL-1), Idaho National Engineering Laboratory, eastern Snake River Plain, Idaho: U.S. Geological Survey Open-File Report 79-1248, 9 p.

Drever, J. I., 1973, The preparation of oriented clay mineral specimens for x-ray diffraction analysis by a filter-membrane peel technique: American Mineralogist, v. 58, p. 553-554.

Fromm, J. M., 1995, Characterizing aquifer hydrogeology and anthropogenic chemical influences on groundwater near the Idaho Chemical Processing Plant, Idaho National Engineering Laboratory, Idaho [M.S. thesis]: Pocatello, Idaho, Idaho State University, 312 p.

Fromm, J. M., Hackett, W. R., and Stephens, J. D., 1994, Primary mineralogy and alteration of basalts and sediments in drillcores from the Idaho National Engineering Laboratory, eastern Snake River Plain *in* Abstracts of the 7th International Symposium on the Observation of the Continental Crust Through Drilling: Santa Fe, New Mexico.

Garabedian, S. P., 1986, Application of a parameter-estimation technique to modeling the regional aquifer underlying the eastern Snake River Plain, Idaho: U.S. Geological Survey Water-Supply Paper 2278, 60 p.

Geist, D. J., Sims, E. N., Hughes, S. S., and McCurry, M., 2002, Open-system evolution of a single episode of Snake River Plain magmatism, *in* Link, P. K., and Mink, L. L., eds., Geology, Hydrogeology, and Environmental Remediation: Idaho National Engineering and Environmental Laboratory, Eastern Snake River Plain, Idaho: Boulder, Colorado, Geological Society of America Special Paper 353, p. 193-204.

Greeley, R., 1982, Snake River Plain, Idaho: representative of a new category of volcanism: Journal of Geophysical Research, v. 87, no. B4, p. 2,705-2,712.

Hackett, W. R., and Smith, R. P., 1992, Quaternary volcanism, tectonics, and sedimentation in the Idaho National Engineering Laboratory area, *in* Wilson, J. R., ed., Field Guide to Geologic Excursions in Utah and Adjacent Areas of Nevada, Idaho, and Wyoming: Salt Lake City, Utah, Utah Geological Survey, p. 1-18.

Heath, R. C., 1984, Ground-water regions of the United States: U.S. Geological Survey Water-Supply Paper 2242, 78 p.

Hughes, S. S., McCurry, M., and Geist, D. J., 2002, Geochemical correlations and implications for the magmatic evolution of basalt flow groups at the Idaho National Engineering and Environmental Laboratory, *in* Link, P. K., and Mink, L. L., eds., Geology, Hydrogeology, and Environmental Remediation: Idaho National Engineering and Environmental Laboratory, Eastern Snake River Plain, Idaho: Boulder, Colorado, Geological Society of America Special Paper 353, p. 151-173.

Johnson, G. S., Olsen, J. H., and Ralston, D. R., 1994, Hydrologic testing in wells near the Idaho Chemical Processing Plant at the Idaho National Engineering Laboratory, *in* Link, P. K., ed., Hydrogeology, Waste Disposal, Science and Politics, Proceedings of the 30th Symposium on Engineering Geology and Geotechnical Engineering: College of Engineering, Idaho State University, Pocatello, Idaho, p. 253-265.

Keith, T. E. C., and Bargar, K. E., 1988, Petrology and hydrothermal mineralogy of U.S. Geological Survey Newberry 2 drill core from Newberry Caldera, Oregon: Journal of Geophysical Research, v. 93, no. B9, p. 10,174-10,190.

Knobel, L. L., Bartholomay, R. C., and Orr, B. R., 1997, Preliminary delineation of natural geochemical reactions, Snake River Plain aquifer system, Idaho National Engineering Laboratory and vicinity, Idaho: U.S. Geological Survey Water-Resources Investigations Report 97-4093, 52 p.

Knutson, C. F., McCormick, K. A., Smith, R. P., Hackett, W. R., O'Brian, J. P., and Crocker, J. C., 1990, FY 89 report Radioactive Waste Management Complex vadose zone basalt characterization: EG&G Idaho Report EGG-WM-8949, 412 p.

Kuntz, M. A., Covington, H. R., and Schorr, L. J., 1992, An overview of basaltic volcanism of the eastern Snake River Plain, Idaho, *in* Link, P. K., Kuntz, M. A., and Platt, L. B., eds., Regional geology of eastern Idaho and western Wyoming: Geological Society of America Memoir, p. 227-267.

Kuntz, M. A., and Dalrymple, G. B., 1979, Geology, geochronology, and potential volcanic hazards in the Lava Ridge-Hells Half Acre area, eastern Snake River Plain, Idaho: U.S. Geological Survey Open-File Report 79-1657, 66 p.

Lanphere, M. A., Champion, D. E., and Kuntz, M. A., 1993, Petrography, age, and paleomagnetism of basalt lava flows in coreholes Well 80, NRF 89-04, NRF 89-05, and ICPP 123, Idaho National Engineering Laboratory: U.S. Geological Survey Open-File Report 93-327, 40 p.

Lanphere, M. A., Kuntz, M. A., and Champion, D. E., 1994, Petrography, age, and paleomagnetism of basaltic lava flows in coreholes at Test Area North (TAN), Idaho National Engineering Laboratory: U.S. Geological Survey Open-File Report 94-686, 49 p.

Le Bas, M. J., Le Maitre, R. W., Streckeisen, A., and Zanettin, B., 1986, A chemical classification of volcanic rocks based on the total alkali-silica diagram: Journal of Petrology, v. 27, p. 745-750.

Leeman, W. P., 1982, Olivine tholeiitic basalts of the Snake River Plain, Idaho, *in* Bonnichsen, B., and Breckenridge, R. M., eds., Cenozoic geology of Idaho: Idaho Bureau of Mines and Geology Bulletin 26, p. 181-192.

Mann, L. J., 1986, Hydraulic properties of rock units and chemical quality of water for INEL-1 — a 10,365-foot deep test hole drilled at the Idaho National Engineering Laboratory, Idaho: U. S. Geological Survey Water-Resources Investigations Report 86-4020, 23 p.

Mark, L. E., and Thackray, G. D., 2002, Sedimentologic and hydrologic characterization of surficial sedimentary facies in the Big Lost Trough, Idaho National Engineering and Environmental Laboratory, eastern Idaho, *in* Link, P. K., and Mink, L. L., eds., Geology, Hydrogeology, and Environmental Remediation: Idaho National Engineering and Environmental Laboratory, Eastern Snake River Plain, Idaho: Boulder, Colorado, Geological Society of America Special Paper 353, p. 61-75.

McLing, T. L., 1994, The pre-anthropogenic groundwater evolution at the Idaho National Engineering Laboratory, Idaho [M.S. thesis]: Pocatello, Idaho, Idaho State University, 62 p.

McLing, T. L., Smith, R. W., and Johnson, T. M., 1997, The effect of hydrothermal water on the Snake River Plain aquifer: Geological Society of America Abstracts with Programs, v. 29, no. 6, p. A323.

McLing, T. L., Smith, R. W., and Johnson, T. M., 2002, Chemical characteristics of thermal water beneath the eastern Snake River Plain, *in* Link, P. K., and Mink, L. L., eds., Geology, Hydrogeology, and Environmental Remediation: Idaho National Engineering and Environmental Laboratory, Eastern Snake River Plain, Idaho: Boulder, Colorado, Geological Society of America Special Paper 353, p. 205-211.

Nace, R. L., 1953, Altitude and configuration of the water table beneath the National Reactor Testing Station, Idaho: U. S. Geological Survey Report IDO-22024-USGS, 5 p.

Nash, W. P., 1992, Analysis of oxygen with the electron microprobe; applications to hydrated glass and minerals: American Mineralogist, v. 77, no. 3-4, p. 453-457.

Nesse, W. D., 1991, Introduction to optical mineralogy: New York, Oxford University Press, 335 p.

Olmsted, F. H., 1962, Chemical and physical character of ground water in the National Reactor Testing Station, Idaho: U. S. Geological Survey Report IDO-22043-USGS, 124 p.

Reed, M. F., Bartholomay, R. C., and Hughes, S. S., 1997, Geochemistry and stratigraphic correlation of basalt lavas beneath the Idaho Chemical Processing Plant, Idaho National Engineering Laboratory: Environmental Geology, v. 30, p. 108-118.

Robertson, J. B., Shoen, R., and Barraclough, J. T., 1974, The influence of liquid waste disposal on the geochemistry of water at the National Reactor Testing Station, Idaho: 1952-1970: U. S. Geological Survey Open-File Report IDO-22053, 231 p.

Self, S., Keszthelyi, L., and Thordarson, T., 1998, The importance of pahoehoe: Annual Reviews in Earth and Planetary Science, v. 26, p. 81-110.

Smith, R. P., Hackett, W. R., Josten, N. E., Knutson, C. F., Jackson, S. M., Barton, C. A., Moos, D., Blackwell, D. D., and Kelley, S., 1994, Synthesis of deep drill hole information at the Idaho National Engineering Laboratory (INEL): Upper crustal environment in the continental track of a mantle hotspot, *in* Proceedings of the 7th International Symposium on the Observation of the Continental Crust Through Drilling, Santa Fe, New Mexico, p. 89-92.

Staff, Basalt Waste Isolation Project, Systems Integration Department, Rock Mechanics and Mining Technology Group, 1979, Geological characterization of drill holes DC-6, DC-8, and DC-4, final report, RHO-BWI-C-69: Richland, Washington, Rockwell Hanford Operations, 24 p.

Welhan, J., and Wylie, A., 1997, Stochastic modeling of hydraulic conductivity in the Snake River Plain aquifer: 2. Evaluation of controls at the core and borehole scales, *in* Proceedings of the 32nd Symposium on Engineering Geology and Geotechnical Engineering: Boise, Idaho, p. 93-107.

Whitehead, R. L., 1992, Geohydrologic framework of the Snake River Plain aquifer system, Idaho and eastern Oregon: U. S. Geological Survey Professional Paper 1408-B, 32 p.

Wood, W. W., and Low, W. H., 1986, Aqueous geochemistry and diagenesis in the eastern Snake River Plain aquifer system, Idaho: Geological Society of America Bulletin, v. 97, p. 1,456-1,466.

Wood, W. W., and Low, W. H., 1988, Solute geochemistry of the Snake River Plain regional aquifer system, Idaho and eastern Oregon: U.S. Geological Survey Professional Paper 1408-D, 79 p.

Wright, K. E., 1998, Geochemistry and petrology of the Tuff of McMullen Creek, Cassia County Idaho [M.S. thesis]: Pocatello, Idaho, Idaho State University, 172 p.

APPENDIX A: CORE LOGS

This appendix contains graphical logs of the core from the five deep wells that was examined in this study. The portrayal of vesicles and fractures is intended to indicate the relative location and abundance of these features. The logs are drawn at a scale of approximately 1:100. Within the description of the core, mineral grain size is defined as follows: fine-grained indicates most crystals are < 0.5 mm; medium-grained indicates most crystals are ≥ 0.5 mm and ≤ 2 mm; coarse-grained indicates most crystals are > 2 mm.

Explanation of Core Log Symbology

Sample number

2-2A-185.3$_{1,2,3,4,5}$

2-2A indicates the sample is from well 2-2A.

185.3 indicates the depth of the core in meters below land surface (BLS) from which the sample was collected.

Subscripts 1-5 indicate the purpose of the sample as follows:

1 - Petrography
2 - Bulk chemical analysis
3 - Microprobe analysis
4 - X-ray powder diffraction analysis
5 - SEM analysis

Sediment interbed

Rubble

Autoclastic breccia; used only for CH-1 log

Vesicles; quantity represents abundance in core

Vesicle zone

Vesicle sheet

Vesicle column

Upper crust

Core

Lower crust

Intense alteration

Moderate alteration

Weak alteration

Flow contact

Flow banding; used only for CH-1 log

Sample location

Fracture without secondary minerals

Fracture with secondary minerals

Sub-vertical fracture

Sub-horizontal fracture

Low-angle ($\leq 45^{o}$) fracture

High-angle ($> 45^{o}$) fracture

Top or bottom of logged core section

Well 2-2A

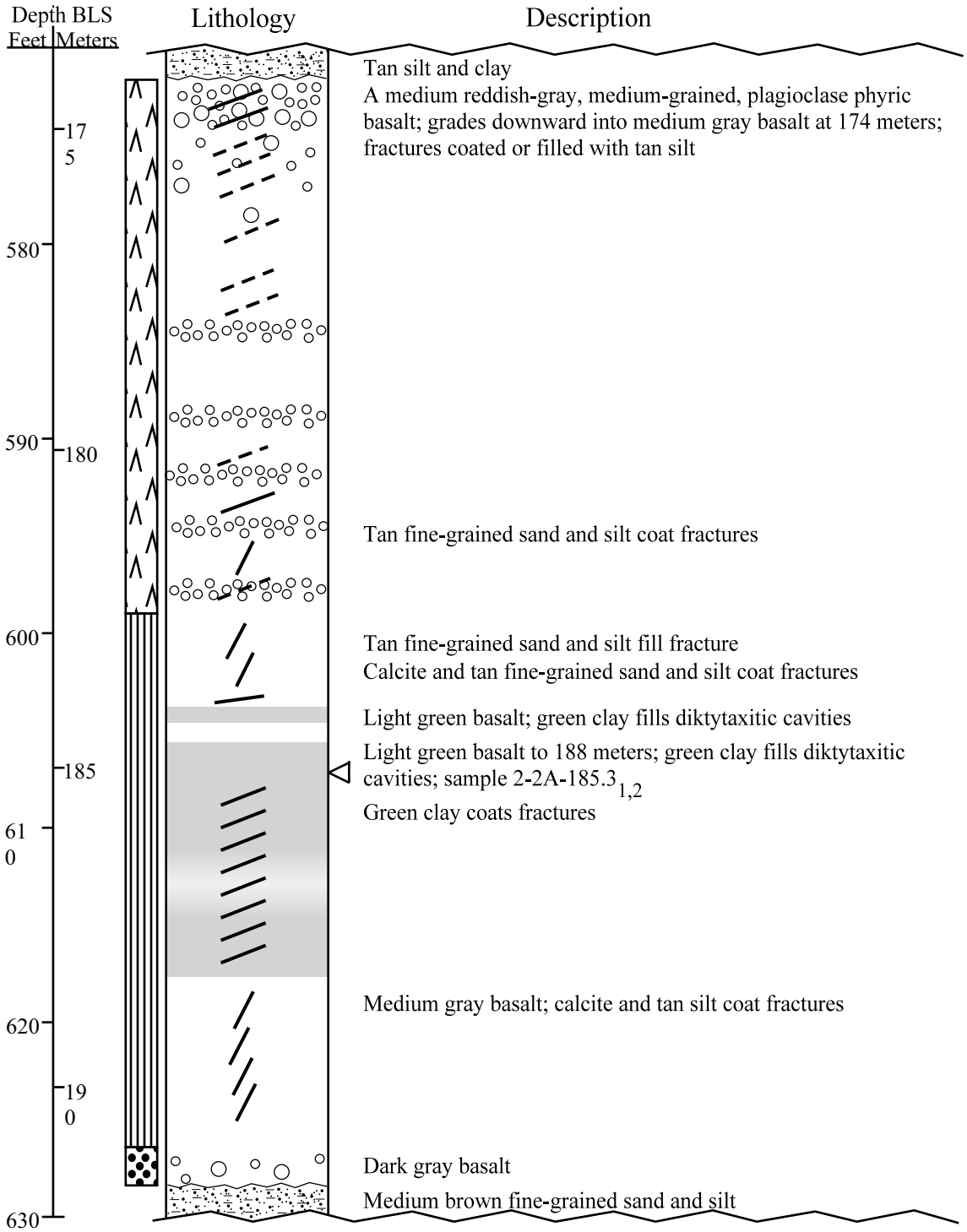
Depth BLS
Feet Meters
Lithology
Description
17
5
580
590
180
600
185
61
0
620
19
0
630
Tan silt and clay
A medium reddish-gray, medium-grained, plagioclase phyric basalt; grades downward into medium gray basalt at 174 meters; fractures coated or filled with tan silt
Tan fine-grained sand and silt coat fractures
Tan fine-grained sand and silt fill fracture
Calcite and tan fine-grained sand and silt coat fractures
Light green basalt; green clay fills diktytaxitic cavities
Light green basalt to 188 meters; green clay fills diktytaxitic cavities; sample 2-2A-185.3 1,2
Green clay coats fractures
Medium gray basalt; calcite and tan silt coat fractures
Dark gray basalt
Medium brown fine-grained sand and silt

Well 2-2A

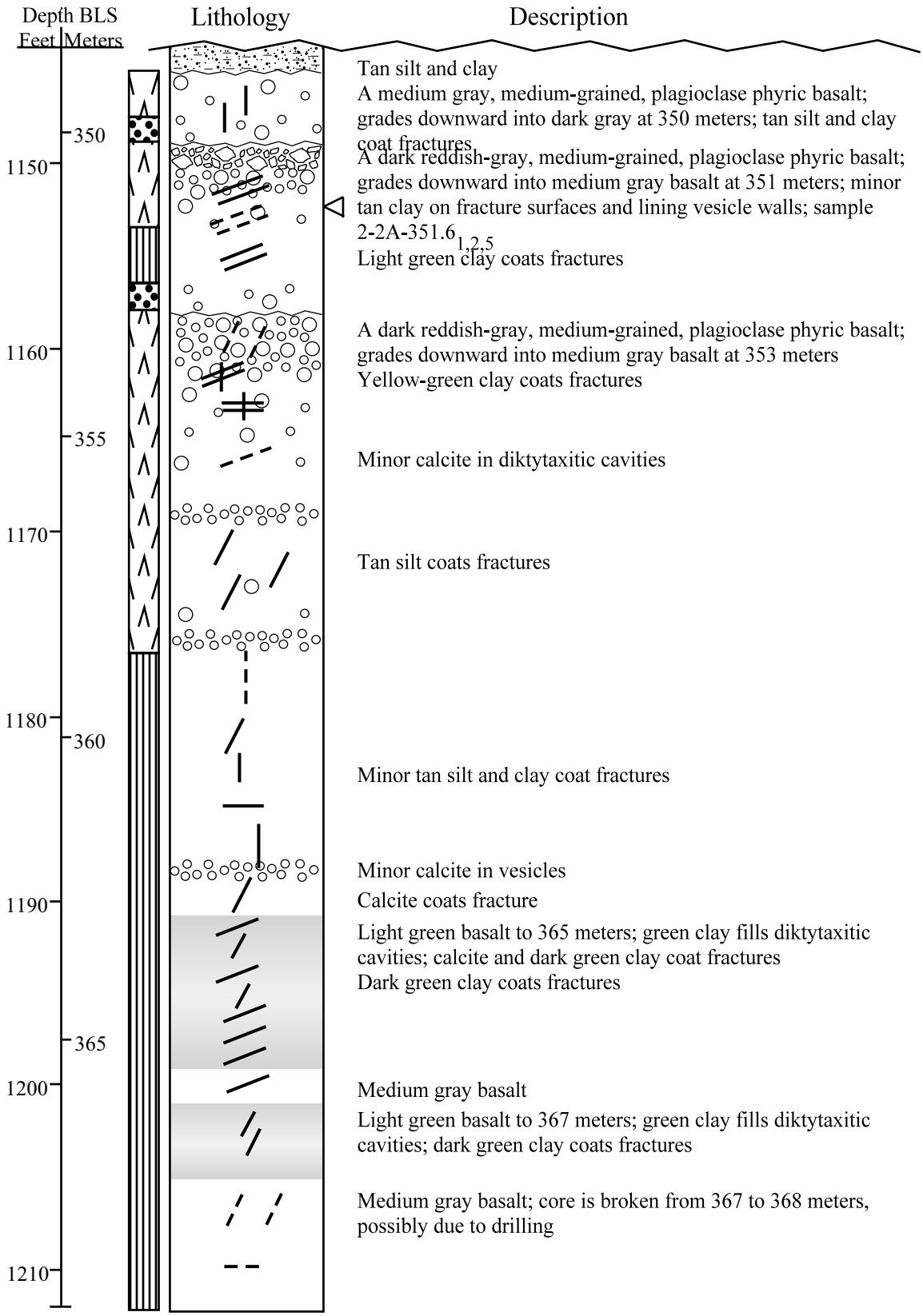
Depth BLS
Feet Meters
Lithology
Description
350
1150
355
1160
360
1170
365
1180
1190
1200
1210
Tan silt and clay
A medium gray, medium-grained, plagioclase phyric basalt; grades downward into dark gray at 350 meters; tan silt and clay coat fractures
A dark reddish-gray, medium-grained, plagioclase phyric basalt; grades downward into medium gray basalt at 351 meters; minor tan clay on fracture surfaces and lining vesicle walls; sample 2-2A-351.6 1,2,5
Light green clay coats fractures
A dark reddish-gray, medium-grained, plagioclase phyric basalt; grades downward into medium gray basalt at 353 meters
Yellow-green clay coats fractures
Minor calcite in diktytaxitic cavities
Tan silt coats fractures
Minor tan silt and clay coat fractures
Minor calcite in vesicles
Calcite coats fracture
Light green basalt to 365 meters; green clay fills diktytaxitic cavities; calcite and dark green clay coat fractures
Dark green clay coats fractures
Medium gray basalt
Light green basalt to 367 meters; green clay fills diktytaxitic cavities; dark green clay coats fractures
Medium gray basalt; core is broken from 367 to 368 meters, possibly due to drilling

Well 2-2A

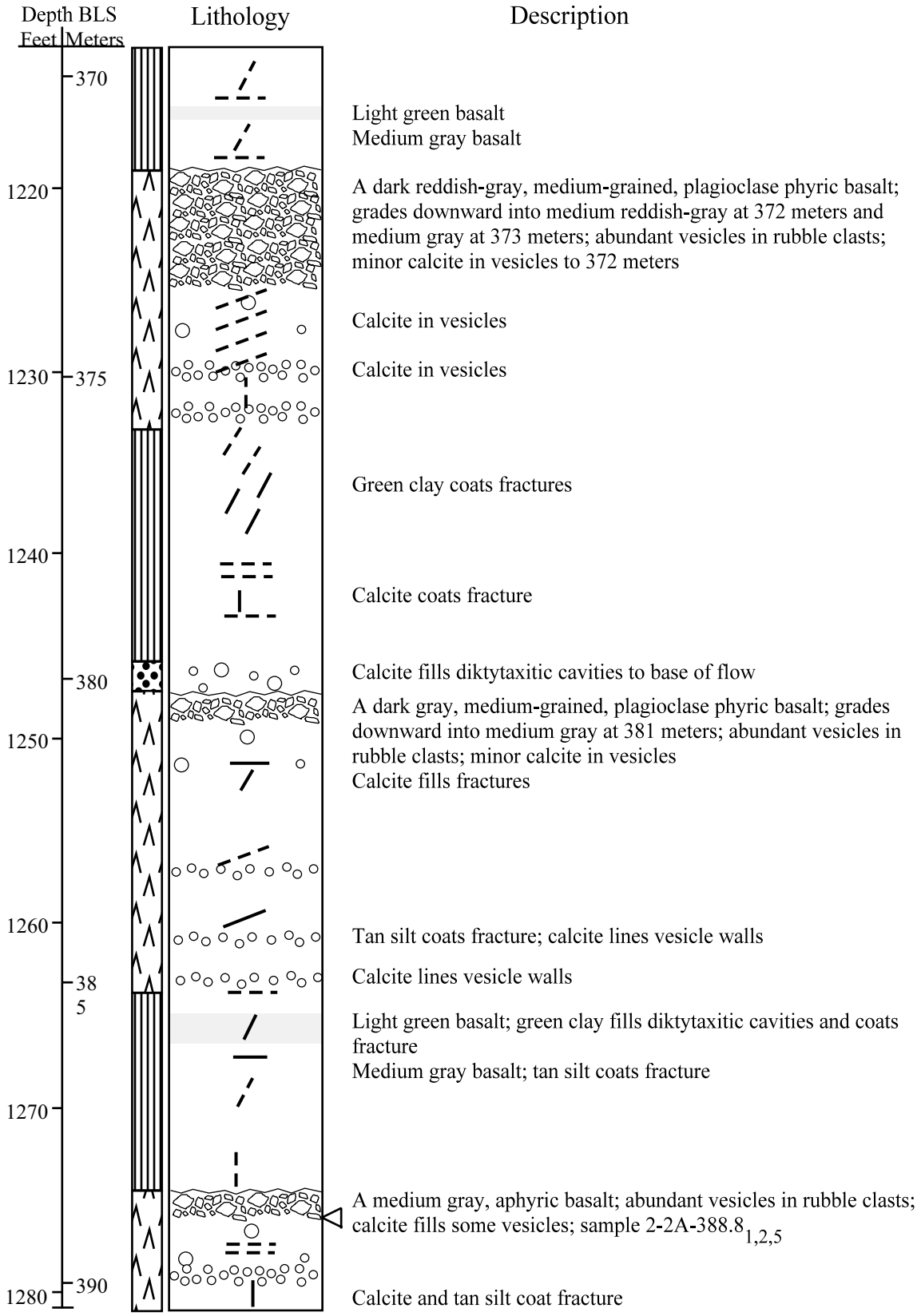
Depth BLS
Feet Meters
Lithology
Description
370
1220
1230
375
1240
380
1250
1260
38
5
1270
390
1280
Light green basalt
Medium gray basalt
A dark reddish-gray, medium-grained, plagioclase phyric basalt; grades downward into medium reddish-gray at 372 meters and medium gray at 373 meters; abundant vesicles in rubble clasts; minor calcite in vesicles to 372 meters
Calcite in vesicles
Calcite in vesicles
Green clay coats fractures
Calcite coats fracture
Calcite fills diktytaxitic cavities to base of flow
A dark gray, medium-grained, plagioclase phyric basalt; grades downward into medium gray at 381 meters; abundant vesicles in rubble clasts; minor calcite in vesicles
Calcite fills fractures
Tan silt coats fracture; calcite lines vesicle walls
Calcite lines vesicle walls
Light green basalt; green clay fills diktytaxitic cavities and coats fracture
Medium gray basalt; tan silt coats fracture
A medium gray, aphyric basalt; abundant vesicles in rubble clasts; calcite fills some vesicles; sample 2-2A-388.8 1,2,5
Calcite and tan silt coat fracture

Well 2-2A

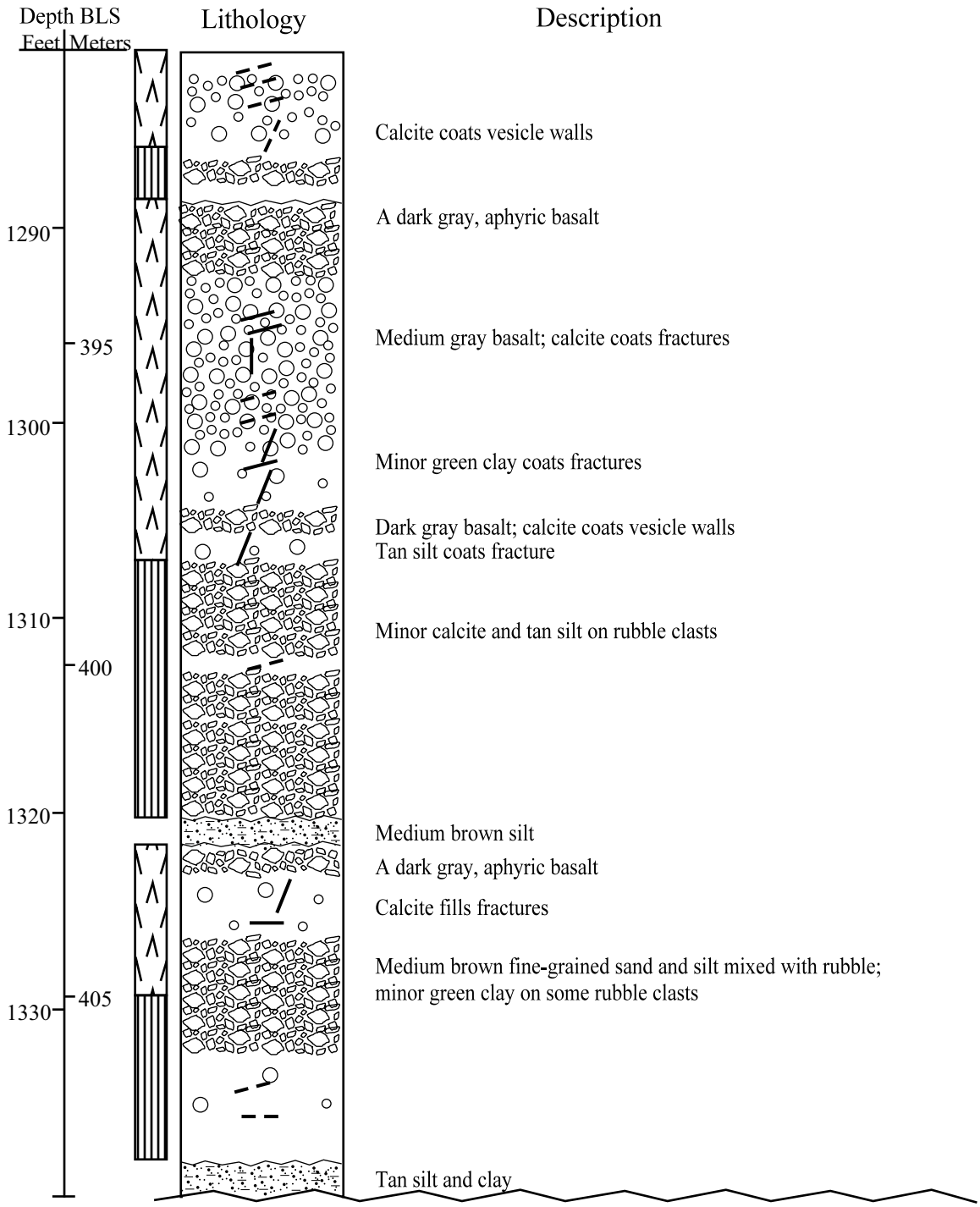
Depth BLS
Feet Meters
Lithology
Description
1290
395
1300
1310
400
1320
405
1330
Calcite coats vesicle walls
A dark gray, aphyric basalt
Medium gray basalt; calcite coats fractures
Minor green clay coats fractures
Dark gray basalt; calcite coats vesicle walls
Tan silt coats fracture
Minor calcite and tan silt on rubble clasts
Medium brown silt
A dark gray, aphyric basalt
Calcite fills fractures
Medium brown fine-grained sand and silt mixed with rubble;
minor green clay on some rubble clasts
Tan silt and clay

Well 2-2A

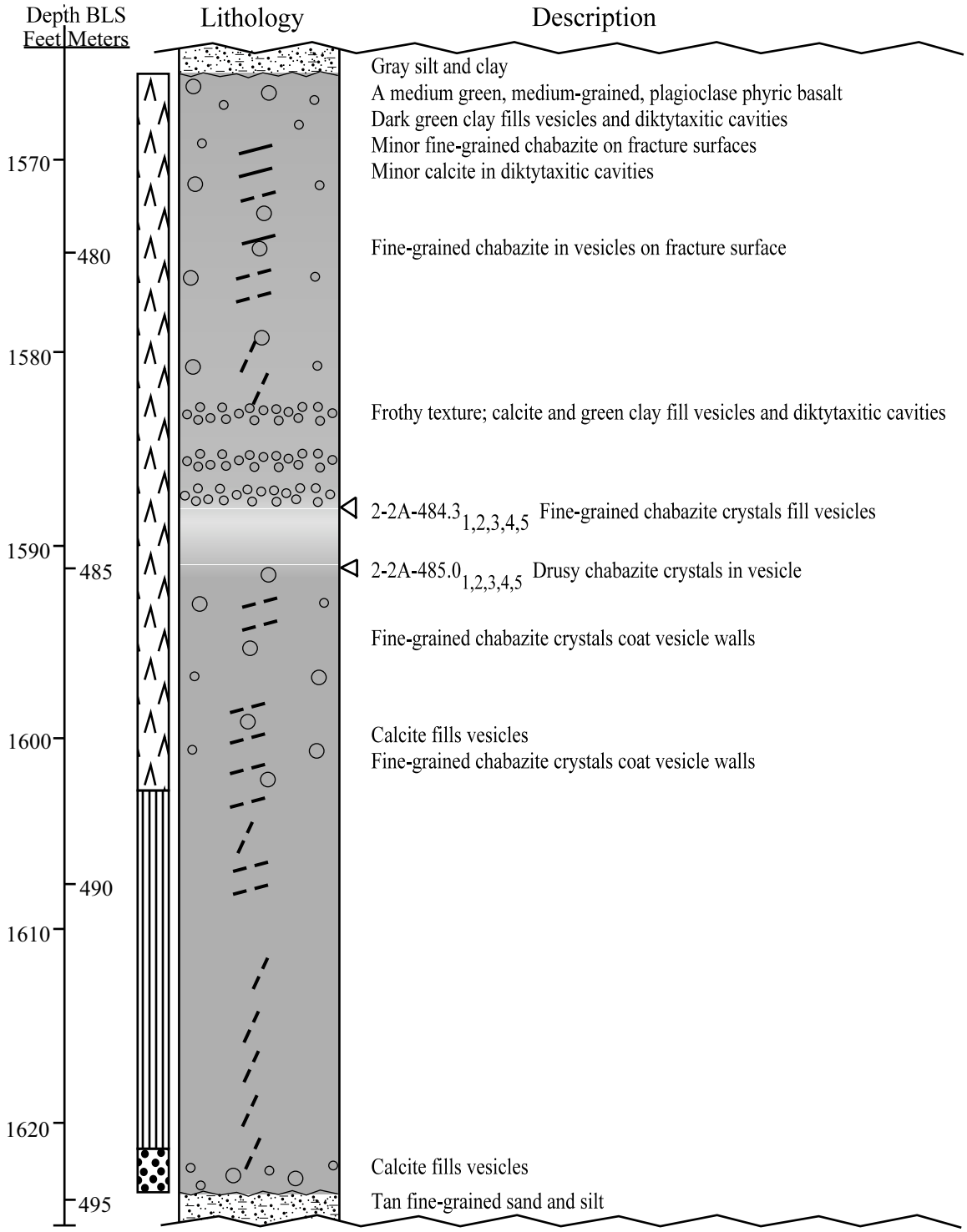
Depth BLS
Feet Meters
Lithology
Description
1570
480
1580
1590
485
1600
490
1610
1620
495
Gray silt and clay
A medium green, medium-grained, plagioclase phyric basalt
Dark green clay fills vesicles and diktytaxitic cavities
Minor fine-grained chabazite on fracture surfaces
Minor calcite in diktytaxitic cavities
Fine-grained chabazite in vesicles on fracture surface
Frothy texture; calcite and green clay fill vesicles and diktytaxitic cavities
2-2A-484.3 1,2,3,4,5 Fine-grained chabazite crystals fill vesicles
2-2A-485.0 1,2,3,4,5 Drusy chabazite crystals in vesicle
Fine-grained chabazite crystals coat vesicle walls
Calcite fills vesicles
Fine-grained chabazite crystals coat vesicle walls
Calcite fills vesicles
Tan fine-grained sand and silt

Well 2-2A

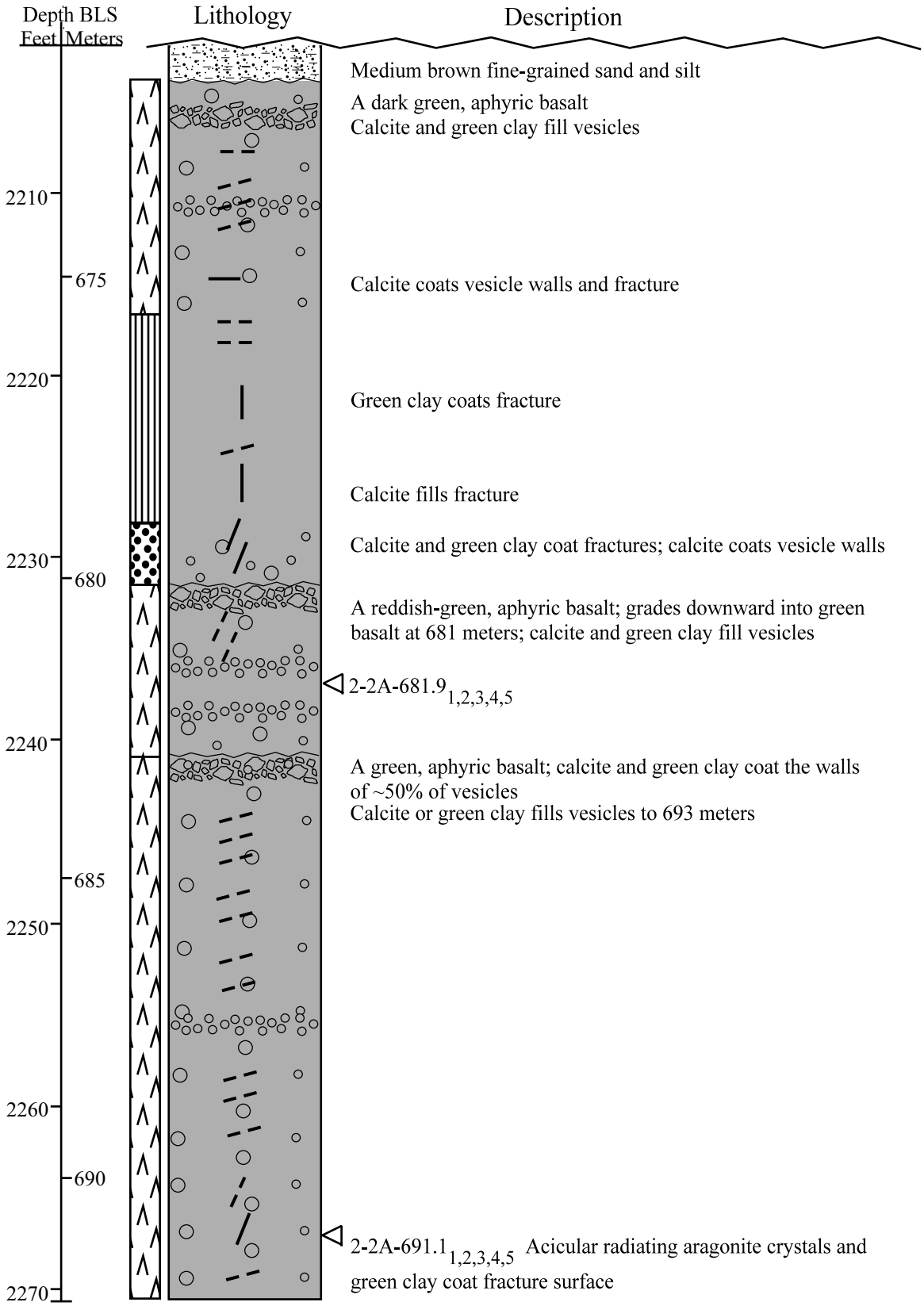
Depth BLS
Feet Meters
Lithology
Description
Medium brown fine-grained sand and silt
A dark green, aphyric basalt
Calcite and green clay fill vesicles
2210
675
Calcite coats vesicle walls and fracture
2220
Green clay coats fracture
Calcite fills fracture
Calcite and green clay coat fractures; calcite coats vesicle walls
2230
680
A reddish-green, aphyric basalt; grades downward into green basalt at 681 meters; calcite and green clay fill vesicles
2-2A-681.9 1,2,3,4,5
2240
A green, aphyric basalt; calcite and green clay coat the walls of ~50% of vesicles
Calcite or green clay fills vesicles to 693 meters
685
2250
2260
690
2-2A-691.1 1,2,3,4,5 Acicular radiating aragonite crystals and green clay coat fracture surface
2270

Well 2-2A

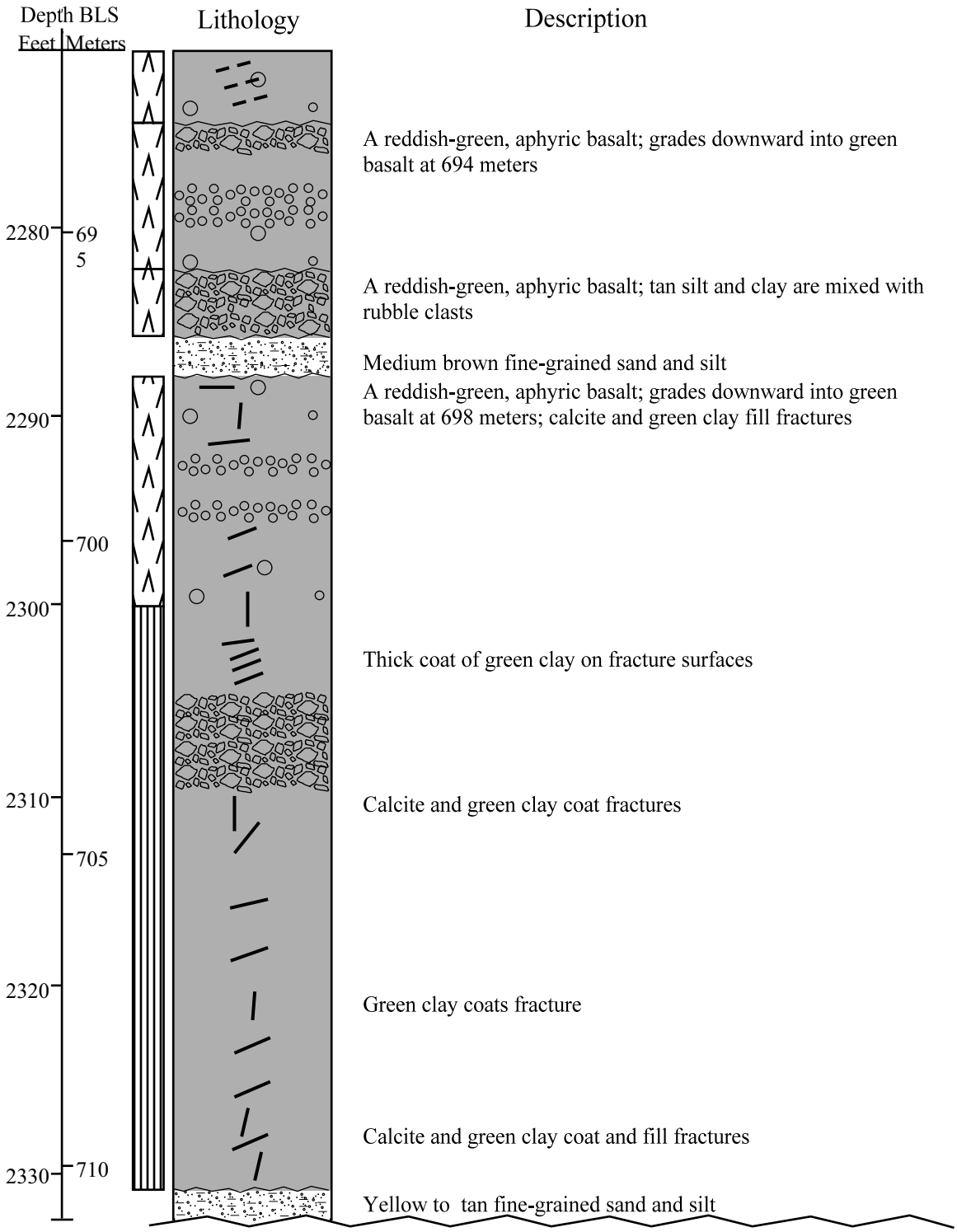
Depth BLS
Feet Meters
Lithology
Description
2280
69
5
2290
700
2300
2310
705
2320
2330
710
A reddish-green, aphyric basalt; grades downward into green basalt at 694 meters
A reddish-green, aphyric basalt; tan silt and clay are mixed with rubble clasts
Medium brown fine-grained sand and silt
A reddish-green, aphyric basalt; grades downward into green basalt at 698 meters; calcite and green clay fill fractures
Thick coat of green clay on fracture surfaces
Calcite and green clay coat fractures
Green clay coats fracture
Calcite and green clay coat and fill fractures
Yellow to tan fine-grained sand and silt

Well WO2

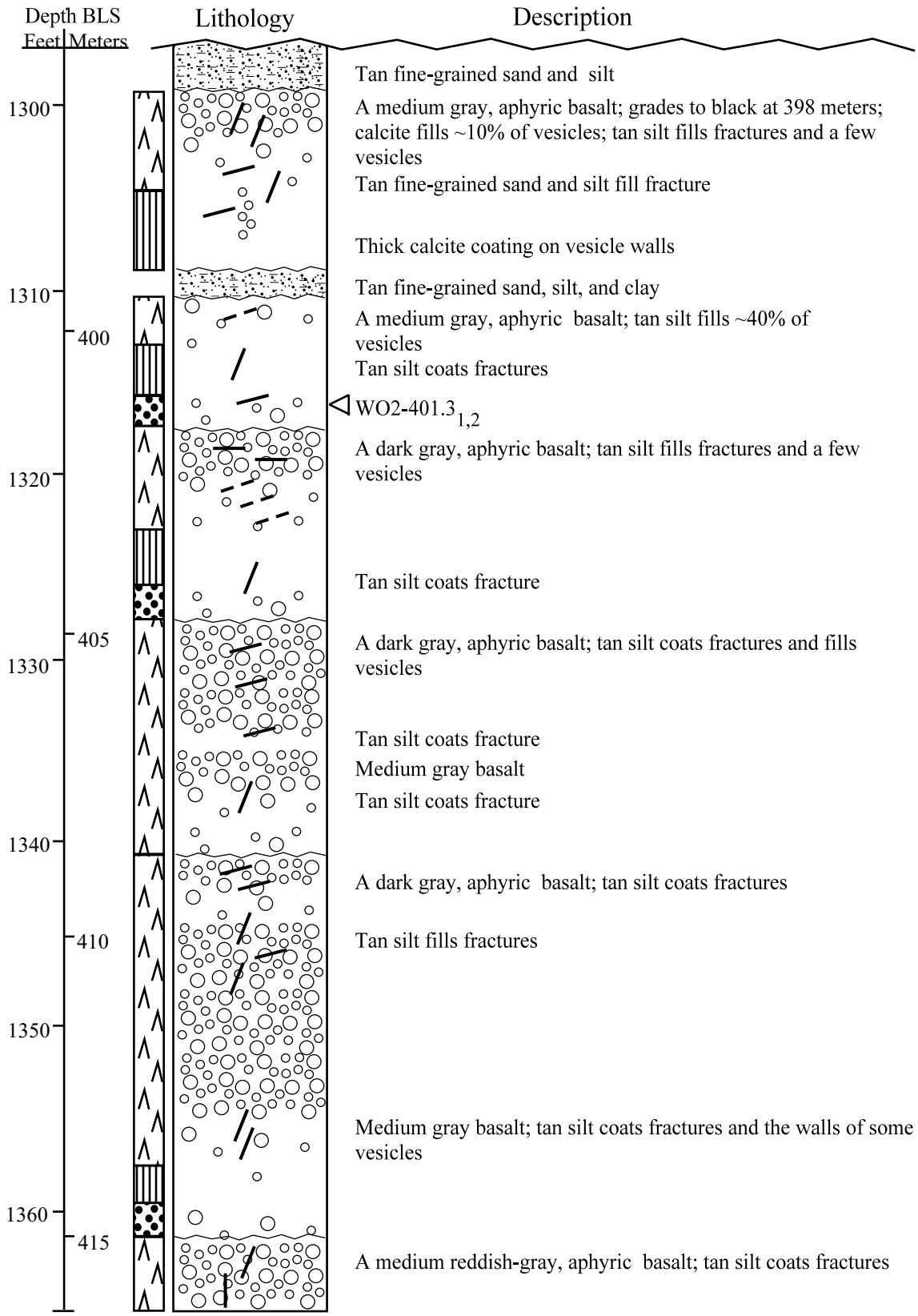
Depth BLS
Feet Meters
Lithology
Description
1300
1310
400
1320
405
1330
1340
410
1350
1360
415
Tan fine-grained sand and silt
A medium gray, aphyric basalt; grades to black at 398 meters; calcite fills ~10% of vesicles; tan silt fills fractures and a few vesicles
Tan fine-grained sand and silt fill fracture
Thick calcite coating on vesicle walls
Tan fine-grained sand, silt, and clay
A medium gray, aphyric basalt; tan silt fills ~40% of vesicles
Tan silt coats fractures
WO2-401.3 1,2
A dark gray, aphyric basalt; tan silt fills fractures and a few vesicles
Tan silt coats fracture
A dark gray, aphyric basalt; tan silt coats fractures and fills vesicles
Tan silt coats fracture
Medium gray basalt
Tan silt coats fracture
A dark gray, aphyric basalt; tan silt coats fractures
Tan silt fills fractures
Medium gray basalt; tan silt coats fractures and the walls of some vesicles
A medium reddish-gray, aphyric basalt; tan silt coats fractures

Well WO2

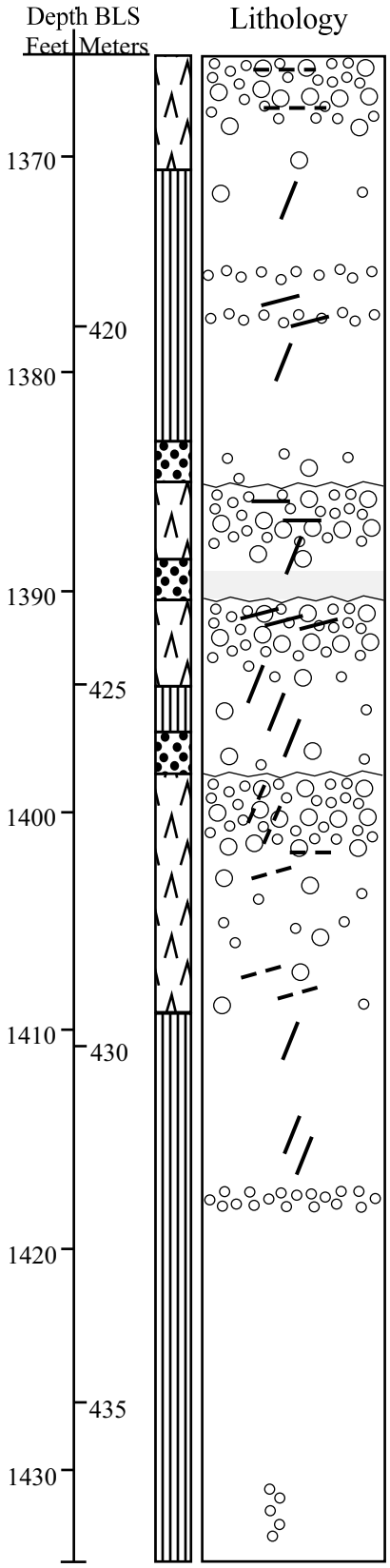

Description

Medium gray basalt

Minor calcite coats vesicle walls

Tan silt coats fracture

Tan silt coats fractures

Dark gray basalt
A dark reddish-gray, medium-grained, plagioclase phyric basalt; tan silt fills fractures and ~10% of vesicles

Light green basalt
A dark gray, medium-grained, plagioclase phyric basalt; tan silt coats fractures

A dark gray, medium-grained, plagioclase phyric basalt; grades downward to medium gray at 428 meters

Minor tan silt in vesicles

Tan silt coats fracture

Tan silt coats fractures

Well WO2

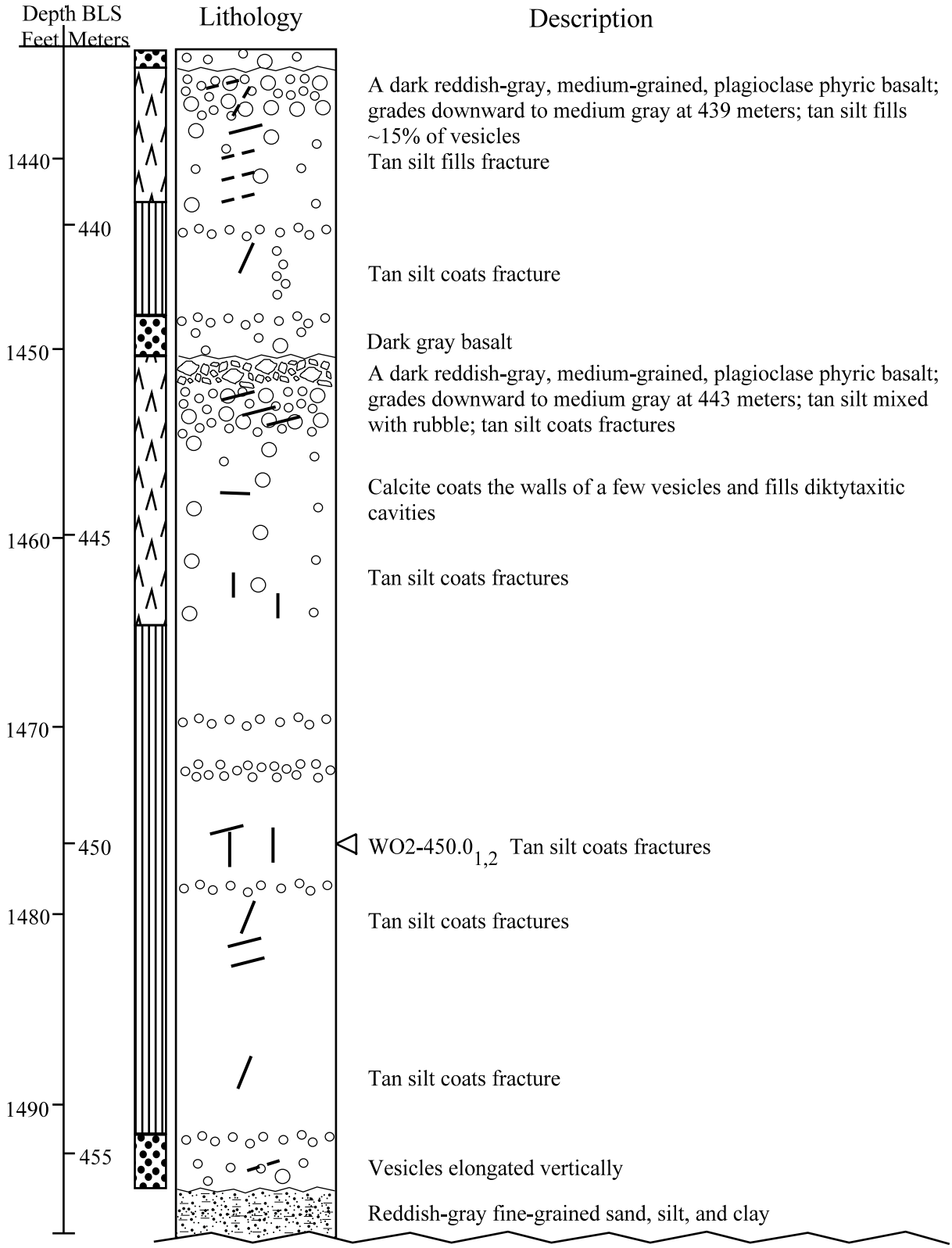
Depth BLS
Feet Meters
Lithology
Description
1440
440
1450
445
1460
1470
450
1480
1490
455
A dark reddish-gray, medium-grained, plagioclase phyric basalt; grades downward to medium gray at 439 meters; tan silt fills ~15% of vesicles
Tan silt fills fracture
Tan silt coats fracture
Dark gray basalt
A dark reddish-gray, medium-grained, plagioclase phyric basalt; grades downward to medium gray at 443 meters; tan silt mixed with rubble; tan silt coats fractures
Calcite coats the walls of a few vesicles and fills diktytaxitic cavities
Tan silt coats fractures
WO2-450.0 1,2 Tan silt coats fractures
Tan silt coats fractures
Tan silt coats fracture
Vesicles elongated vertically
Reddish-gray fine-grained sand, silt, and clay

Well WO2

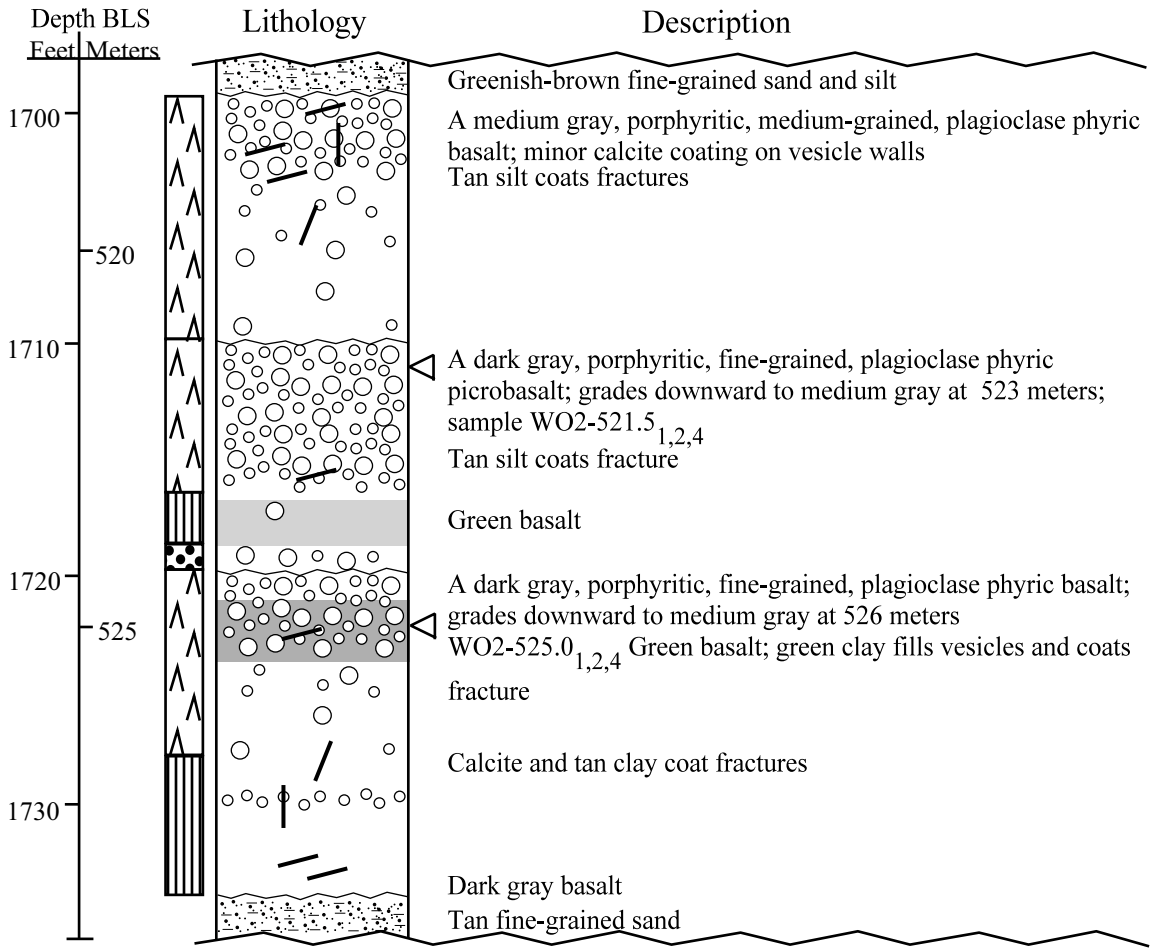
Depth BLS
Feet Meters
Lithology
Description
1700
520
1710
1720
525
1730
Greenish-brown fine-grained sand and silt
A medium gray, porphyritic, medium-grained, plagioclase phyric basalt; minor calcite coating on vesicle walls
Tan silt coats fractures
A dark gray, porphyritic, fine-grained, plagioclase phyric picrobasalt; grades downward to medium gray at 523 meters; sample WO2-521.5 1,2,4
Tan silt coats fracture
Green basalt
A dark gray, porphyritic, fine-grained, plagioclase phyric basalt; grades downward to medium gray at 526 meters
WO2-525.0 1,2,4 Green basalt; green clay fills vesicles and coats fracture
Calcite and tan clay coat fractures
Dark gray basalt
Tan fine-grained sand

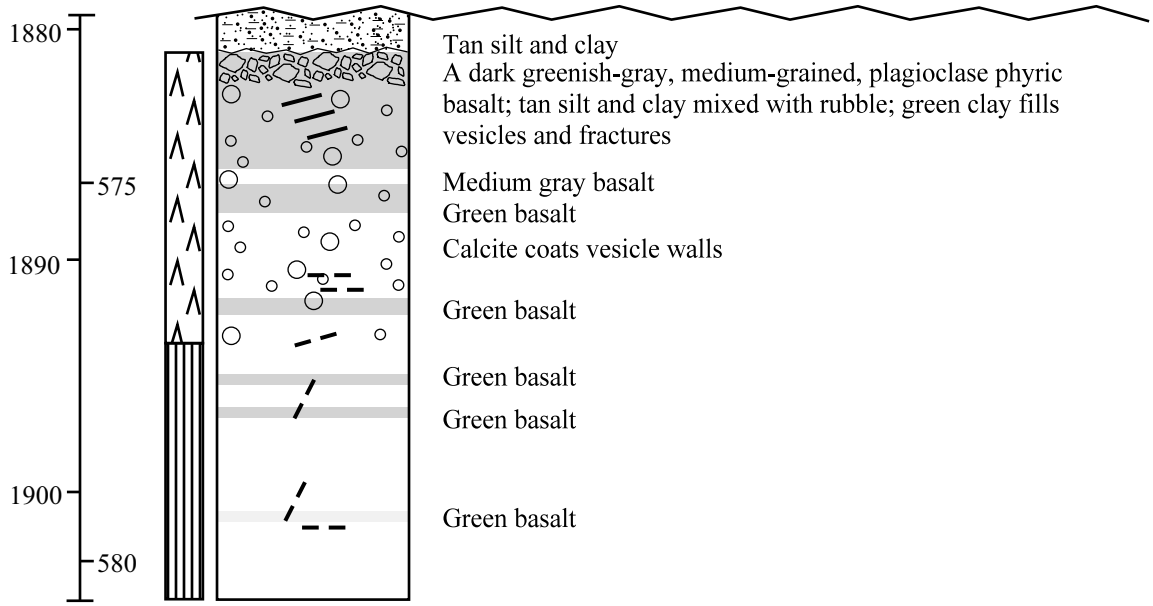
1880
575
1890
1900
580
Tan silt and clay
A dark greenish-gray, medium-grained, plagioclase phyric basalt; tan silt and clay mixed with rubble; green clay fills vesicles and fractures
Medium gray basalt
Green basalt
Calcite coats vesicle walls
Green basalt
Green basalt
Green basalt
Green basalt

Well WO2

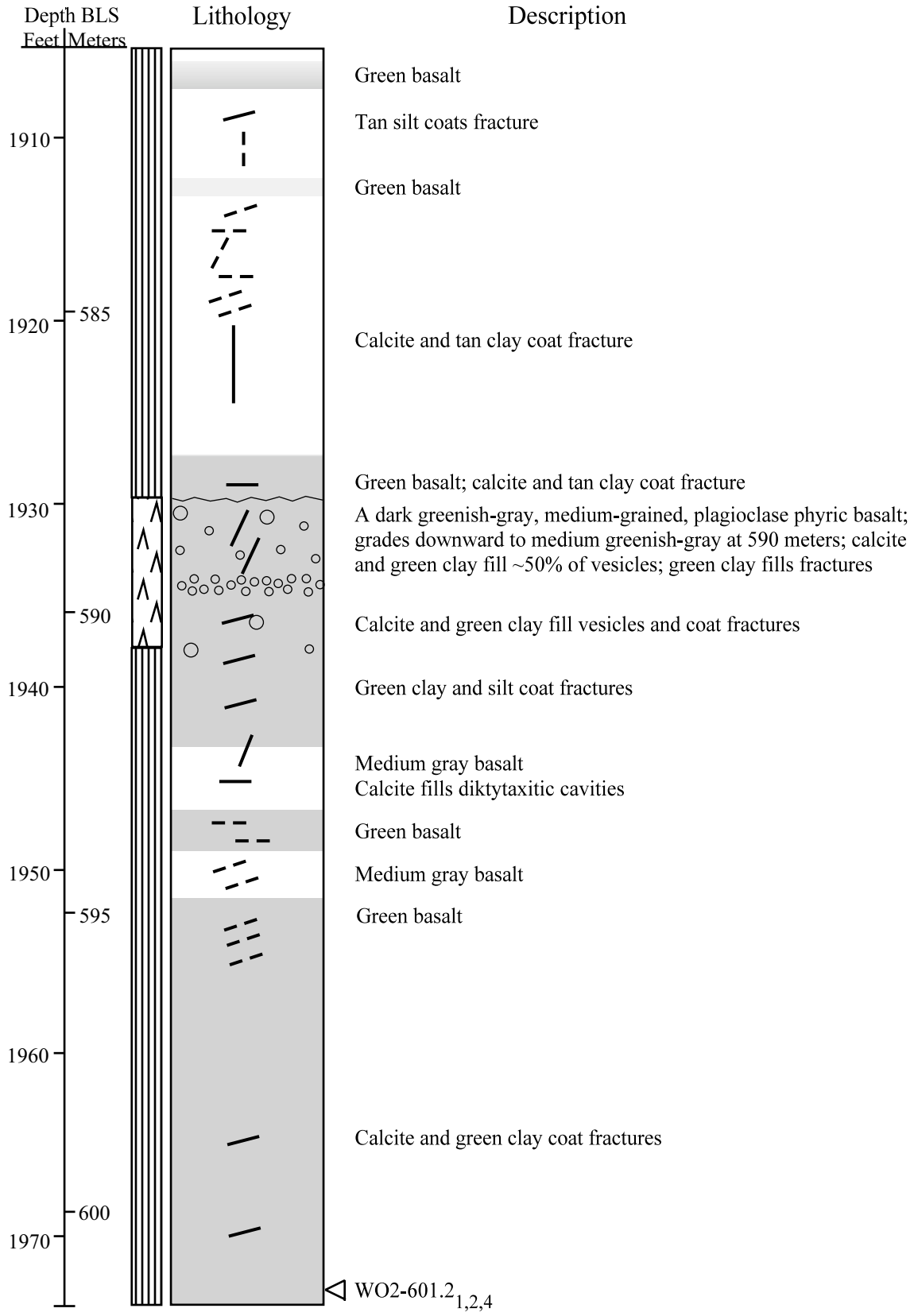
Depth BLS
Feet Meters
Lithology
Description
1910
1920
585
1930
590
1940
1950
595
1960
600
1970
Green basalt
Tan silt coats fracture
Green basalt
Calcite and tan clay coat fracture
Green basalt; calcite and tan clay coat fracture
A dark greenish-gray, medium-grained, plagioclase phyric basalt; grades downward to medium greenish-gray at 590 meters; calcite and green clay fill ~50% of vesicles; green clay fills fractures
Calcite and green clay fill vesicles and coat fractures
Green clay and silt coat fractures
Medium gray basalt
Calcite fills diktytaxitic cavities
Green basalt
Medium gray basalt
Green basalt
Calcite and green clay coat fractures
WO2-601.2 1,2,4

Well WO2

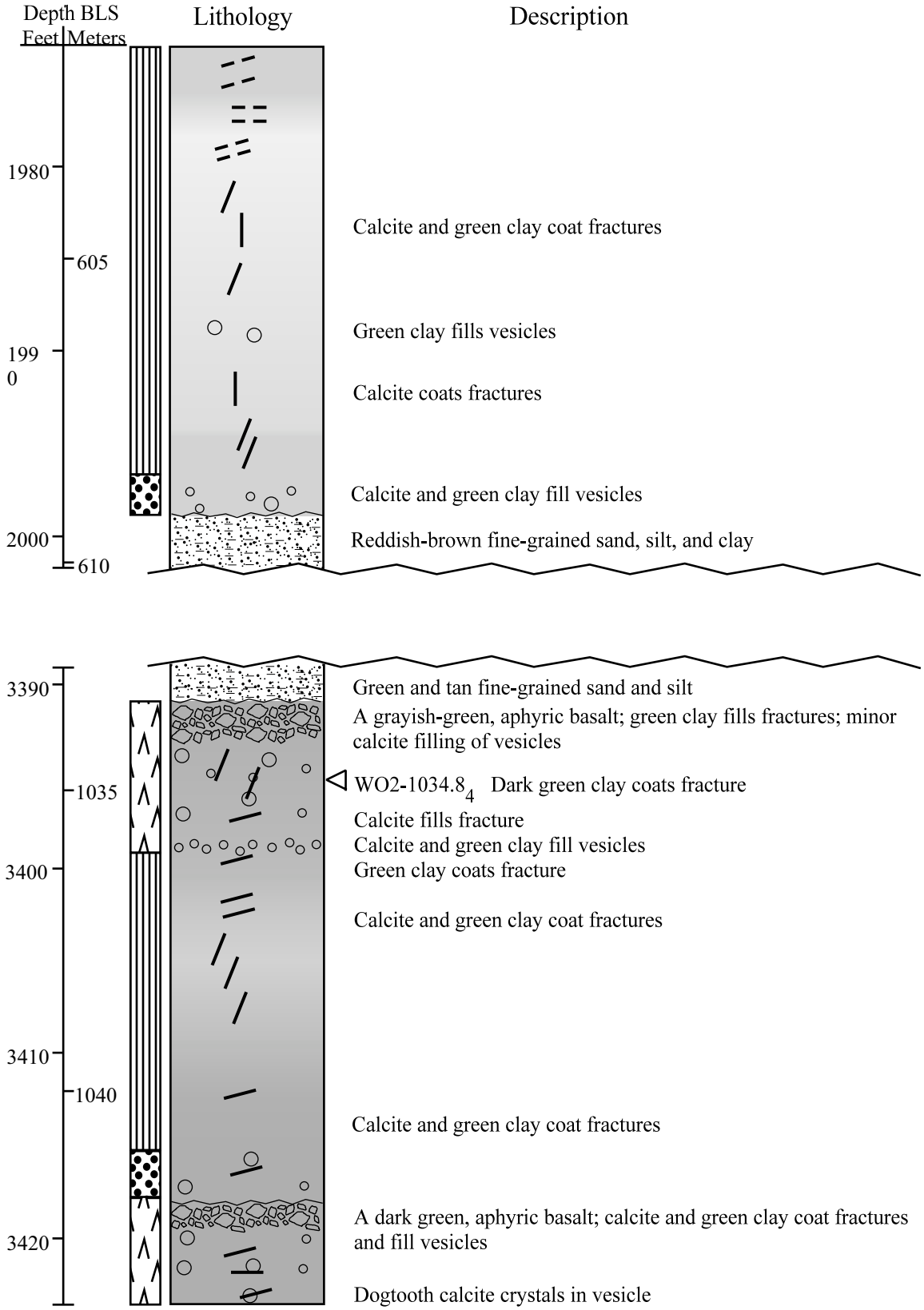
Depth BLS
Feet Meters
Lithology
Description
1980
605
199
0
2000
610
Calcite and green clay coat fractures
Green clay fills vesicles
Calcite coats fractures
Calcite and green clay fill vesicles
Reddish-brown fine-grained sand, silt, and clay
3390
1035
3400
3410
1040
3420
Green and tan fine-grained sand and silt
A grayish-green, aphyric basalt; green clay fills fractures; minor calcite filling of vesicles
WO2-1034.8 4 Dark green clay coats fracture
Calcite fills fracture
Calcite and green clay fill vesicles
Green clay coats fracture
Calcite and green clay coat fractures
Calcite and green clay coat fractures
A dark green, aphyric basalt; calcite and green clay coat fractures and fill vesicles
Dogtooth calcite crystals in vesicle

Well WO2

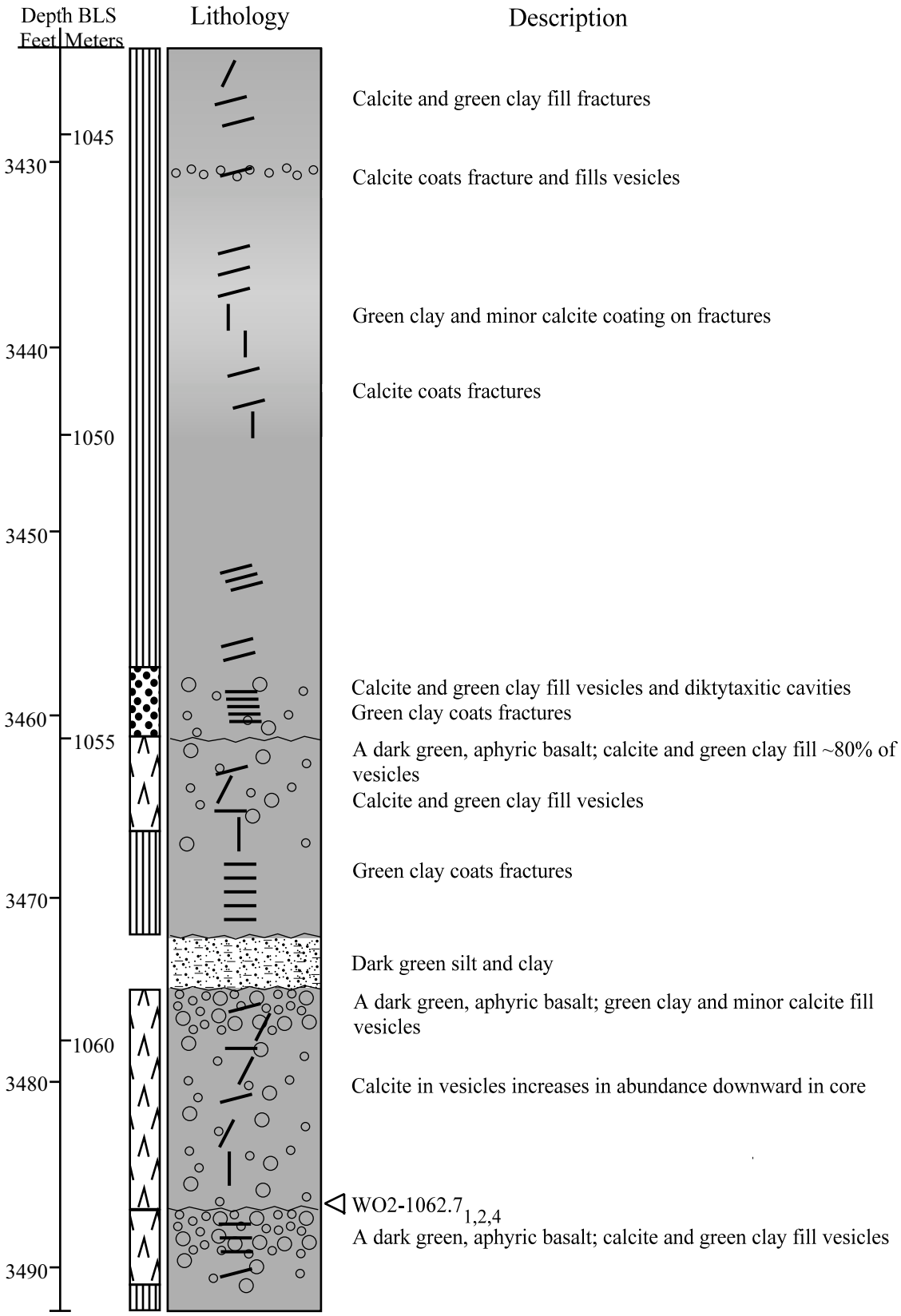
Depth BLS
Feet Meters
Lithology
Description
1045
3430
1050
3440
3450
1055
3460
3470
1060
3480
3490
Calcite and green clay fill fractures
Calcite coats fracture and fills vesicles
Green clay and minor calcite coating on fractures
Calcite coats fractures
Calcite and green clay fill vesicles and diktytaxitic cavities
Green clay coats fractures
A dark green, aphyric basalt; calcite and green clay fill ~80% of vesicles
Calcite and green clay fill vesicles
Green clay coats fractures
Dark green silt and clay
A dark green, aphyric basalt; green clay and minor calcite fill vesicles
Calcite in vesicles increases in abundance downward in core
WO2-1062.7 1,2,4
A dark green, aphyric basalt; calcite and green clay fill vesicles

Well WO2

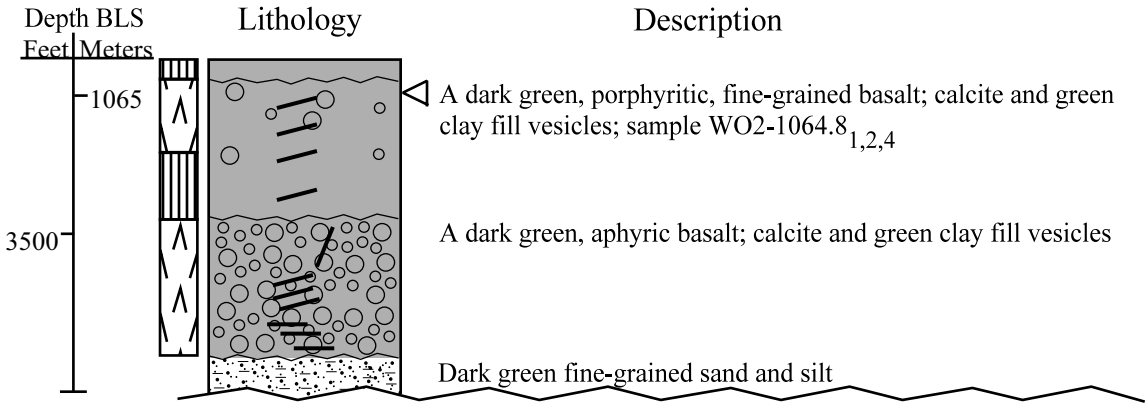
Depth BLS
Feet Meters
Lithology
Description
1065
3500
A dark green, porphyritic, fine-grained basalt; calcite and green clay fill vesicles; sample WO2-1064.8 1,2,4
A dark green, aphyric basalt; calcite and green clay fill vesicles
Dark green fine-grained sand and silt

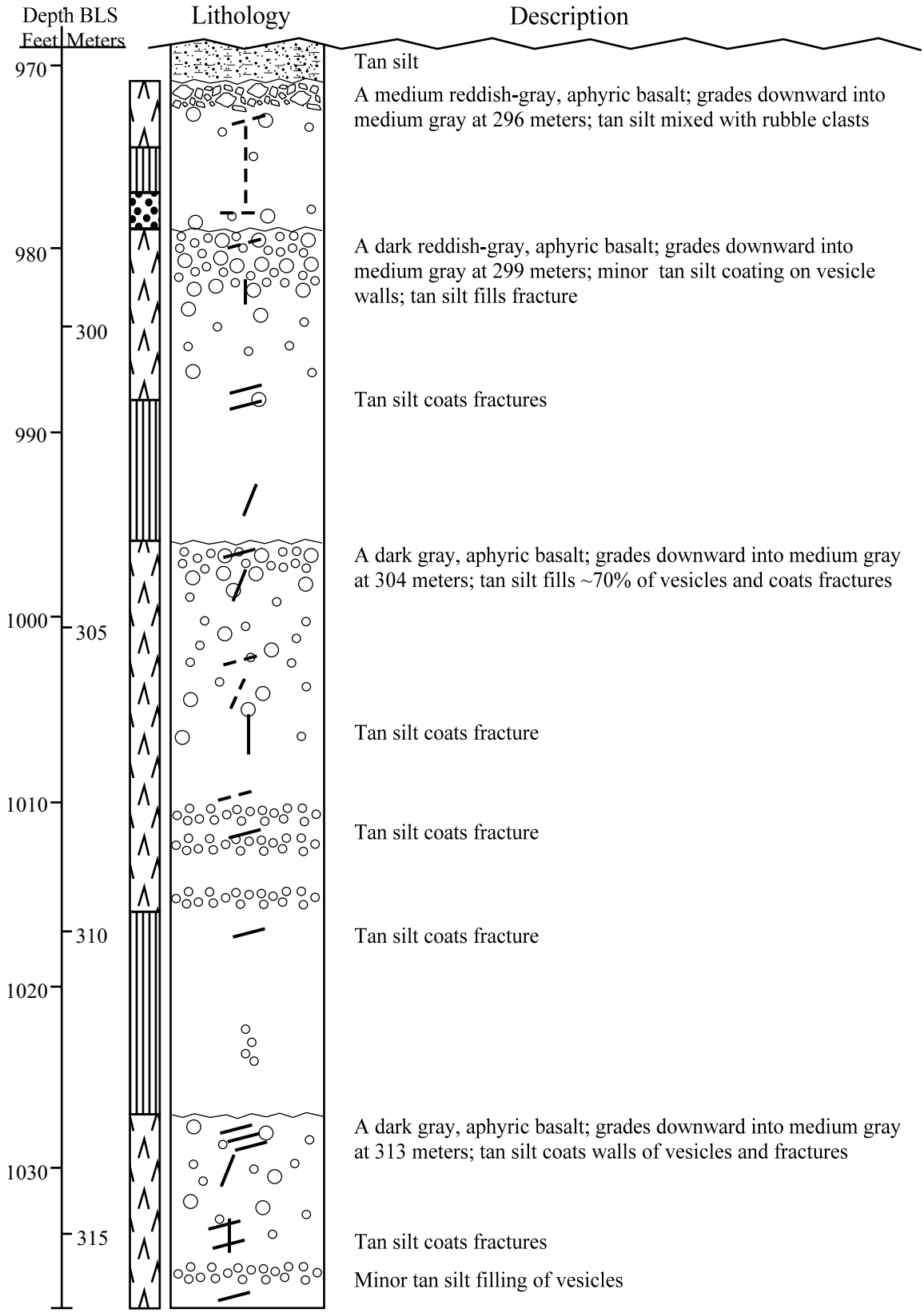
Depth BLS
Feet Meters
Lithology
Description
970
980
990
1000
1010
1020
1030
300
305
310
315
Tan silt
A medium reddish-gray, aphyric basalt; grades downward into medium gray at 296 meters; tan silt mixed with rubble clasts
A dark reddish-gray, aphyric basalt; grades downward into medium gray at 299 meters; minor tan silt coating on vesicle walls; tan silt fills fracture
Tan silt coats fractures
A dark gray, aphyric basalt; grades downward into medium gray at 304 meters; tan silt fills ~70% of vesicles and coats fractures
Tan silt coats fracture
Tan silt coats fracture
Tan silt coats fracture
A dark gray, aphyric basalt; grades downward into medium gray at 313 meters; tan silt coats walls of vesicles and fractures
Tan silt coats fractures
Minor tan silt filling of vesicles

Well C1A

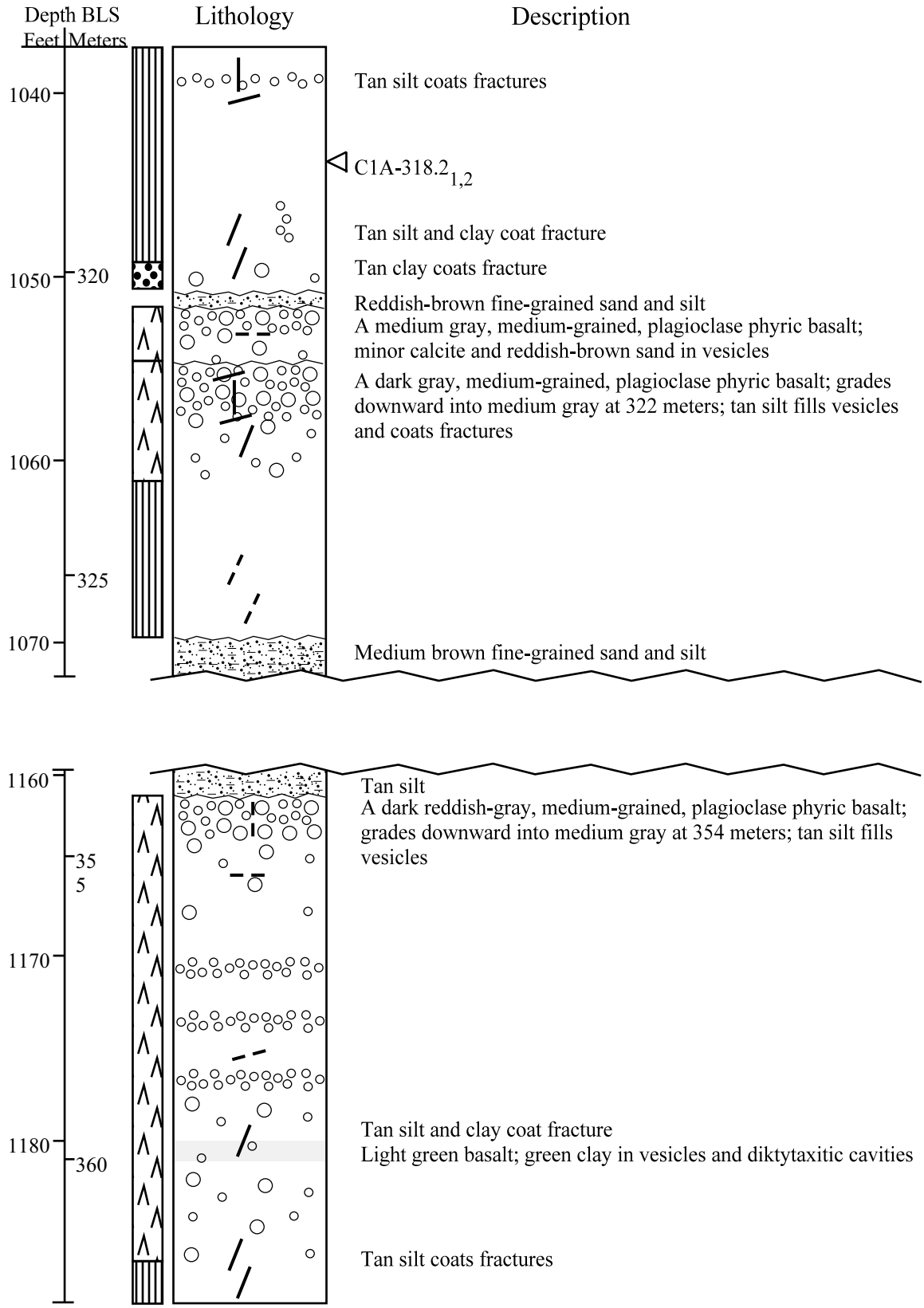
Depth BLS
Feet Meters
Lithology
Description
1040
1050
320
1060
325
1070
Tan silt coats fractures
C1A-318.2 1,2
Tan silt and clay coat fracture
Tan clay coats fracture
Reddish-brown fine-grained sand and silt
A medium gray, medium-grained, plagioclase phyric basalt; minor calcite and reddish-brown sand in vesicles
A dark gray, medium-grained, plagioclase phyric basalt; grades downward into medium gray at 322 meters; tan silt fills vesicles and coats fractures
Medium brown fine-grained sand and silt
1160
35
5
1170
1180
360
Tan silt
A dark reddish-gray, medium-grained, plagioclase phyric basalt; grades downward into medium gray at 354 meters; tan silt fills vesicles
Tan silt and clay coat fracture
Light green basalt; green clay in vesicles and diktytaxitic cavities
Tan silt coats fractures

Well C1A

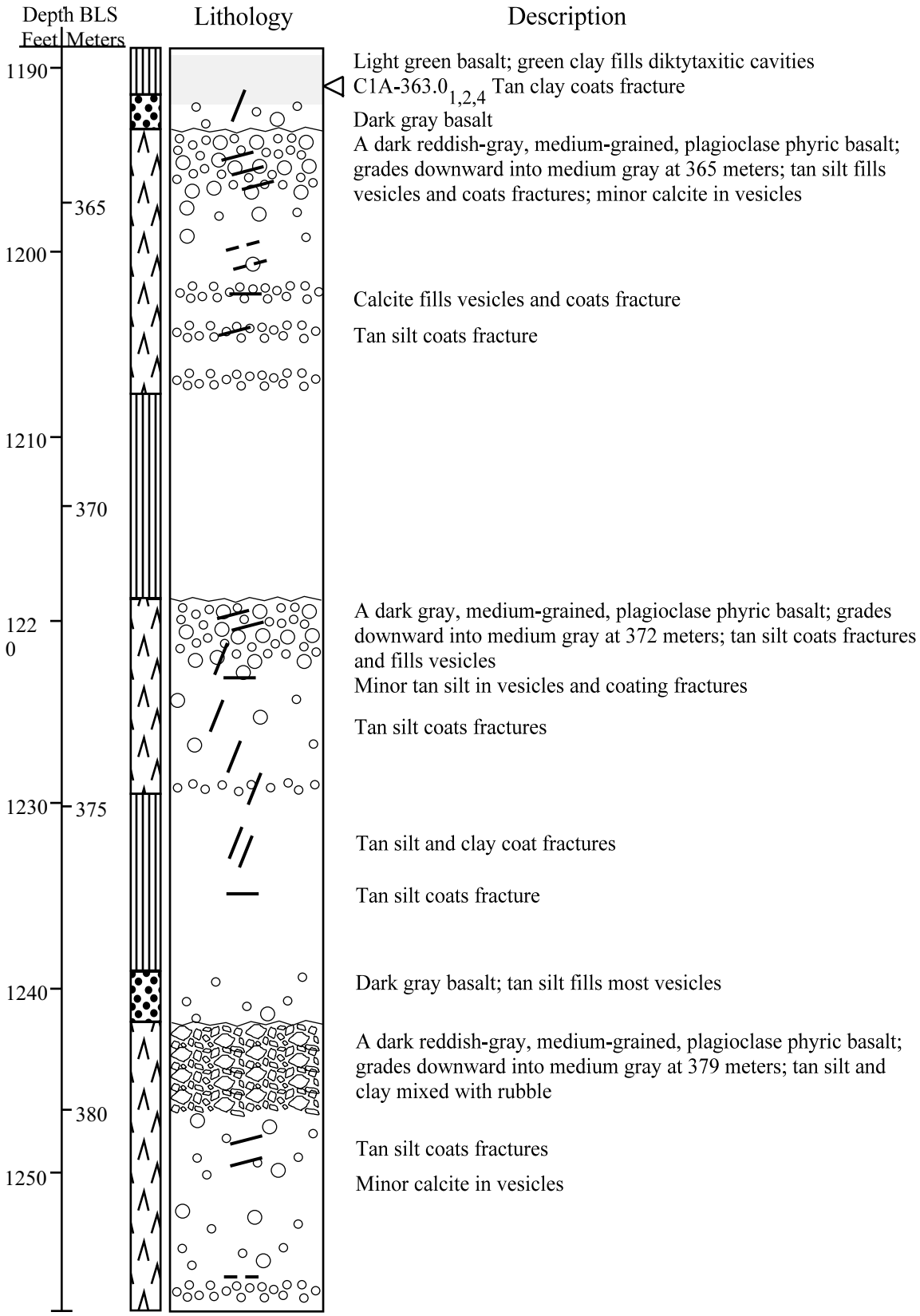
Depth BLS
Feet
Meters
Lithology
Description
1190
365
1200
1210
370
122
0
1230
375
1240
380
1250
Light green basalt; green clay fills diktytaxitic cavities
C1A-363.0 1,2,4 Tan clay coats fracture
Dark gray basalt
A dark reddish-gray, medium-grained, plagioclase phyric basalt; grades downward into medium gray at 365 meters; tan silt fills vesicles and coats fractures; minor calcite in vesicles
Calcite fills vesicles and coats fracture
Tan silt coats fracture
A dark gray, medium-grained, plagioclase phyric basalt; grades downward into medium gray at 372 meters; tan silt coats fractures and fills vesicles
Minor tan silt in vesicles and coating fractures
Tan silt coats fractures
Tan silt and clay coat fractures
Tan silt coats fracture
Dark gray basalt; tan silt fills most vesicles
A dark reddish-gray, medium-grained, plagioclase phyric basalt; grades downward into medium gray at 379 meters; tan silt and clay mixed with rubble
Tan silt coats fractures
Minor calcite in vesicles

Well C1A

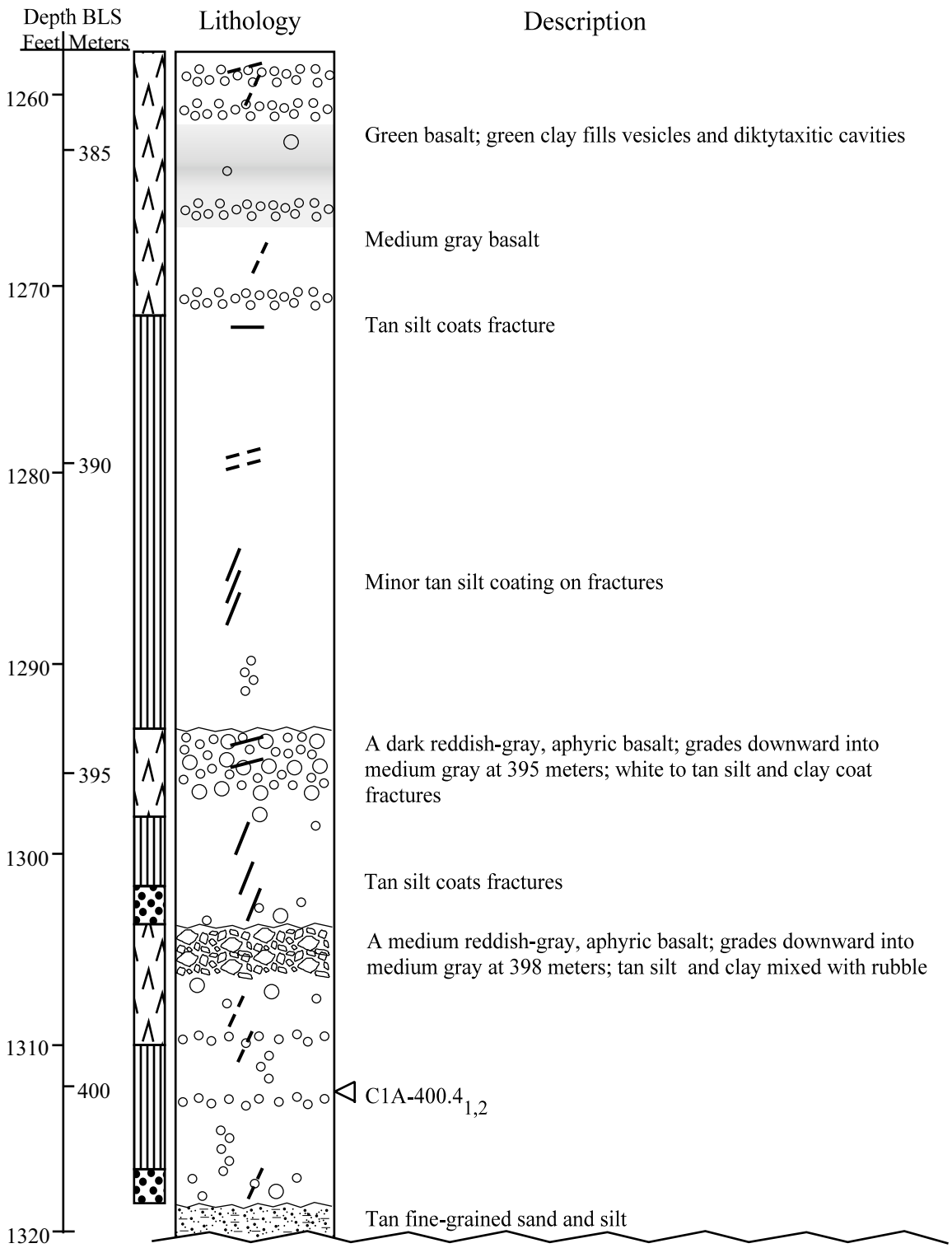
Depth BLS
Feet Meters
Lithology
Description
1260
385
1270
1280
390
1290
395
1300
1310
400
1320
Green basalt; green clay fills vesicles and diktytaxitic cavities
Medium gray basalt
Tan silt coats fracture
Minor tan silt coating on fractures
A dark reddish-gray, aphyric basalt; grades downward into medium gray at 395 meters; white to tan silt and clay coat fractures
Tan silt coats fractures
A medium reddish-gray, aphyric basalt; grades downward into medium gray at 398 meters; tan silt and clay mixed with rubble
C1A-400.4 1,2
Tan fine-grained sand and silt

Well C1A

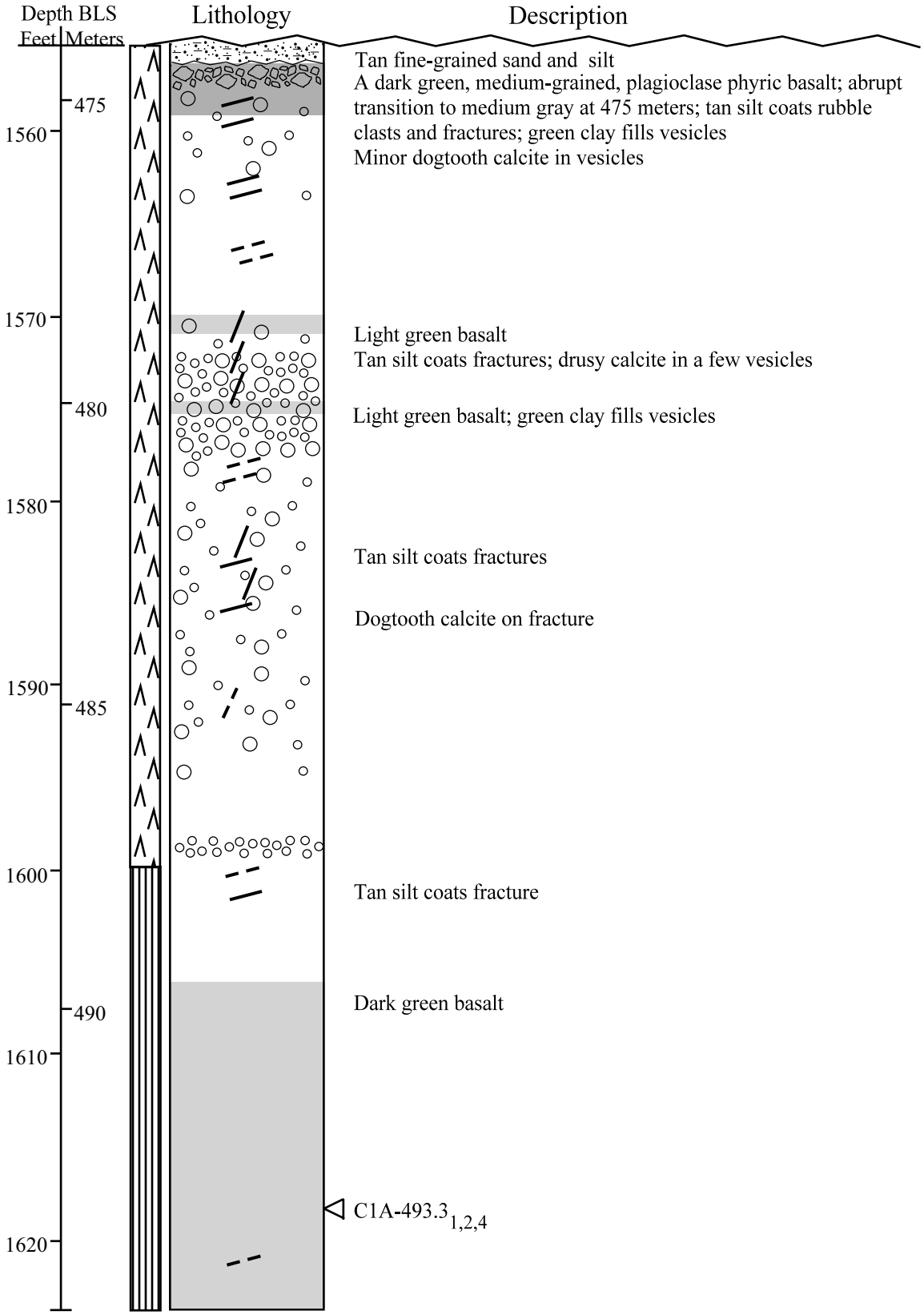
Depth BLS
Feet Meters
Lithology
Description
475
1560
1570
480
1580
1590
485
1600
490
1610
1620
Tan fine-grained sand and silt
A dark green, medium-grained, plagioclase phyric basalt; abrupt transition to medium gray at 475 meters; tan silt coats rubble clasts and fractures; green clay fills vesicles
Minor dogtooth calcite in vesicles
Light green basalt
Tan silt coats fractures; drusy calcite in a few vesicles
Light green basalt; green clay fills vesicles
Tan silt coats fractures
Dogtooth calcite on fracture
Tan silt coats fracture
Dark green basalt
C1A-493.3 1,2,4

Well C1A

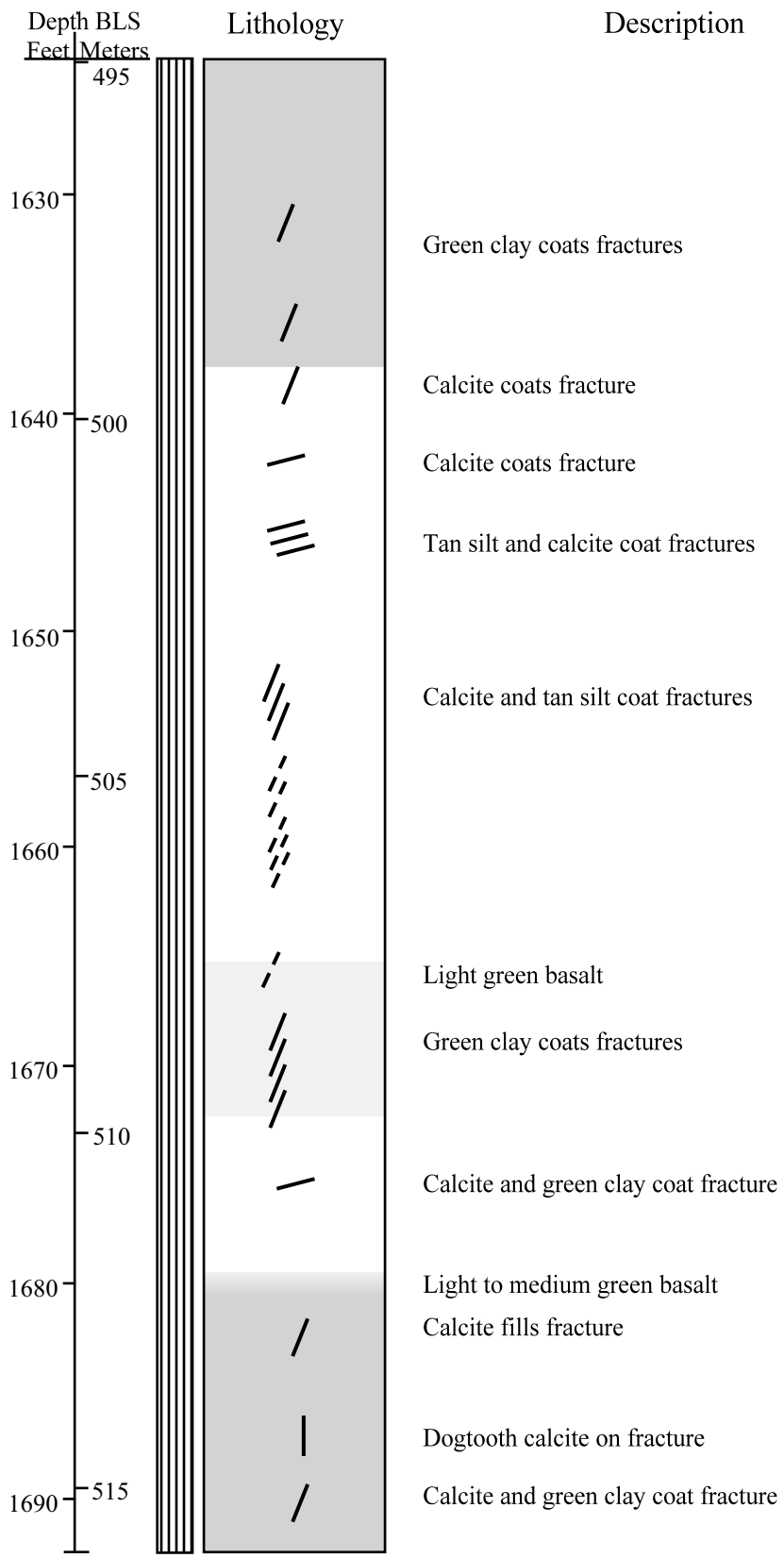
Depth BLS
Feet Meters
Lithology
Description
495
1630
Green clay coats fractures
Calcite coats fracture
1640
500
Calcite coats fracture
Tan silt and calcite coat fractures
1650
Calcite and tan silt coat fractures
505
1660
Light green basalt
Green clay coats fractures
1670
510
Calcite and green clay coat fracture
1680
Light to medium green basalt
Calcite fills fracture
Dogtooth calcite on fracture
1690
515
Calcite and green clay coat fracture

Well C1A

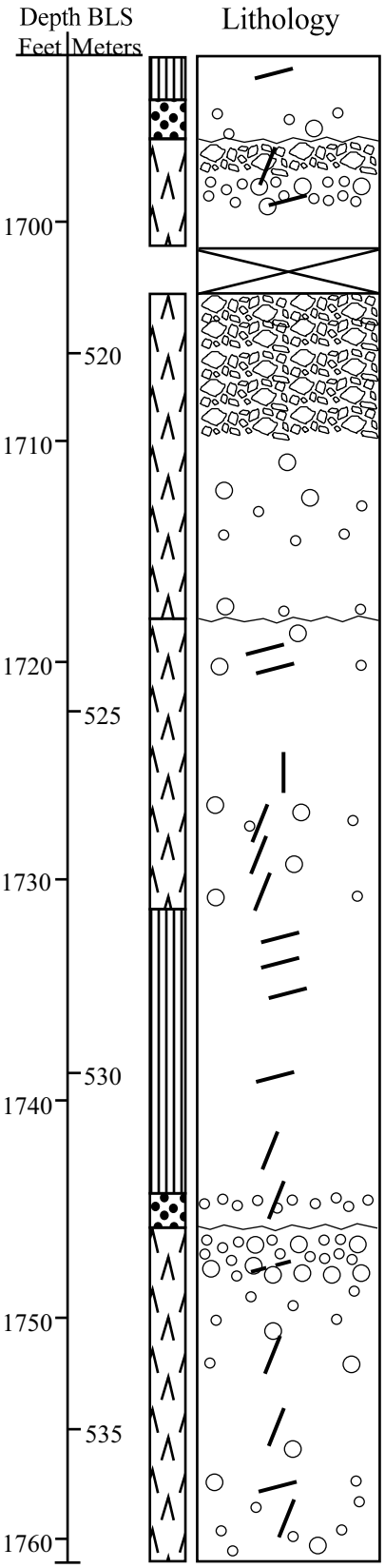

Description

Green clay coats fracture

Minor calcite in vesicles

A dark reddish-gray, medium-grained, plagioclase phyric basalt; minor calcite and tan silt coating on fractures

Missing core

A medium reddish-gray, medium-grained, plagioclase phyric basalt; grades downward into medium gray at 520 meters; minor calcite in vesicles; fine-grained sand and silt mixed with rubble clasts; rhombohedral calcite in vesicle

Minor calcite filling of diktytaxitic cavities and vesicles

Minor calcite in vesicles.

A medium reddish-gray, medium-grained, plagioclase phyric basalt; grades downward into medium gray at 524 meters; calcite and tan silt coat fractures

Calcite fills fracture

Tan silt coats fractures

Calcite and tan clay coat fractures

Tan silt coats fractures

A dark gray, aphyric basalt; grades downward into medium gray at 533 meters; calcite and tan silt and clay in vesicles

Tan silt coats fractures

Minor calcite in vesicles
Tan silt and clay coat fractures

Well C1A

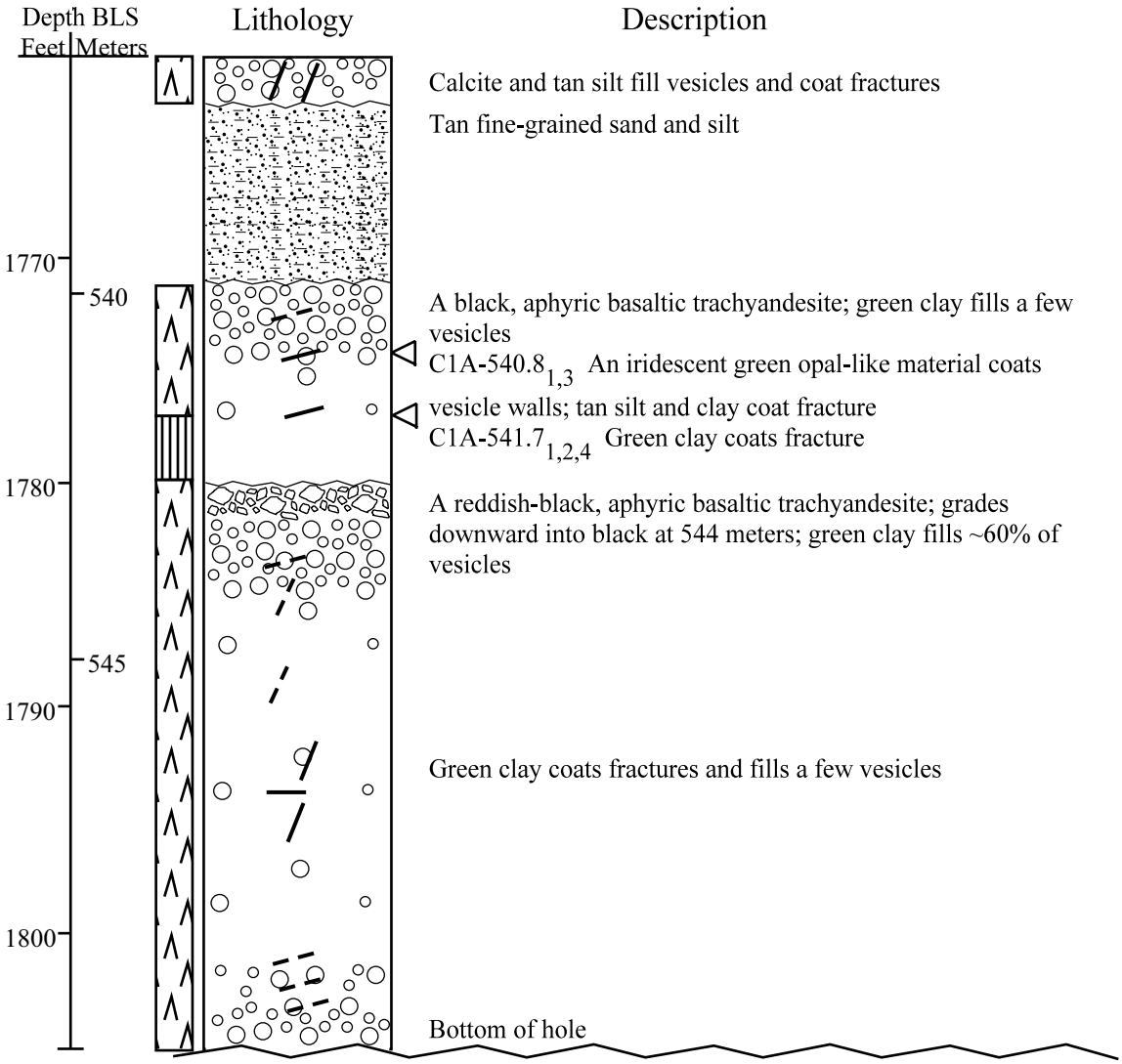
Depth BLS
Feet Meters
Lithology
Description
1770
540
1780
545
1790
1800
Calcite and tan silt fill vesicles and coat fractures
Tan fine-grained sand and silt
A black, aphyric basaltic trachyandesite; green clay fills a few vesicles
C1A-540.8 1,3 An iridescent green opal-like material coats vesicle walls; tan silt and clay coat fracture
C1A-541.7 1,2,4 Green clay coats fracture
A reddish-black, aphyric basaltic trachyandesite; grades downward into black at 544 meters; green clay fills ~60% of vesicles
Green clay coats fractures and fills a few vesicles
Bottom of hole

Well ANL-1

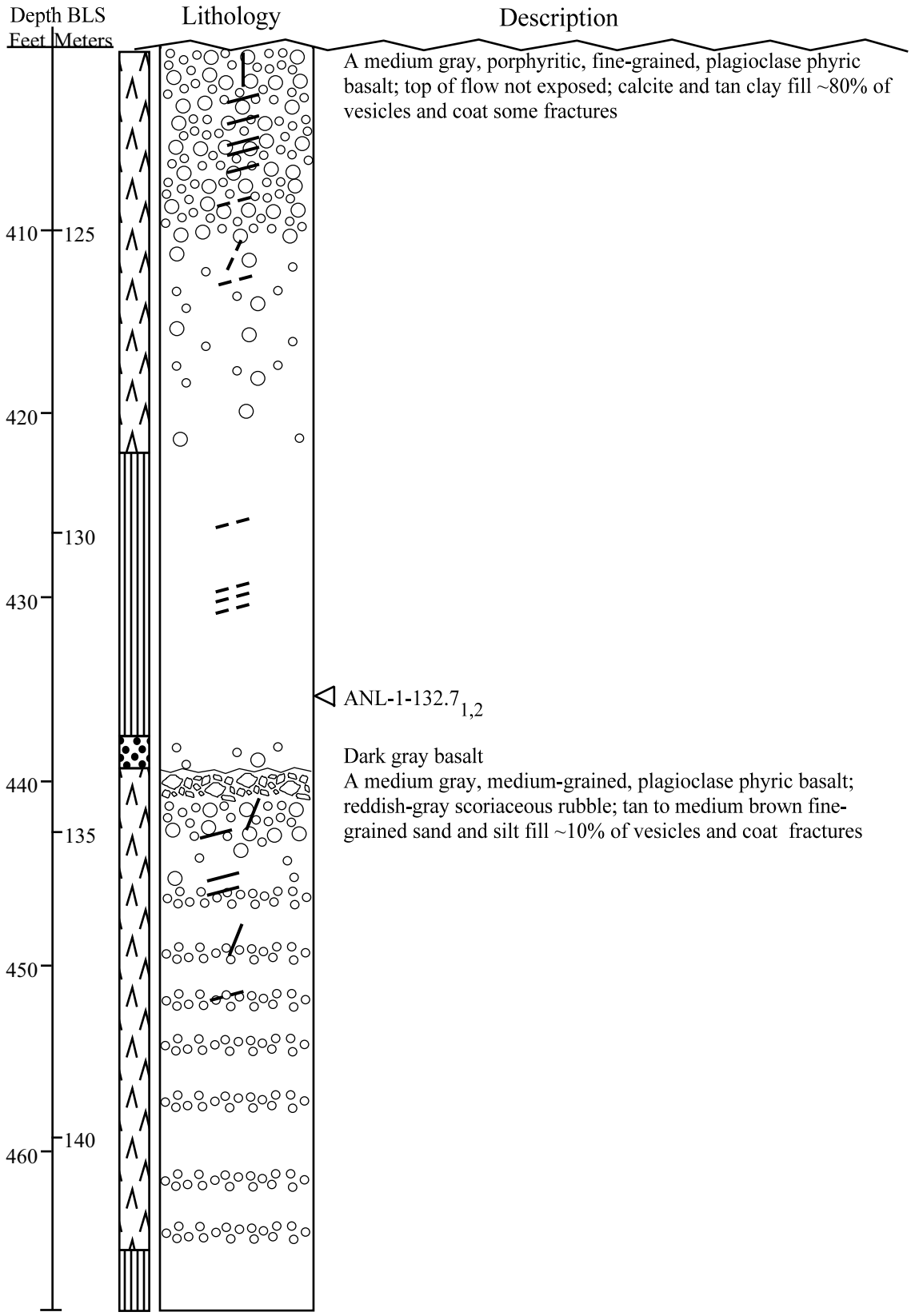
Depth BLS
Feet Meters
Lithology
Description
A medium gray, porphyritic, fine-grained, plagioclase phyric basalt; top of flow not exposed; calcite and tan clay fill ~80% of vesicles and coat some fractures
410
125
420
130
430
ANL-1-132.7 1,2
Dark gray basalt
A medium gray, medium-grained, plagioclase phyric basalt; reddish-gray scoriaceous rubble; tan to medium brown fine-grained sand and silt fill ~10% of vesicles and coat fractures
440
135
450
140
460

Well ANL-1

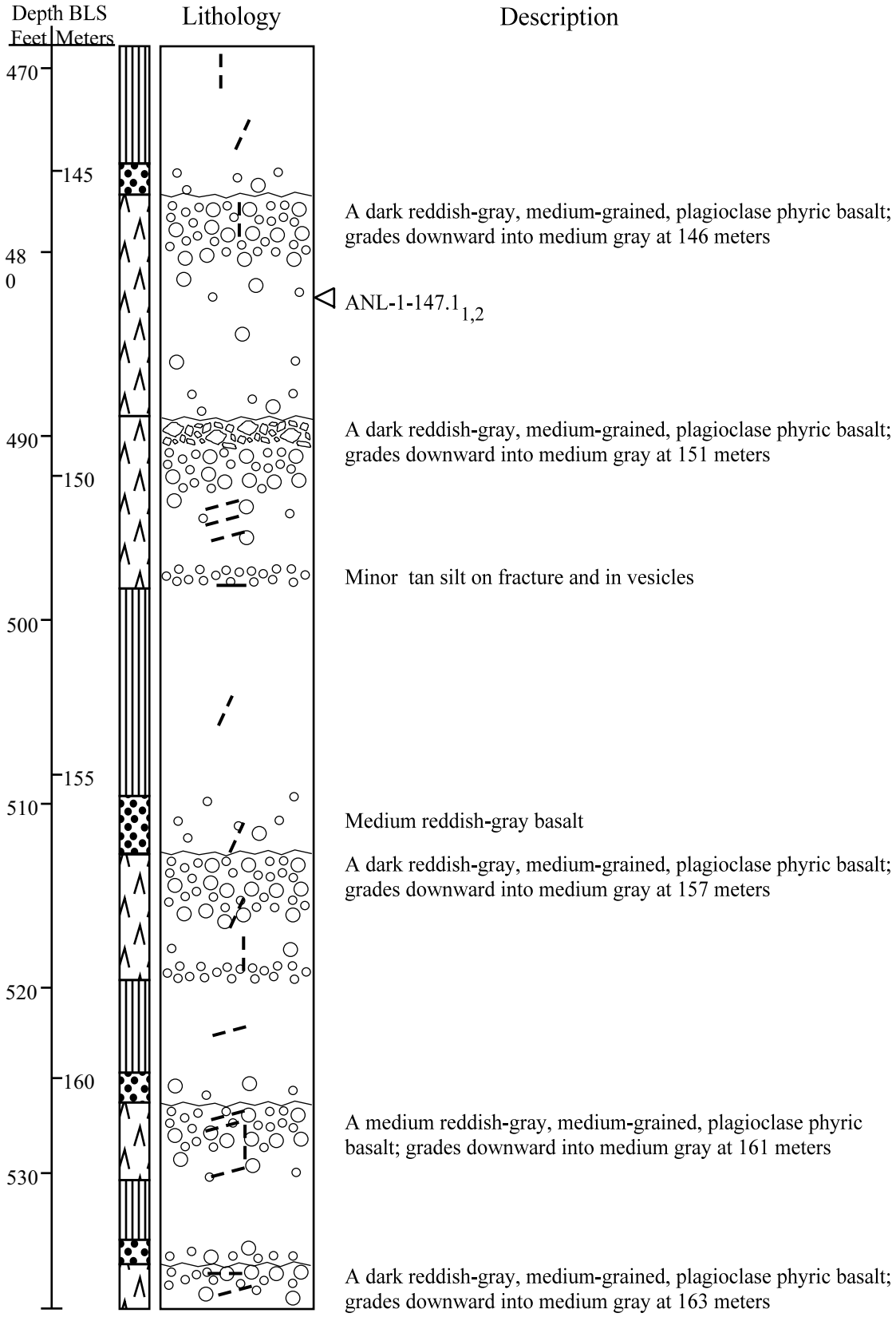
Depth BLS
Feet Meters
Lithology
Description
470
145
48
0
490
150
500
155
510
520
160
530
A dark reddish-gray, medium-grained, plagioclase phyric basalt; grades downward into medium gray at 146 meters
ANL-1-147.1 1,2
A dark reddish-gray, medium-grained, plagioclase phyric basalt; grades downward into medium gray at 151 meters
Minor tan silt on fracture and in vesicles
Medium reddish-gray basalt
A dark reddish-gray, medium-grained, plagioclase phyric basalt; grades downward into medium gray at 157 meters
A medium reddish-gray, medium-grained, plagioclase phyric basalt; grades downward into medium gray at 161 meters
A dark reddish-gray, medium-grained, plagioclase phyric basalt; grades downward into medium gray at 163 meters

Well ANL-1

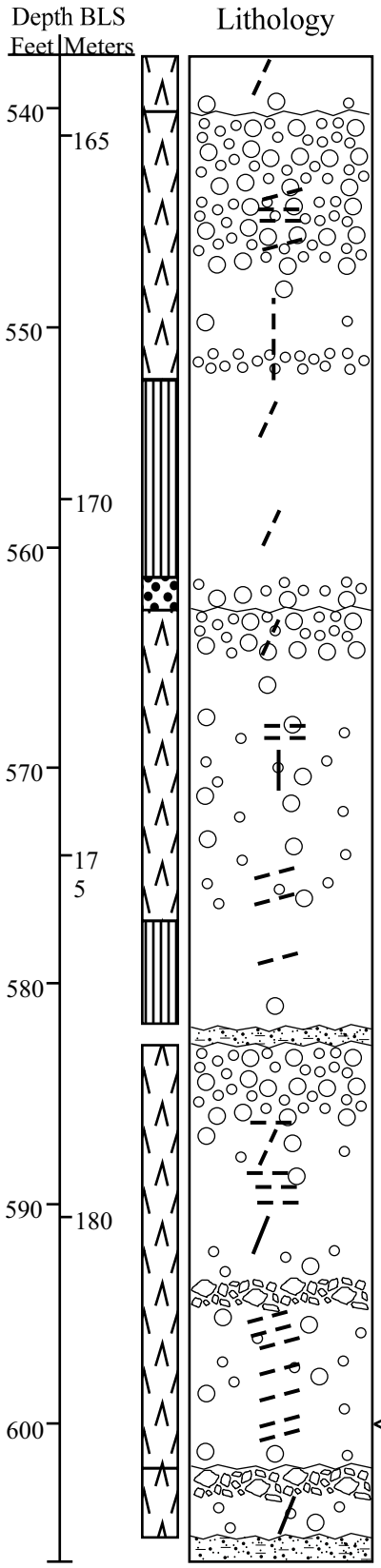

Description

A dark reddish-gray, medium-grained, plagioclase phyric basalt; grades downward into dark gray at 165 meters

A medium reddish-gray, aphyric basalt; grades downward into medium gray at 172 meters; calcite in ~20% of vesicles

Tan fine-grained sand and silt coat fracture

Light gray basalt

Tan fine-grained sand and silt

A dark gray, medium-grained, plagioclase phyric basalt; tan sand and silt fill ~50% of vesicles

Minor tan sand and silt in vesicles

Minor calcite in vesicle

Medium gray basalt

Tan fine-grained sand and silt coat fracture

ANL-1-182.9[1,2]

Dark gray basalt

A dark gray, medium-grained, plagioclase phyric basalt; tan fine-grained sand and silt coat fracture

Tan fine-grained sand and clay with basalt clasts

Well ANL-1

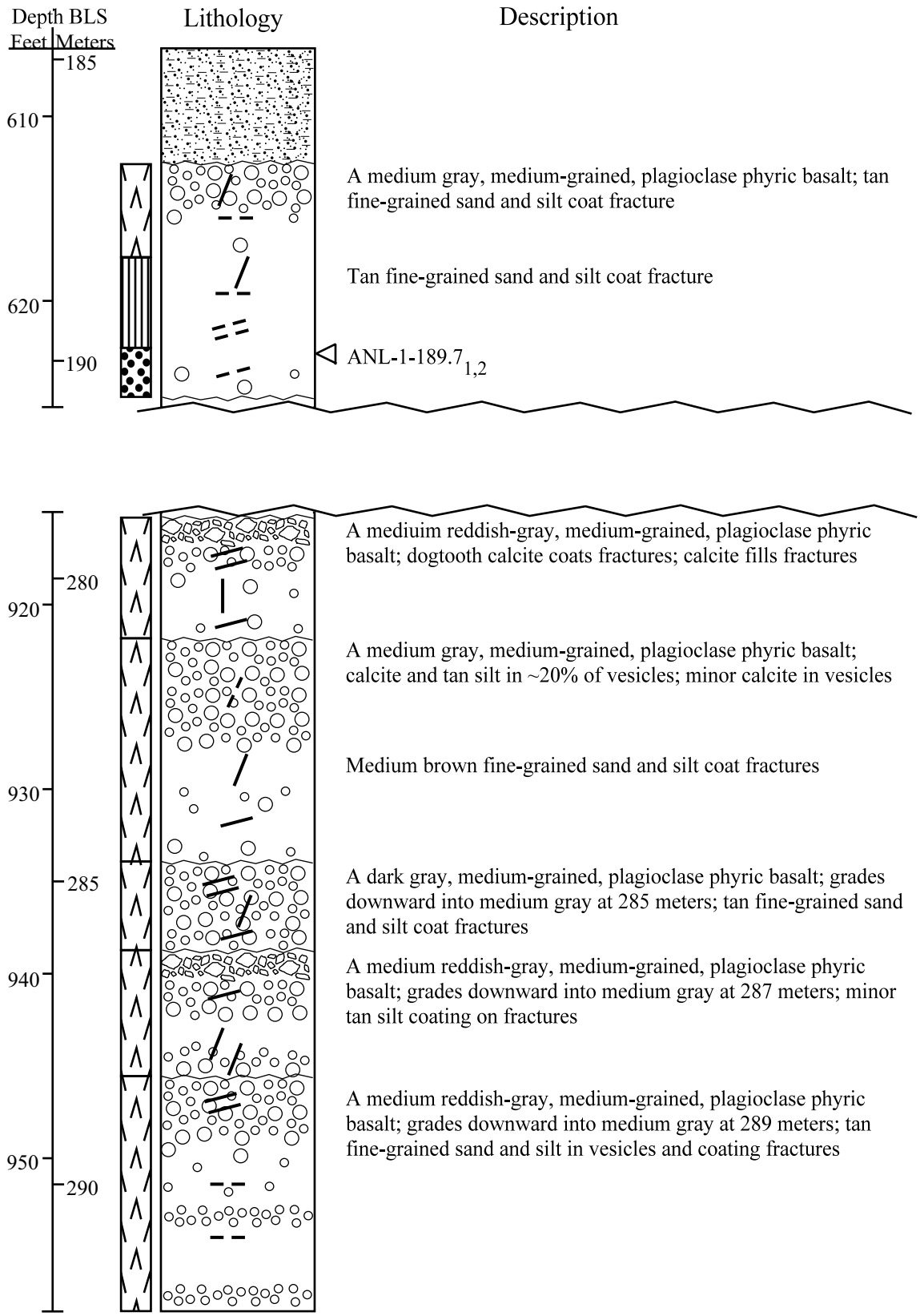
Depth BLS
Feet Meters
Lithology
Description
185
610
620
190
280
920
930
285
940
950
290
A medium gray, medium-grained, plagioclase phyric basalt; tan fine-grained sand and silt coat fracture
Tan fine-grained sand and silt coat fracture
ANL-1-189.7 1,2
A mediuim reddish-gray, medium-grained, plagioclase phyric basalt; dogtooth calcite coats fractures; calcite fills fractures
A medium gray, medium-grained, plagioclase phyric basalt; calcite and tan silt in ~20% of vesicles; minor calcite in vesicles
Medium brown fine-grained sand and silt coat fractures
A dark gray, medium-grained, plagioclase phyric basalt; grades downward into medium gray at 285 meters; tan fine-grained sand and silt coat fractures
A medium reddish-gray, medium-grained, plagioclase phyric basalt; grades downward into medium gray at 287 meters; minor tan silt coating on fractures
A medium reddish-gray, medium-grained, plagioclase phyric basalt; grades downward into medium gray at 289 meters; tan fine-grained sand and silt in vesicles and coating fractures

Well ANL-1

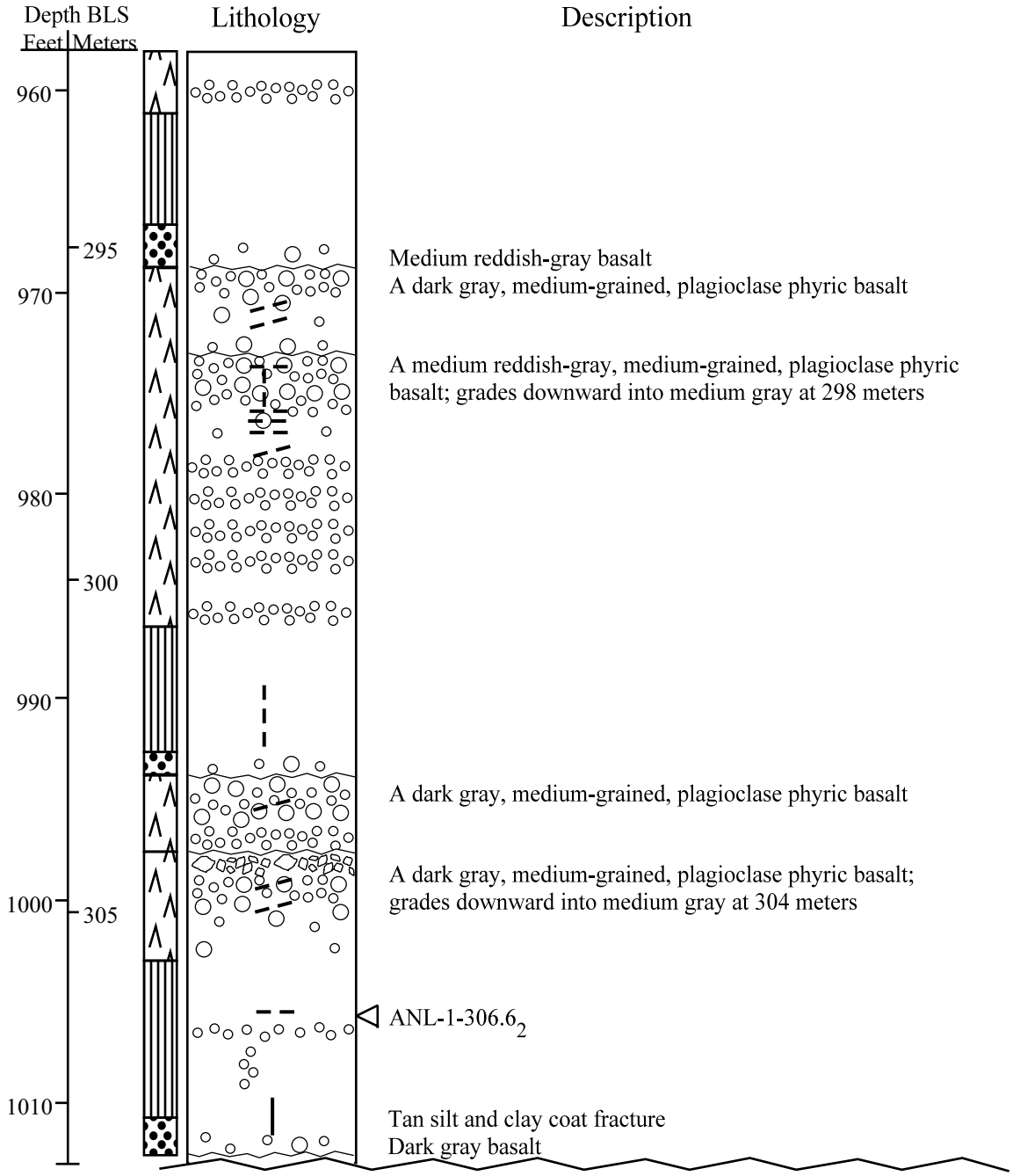
Depth BLS
Feet Meters
Lithology
Description
960
295
970
980
300
990
1000
305
1010
Medium reddish-gray basalt
A dark gray, medium-grained, plagioclase phyric basalt
A medium reddish-gray, medium-grained, plagioclase phyric basalt; grades downward into medium gray at 298 meters
A dark gray, medium-grained, plagioclase phyric basalt
A dark gray, medium-grained, plagioclase phyric basalt; grades downward into medium gray at 304 meters
ANL-1-306.6$_2$
Tan silt and clay coat fracture
Dark gray basalt

Well ANL-1

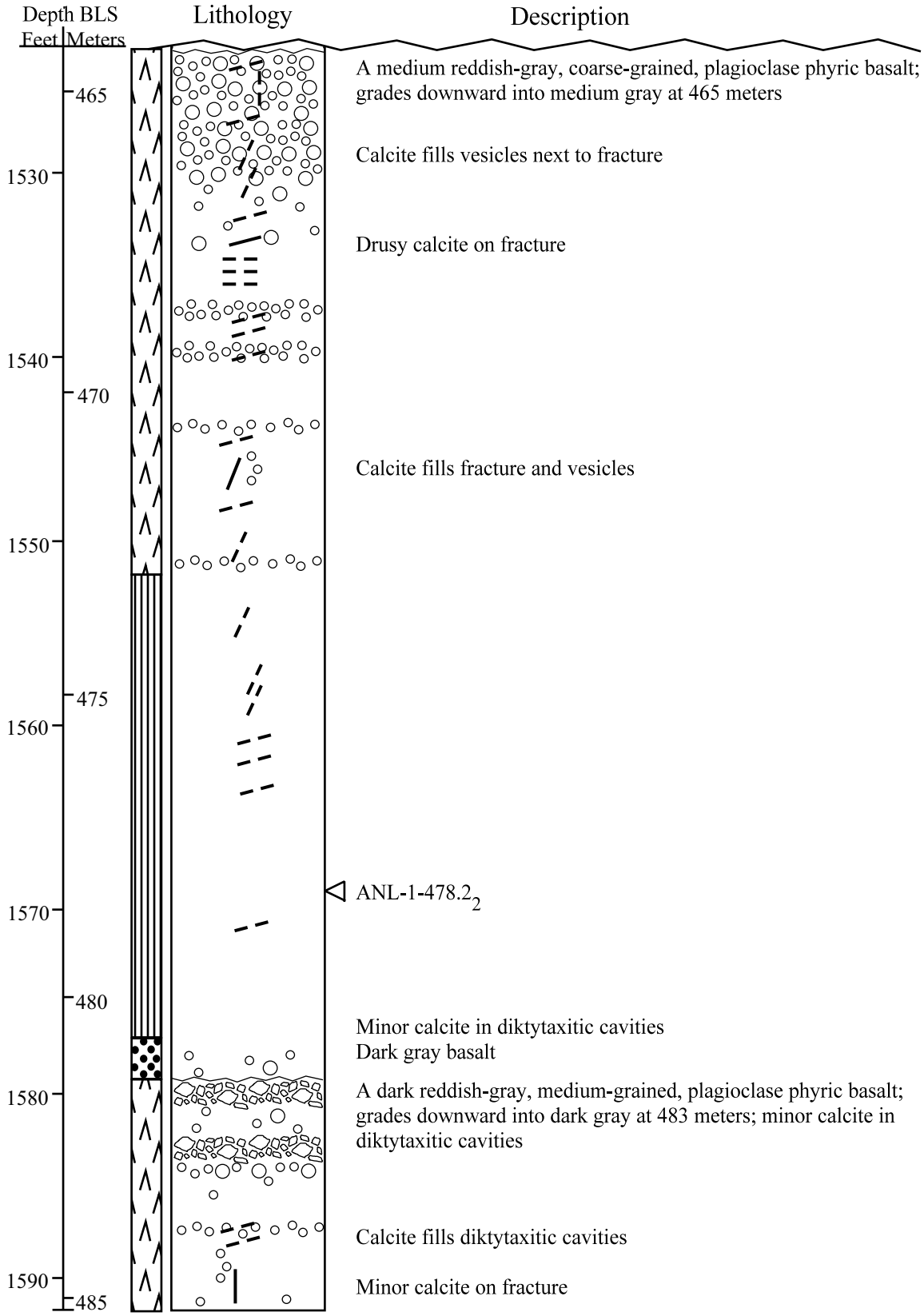
Depth BLS
Feet Meters
Lithology
Description
465
1530
1540
470
1550
475
1560
1570
480
1580
1590
485
A medium reddish-gray, coarse-grained, plagioclase phyric basalt; grades downward into medium gray at 465 meters
Calcite fills vesicles next to fracture
Drusy calcite on fracture
Calcite fills fracture and vesicles
ANL-1-478.2$_2$
Minor calcite in diktytaxitic cavities
Dark gray basalt
A dark reddish-gray, medium-grained, plagioclase phyric basalt; grades downward into dark gray at 483 meters; minor calcite in diktytaxitic cavities
Calcite fills diktytaxitic cavities
Minor calcite on fracture

Well ANL-1

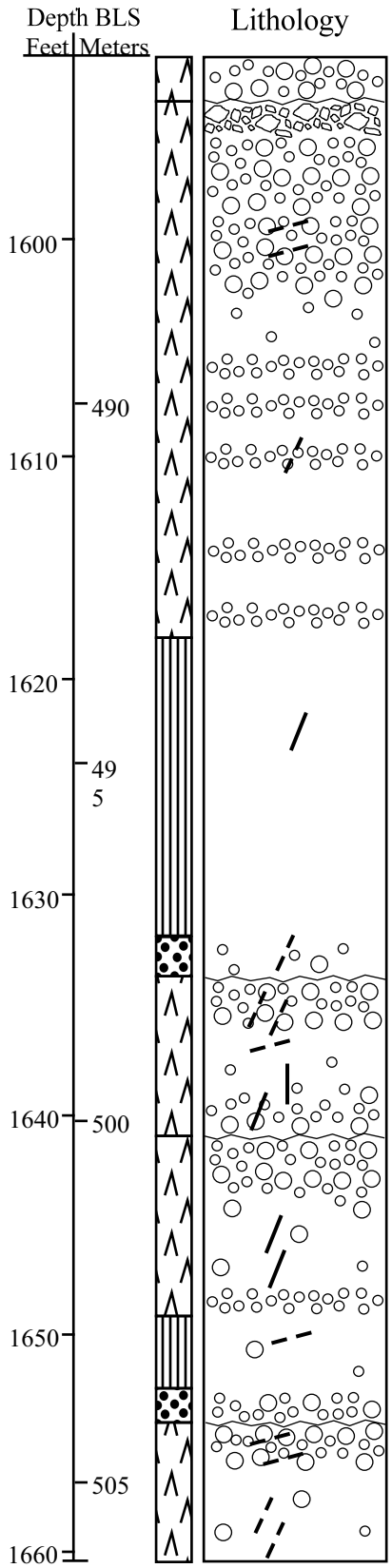

Description

A dark reddish-gray, medium-grained, plagioclase phyric basalt; grades downward into dark gray at 486 meters

Minor calcite filling of vesicles and diktytaxitic cavities

Tan silt coats fracture

Calcite fills diktytaxitic cavities
A dark reddish-gray, medium-grained, plagioclase phyric basalt; grades downward into dark gray at 499 meters
Minor calcite filling of vesicles

Calcite fills fractures
A dark reddish-gray, medium-grained, plagioclase phyric basalt; grades downward into dark gray at 501 meters
Minor calcite in diktytaxitic cavities

Calcite fills fractures

Minor calcite in diktytaxitic cavities

A dark reddish-gray, medium-grained, plagioclase phyric basalt.; grades downward into dark gray at 505 meters; minor calcite in vesicles

Well ANL-1

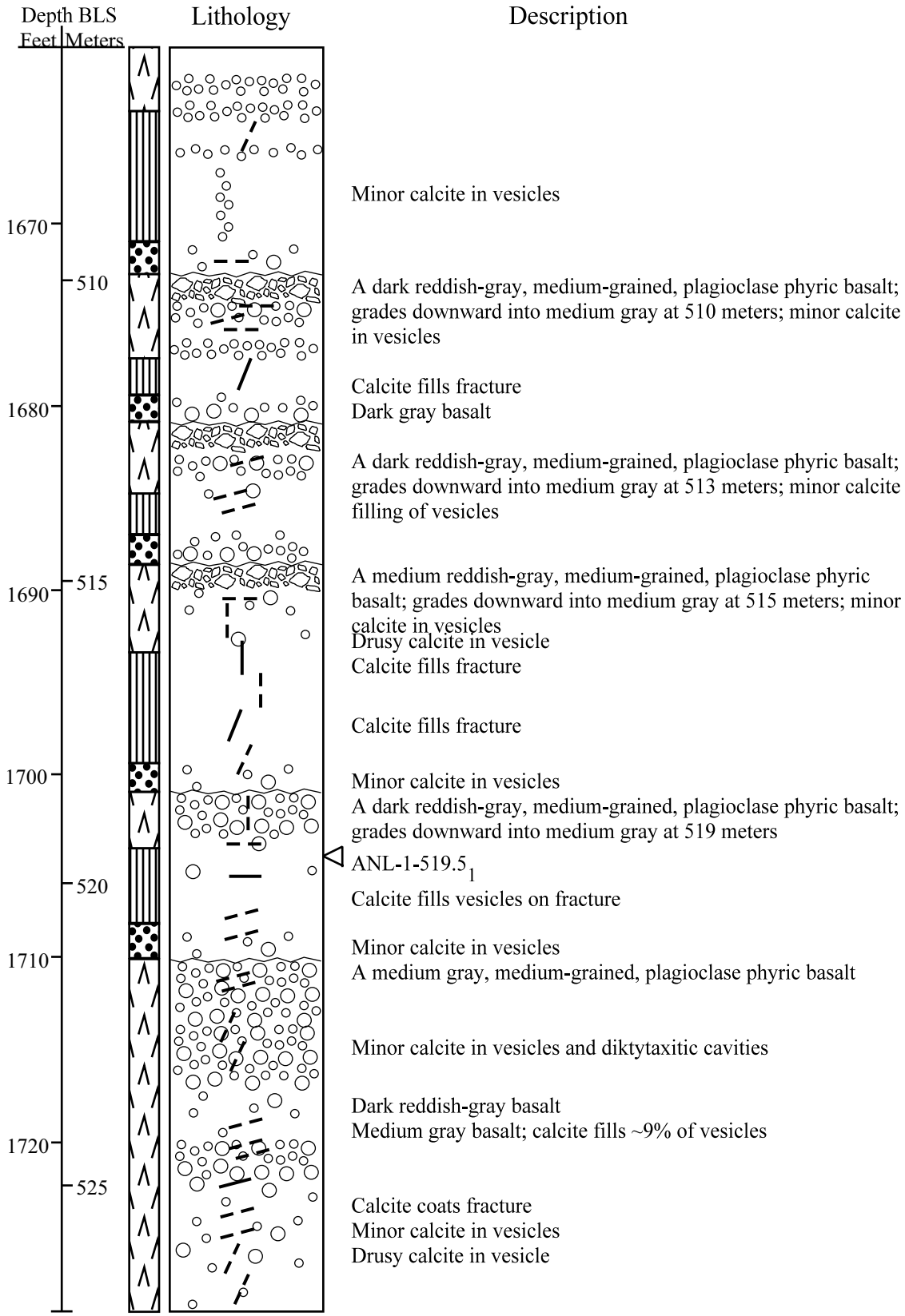
Depth BLS
Feet Meters
Lithology
Description
1670
510
1680
515
1690
1700
520
1710
1720
525
Minor calcite in vesicles
A dark reddish-gray, medium-grained, plagioclase phyric basalt; grades downward into medium gray at 510 meters; minor calcite in vesicles
Calcite fills fracture
Dark gray basalt
A dark reddish-gray, medium-grained, plagioclase phyric basalt; grades downward into medium gray at 513 meters; minor calcite filling of vesicles
A medium reddish-gray, medium-grained, plagioclase phyric basalt; grades downward into medium gray at 515 meters; minor calcite in vesicles
Drusy calcite in vesicle
Calcite fills fracture
Calcite fills fracture
Minor calcite in vesicles
A dark reddish-gray, medium-grained, plagioclase phyric basalt; grades downward into medium gray at 519 meters
ANL-1-519.5 1
Calcite fills vesicles on fracture
Minor calcite in vesicles
A medium gray, medium-grained, plagioclase phyric basalt
Minor calcite in vesicles and diktytaxitic cavities
Dark reddish-gray basalt
Medium gray basalt; calcite fills ~9% of vesicles
Calcite coats fracture
Minor calcite in vesicles
Drusy calcite in vesicle

Well ANL-1

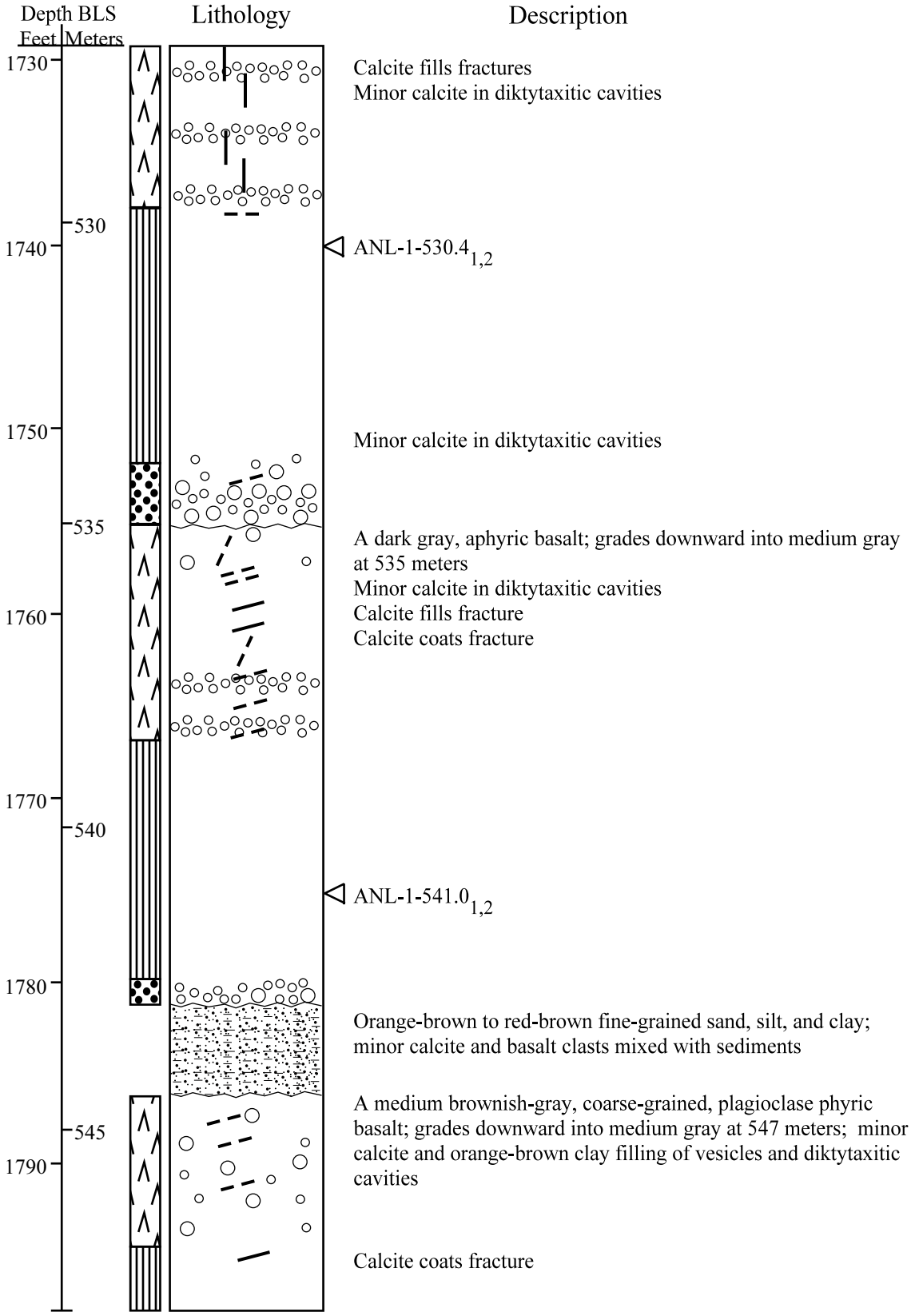
Depth BLS
Feet Meters
Lithology
Description
1730
530
1740
1750
535
1760
1770
540
1780
545
1790
Calcite fills fractures
Minor calcite in diktytaxitic cavities
ANL-1-530.4 1,2
Minor calcite in diktytaxitic cavities
A dark gray, aphyric basalt; grades downward into medium gray at 535 meters
Minor calcite in diktytaxitic cavities
Calcite fills fracture
Calcite coats fracture
ANL-1-541.0 1,2
Orange-brown to red-brown fine-grained sand, silt, and clay; minor calcite and basalt clasts mixed with sediments
A medium brownish-gray, coarse-grained, plagioclase phyric basalt; grades downward into medium gray at 547 meters; minor calcite and orange-brown clay filling of vesicles and diktytaxitic cavities
Calcite coats fracture

Well ANL-1

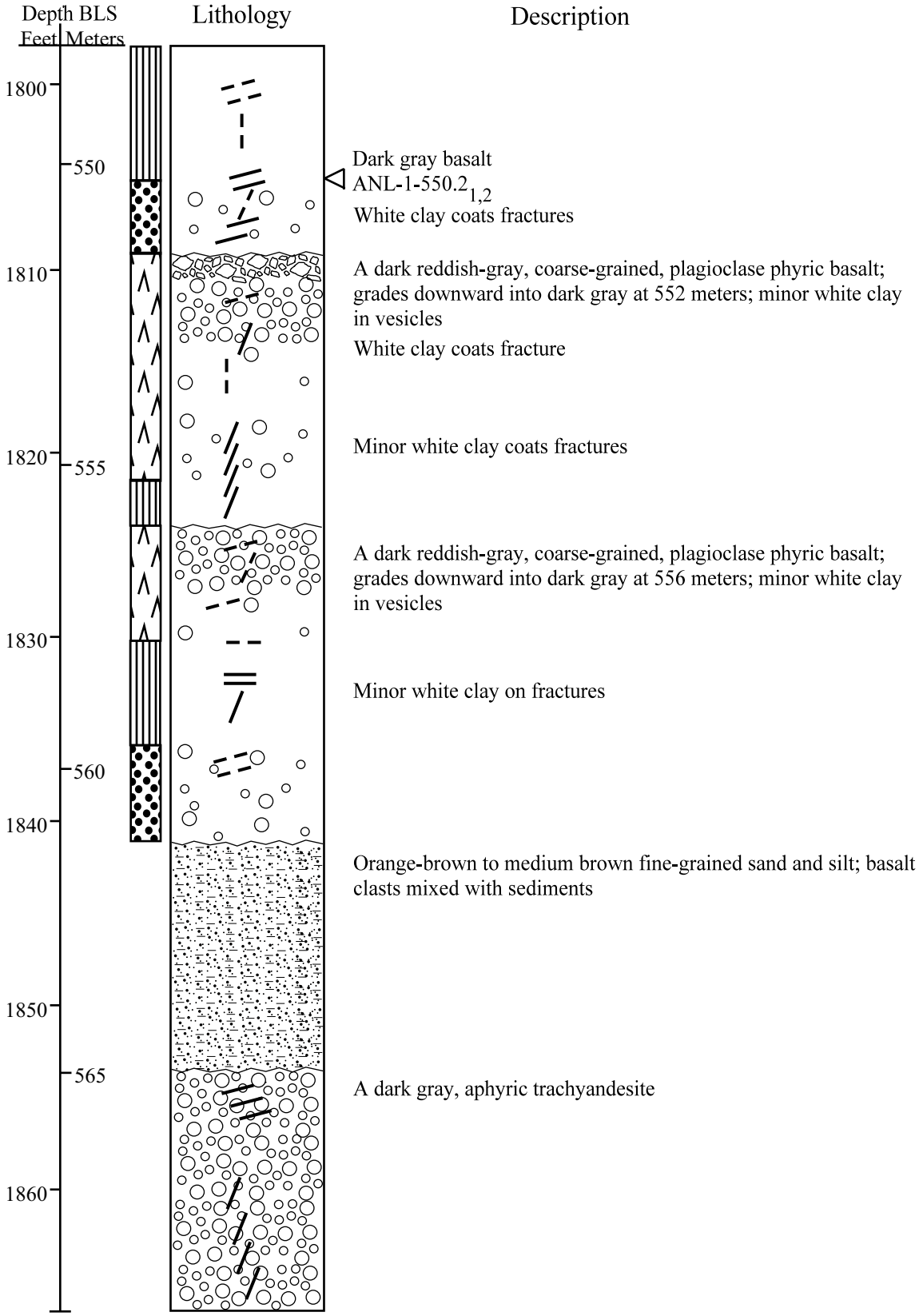
Depth BLS
Feet Meters
Lithology
Description
1800
550
1810
1820
555
1830
560
1840
1850
565
1860
Dark gray basalt
ANL-1-550.2 1,2
White clay coats fractures
A dark reddish-gray, coarse-grained, plagioclase phyric basalt; grades downward into dark gray at 552 meters; minor white clay in vesicles
White clay coats fracture
Minor white clay coats fractures
A dark reddish-gray, coarse-grained, plagioclase phyric basalt; grades downward into dark gray at 556 meters; minor white clay in vesicles
Minor white clay on fractures
Orange-brown to medium brown fine-grained sand and silt; basalt clasts mixed with sediments
A dark gray, aphyric trachyandesite

Well ANL-1

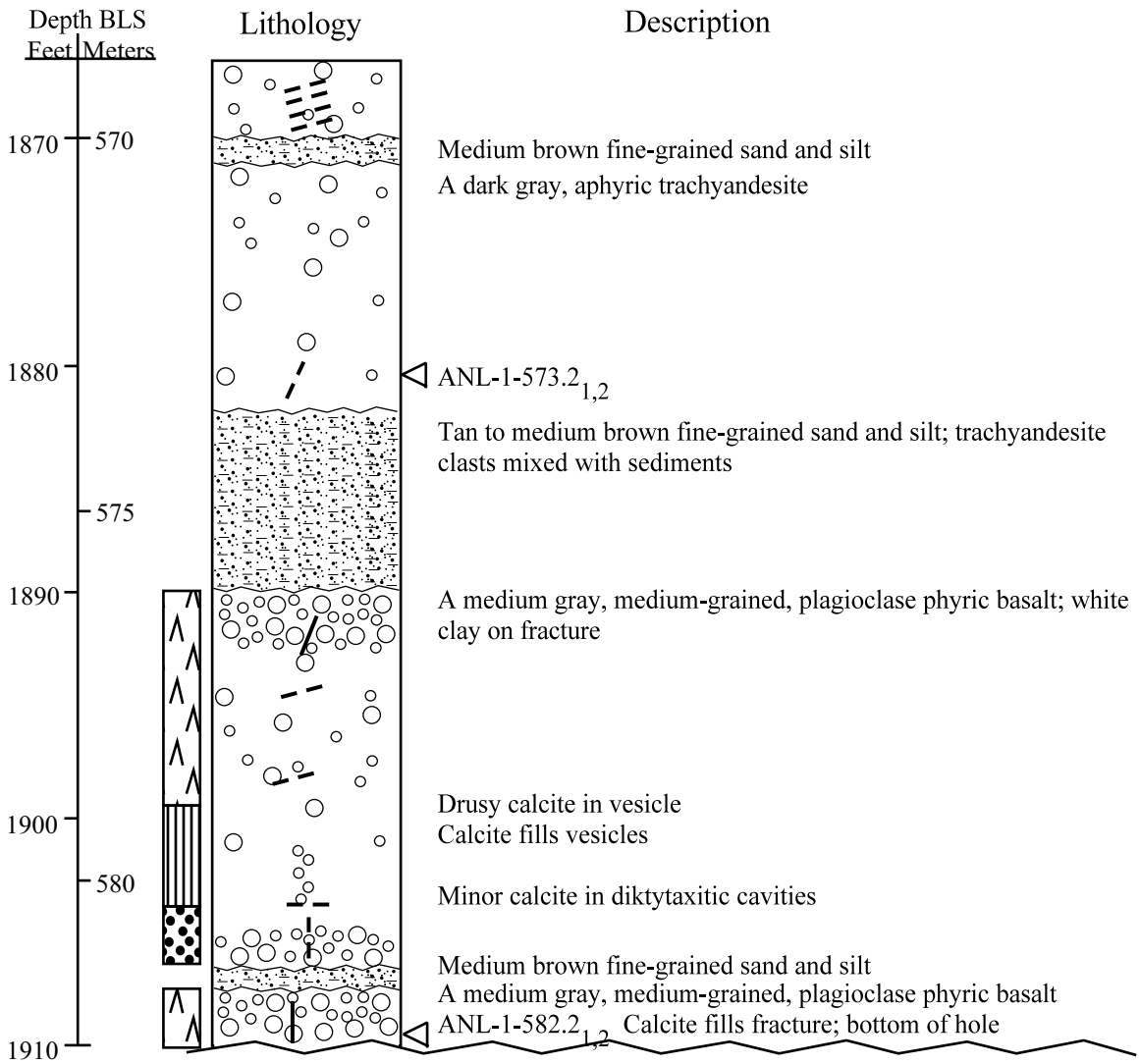
Depth BLS
Feet Meters
Lithology
Description
1870
570
1880
575
1890
1900
580
1910
Medium brown fine-grained sand and silt
A dark gray, aphyric trachyandesite
ANL-1-573.2 1,2
Tan to medium brown fine-grained sand and silt; trachyandesite clasts mixed with sediments
A medium gray, medium-grained, plagioclase phyric basalt; white clay on fracture
Drusy calcite in vesicle
Calcite fills vesicles
Minor calcite in diktytaxitic cavities
Medium brown fine-grained sand and silt
A medium gray, medium-grained, plagioclase phyric basalt
ANL-1-582.2 1,2
Calcite fills fracture; bottom of hole

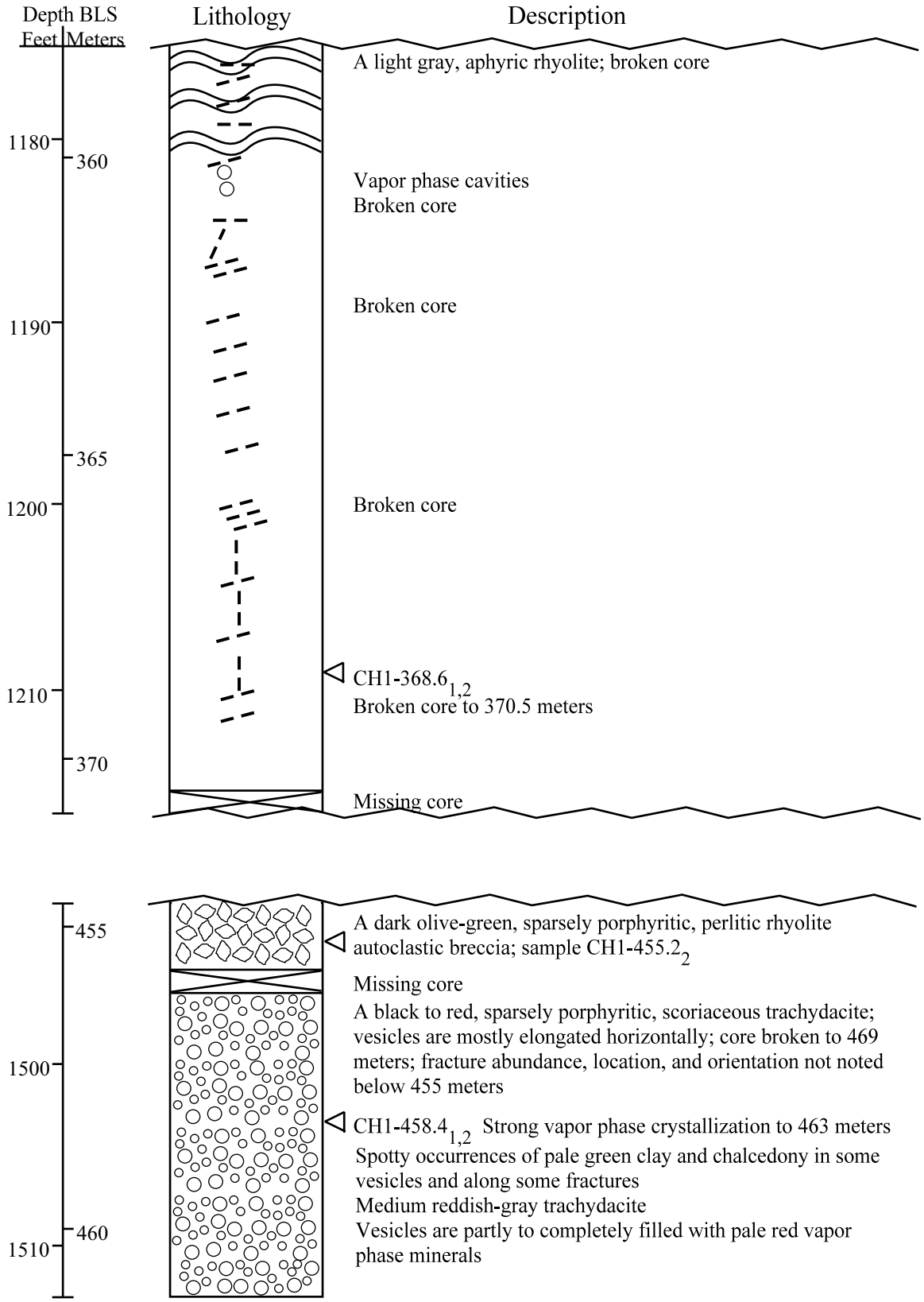
Depth BLS
Feet Meters
Lithology
Description
A light gray, aphyric rhyolite; broken core
1180
360
Vapor phase cavities
Broken core
Broken core
1190
365
1200
Broken core
CH1-368.6 1,2
Broken core to 370.5 meters
1210
370
Missing core
455
A dark olive-green, sparsely porphyritic, perlitic rhyolite autoclastic breccia; sample CH1-455.2 2
Missing core
A black to red, sparsely porphyritic, scoriaceous trachydacite; vesicles are mostly elongated horizontally; core broken to 469 meters; fracture abundance, location, and orientation not noted below 455 meters
1500
CH1-458.4 1,2 Strong vapor phase crystallization to 463 meters
Spotty occurrences of pale green clay and chalcedony in some vesicles and along some fractures
Medium reddish-gray trachydacite
Vesicles are partly to completely filled with pale red vapor phase minerals
460
1510

Well CH-1

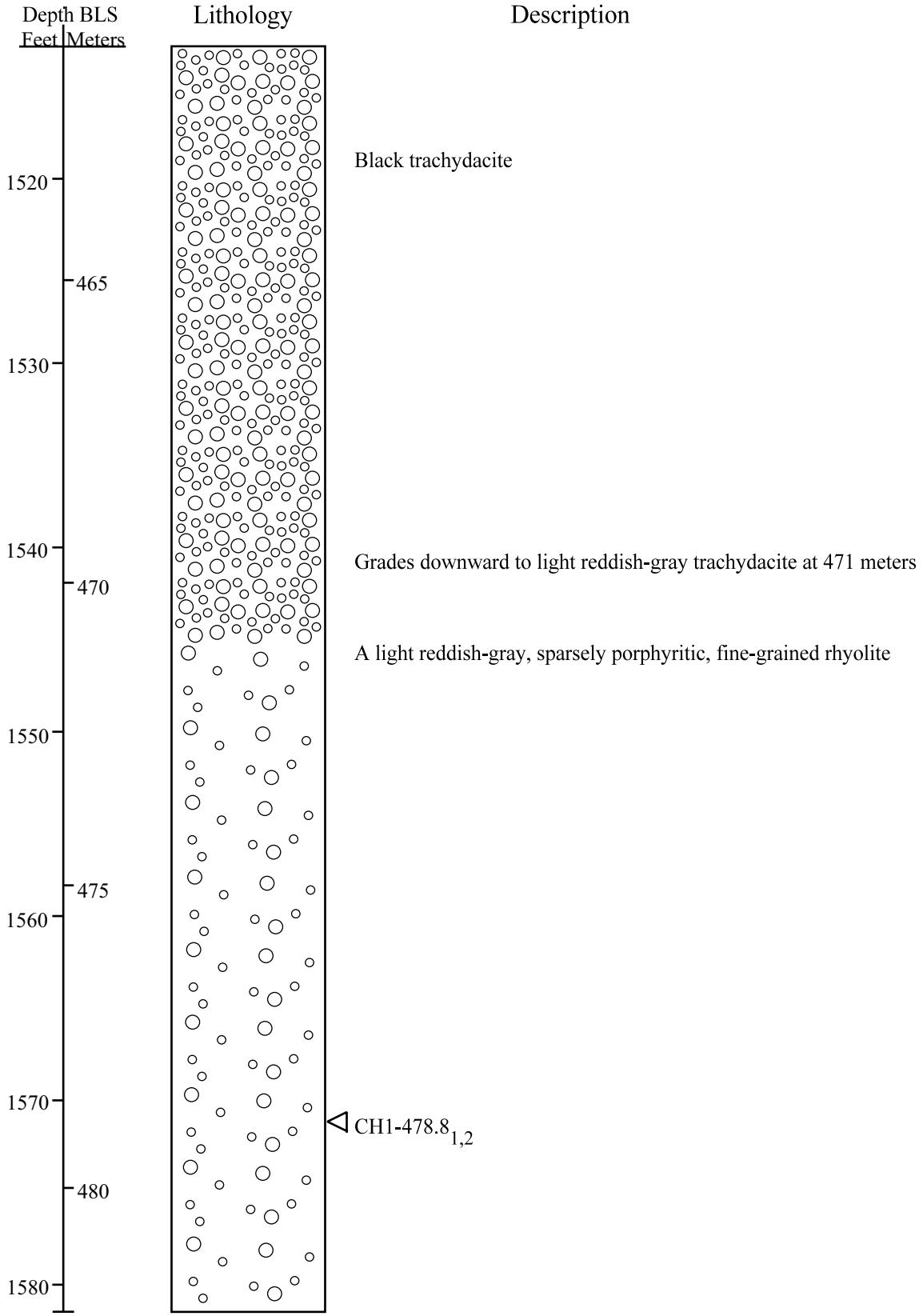
Depth BLS
Feet Meters
Lithology
Description
1520
465
1530
1540
470
1550
475
1560
1570
480
1580
Black trachydacite
Grades downward to light reddish-gray trachydacite at 471 meters
A light reddish-gray, sparsely porphyritic, fine-grained rhyolite
CH1-478.8 1,2

Well CH-1

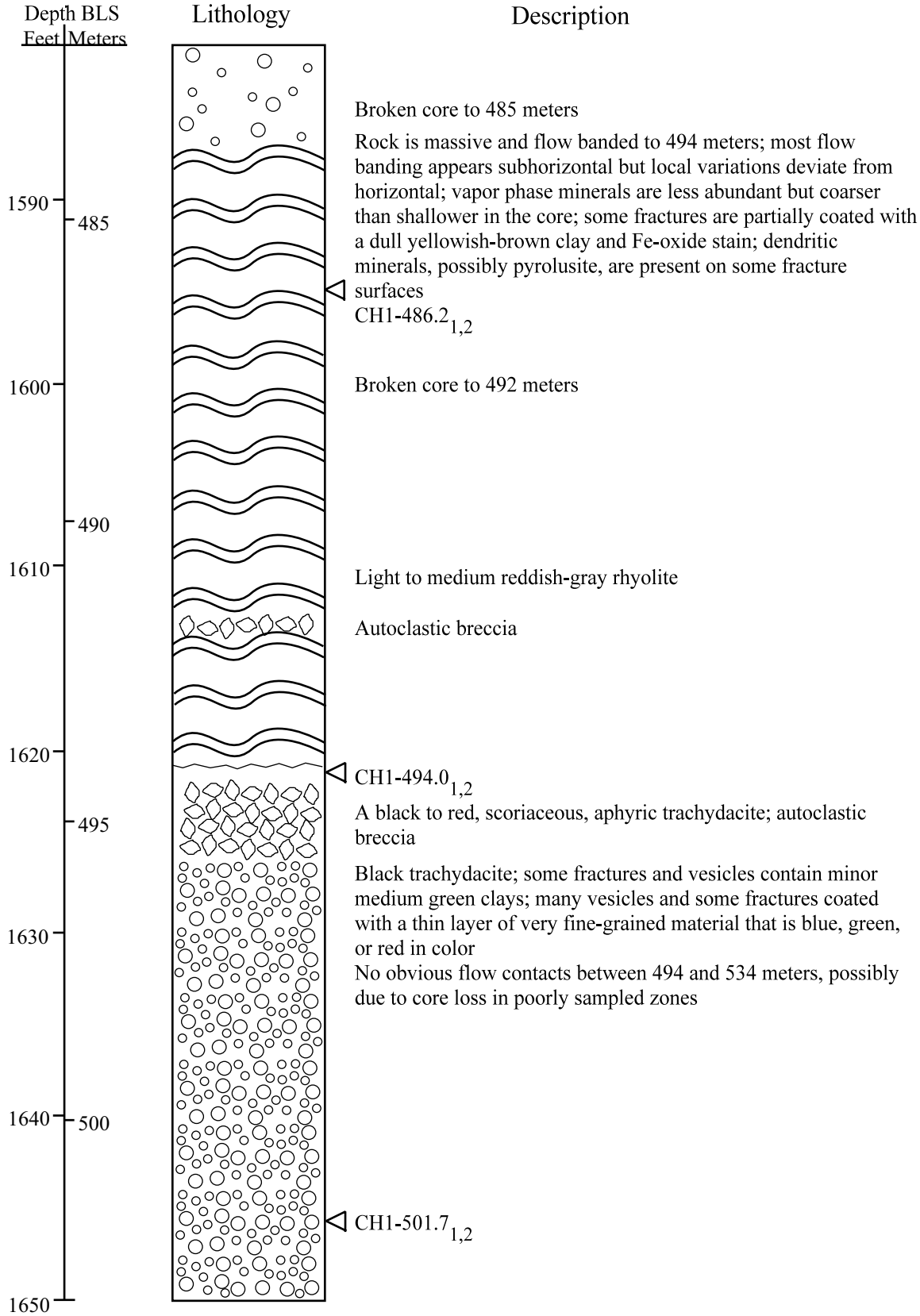
Depth BLS
Feet Meters
Lithology
Description
1590
485
1600
490
1610
1620
495
1630
1640
500
1650
Broken core to 485 meters
Rock is massive and flow banded to 494 meters; most flow banding appears subhorizontal but local variations deviate from horizontal; vapor phase minerals are less abundant but coarser than shallower in the core; some fractures are partially coated with a dull yellowish-brown clay and Fe-oxide stain; dendritic minerals, possibly pyrolusite, are present on some fracture surfaces
CH1-486.2 1,2
Broken core to 492 meters
Light to medium reddish-gray rhyolite
Autoclastic breccia
CH1-494.0 1,2
A black to red, scoriaceous, aphyric trachydacite; autoclastic breccia
Black trachydacite; some fractures and vesicles contain minor medium green clays; many vesicles and some fractures coated with a thin layer of very fine-grained material that is blue, green, or red in color
No obvious flow contacts between 494 and 534 meters, possibly due to core loss in poorly sampled zones
CH1-501.7 1,2

Well CH-1

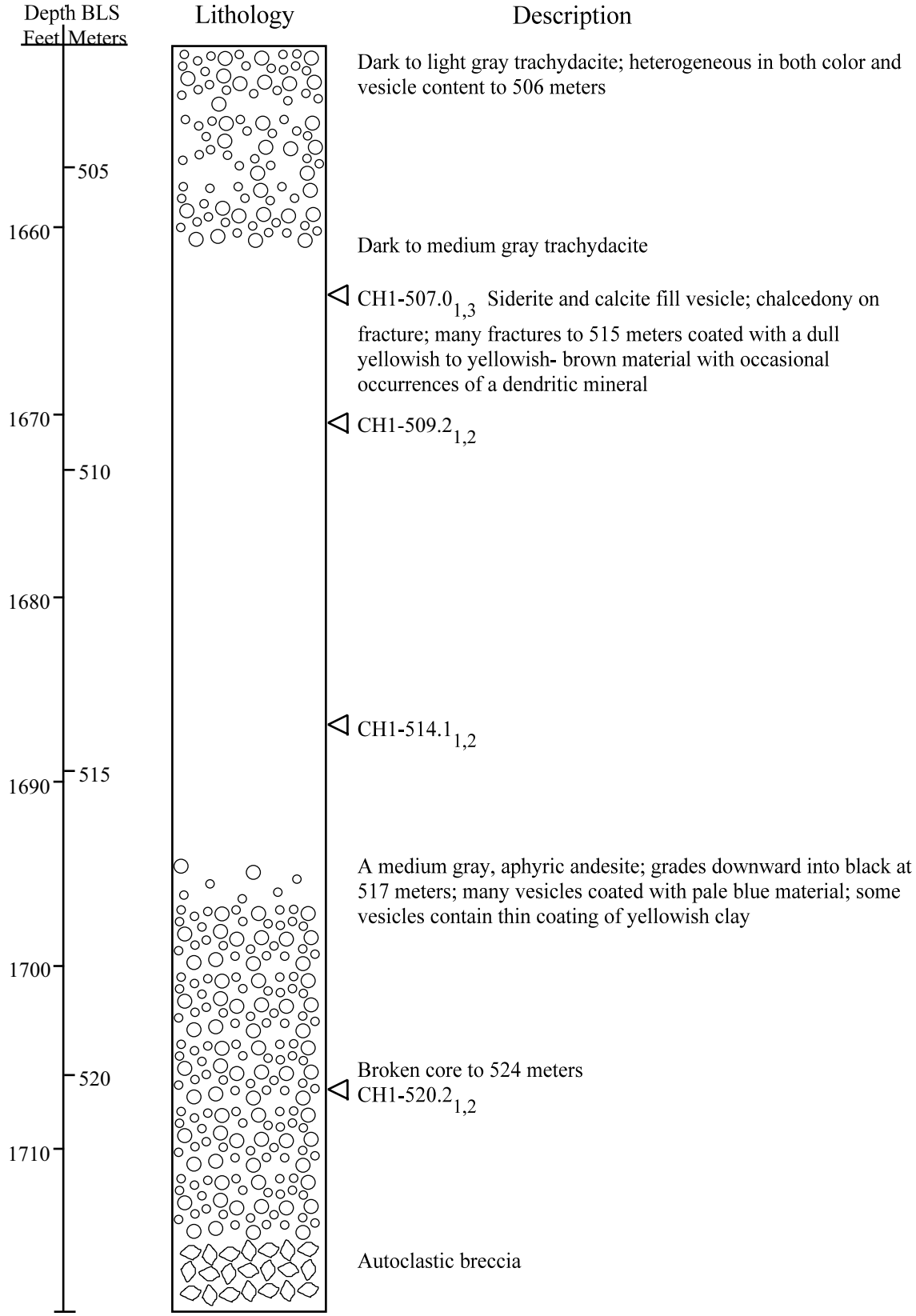
Depth BLS
Feet Meters
Lithology
Description
505
1660
1670
510
1680
515
1690
1700
520
1710
Dark to light gray trachydacite; heterogeneous in both color and vesicle content to 506 meters
Dark to medium gray trachydacite
CH1-507.0 1,3 Siderite and calcite fill vesicle; chalcedony on fracture; many fractures to 515 meters coated with a dull yellowish to yellowish- brown material with occasional occurrences of a dendritic mineral
CH1-509.2 1,2
CH1-514.1 1,2
A medium gray, aphyric andesite; grades downward into black at 517 meters; many vesicles coated with pale blue material; some vesicles contain thin coating of yellowish clay
Broken core to 524 meters
CH1-520.2 1,2
Autoclastic breccia

Well CH-1

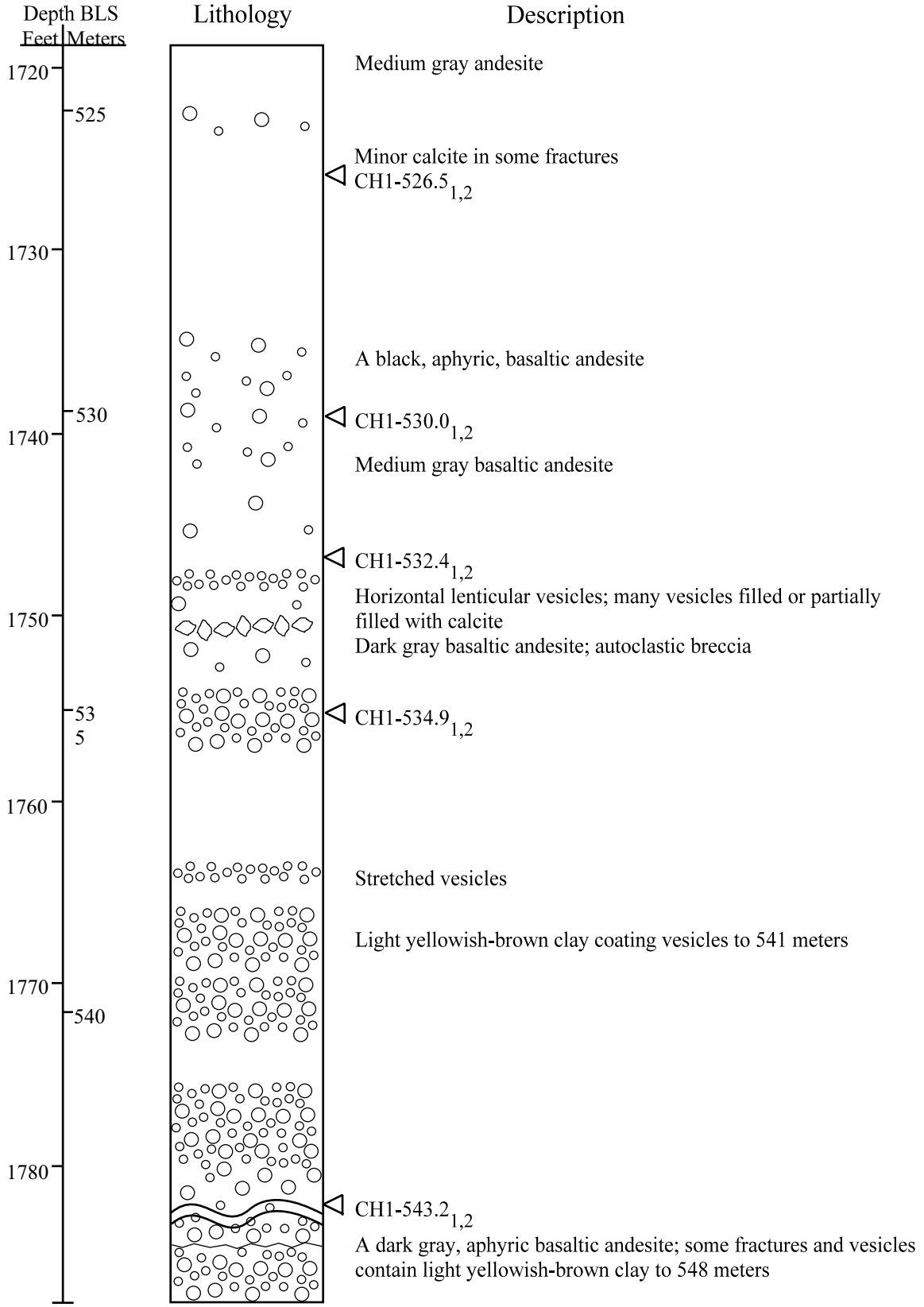
Depth BLS
Feet Meters
Lithology
Description
1720
525
1730
530
1740
1750
53
5
1760
1770
540
1780
Medium gray andesite
Minor calcite in some fractures
CH1-526.5 1,2
A black, aphyric, basaltic andesite
CH1-530.0 1,2
Medium gray basaltic andesite
CH1-532.4 1,2
Horizontal lenticular vesicles; many vesicles filled or partially filled with calcite
Dark gray basaltic andesite; autoclastic breccia
CH1-534.9 1,2
Stretched vesicles
Light yellowish-brown clay coating vesicles to 541 meters
CH1-543.2 1,2
A dark gray, aphyric basaltic andesite; some fractures and vesicles contain light yellowish-brown clay to 548 meters

Well CH-1

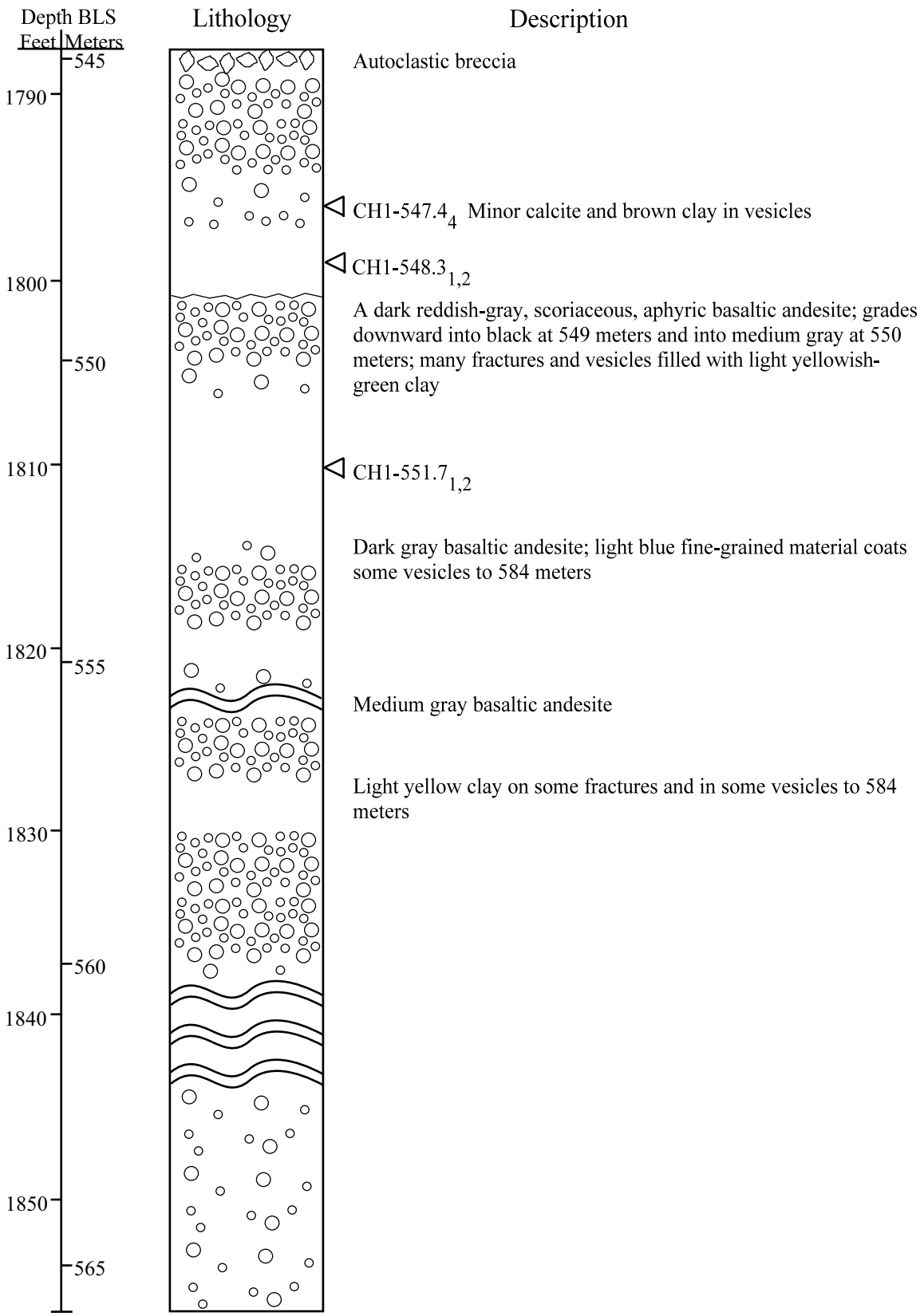
Depth BLS
Feet | Meters
Lithology
Description
545
1790
1800
550
1810
1820
555
1830
560
1840
1850
565
Autoclastic breccia
CH1-547.4$_4$ Minor calcite and brown clay in vesicles
CH1-548.3$_{1,2}$
A dark reddish-gray, scoriaceous, aphyric basaltic andesite; grades downward into black at 549 meters and into medium gray at 550 meters; many fractures and vesicles filled with light yellowish-green clay
CH1-551.7$_{1,2}$
Dark gray basaltic andesite; light blue fine-grained material coats some vesicles to 584 meters
Medium gray basaltic andesite
Light yellow clay on some fractures and in some vesicles to 584 meters

Well CH-1

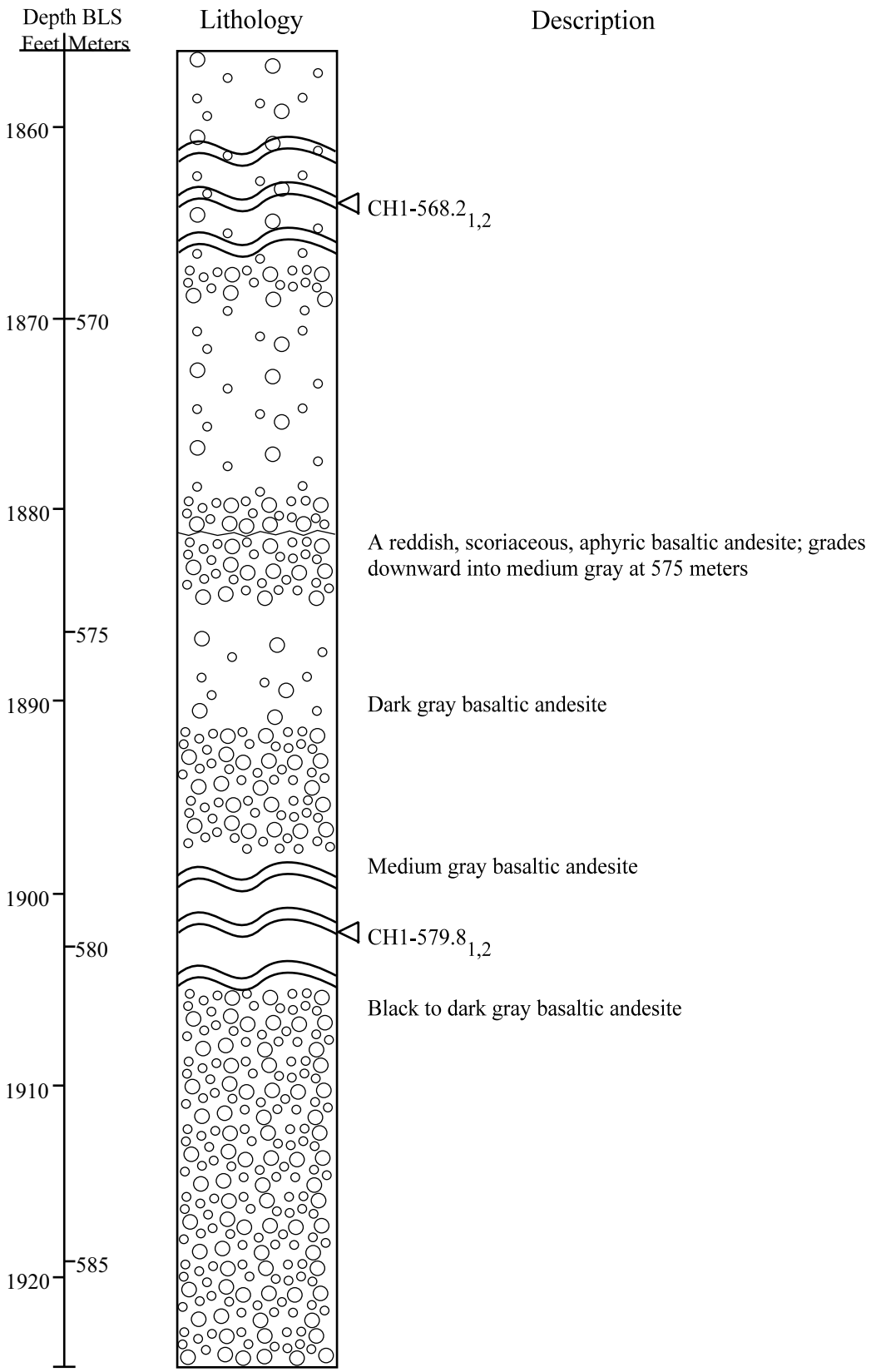
Depth BLS
Feet Meters
Lithology
Description
1860
1870
570
1880
575
1890
1900
580
1910
585
1920
CH1-568.2 1,2
A reddish, scoriaceous, aphyric basaltic andesite; grades downward into medium gray at 575 meters
Dark gray basaltic andesite
Medium gray basaltic andesite
CH1-579.8 1,2
Black to dark gray basaltic andesite

Well CH-1

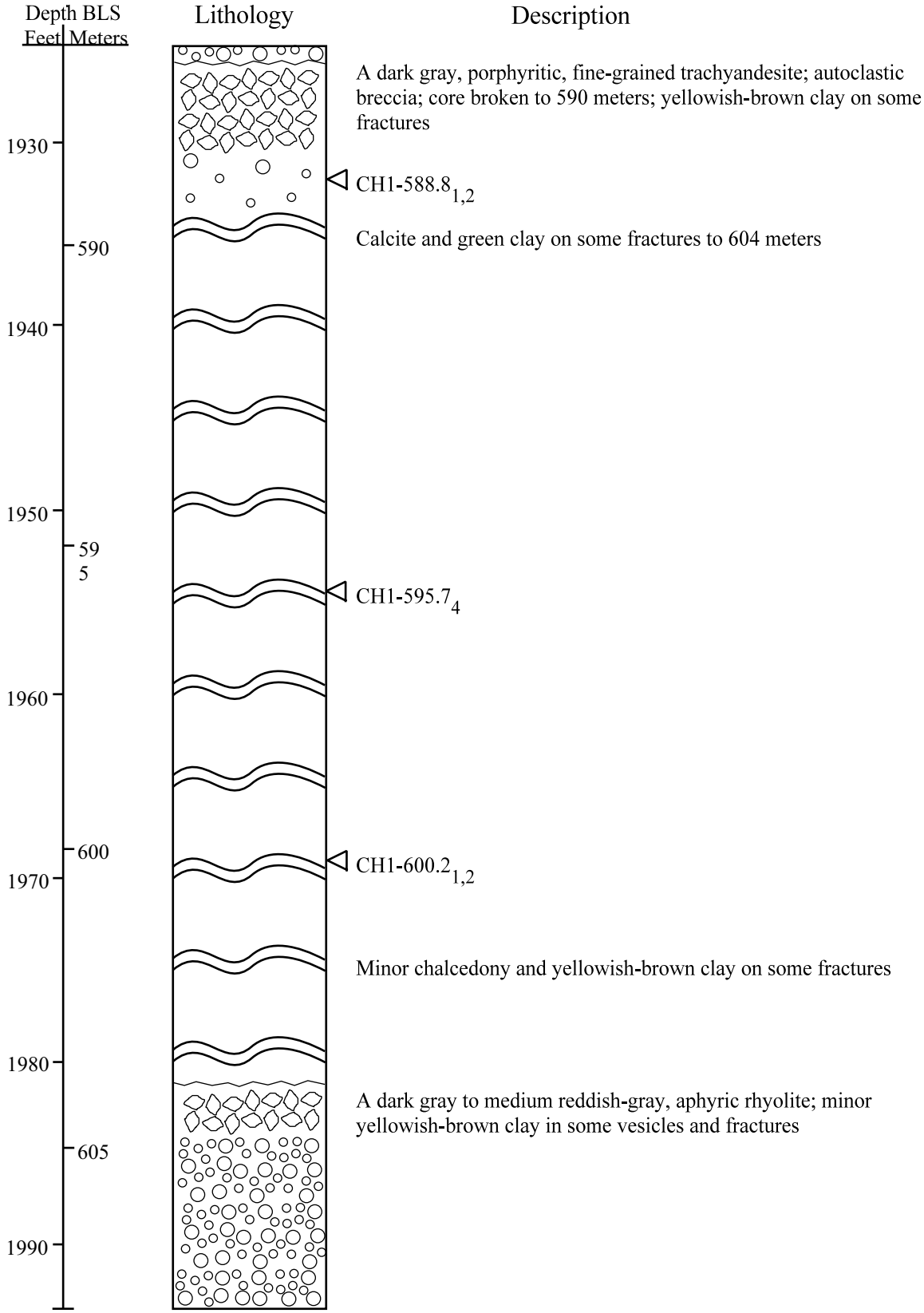
Depth BLS
Feet Meters
Lithology
Description
1930
590
1940
1950
59
5
1960
600
1970
1980
605
1990
A dark gray, porphyritic, fine-grained trachyandesite; autoclastic breccia; core broken to 590 meters; yellowish-brown clay on some fractures
CH1-588.8 1,2
Calcite and green clay on some fractures to 604 meters
CH1-595.7 4
CH1-600.2 1,2
Minor chalcedony and yellowish-brown clay on some fractures
A dark gray to medium reddish-gray, aphyric rhyolite; minor yellowish-brown clay in some vesicles and fractures

Well CH-1

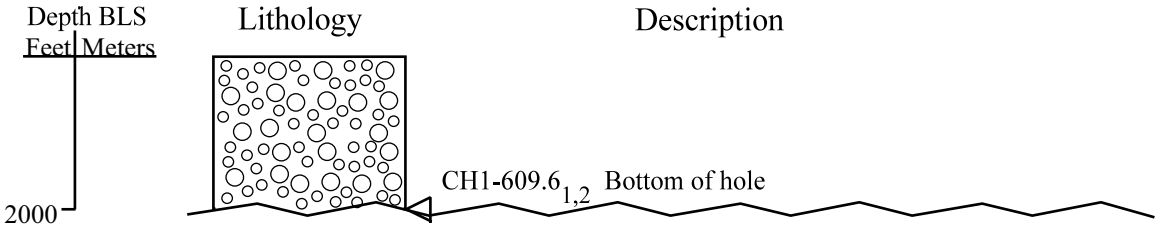
Depth BLS
Feet Meters
Lithology
Description
2000
CH1-609.6 1,2 Bottom of hole

APPENDIX B: PETROGRAPHIC DESCRIPTIONS

This appendix contains petrographic descriptions of 29 thin sections of selected core samples. The thin sections were examined using a Nikon petrographic binocular microscope at Idaho State University. The modal percentages expressed in the descriptions are based on point counts (1,000 counts per thin section) for the first three samples from well 2-2A; all others are based on estimating the percentages by eye using the binocular microscope. Grain size is defined as follows: fine-grained indicates most crystals < 0.5 mm; medium-grained indicates most crystals ≥ 0.5 mm and ≤ 2 mm; and coarse-grained indicates most crystals > 2 mm. Olivine composition was determined using Figure 11.2 of Nesse (1986). Opaques are identified by their shape. Elongate opaques are probably mostly ilmenite (solid solution) and are identified as "ilmenite$_{ss}$". Equant opaques are probably mostly magnetite (solid solution) and are identified as "magnetite$_{ss}$" .

Well 2-2A

2-2A-185.3

An aphyric, medium-grained, equigranular, intergranular, diktytaxitic basalt consisting of hypidiomorphic, randomly oriented, interlocking and intergranular plagioclase laths (~54%), intergranular olivine (~14%), opaques (~9%), and tachylite (~6%), subophitic augite (~15%), and accessory apatite. Plagioclase is euhedral to subhedral, 0.5 - 1.7 mm in maximum dimension, and exhibits moderate normal zoning. Augite is pale brown and varies from 0.5 - 1.5 mm. Olivine is colorless, subhedral to anhedral, and 0.2 - 0.6 mm in maximum dimension, with a negative 2V of ~85°, indicating a composition of ~Fo_{78}. Some olivines have a minor red-brown stain, possibly due to oxidation, along rims and fractures. Opaques are both elongate (~4%, ilmenite$_{ss}$?), 0.4 - 1 mm long, and equant (~5%, magnetite$_{ss}$?), 0.1 - 0.2 mm across. Tachylite is turbid and very dark brown; some has

altered to dark brown clay. The sample consists of ~2% diktytaxitic cavities varying from 0.1 - 1 mm in maximum dimension. All diktytaxitic cavities are filled with dark brown clay.

2-2A-351.6

A sparsely porphyritic, intersertal, vesicular, diktytaxitic, plagioclase and olivine phyric basalt consisting of hypidiomorphic, randomly oriented and interlocking plagioclase laths (~35%), olivine (~13%), subophitic augite (~17%), opaques (~10%), and tachylite (~13%) in a fine grained groundmass. Plagioclase is euhedral to subhedral, 0.5 - 1 mm in maximum dimension, and exhibits moderate normal zoning, except for a few large phenocrysts that exhibit oscillatory zoning. Some plagioclase laths exhibit a "dovetail" texture. Olivine is colorless, subhedral to anhedral, and 0.1 - 1 mm in maximum dimension, with a 2V ~90°, indicating a composition of ~Fo_{84}. Olivine phenocrysts form glomeroporphyritic aggregates. Equant black inclusions in olivines may be spinel. Augite is pale brown and varies from 0.2 - 0.5 mm. Opaques are both elongate (~6%, $ilmenite_{ss}$?), 0.2 - 0.5 mm long, and equant (~4%, $magnetite_{ss}$?), 0.1 - 0.2 mm across. Tachylite is turbid and very dark brown. The sample consists of ~6% round to elongate vesicles varying from 1.5 - 6 mm in maximum dimension and ~6% diktytaxitic cavities varying from 0.1 - 0.9 mm in maximum dimension. Several vesicles are mantled by a zone of fine-grained minerals. Light brown clay coats the walls of some vesicles and fills or partially fills ~40% of the diktytaxitic cavities. Calcite fills a few diktytaxitic cavities and vesicles. There is a minor clay coating on some of the calcite. A clay filled vug contains a single crystal of a mineral that is colorless, has a rectangular habit with perfect cleavage parallel to the long axis, near parallel extinction, moderately high positive relief relative to "balsam", and is biaxial positive. This mineral may be anhydrite.

2-2A-388.8

An aphyric, fine grained, equigranular, intersertal, vesicular, diktytaxitic basalt consisting of hypidiomorphic, randomly oriented and interlocking plagioclase laths (~34%), olivine (~16%), augite (~11%), opaques (~9%), and tachylite (~14%). Plagioclase is euhedral to subhedral, 0.3 - 0.7 mm in maximum dimension, and exhibits moderate normal zoning. Some plagioclase laths exhibit a "dovetail" texture. Augite is pale brown, subhedral to anhedral, and varies from 0.1 - 0.5 mm. Olivine is colorless, subhedral to anhedral, and 0.1 - 0.4 mm in maximum dimension. Many olivines have a minor red-brown stain, possibly due to oxidation. Opaques are both elongate (~4%, $ilmenite_{ss}$?), 0.2 - 0.4 mm long, and equant (~5%, $magnetite_{ss}$?), 0.1 - 0.2 mm across. Tachylite is turbid and very dark brown. The sample consists of ~9% round to elongate vesicles varying from 0.5 - 6 mm in maximum dimension and ~7% diktytaxitic cavities varying from 0.1 - 1 mm in maximum dimension. Several vesicles are mantled by a zone of fine-grained minerals. Minor light brown to light green clay is present in three vesicles.

2-2A-484.3

A sparsely porphyritic, intergranular, vesicular, diktytaxitic, olivine phyric basalt consisting of olivine phenocrysts (~2%), hypidiomorphic, randomly oriented, interlocking and intergranular plagioclase laths (~45%), intergranular olivine (~15%), opaques (~6%), and tachylite (~2%), and subophitic augite (~20%) in a fine grained groundmass. Olivine is colorless, subhedral to anhedral, and 0.1 - 5 mm in maximum dimension, with a negative 2V of ~85°, indicating a composition of ~Fo_{78}. Most olivines have a red-brown stain, possibly due to oxidation, and there is very minor alteration of a few olivines to light brown clay. Olivine phenocrysts form glomeroporphyritic aggregates. Equant black inclusions in the olivines may be spinel. Plagioclase is euhedral to subhedral, 0.1 - 1.2 mm in maximum dimension, and exhibits moderate normal zoning. Augite is pale brown and varies from 0.5 - 1.5 mm. Opaques are both elongate (~4%, $ilmenite_{ss}$?), 0.2 - 0.5 mm long, and equant

(~2%, magnetite$_{ss}$?), 0.1 - 0.2 mm across. Tachylite is turbid and very dark brown. The sample consists of ~3% round to elongate vesicles varying from 0.3 - 6 mm in maximum dimension and ~7% diktytaxitic cavities varying from 0.2 - 2 mm in maximum dimension. A large (6 mm) vesicle is partially filled with calcite, chabazite, and light brown clay. Calcite adheres to the vesicle wall and has a light coating of clay. Clay also coats the remainder of the vesicle. Chabazite forms a coating over the clay. Several other vesicles are filled with calcite or light brown clay. Most (~90%) of the diktytaxitic cavities are completely or partially filled with one or more of the following authigenic minerals: light brown clay, chabazite, fluorapophyllite, calcite, and an unidentified zeolite-like silicate mineral. Clay lines cavities that contain chabazite, fluorapophyllite, and the zeolite-like mineral. Clay does not line cavities filled with calcite, but is sometimes intergrown with the calcite. The zeolite-like mineral has a moderate negative relief relative to fluorapophyllite, is colorless, and has a birefringence of ~0.001. It may be isotropic. The mineral has a radiating habit and is found with fluorapophyllite or chabazite; most frequently it is found with fluorapophyllite. A few cavities contain fluorapophyllite, chabazite, and the zeolite-like mineral. Authigenic minerals in the diktytaxitic cavities are present in the following proportions: chabazite, ~65%; calcite, ~25%; fluorapophyllite, ~7%; light brown clay, ~2%; zeolite-like mineral, ~1%.

2-2A-485.0

A sparsely porphyritic, intergranular, vesicular, diktytaxitic, olivine phyric basalt consisting of olivine phenocrysts (~1%), hypidiomorphic, randomly oriented, interlocking and intergranular plagioclase laths (~45%), intergranular olivine (~9%), opaques (~7%), and tachylite (~3%), subophitic augite (~13%), and chabazite (~10%) in a medium-grained groundmass. Olivine is colorless, subhedral to anhedral, and 0.2 - 1.5 mm in maximum dimension, with a 2V of ~90°, indicating a composition of ~Fo_{84}. Olivine phenocrysts form glomeroporphyritic aggregates. Plagioclase is euhedral to subhedral, 0.5 - 1 mm in

maximum dimension, and exhibits moderate normal zoning. Augite is pale brown and varies from 0.5 - 1.5 mm. Opaques are both elongate (~5%, ilmenite$_{ss}$?), 0.2 - 0.5 mm long, and equant (~2%, magnetite$_{ss}$?), 0.1 - 0.2 mm across. Chabazite is colorless, subhedral to anhedral, and 0.5 - 3 mm in maximum dimension. Tachylite is turbid and very dark brown. There is a single large vesicle, ~15 mm in length, that is lined with chabazite and medium brown clay. The sample consists of ~12% diktytaxitic cavities varying from 0.1 - 1.5 mm in maximum dimension. All diktytaxitic cavities are filled with clays, either completely with medium brown clay, or lined with medium brown clay with spherulitic medium green clay in the center of the cavity. There is a greater abundance of medium brown clay in cavities near the vesicle wall. Plagioclase is moderately to strongly altered to light brown clay near the vesicle wall. Olivines near the vesicle wall are mostly to completely altered to light brown clay; other olivines exhibit incipient alteration to dark brown and dark green clays. There is moderate alteration of tachylite to dark brown clay.

2-2A-681.9

An aphyric, fine grained, inequigranular, intergranular, vesicular, diktytaxitic basalt consisting of hypidiomorphic, randomly oriented, interlocking and intergranular plagioclase laths (~40%), intergranular olivine (~12%), opaques (~11%), and tachylite (~1%), and subophitic augite (~20%). Plagioclase is euhedral to subhedral, 0.2- 1.5 mm in maximum dimension, and exhibits moderate normal zoning. Augite is pale brown and varies from 0.3 - 1 mm. Olivine is subhedral to anhedral and 0.05 - 0.2 mm in maximum dimension. All olivines have a red-brown stain, possibly due to oxidation. Opaques are both elongate (~3%, ilmenite$_{ss}$?), 0.05 - 0.2 mm long, and equant (~8%, magnetite$_{ss}$?), 0.05 - 0.2 mm across. Tachylite is turbid and very dark brown. The sample consists of ~12% irregularly shaped vesicles varying from 0.2 - 4 mm in maximum dimension and ~4% diktytaxitic cavities varying from 0.2 - 1 mm in maximum dimension. Most vesicles and diktytaxitic cavities are filled with light brown clay, calcite, or intergrowths of dark brown clay and

calcite. Light brown clay either completely fills or coats the walls of the vesicles and diktytaxitic cavities. Calcite occurs most frequently in the center of vesicles and diktytaxitic cavities lined by clay. Calcite with dark brown clay intergrowths exhibits a fan texture in some vesicles. All olivine is either partly or completely altered to light brown clay. Much of the tachylite is altered to light brown clay. A fracture is filled with light brown clay.

2-2A-691.1

A porphyritic, intergranular, vesicular, diktytaxitic, augite phyric basalt consisting of ophitic augite (~31%), hypidiomorphic, pilotaxitic, interlocking and intergranular plagioclase laths (~40%), and intergranular olivine (~14%), opaques (~8%), and tachylite (~2%) in a fine grained groundmass. Augite is pale brown and varies from 0.5 - 2.5 mm. Plagioclase is euhedral to subhedral, 0.2- 0.7 mm in maximum dimension, and exhibits moderate normal zoning. Olivine is subhedral to anhedral and 0.1 - 0.5 mm in maximum dimension. Opaques are both elongate (~1%, $ilmenite_{ss}$?), 0.2 - 0.4 mm long, and equant (~7%, $magnetite_{ss}$?), 0.1 - 0.3 mm across. The sample consists of ~2% round to elongate vesicles varying from 0.5 - 3 mm in maximum dimension and ~3% diktytaxitic cavities varying from 0.1 - 0.6 mm in maximum dimension. Vesicles are concentrated at one end of the thin section. All vesicles are filled with dark green, light green, or dark brown clays. Light green and light brown clays are often intergrown. All diktytaxitic cavities are filled with light green and light brown clays, either separately or together. Most olivines are altered to bright green or dark brown clays. There are a few olivine relics. Euhedral pseudomorphs of bright green or dark brown clay after olivine are present. Plagioclase near vesicles is frequently altered to light green and light brown clays. All tachylite is altered to bright green clay.

Well WO2

WO2-401.3

An aphyric, fine grained, inequigranular, intersertal, vesicular, diktytaxitic basalt consisting of hypidiomorphic, randomly oriented and interlocking plagioclase laths (~35%), subophitic augite (~18%), olivine (~15%), opaques (~7%), and tachylite (~8%). Plagioclase is euhedral to subhedral, 0.4 - 1 mm in maximum dimension, and exhibits moderate normal zoning, except for a few large laths that exhibit oscillatory zoning. Augite is pale brown and varies from 0.5 - 1.5 mm. Olivine is colorless, subhedral to anhedral, and 0.2 - 0.7 mm in maximum dimension, with a 2V of ~90°, indicating a composition of ~Fo_{84}. Some olivines have a minor red-brown stain, possibly due to oxidation, along rims and fractures. Equant black inclusions in the olivines may be spinel. Opaques are both elongate (~5%, $ilmenite_{ss}$?), 0.1 - 0.3 mm long, and equant (~2%, $magnetite_{ss}$?), 0.1 - 0.2 mm across. Tachylite is turbid and very dark brown. The sample consists of ~8% round vesicles varying from 0.5 - 4 mm in maximum dimension and ~9% diktytaxitic cavities varying from 0.2 - 1 mm in maximum dimension.

WO2-450.0

An aphyric, fine grained, equigranular, intergranular, diktytaxitic basalt consisting of hypidiomorphic, randomly oriented, interlocking and intergranular plagioclase laths (~40%), intergranular olivine (~17%), opaques (~6%), and tachylite (~1%), and subophitic augite (~20%). Plagioclase is euhedral to subhedral, 0.3 - 0.8 mm in maximum dimension, and exhibits moderate normal zoning. Augite is pale brown and varies from 1 - 2 mm. Olivine is colorless, subhedral to anhedral, and 0.1 - 0.7 mm in maximum dimension, with a 2V of ~90°, indicating a composition of ~Fo_{84}. A few olivines have a minor red-brown stain, possibly due to oxidation, along rims and fractures. Olivine microphenocrysts form glomeroporphyritic aggregates. Opaques are both elongate (~4%, $ilmenite_{ss}$?), 0.2 - 0.5 mm long, and equant (~2%, $magnetite_{ss}$?), 0.1 - 0.2 mm across. Tachylite is turbid and very dark

brown. The sample consists of ~16% diktytaxitic cavities varying from 0.2 - 1 mm in maximum dimension.

WO2-521.5

A seriate porphyritic, vesicular, plagioclase and olivine phyric picrobasalt consisting of randomly oriented and interlocking plagioclase laths (~15%) and olivine (~12%) in a tachylite (~50%) groundmass. Plagioclase is euhedral to subhedral, 0.7- 3 mm in maximum dimension, and exhibits moderate normal zoning. Many phenocrysts are broken. Olivine is subhedral to anhedral and 0.7 - 3 mm in maximum dimension, with a negative 2V of ~85°, indicating a composition of ~Fo_{78}. Phenocrysts are dark red-brown, possibly due to oxidation. Tachylite is black and opaque, with randomly oriented plagioclase microlaths. The sample consists of ~10 % round to irregular vesicles varying from 0.5 - 4 mm in maximum dimension and ~13% anastomosing fractures. Fractures and vesicles are mostly filled with calcite and light brown clay (~85% calcite, ~13% clay). An unidentified, biaxial positive mineral (possibly a zeolite) with low birefringence (< 0.002) and high negative relief relative to "balsam" fills ~2% of fractures.

WO2-525.0

A strongly porphyritic, vesicular, diktytaxitic, plagioclase phyric basalt consisting of hypidiomorphic, randomly oriented and interlocking plagioclase laths (~15%) in a fine grained intersertal groundmass of plagioclase laths (~28%), augite (~15%), olivine (~15%), opaques (~11%), and tachylite (~3%). Plagioclase phenocrysts are euhedral to subhedral, 1 - 5 mm in maximum dimension, and exhibit moderate normal zoning. Groundmass plagioclase laths vary from 0.1 - 0.3 mm in maximum dimension and exhibit moderate normal zoning. Most are weakly to strongly altered to light green clay. Augite is pale brown, subhedral to anhedral, and varies from 0.05 - 0.2 mm. Olivine is subhedral to anhedral and 0.05 - 1 mm in maximum dimension, with a negative 2V of ~85°, indicating a

composition of ~Fo_{78}. All olivine is altered to light green and light brown clays, with a few relics. Plagioclase phenocrysts and pseudomorphs of olivine microphenocrysts form glomeroporphyritic aggregates. Opaques are both elongate (~5%, $ilmenite_{ss}$?), 0.1 - 0.2 mm long, and equant (~6%, $magnetite_{ss}$?), 0.05 - 0.1 mm across. Tachylite is turbid and very dark brown. Some tachylite has altered to light brown clay. The sample consists of ~11% round to elongate vesicles varying from 1 - 4.5 mm in maximum dimension and ~2% diktytaxitic cavities varying from 0.1 - 0.3 mm in maximum dimension. All vesicles are filled with light green and light brown clays and minor calcite. Light brown clay frequently coats the walls of vesicles, with spherulitic light green clay in the middle of the vesicles. Light brown clay within the light green clay has a "caterpillar" texture. Calcite is present in only a few vesicles. Diktytaxitic cavities are all filled with calcite or light brown clay.

WO2-601.2

An aphyric, medium-grained, equigranular, intergranular, diktytaxitic basalt consisting of hypidiomorphic, randomly oriented, interlocking and intergranular plagioclase laths (~45%), intergranular olivine (~10%), opaques (~13%), and tachylite (~1%), subophitic augite (~21%), and accessory apatite. Plagioclase is euhedral to subhedral, 0.7 - 1.5 mm in maximum dimension, and exhibits moderate normal zoning. There is minor alteration of a few plagioclase laths to light brown clay. Fractures in plagioclase laths are filled with light brown clay. Augite is pale brown and varies from 1 - 5 mm. Olivine is subhedral to anhedral and 0.1 - 1.5 mm in maximum dimension, with a negative 2V of ~85°, indicating a composition of ~Fo_{78}. All olivine microphenocrysts (0.5 - 1.5 mm) are altered to light brown and red-brown clays, with a few relics. Less than 1% of the small (0.1 - 0.3 mm) olivines are altered to dark green clay. Opaques are both elongate (~7%, $ilmenite_{ss}$?), 0.2 - 0.7 mm long, and equant (~6%, $magnetite_{ss}$?), 0.1 - 0.3 mm across. Tachylite is turbid and very dark brown. Most tachylite has altered to light green and light brown clays. The sample consists of ~10% diktytaxitic cavities varying from 0.1 - 1.5 mm in maximum

dimension. Diktytaxitic cavities are all filled with light brown or dark green clays or calcite. Calcite is present in minor quantities in cavities lined with light brown clay. Dark green clay is present in minor quantities. Some light brown clay in large cavities has a spherulitic texture. A fracture is filled with calcite and light brown clay.

WO2-1062.7

A seriate porphyritic, vesicular, plagioclase and olivine phyric basalt consisting of hypidiomorphic, randomly oriented and interlocking plagioclase laths (~29%) and olivine (~8%) in a tachylite matrix (~45%). Plagioclase is euhedral to subhedral, 0.5 - 1.5 mm in maximum dimension, and exhibits moderate normal zoning. Some plagioclase is weakly to moderately altered to light brown clay. Olivine is subhedral to anhedral and 0.3 - 1 mm in maximum dimension, with a red-brown stain. All olivine is altered to dark green or red-brown clays. Tachylite is turbid and very dark brown to black with randomly oriented plagioclase microlaths. The sample consists of ~15% irregularly shaped vesicles varying from 0.2 - 3 mm in maximum dimension and ~3% anastomosing fractures. Calcite and dark green and light brown clays fill vesicles and fractures.

WO2-1064.8

A seriate porphyritic, vesicular, diktytaxitic, plagioclase and olivine phyric basalt consisting of hypidiomorphic, randomly oriented and interlocking plagioclase laths (~45%) and olivine (~12%) in a tachylite matrix (~31%). Plagioclase is euhedral to subhedral, 0.5 - 1.7 mm in maximum dimension, and exhibits moderate normal zoning. Most plagioclase is weakly to moderately altered to light green and light brown clays, with the strongest alteration occurring near vesicles and fractures. Olivine is subhedral to anhedral and 0.1 - 0.5 mm in maximum dimension. Olivines have a red-brown stain. Most olivine is weakly to strongly altered to dark green clay, with some red-brown relics present. Tachylite is turbid and very dark brown, with minor alteration to dark green clay at the wall of a vesicle.

The sample consists of ~9% round to elongate vesicles varying from 0.3 - 3 mm in maximum dimension and ~3% diktytaxitic cavities varying from 0.1 - 1 mm in maximum dimension. Vesicles are filled with calcite and dark green and light green clays. Diktytaxitic cavities are filled with dark green clay. Fractures are lined or filled with dark green clay.

Well C1A

C1A-318.2

A seriate porphyritic, intergranular, diktytaxitic, olivine phyric basalt consisting of olivine phenocrysts (~3%), hypidiomorphic, randomly oriented, interlocking and intergranular plagioclase laths (~35%), intergranular olivine (~13%), opaques (~8%), and tachylite (~2%), and subophitic augite (~19%) in a medium-grained groundmass. Olivine is colorless, subhedral to anhedral, and 0.1 - 2 mm in maximum dimension, with a 2V of ~90°, indicating a composition of ~Fo_{84}. Some olivines have a minor red-brown stain, possibly due to oxidation, along rims and fractures. Equant black inclusions in phenocrysts may be spinel. Plagioclase is euhedral to subhedral, 0.5 - 1.5 mm in maximum dimension, and exhibits moderate normal zoning. Augite is pale brown and varies from 1 - 2 mm. Opaques are both elongate (~5%, $ilmenite_{ss}$?), 0.2 - 0.4 mm long, and equant (~3%, $magnetite_{ss}$?), 0.1 - 0.2 mm across. Tachylite is turbid and very dark brown. The sample consists of ~20% diktytaxitic cavities varying from 0.5 - 1.5 mm in maximum dimension.

C1A-363.0

A seriate porphyritic, intergranular, vesicular, diktytaxitic, plagioclase and olivine phyric basalt consisting of hypidiomorphic, randomly oriented, interlocking and intergranular plagioclase laths (~46%), sparse olivine phenocrysts and intergranular olivine (~14%), opaques (~10%), and tachylite (~4%), and subophitic augite (~20%) in a fine grained groundmass. Plagioclase is euhedral to subhedral with phenocrysts (~34%) 0.7 - 2 mm in

maximum dimension and groundmass plagioclase (~12%) 0.1 - 0.2 mm in maximum dimension. Plagioclase exhibits moderate normal zoning, except for a few large phenocrysts that exhibit oscillatory zoning. There is minor filling of fractures in plagioclase laths with light brown clay. Olivine is colorless and subhedral to anhedral, with sparse phenocrysts 0.5 - 2 mm in maximum dimension and groundmass olivines 0.1 - 0.3 mm in maximum dimension, with a 2V of ~90°, indicating a composition of ~Fo_{84}. Olivines have partially to completely altered to dark green and light brown clays. Augite is pale brown and varies from 0.4 - 0.8 mm. Opaques are both elongate (~4%, $ilmenite_{ss}$?), 0.2 - 0.4 mm long, and equant (~6%, $magnetite_{ss}$?), 0.05 - 0.2 mm across. Tachylite is turbid and very dark brown; some has altered to dark green and light brown clays. The sample consists of ~3% round to elongate vesicles varying from 0.2 - 2 mm in maximum dimension and ~3% diktytaxitic cavities varying from 0.1 - 1.5 mm in maximum dimension. All vesicles are filled with dark green and light brown clays. Dark green clays frequently have a spheriodal texture and are more abundant than light brown clays. Light brown clay coats the walls of vesicles filled with dark green clay, and is also present as "caterpillars" within the dark green clay in many vesicles. All diktytaxitic cavities are filled with dark green and light brown clays.

C1A-400.4

A porphyritic, intergranular, diktytaxitic, olivine phyric basalt consisting of olivine phenocrysts (~3%), hypidiomorphic, pilotaxitic and intergranular plagioclase (~40%), intergranular olivine (~12%), opaques (~8%), and tachylite (~2%), and subophitic augite (~19%) in a fine-grained groundmass. Olivine is colorless and subhedral to anhedral with phenocrysts 0.5 - 1.5 mm in maximum dimension and groundmass olivines 0.1 - 0.3 mm in maximum dimension. Some olivines have a minor red-brown stain, possibly due to oxidation. Equant black inclusions in olivine phenocrysts may be spinel. Plagioclase is euhedral to subhedral, 0.2 - 0.4 mm in maximum dimension, and exhibits moderate normal

zoning. Some plagioclase laths exhibit a "dovetail" texture. Augite is pale brown and varies from 0.4 - 1 mm. Opaques are both elongate (~6%, ilmenite$_{ss}$?), 0.1 - 0.2 mm long, and equant (~2%, magnetite$_{ss}$?), 0.05 - 0.1 mm across. Tachylite is turbid and very dark brown. The sample consists of ~16% diktytaxitic cavities varying from 0.2 - 1 mm in maximum dimension.

C1A-493.3

An aphyric, medium-grained, equigranular, intergranular, diktytaxitic basalt consisting of hypidiomorphic, randomly oriented, interlocking and intergranular plagioclase (~47%), intergranular olivine (~18%), opaques (~10%), and tachylite (~2%), subophitic augite (~19%), and accessory apatite. Plagioclase is euhedral to subhedral, 0.5 - 2 mm in maximum dimension, and exhibits moderate normal zoning. Augite is pale brown and varies from 1 - 2 mm. Olivine is colorless, subhedral to anhedral, and 0.3 - 1.5 mm in maximum dimension, with a 2V of ~90°, indicating a composition of ~Fo_{84}. Many olivines have a minor red-brown stain, possibly due to oxidation, along rims and fractures. A few exhibit minor alteration to light green clay. Equant black inclusions in olivine phenocrysts may be spinel. Olivines form glomeroporphyritic aggregates. Opaques are both elongate (~5%, ilmenite$_{ss}$?), 0.2 - 0.6 mm long, and equant (~5%, magnetite$_{ss}$?), 0.1 - 0.2 mm across. Tachylite is turbid and very dark brown. The sample consists of ~4% diktytaxitic cavities varying from 0.2 - 1 mm in maximum dimension. All the cavities are filled with medium brown and dark green clays. Some cavities are filled with only medium brown clay. Others are lined with medium brown clay and the cavity centers are filled with spherulitic dark green clay. A narrow fracture is filled with medium brown clay.

C1A-540.8

An aphyric, fine grained, equigranular, vesicular, diktytaxitic basaltic trachyandesite consisting of hypidiomorphic, pilotaxitic and interlocking plagioclase laths (~25%), olivine (~10%), and opaques (~5%) in a tachylite groundmass (~45%). Plagioclase is euhedral to subhedral, 0.1 - 0.2 mm in maximum dimension, and exhibits moderate normal zoning. A single large (1.1 mm) plagioclase xenocryst has inclusions of brown glass and a boxy cellular texture. Olivine is colorless, subhedral to anhedral, and 0.05 - 0.1 mm in maximum dimension, with a negative 2V of ~80°, indicating a composition of ~Fo_{65}. Opaques are equant ($magnetite_{ss}$?), 0.01 - 0.03 mm across. Tachylite is turbid and very dark brown. The sample consists of ~9% round to irregular vesicles varying from 2 -20 mm in maximum dimension and ~6% diktytaxitic cavities varying from 0.05 - 2 mm in maximum dimension. A large vesicle ~20 mm long is coated with a colorless opal-like material that is isotropic, has moderate negative relief relative to "balsam", and has randomly oriented fractures. There are inclusions of a light brown material within the colorless opal-like material that looks like clay, but is also isotropic. The colorless opal-like material lining the vesicle has a thin coating of the light brown material. Some diktytaxitic cavities are empty, but most are filled with a light brown opal-like material.

C1A-541.7

An aphyric, fine grained, equigranular, vesicular, diktytaxitic basaltic trachyandesite consisting of hypidiomorphic, pilotaxitic and interlocking plagioclase laths (~35%), olivine (~10%), and opaques (~5%) in a tachylite groundmass (~43%). Plagioclase is euhedral to subhedral, 0.1 - 0.2 mm in maximum dimension, and exhibits moderate normal zoning. Olivine is colorless, subhedral to anhedral, and 0.05 - 0.1 mm in maximum dimension, with a negative 2V of ~80°, indicating a composition of ~Fo_{65}. Opaques are equant ($magnetite_{ss}$?), 0.01 - 0.03 mm across. Tachylite is turbid and very dark brown. The sample consists of sparse vesicles varying from 0.1 - 2.5 mm in maximum dimension and ~7%

diktytaxitic cavities varying from 0.1 - 0.5 mm in maximum dimension. The vesicles are filled with a light brown opal-like material that is isotropic, has moderate negative relief relative to "balsam", and has randomly oriented fractures. All diktytaxitic cavities are filled with the light brown opal-like material or with light brown clay.

Well ANL-1

Thin sections from 10 samples from ANL-1 were examined. The samples were collected from the following depths: 132.7, 147.1, 182.9, 189.7, 519.5, 530.4, 541.0, 550.2, 573.2, and 582.2 meters. None of the samples exhibited evidence of alteration. Authigenic mineralization was limited to precipitation of minor amounts of calcite and clay. All of the samples were fresh appearing basalt, except sample ANL-1-573.2, which is a trachyandesite. The following descriptions are of representative samples.

ANL-1-519.5

An aphyric, medium-grained, equigranular, intergranular, diktytaxitic basalt consisting of hypidiomorphic, randomly oriented, interlocking and intergranular plagioclase laths (~40%), intergranular olivine (~13%), opaques (~5%), and tachylite (~8%), and subophitic augite (~16%). Plagioclase is euhedral to subhedral, 0.5 - 1 mm in maximum dimension, and exhibits moderate normal zoning. Some laths exhibit a "dovetail" texture. Augite is pale brown and varies from 0.5 - 1 mm. Olivine is colorless, subhedral to anhedral and 0.2 - 0.5 mm in maximum dimension, with a negative 2V of ~85°, indicating a composition of ~Fo_{78}. Most olivines have a red-brown stain, possibly due to oxidation, along rims and fractures. Opaques are both elongate (~3%, $ilmenite_{ss}$?), 0.2 - 0.4 mm long, and equant (~2%, $magnetite_{ss}$?), 0.1 - 0.2 mm across. Tachylite is turbid and very dark brown. The sample consists of ~18% diktytaxitic cavities varying from 0.5 - 1.5 mm in maximum dimension. Calcite fills ~10% of the diktytaxitic cavities.

ANL-1-550.2

A strongly porphyritic, vesicular, diktytaxitic, plagioclase and olivine phyric basalt consisting of hypidiomorphic, randomly oriented and interlocking plagioclase laths (~25%), olivine (~15%), and opaques (~7%) in a tachylite groundmass (~40%). Plagioclase is euhedral to subhedral, 1 - 3 mm in maximum dimension, and exhibits moderate normal zoning. Olivine is colorless, subhedral to anhedral, and 0.3 - 1 mm in maximum dimension, with a 2V ~90°, indicating a composition of ~Fo_{84}. Equant black inclusions in olivine phenocrysts may be spinel. Some olivines have a minor red-brown stain, possibly due to oxidation, along rims and fractures. Phenocrysts of plagioclase and olivine form glomeroporphyritic aggregates. Opaques are both elongate (~5%, $ilmenite_{ss}$?), 0.2 - 0.4 mm long, and equant (~2%, $magnetite_{ss}$?), 0.1 - 0.2 mm across. Tachylite is turbid and very dark brown at one end of the thin section, and opaque and black at the other end. The sample is from a flow margin and the black tachylite is found at the end of the thin section nearest the flow margin. The sample consists of ~6% round to elongate vesicles varying from 0.2 - 3 mm in maximum dimension and ~7% diktytaxitic cavities varying from 0.2 - 2 mm in maximum dimension.

ANL-1-573.2

A porphyritic, vesicular, plagioclase, olivine and augite phyric trachyandesite consisting of hypidiomorphic, randomly oriented plagioclase laths (~3%), augite (~1%), olivine (~1%), opaques (~1%), and accessory apatite in a felty fine-grained groundmass. Plagioclase is euhedral to subhedral, 0.3 - 3 mm in maximum dimension, and exhibits moderate normal zoning. Several plagioclase phenocrysts exhibit a boxy cellular texture, and a few have fritted rims. Augite is pale brown, subhedral to anhedral, and varies from 0.2 - 0.6 mm. Olivine is colorless, subhedral to anhedral, and 0.4 - 1.2 mm in maximum dimension, with a negative 2V ~80°, indicating a composition of ~Fo_{65}. Some olivine phenocrysts have a minor red-brown stain, possibly due to oxidation, along rims and fractures. Opaques are

equant (magnetite$_{ss}$?), 0.1 - 0.3 mm across. A single quartz xenocryst rimmed by augite is present in the sample. The felty groundmass consists of plagioclase microlaths, tachylite, equant opaques, and olivine. The sample consists of ~2% round to elongate vesicles varying from 0.4 - 2.8 mm in maximum dimension. Three small vesicles are filled with calcite.

ANL-1-582.2

An aphyric, medium-grained, equigranular, intergranular, vesicular, diktytaxitic basalt consisting of hypidiomorphic, randomly oriented, interlocking and intergranular plagioclase laths (~35%), intergranular olivine (~12%), opaques (~9%), and tachylite (~7%), and subophitic augite (~17%). Plagioclase is euhedral to subhedral, 0.5 - 1 mm in maximum dimension, and exhibits moderate normal zoning. Augite is pale brown and varies from 0.7 - 1.5 mm. Olivine is colorless, subhedral to anhedral, and 0.2 - 0.6 mm in maximum dimension, with a 2V ~90°, indicating a composition of ~Fo_{84}. Most olivines have a red-brown stain, possibly due to oxidation, along rims and fractures. Opaques are both elongate (~5%, ilmenite$_{ss}$?), 0.3 - 0.5 mm long, and equant (~4%, magnetite$_{ss}$?), 0.1 - 0.2 mm across. Tachylite is turbid and very dark brown. The sample consists of ~8% irregular vesicles varying from 1 - 5 mm in maximum dimension and ~12% diktytaxitic cavities varying from 0.5 - 2 mm in maximum dimension.

Well CH-1

Thin sections from 22 samples from CH-1 were examined. The samples were collected from the following depths: 368.6, 458.4, 478.8, 486.2, 494.0, 501.7, 507.0, 509.2, 514.1, 520.2, 526.5, 530.0, 532.4, 534.9, 543.2, 548.3, 551.7, 568.2, 579.8, 588.8, 600.2, and 609.6 meters. The rocks examined from this corehole vary in composition from basaltic andesite to rhyolite, with silica contents ranging from 54.8 to 75.9 weight percent. Only one of the samples exhibited minor evidence of alteration. Authigenic mineralization

was limited to precipitation of minor amounts of clay in twelve samples and precipitation of minor to moderate amounts of siderite in eight samples, calcite in four samples, and an unidentified golden-brown mineral in four samples. The following descriptions are of representative samples.

CH1-368.6

A sparsely porphyritic rhyolite consisting of hypidiomorphic plagioclase laths (~2%), quartz (~2%), sanidine (~2%), orthopyroxene (~1%), and opaques (~1%) in a light gray devitrified lithoidal matrix. Plagioclase is euhedral to subhedral, 0.3 - 1.5 mm in maximum dimension, and exhibits moderate normal zoning. Quartz is subhedral to anhedral, equant, and 0.2 - 1 mm across. Sanidine is subhedral to anhedral, mostly equant, and varies from 0.3 - 1 mm. Orthopyroxene is pale green, subhedral to anhedral, and 0.2 - 0.7 mm in maximum dimension. Opaques are both elongate (<1%, $ilmenite_{ss}$?), 0.2 - 1 mm long, and equant (<1%, $magnetite_{ss}$?), 0.3 - 0.7 mm across. Plagioclase, orthopyroxene, and opaques are present as individual phenocrysts and in glomeroporphyritic aggregates.

CH1-507.0

A sparsely porphyritic, vesicular trachydacite consisting of hypidiomorphic plagioclase laths (~2%), orthopyroxene (~2%), olivine (~1%), and accessory quartz in a tachylite groundmass. Plagioclase is euhedral to subhedral, 0.2 - 1 mm in maximum dimension, and exhibits moderate normal zoning. Orthopyroxene is pale green, subhedral to anhedral, and 0.2 - 0.6 in maximum dimension. Plagioclase and orthopyroxene are present as individual phenocrysts and also form glomeroporphyritic aggregates. Olivine is colorless, subhedral to anhedral, and 0.2 - 0.4 mm in maximum dimension, with a negative 2V ~60°, indicating a composition of ~Fo_{27}. Some olivine phenocrysts have a minor red-brown stain, possibly due to oxidation, along fractures. Quartz is subhedral to anhedral, equant, and 0.2 - 0.8 mm across. Most phenocrysts have fritted rims. Tachylite is turbid and very dark brown.

There is minor alteration of tachylite to light brown clay along the walls of vesicles. The sample consists of two elongate vesicles, one ~8 mm long and the other ~2.5 mm long. Small aggregates of radiating prisms of tridymite are located on the walls of both vesicles. The larger vesicle is filled with tridymite, pale yellow-brown siderite, calcite, and clay. Siderite lines the vesicle walls and has a weak fan shaped habit. The central portion of the vesicle is filled with calcite with dark brown clay intergrowths. Between the siderite and this calcite is a clay free calcite. The small vesicle is filled with siderite with a weak fan shaped habit. A fracture is filled with light brown clay.

CH1-526.5

A porphyritic, vesicular andesite consisting of hypidiomorphic plagioclase laths (~2%), orthopyroxene (~6%), and augite (~1%) in a tachylite groundmass. Plagioclase is euhedral to subhedral, 0.3 - 0.8 mm in maximum dimension, and exhibits moderate normal zoning. Orthopyroxene is pale green, subhedral to anhedral, and 0.4 - 1.2 mm in maximum dimension. Plagioclase and orthopyroxene are present as individual phenocrysts and as glomeroporphyritic aggregates. Augite is pale brown, subhedral to anhedral, and 0.1 - 0.6 mm in maximum dimension. Augite is present as individual phenocrysts and in mafic blebs of small (<0.2 mm) crystals. Augite mantles some orthopyroxene phenocrysts. Tachylite is turbid and very dark brown. The sample consists of <1% round to elongate vesicles varying from 0.4 - 0.6 mm in maximum dimension. One vesicle is filled with pale yellow-brown siderite and small aggregates of radiating prisms of tridymite. Siderite is present in one glomeroporphyritic aggregate of orthopyroxene and plagioclase. The siderite may be the product of alteration of orthopyroxene (as it appears to pseudomorph some of the orthopyroxene) or it may have precipitated from solution.

CH1-548.3

A porphyritic, vesicular basaltic andesite consisting of hypidiomorphic plagioclase laths (~6%), orthopyroxene (~8%), and augite (~2%) in a tachylite groundmass. Plagioclase is euhedral to subhedral, 0.3 - 1 mm in maximum dimension, and exhibits moderate normal zoning. Orthopyroxene is pale green, subhedral to anhedral, and 0.2 - 0.6 mm in maximum dimension. Plagioclase and orthopyroxene are present as individual phenocrysts and as glomeroporphyritic aggregates. Augite is pale brown, subhedral to anhedral, and 0.05 - 0.4 mm in maximum dimension. Augite is present as individual phenocrysts and in mafic blebs of small (<0.2 mm) crystals. Tachylite is turbid and very dark brown. The sample consists of ~2% round to elongate vesicles varying from 0.2 - 0.6 mm in maximum dimension. Most vesicles are either filled with pale yellow-brown siderite or lined with siderite. In some vesicles siderite forms concentric rings around a dark brown core. In other vesicles siderite forms concentric rings outward from the vesicle wall. Minor tridymite is present in one vesicle. A fracture is filled with calcite and siderite. Siderite lines both sides of the fracture and exhibits a rhombohedral habit with growth rings. Calcite fills the center of the fracture.

CH1-588.8

A sparsely porphyritic, vesicular trachyandesite consisting of hypidiomorphic plagioclase laths (~1%) and accessory opaques and augite in a tachylite groundmass. Plagioclase is euhedral to subhedral, 0.5 - 3 mm in maximum dimension, and exhibits moderate normal zoning. Augite is pale brown, subhedral to anhedral, and varies from 0.3 - 0.4 mm. Opaques are equant (magnetite$_{ss}$?), 0.1 - 0.2 mm across. Tachylite is turbid and very dark brown. The sample consists of ~8% round to elongate vesicles varying from 0.3 - 3.5 mm in maximum dimension. Many vesicles are completely or partially filled with pale yellow-brown siderite, light brown clay, and/or an unidentified golden-brown mineral. The unidentified mineral has moderate negative relief relative to “balsam” and appears to be

isotropic, though some may be very weakly birefringent. It is associated with siderite or clay in some vesicles, and present with neither siderite nor clay in other vesicles. When the unidentified mineral and siderite are present in the same vesicle, the unidentified mineral lines the vesicle and the siderite is in the center of the vesicle. When the unidentified mineral and light brown clay are present in the same vesicle, the clay lines the vesicle and the unidentified mineral is in the center of the vesicle.

APPENDIX C: ANALYTICAL DATA

This appendix contains bulk geochemical and trace element data from ICP-AES and INAA analyses, data from electron microprobe analyses, and data from X-ray powder diffraction analyses. Mineral structural data presented in the electron microprobe data tables were calculated using the computer software MinTab, version 1.1 (Carroll, 1991).

ulk rock analytical data

orehole	2-2A	2-2A	2-2A	2-2A	2-2A	2-2A	2-2A	2	2
ample epth meters	18 .3	3 1.6	388.8	8 .3	8 .0	681.9	691.1	01.3	0.0
a or elements wt.									
i 2	8.0	.11	.38	6. 1	.21	8.60	6. 6	.2	6.8
i 2	2.66	3.29	2.9	2.29	2.30	2.20	2.26	2.01	2.68
Al2 3	1 .11	13.9	1 . 8	1 .91	1 .10	1 . 9	1 . 9	1 .1	1 .1
Fe	13.33	1 . 8	1 .3	12.93	12.80	12.83	13.13	12.	13.
n	0.20	0.22	0.21	0.20	0.20	0.16	0.20	0.19	0.20
g	.38	.1	.22	9.2	9.31	.6	9.00	9. 0	.88
Ca	9.39	9.8	9.62	10. 8	10.20	11.63	10.12	10.0	9. 8
a2	2.61	2. 3	2.	2. 0	2.28	2. 2	2.3	2. 1	2.6
2	0.61	0.6	0. 0	0. 1	0.20	0. 2	0.31	0.	0. 2
P2	0.6	0. 6	0.	0.39	0. 1	0. 1	0.39	0. 3	0.
riginal otal	98. 6	98.9	9 .09	9 .23	98.18	9 . 6	9 . 2	98.3	9 . 3
g	0. 9	0. 66	0. 3	0. 61	0. 6	0. 39	0. 0	0. 2	0. 0
race elements ppm									
c	28.6	31.3	30.0	29.9	29.0	31.3	33.3	31.2	29.
Cr	216	21	22	281	2 9	1 8	161	3 8	209
Co	.0	6 .9	.2	.8	.8	60.	.	68.	.
i	90	120	110	1 0	90	30	110	110	100
		8			6	22		9.	6
r	333	320	32	282	230	2 0	20	2 3	2 8
Cs	0.1	0.39	0.2	0.30	0.08	30.2	1. 1	0.11	0.10
a	388	2	3	231	218	2	19	33	308
a	31.	30.	21.	1 .6	1 .0	1 .1	1 .1	18.	18.6
Ce	1.1	69.9	1.9	33.0	3 .	36.8	3 .1	2.	2.6
d	28	39	30	19	19	19	19	26.9	31.1
m	.	8.86	.09	.90	. 2	. 3	.86	.0	.91
u	2. 1	3.3	2.6	1.8	1. 6	1.82	1.90	1.9	2.2
	1.26	1.66	1.31	0.8	0.	0.9	0.9	0.91	1.2
	3. 6	.12	3. 0	2.6	2. 0	2.8	2.	2. 2	2.98
u	0.	0.	0.	0.38	0.3	0.38	0.36	0. 0	0. 8
r	2 0	29	2 1	1	1 9	1	1 8	191	201
Hf	.9	. 2	6.21	3.	3.68	3. 2	3.8	.66	.06
a	1. 0	1. 3	1.00	0. 2	0.82	0.83	0.	0.92	0.99
h	1.22	0.93	0. 2	0.66	0. 9	0. 9	na	1.0	0.93
	0.8	1.0	0.9	0.2	0.	1.2	0.	0.2	0.
	na	na	na	na	na	na	na	na	na
n	138	19	1	109	110	106	96	1 9	1 2

enotes all Fe expressed as Fe
xides normalized to 100
na not analyzed for this constituent

ulk rock analytical data

orehole	2	2	2	2	2	C1A	C1A	C1A	C1A
ample epth meters	21.	2 .0	601.2	1062.	106 .8	318.2	363.0	00.	93.3
a or elements wt.									
i 2	3.86	6. 9	.30	9.0	9.6	.	.1	.30	6. 0
i 2	3.39	3.3	2. 3	1. 6	1.32	2.0	2.	2.38	2.6
Al2 3	1 .11	1 .2	1 .96	1 .32	1 .12	1 .16	1 .18	1 .99	1 .9
Fe	1 . 3	1 .12	13.09	11.80	11.2	12.26	13.69	12.83	13.
n	0.2	0.18	0.19	0.1	0.21	0.19	0.19	0.19	0.20
g	6.12	8.	8.31	. 9	.89	9.09	.86	8.6	8.6
Ca	13. 0	8.92	10.20	10.99	9. 0	10. 2	9.38	9.9	10.23
a2	2.2	1.98	2. 9	2. 6	2.6	2.	2. 8	2.	2. 0
2	0.26	0. 0	0.	0.3	0.29	0. 0	0.	0. 9	0.38
P2	0.82	0.6	0. 6	0.29	0.19	0. 3	0.63	0. 6	0. 1
riginal otal	9 . 9	96.80	9 .63	9 .62	98.6	99.93	96. 3	96.8	9 . 9
g	0. 1	0. 02	0. 31	0. 66	0. 6	0. 69	0. 06	0. 6	0. 3
race elements ppm									
c	31.	31.3	33	29.9	26.9	3 .	28.1	33.3	3 .0
Cr	23	2 2	29	212	196	1	190	19	3 3
Co	.1		8	3.	.	68.0	1.3	63.6	66.
i	80	90	90	na	na	na	90	na	na
			8	8	9.2	19		1	11
r	26	223	230	238	230	238	2	2	26
Cs	0.11	0.1	0.03	0.21	0.16	0.1	0.13	0.21	0.1
a	0	369	30	21	21	2	3 0	322	26
a	2	20.6	18.3	1 .9	1 .1	1 .6	2 .2	2 .3	1 .1
Ce	2.3	0.2	3.9	38.3	31.1	0.1	61.	3.1	3 .9
d	36.6	2 .2	2 .	21.2	19.3	2	3	29	2
m	.29		. 8	.	.11	. 1	6.90	6.28	. 8
u	2. 6	2. 6	2.2	1.36	1.3	2.0	2.3	2.22	2.0
	1.26	1.13	1.1	0.89	0.	0.61	1.22	1.2	0.9
	.28	3.	2.9	3.1	2.3	2.88	3.2	3.08	2.8
u	0.62	0. 8	0. 8	0. 2	0.3	0.39	0. 6	0.	0.39
r	266	260	20	1 3	133	1 9	2 1	213	1 8
Hf	6. 6	6.68	.3	.	3.63	.81	. 1	.36	. 8
a	1.1	1.1	0.96	0. 6	0. 6	1.23	1.39	1.3	0. 9
h	1.22	0. 8	0.3	2.0	1. 6	0.98	0. 1	1.09	0. 0
	0.	0.3	na	1.2	1.	0.	0.2	1.2	0.9
	na	na	na	na	na	na	na	na	na
n	18	18	1 2	0	102	112	1 8	1 0	13

enotes all Fe expressed as Fe
xides normalized to 100
na not analyzed for this constituent

ulk rock analytical data

orehole	C1A	A -1	A -1	A -1	A -1	A -1	A -1	A -1	A -1
ample epth meters	1.	132.	1 .1	182.9	189.	306.6	8.2	30.	1.0
a or elements wt.									
i 2	2.	6.8	6.88	6.9	.	6.83	6.10	6.66	6.93
i 2	2.22	3. 0	3.	3.00	3.19	3.0	3.08	2.	2.30
Al2 3	12.9	1 .66	1 . 1	1 .26	1 . 2	1 .8	1 .61	1 . 8	1 . 6
Fe	16.22	1 .	1 .81	13.	1 .00	13.98	1 .23	12. 6	12.26
n	0.3	0.22	0.23	0.21	0.21	0.21	0.22	0.19	0.19
g	2.20	6.90	6.32	.1	6.6	.29	.80	8. 8	8.82
Ca	6.31	9.31	9.29	9.	9.	9. 3	10.23	10.36	10. 0
a2	3. 0	2.	2.	2.69	2. 6	2.69	2.	2.	2. 1
2	2.	0.	1.02	0.86	0.83	0.6	0. 6	0.	0.
P2	1.11	0.69	0.8	0.68	0.9	0. 1	0. 3	0.	0.36
riginal otal	9 .0	99.20	98.83	99.01	98.28	98. 6	98.36	98.12	9 .96
g	0.19	0. 60	0. 32	0. 81	0. 8	0. 82	0. 9	0. 9	0. 62
race elements ppm									
c	0.1	30.3	na	28.9	30.0	30.1	31.	32.2	32.
Cr	16.1	16	na	1 9	1 2	196	209	286	33
Co	18.	1.	na	0.8	.	2.	6.	0.	2.0
i	na	30	na	0	60	60	80	30	0
	9	16.6	na	18.1	20.	22.6	10.6	10.	13.
r	2	329	329	323	313	306	300	266	2 3
Cs	0.6	0.20	na	0. 6	0.20	0.2	0.16	0.22	0.28
a	1 00	8	02	82	0	38	32	2 3	2 0
a	1 6	29.	na	29.	.0	28.	28.	18.6	1 .8
Ce	331	6 .8	na	66.	96.0	63.1	60.	2.2	3 .6
d	18	33.	na	33.3	.	33.	28.8	22.1	19
m	36.2	8.31	na	8.0	10.30	8.00	. 3	.	.9
u	10.	3.1	na	2.89	3. 2	2.8	2.6	2.13	1.81
	.8	1.	na	1.28	1. 2	1.3	1.09	0.86	0.96
	18.60	3.90	na	3.62	.1	3. 8	3.3	2.90	2. 8
u	2.33	0. 1	na	0. 9	0. 1	0. 1	0. 2	0. 3	0.36
r	13 0	320		291	3 0	2	2 0	181	1 9
Hf	.2	.80	na	.12	8.0	6.3	.80	. 3	.01
a	8. 6	1. 0	na	1. 1	2.06	1.60	1.29	0.99	0.9
h	9.06	1.21	na	1.31	2.61	1. 9	0.62	0.91	1.0
	.0	0.	na	1.0	1.	0.6	1.3	0.8	0.6
	na	.1	2.	2.0	9.0	3.	38.6	32.1	30.
n	00	1 1	na	1 3	1 1	162	1 3	88	122

enotes all Fe expressed as Fe
xides normalized to 100
na not analyzed for this constituent

ulk rock analytical data

orehole	A -1	A -1	A -1	CH-1	CH-1	CH-1	CH-1	CH-1	CH-1
ample epth meters	0.2	3.2	82.2	368.6	.2	8.	8.8	86.2	9 .0
a or elements wt.									
i 2	6.21	61.	.10	.88	2. 0	6 .	1. 2	0.01	6 .9
i 2	3.1	1.10	2. 1	0.20	0. 2	1.00	0.61	0. 8	1.03
Al2 3	1 . 8	1 .82	1 .38	12.19	12.	12.	12.6	12.66	12.86
Fe	1 .8	9.08	12.98	2.1	3. 8	. 8	3.82	.	. 2
n	0.21	0.2	0.21	0.0	0.0	0.09	0.06	0.06	0.06
g	. 6	0.81	.6	0.06	0. 9	1.9	0. 8	1.2	1. 6
Ca	9.90	3. 0	10.3	0.38	1.	3.02	1.32	2.0	2.
a2	2.	3. 3	2. 3	3.91	3. 2	3.08	3. 6	3.66	3.63
2	0.	. 8	0.61	.16	.98	.81	.1	.81	.32
P2	0. 2	0.38	0.69	0.03	0.11	0.22	0.12	0.1	0.22
riginal otal	100.39	96.8	9 .6	98. 3	98.0	99.02	96.38	9 .3	9 .81
g	0. 3	0.13	0. 12	0.0 0	0.289	0.388	0.266	0.329	0.366
race elements ppm									
c	29.2	2 .3	32.1	0.	na	9.2	.	6.	9.0
Cr	198	.8	23	11.	na	82.3	3 .6	2.1	.9
Co	66.	.1	0.6	18.	na	1.3	28.	2 .8	30.3
i	120	0	90	na	na	na	na	na	na
	2.0	100	1 .2	21	na	1 6	193	180	1
r	32	1 9	22	10	39	88	8	66	90
Cs	0.23	1.	0.2	1. 8	na	2.66	1.63	1.	3.12
a	39	603	2	2	9	1 2	90	112	1
a	2 .2	132	30.3	108	na	8 .9	9 .	91.3	82.0
Ce	62.3	280	6 .3	221	na	180	221	20	193
d	3	121	0	10	na	80.	89.	.	8.6
m	8.0	2 .8	.81	2 .	na	20.6	22.6	21.2	19.6
u	2.90	10.6	2.61	0. 3	na	1. 8	1.10	1.2	1.33
	1.29	.1	1. 0	.8	na	3.89	.19	.9	.3
	3.3	1 .6	.02	19.	na	16.2	16.	1 .9	1 .
u	0. 8	1.8	0. 6	2.1	na	1.81	2.16	1.9	1.82
r	2	2160	332	69	0	03	13	09	396
Hf	6.2	0.1	. 2	20.1	na	16.2	18.0	1 .3	18.1
a	1.31	6.6	1.29	1 .1	na	10.2	9.69	8.99	9.18
h	0.3	1 .3	1.31	26.1	na	19.3	23.	21.	19.8
	0.	.3	na	8.8	na	.2	.9	6.8	6.9
	na	1 1	na	na	na	na	na	na	na
n	23 .	2 6	138	8	na	3	na	na	na

enotes all Fe expressed as Fe
xides normalized to 100
na not analyzed for this constituent

ulk rock analytical data

orehole	CH-1	CH-1	CH-1	CH-1	CH-1	CH-1	CH-1	CH-1	CH-1
ample epth meters	01.	09.2	1 .1	20.2	26.	30.0	32.	3 .9	3.2
a or elements wt.									
i 2	6 .92	6 .22	6 . 6	61. 1	61.	6.90	6. 1	6.21	.86
i 2	1.31	1.29	1.32	1.66	1.66	2.16	2.18	2.2	2.2
Al2 3	13.18	13.1	13.0	13.31	13.31	13.66	13. 3	13.69	13. 6
Fe	6.69	6.32	6.6	8.02	8.21	10.3	10.28	10.	10.60
n	0.11	0.10	0.11	0.13	0.13	0.16	0.1	0.16	0.21
g	2.	2. 1	2.66	3.	3.33	. 8	.66	.	.82
Ca	3. 2	3. 0	3.9	.9	. 3	6. 6	6. 9	6.69	6.83
a2	3.16	3. 8	3.2	3.1	3.3	3.02	3.0	2.89	2.8
2	.1	.06	.1	3.2	3.13	2.21	2.	2.33	2.28
P2	0.29	0.29	0.30	0.3	0.3	0. 9	0. 8	0. 0	0. 2
riginal otal	98.	96.81	96.	99.12	99.13	9 . 3	99.89	9 .9	98.01
g	0.39	0. 0	0. 16	0. 3	0. 20	0. 1	0.	0.	0. 8
race elements ppm									
c	11.1	11.3	11.	1 .0	20.	20.3	20.2	na	20.8
Cr	8.1	69.0	.3	99.9	12	121	126	na	132
Co	2 .	28.	2 .1	30.6	38.9	.	2.3	na	0.6
i	na	na	na	na	na	na	na	na	na
	1 2	1	1	11	6	3	81	na	69
r	11	11	11	1	1	199	200	206	212
Cs	2.09	1.83	2.22	1.9	1. 1	1.39	1.1	na	1. 0
a	182	1 9	186	2 0	233	300	29	300	319
a	.1	6.9	.1	69.3	.	.8	.8	na	.
Ce	169	1 8	169	1	126	131	128	na	123
d	1	3	0	6		61	62	na	
m	18.6	18.6	18.2	16.9	13.	1 .0	1 .	na	13.3
u	1. 0	1.61	1.	2.02	2. 6	2. 9	2.29	na	2. 9
	.18	.20	.03	3.8	2.93	3.13	2.92	na	2.8
	12.1	13.2	12.	11.	8. 6	8. 9	8.90	na	.
u	1.61	1. 0	1.62	1.	1.11	1.1	1.13	na	1.08
r	393	393	389	383	38	360	363	3 3	3
Hf	1 .	1 .2	1 .3	1 .1	11.9	13.1	12.6	na	11.1
a	.	.0	.0	6.	.8	. 1	.1	na	. 1
h	16.2	16.	1 .9	1 .2	9.1	10.	10.2	na	8.3
	6.0	6.	6.	.	3.6	3.	.1	na	3.2
	na	na	na	na	na	na	na	na	na
n	na	na	na	na	na	na	na	na	na

enotes all Fe expressed as Fe
xides normalized to 100
na not analyzed for this constituent

ulk rock analytical data

orehole	CH-1	CH-1	CH-1	CH-1	CH-1	CH-1	CH-1
ample epth meters	8.3	1.	68.2	9.8	88.8	600.2	609.6
a or elements wt.							
i 2	.81	.	.80	.03	60.62	60. 2	69.29
i 2	2.30	2.29	2.29	2.21	1.1	1.1	0. 0
Al2 3	13.80	13.62	1 . 8	1 .13	1 . 9	1 .	1 .0
Fe	10.6	10.	10.31	10.69	9.39	9.82	.
n	0.1	0.18	0.23	0.19	0.2	0.23	0.10
g	. 8	.93	.	.9	0.93	0.98	0.1
Ca	6. 3	6.9	.28	. 1	.36	3. 2	1. 1
a2	3.08	2.91	3.0	2. 6	3. 9	3.8	3.6
2	2.1	2. 1	2.22	2.1	.	.63	6.02
P2	0. 3	0.	0. 0	0.	0.	0. 3	0.06
riginal otal	9 .	9 .83	96.89	9 .38	9 .92	9 .92	9 .
g	0.	0. 0	0. 0	0. 3	0.1 0	0.1 1	0.0 9
race elements ppm							
c	21.	21.	23.0	na	23.8	2 .	6.0
Cr	133	138	1	na	. 9	8.8	10.
Co	1.0	2.3	3.3	na	11.	10.8	8.3
i	na	na	na	na	na	na	na
	3	6	62	na	98	8	1 3
r	213	210	21	20	193	188	28
Cs	1.06	1.0	1.81	na	2.06	0.88	2.16
a	31	311	32	310	2	33	1 0
a	6.	.1	0.0	na	128	12	21
Ce	12	122	109	na	269	2 3	0
d	9			na	1 1	1 0	206
m	1 .2	13.	12.9	na	2 .	2 .9	3 .8
u	2.3	2.33	2.3	na	10.2	10.3	6.26
	2.92	2. 0	2.6	na	. 2	.92	6.03
	8.	8.0	.29	na	13.6	13.6	18.
u	1.0	1.08	1.00	na	1.90	1.96	2. 8
r	3 9	363	3	33	2226	226	100
Hf	11.8	11.	10.8	na	3.	.	30.9
a	.63	.6	.1	na	6.2	6.	10.0
h	9.29	9.18	8.28	na	13.9	1 .2	2 .8
	.0	3.	3.0	na	.	.8	.9
	na	na	na	na	na	na	na
n	na	na	na	na	na	na	na

enotes all Fe expressed as Fe
xides normalized to 100
na not analyzed for this constituent

Clay micropro e data

ample	2-2A- 8 cl1	2-2A- 8 cl2	2-2A- 8 cl3	2-2A-682cl1l	2-2A-682cl2l
i 2	.1	3.	6.91	.6	2.0
i 2	0.00	0.00	0.00	0.00	0.00
Al2 3	6.8	6. 1	.29	3.09	.
Fe2 3	2 .8	2 .82	18.08	2 .91	36.06
n	0.00	0.00	0.00	0.00	0.00
g	13.12	12.39	1 .62	6.62	. 6
Ca	3.0	2.	2. 3	1.9	1.86
a2	0.28	0.28	0.2	0.22	0.11
2	0.33	0.61	0.3	0.60	0.23
Cr2 3	0.00	0.00	0.00	0.00	0.00
r	0.02	0.0	0.00	0.00	0.02
otal	93.68	91.86	90.22	93.06	91.
tructural formula calculated on the asis of 22 oxygens					
i	6. 6	6.39	6. 8	. 8	6.3
Al	1.16	1.13	1.2	0. 1	0.98
Fe3	2.6	2.86	1.9	2.62	.11
g	2.80	2. 2	3.1	1.38	1.30
Ca	0.	0. 3	0. 2	0.30	0.30
a	0.08	0.08	0.0	0.06	0.03
	0.06	0.12	0.06	0.11	0.0
i	0.00	0.00	0.00	0.00	0.00
n	0.00	0.00	0.00	0.00	0.00
Cr	0.00	0.00	0.00	0.00	0.00
r	0.00	0.00	0.00	0.00	0.00
otal Cat	13. 0	13. 2	13.69	12.	13.13

ample num er indicates well depth of sample and mineral grain analyzed e.g. 2-2A- 8 cl1 well 2-2A sample depth is 8 meters cl1 is mineral grain 1 from this sample denotes color of clay

rown l light rown d dark rown g right green dg dark green

xide analyses in weight percent

Clay micropro e data

ample	2-2A-682cl3l	2-2A-682cl3l	2-2A-691cl1dg	2-2A-691cl1dg	2-2A-691cl1dg
i 2	2.33	0.	39.02	3 .8	3 .22
i 2	0.00	0.01	0.00	0.00	0.00
Al2 3	6. 1	6. 1	10.09	10. 0	10.26
Fe2 3	23.0	23.98	13. 9	16. 2	21.66
n	0.00	0.00	0.00	0.00	0.00
g	10.11	9.13	13. 0	16.83	1 .
Ca	2.36	2.38	0.00	0.00	0.00
a2	0.16	0.19	0.02	0.06	0.03
2	0.30	0.3	0.01	0.01	0.00
Cr2 3	0.00	0.00	0.00	0.01	0.00
r	0.00	0.00	0.00	0.00	0.00
otal	9 .8	93.	6.3	81.9	82.6
tructural formula calculated on the asis of 22 oxygens					
i	.19	.11	6. 3	6.02	.69
Al	1.0	1.11	1.99	1.9	1.9
Fe3	2.39	2. 3	1.	2.00	2.63
g	2.0	1.91	3.3	3.99	3. 3
Ca	0.3	0.36	0.00	0.00	0.00
a	0.0	0.0	0.01	0.02	0.01
	0.0	0.06	0.00	0.00	0.00
i	0.00	0.00	0.00	0.00	0.00
n	0.00	0.00	0.00	0.00	0.00
Cr	0.00	0.00	0.00	0.00	0.00
r	0.00	0.00	0.00	0.00	0.00
otal Cat	13.1	13.13	13.61	1 .00	1 .02

ample num er indicates well depth of sample and mineral grain analyzed e.g. 2-2A- 8 cl1 well 2-2A sample depth is 8 meters cl1 is mineral grain 1 from this sample denotes color of clay

rown l light rown d dark rown g right green dg dark green

xide analyses in weight percent

Clay micropro e data

ample	2-2A-691cl1dg	2-2A-691cl2 g	2-2A-691cl2d	2-2A-691cl3	2-2A-691cl d
i 2	38.82	3 .60	33. 2	39.1	.6
i 2	0.00	0.00	0.01	0.10	0.0
Al2 3	9.20	10. 0	11.80	9.8	6.3
Fe2 3	1.	2 . 8	26.16	18.62	19.6
n	0.00	0.00	0.00	0.00	0.00
g	11. 6	1 .93	1 .69	1 . 3	1 . 3
Ca	0.00	0. 8	0.	1.19	1. 3
a2	0.03	0.0	0.08	0.16	0.11
2	0.01	0.03	0.03	0.08	0.0
Cr2 3	0.01	0.00	0.01	0.01	0.00
r	0.00	0.00	0.00	0.00	0.00
otal	61. 1	89.38	89.	86. 0	89.0
tructural formula calculated on the asis of 22 oxygens					
i	.	.28	.10	.96	6. 0
Al	2.11	1.8	2.12	1.	1.10
Fe3	0.26	2.96	3.00	2.13	2.1
g	3.3	.08	.02	3.96	3.
Ca	0.00	0.10	0.09	0.19	0.2
a	0.01	0.01	0.02	0.0	0.03
	0.00	0.01	0.01	0.02	0.01
i	0.00	0.00	0.00	0.01	0.00
n	0.00	0.00	0.00	0.00	0.00
Cr	0.00	0.00	0.00	0.00	0.00
r	0.00	0.00	0.00	0.00	0.00
otal Cat	13.28	1 .31	1 .36	1 .10	13.69

ample num er indicates well depth of sample and mineral grain analyzed e.g. 2-2A- 8 cl1 well 2-2A sample depth is 8 meters cl1 is mineral grain 1 from this sample denotes color of clay

rown l light rown d dark rown g right green dg dark green

xide analyses in weight percent

Clay micropro e data

ample	2-2A-691cl dg	2-2A-691cl dg	2-2A-691cl6	2-2A- 16ol1c	2-2A- 16ol2c
i 2	28.91	3 . 0	.28	.9	9.0
i 2	0.00	0.00	0.12	0.11	0.02
Al2 3	.82	.69	6. 2	.0	3.28
Fe2 3	.00	18.2	18.18	23.6	23.91
n	0.00	0.00	0.13	0.18	0.1
g	13.20	16.3	16.26	9.62	11.66
Ca	0. 9	0.88	1.0	1.91	1. 6
a2	0.10	0.13	0.20	0.22	0.1
2	0.0	0.0	0.1	0.1	0.13
Cr2 3	0.00	0.00	0.00		
r	0.00	0.00	0.00		
otal	3.6	8.09	86.6	8 .89	89.9
tructural formula calculated on the asis of 22 oxygens					
i	6.	.91	6.66	.19	.18
Al	1.60	1.	1.1	0. 1	0.
Fe3	0.88	2.3	2.06	2.6	2.6
g	.60	.16	3.6	2.1	2.
Ca	0.1	0.16	0.1	0.31	0.23
a	0.0	0.0	0.06	0.06	0.0
	0.01	0.01	0.03	0.03	0.03
i	0.00	0.00	0.01	0.01	0.00
n	0.00	0.00	0.02	0.02	0.02
Cr	0.00	0.00	0.00	0.00	0.00
r	0.00	0.00	0.00	0.00	0.00
otal Cat	1 .0	1 .1	13. 8	13.1	13.2

ample num er indicates well depth of sample and mineral grain analyzed e.g. 2-2A- 8 cl1 well 2-2A sample depth is 8 meters cl1 is mineral grain 1 from this sample denotes color of clay

rown l light rown d dark rown g right green dg dark green

xide analyses in weight percent

Clay micropro e data

ample	2-2A- 16ol3	c1a 1cl1l	c1a 1cl1l	c1a 1cl1l
i 2	.66	. 6	68.02	.
i 2	0.1	0.00	0.06	0.01
Al2 3	.6	6.2	. 1	6.91
Fe2 3	2 . 1	1 .20	11.60	18.68
n	0.11	0.00	0.00	0.00
g	9.10	0.00	2.39	3.61
Ca	1.9	1.99	1.32	1. 0
a2	0.19	0.16	0.08	0.22
2	0.1	0.1	0.09	0.28
Cr2 3		0.00	0.00	0.00
r		0.00	0.00	0.00
otal	88.	80. 2	8 .91	6.96
tructural formula calculated on the asis of 22 oxygens				
i	.12	8. 6	9.23	. 9
Al	0.82	1.1	0. 1	1.36
Fe3	2.	2.00	1.19	2.3
g	2.03	0.00	0. 8	0.90
Ca	0.31	0.33	0.19	0.30
a	0.0	0.0	0.02	0.0
	0.03	0.03	0.02	0.06
i	0.02	0.00	0.01	0.00
n	0.01	0.00	0.00	0.00
Cr	0.00	0.00	0.00	0.00
r	0.00	0.00	0.00	0.00
otal Cat	13.13	12.01	11.8	12.62

ample num er indicates well depth of sample and mineral grain analyzed e.g. 2-2A- 8 cl1 well 2-2A sample depth is 8 meters cl1 is mineral grain 1 from this sample denotes color of clay

rown l light rown d dark rown g right green dg dark green

xide analyses in weight percent

Cha azite micropro e data

ell 2-2A zeolite analyses

ample	8 z6	8 z6	8 z6	8 z8	8 z13	8 z13	8 z13
i 2	0.96	6.32	1. 3	3.8	1.9	2.8	0.8
Al2 3	2 .39	23.26	2 .12	23.63	2 .1	2 . 1	23.86
Fe2 3	0.0	0.0	0.08	0.13	0.03	0	0.0
g	0	0	0	0	0	0	0
Ca	.2	. 6	.12	6. 2	6.88	6.8	6.6
a2	2.2	3.	2.36	2.92	2. 8	2. 9	2. 2
2	. 9	.6	. 1	.1	.16	.29	.32
r	0.01	0	0	0.06	0	0	0
a	0.	0. 2	0.	0.0	0. 8	0.3	0.06
H2	.61	. 9	.91	6.6	.8	.	8. 9
otal	98.8	99.9	99.28	98.89	99.06	100.0	9 . 9
tructural Formula 2 oxygens							
i	.	8.1	.	.9	.8	.82	. 8
Al	.3	3.9	.28	.11	.2	.26	.3
Fe3	0.01	0	0.01	0.02	0	0	0.01
Ca	1.1	0.89	1.1	1.03	1.11	1.08	1.09
a	0.66	1.0	0.69	0.83	0. 2	0.	0.
	1.12	0.86	1.1	0.9	0.99	1	1.0
r	0	0	0	0.01	0	0	0
a	0.03	0.03	0.03	0	0.03	0.02	0
otal Cat	1 .02	1 .8	1	1 .9	1 .92	1 .92	1 .96

ample	8 z1	8 z1	8 z2	8 z2	8 z3	8 z
i 2	1.69	1. 3	1.83	3.38	3.03	2. 1
Al2 3	21.92	22.1	23. 9	23.6	23.6	22.88
Fe2 3	0	0	0.03	0	0	0.01
g	0	0	0	0	0	0
Ca	8. 1	8. 9	6.8	6.98	6.8	6.0
a2	2.62	2.38	1.82	1. 1	1.98	2.0
2	1.8	1.88	.3	.69	.11	.1
r	1.83	1.8	0	0.01	0	0
a	0.0	0.0	0.2	0.19	0.28	0.2
H2	0	0	0	0	0	0
otal	88.3	88.6	89.6	91.61	90.9	88.86
tructural Formula 2 oxygens						
i	.96	.9	.88	.9	.93	8.01
Al	3.98		.21	.1	.1	.11
Fe3	0	0	0	0	0	0
Ca	1.39	1. 1	1.12	1.11	1.1	0.99
a	0. 8	0. 1	0.	0. 9	0.	0.6
	0.36	0.3	1.0	1.08	0.98	1
r	0.16	0.1	0	0	0	0
a	0	0	0.02	0.01	0.02	0.01
otal Cat	1 .63	1 .6	1 .8	1 . 8	1 . 6	1 .

ample num er indicates depth of sample and mineral grain analyzed e.g. 8 z6
sample depth is 8 meters z6 is mineral grain 6 from this sample
xide analyses in weight percent
H2 calculated from oxygen remaining after assigning oxygens to oxides

Fluorapophyllite micropro e data

ell 2-2A fluorapophyllite analyses

ample	8 z1a1	8 z1a2	8 z1a3	8 z2a1	8 z2a2	8 z a1	8 z a2	8 z a1
i 2	.26	1.62	0.81	2. 1	0. 3	1.86	1.08	1.90
Al2 3	1.20	1.19	0. 3	0.90	1. 0	1.0	0. 2	1. 3
Fe2 3	0.08	0.08	0.1	0.11	0.0	0.1	0.18	0.10
g	0.00	0.00	0.00	0.00	0.00	0.00	0.00	0.00
Ca	23. 8	23.6	23.20	23. 8	23. 8	23. 0	23.2	23.
a2	0.2	0.21	0.38	0.21	0.32	0.28	0.21	0.26
2	3.96	.0	3.32	.19	3.	.01	3.61	.08
r	0.01	0.00	0.03	0.00	0.00	0.00	0.00	0.00
a	0.08	0.00	0.00	0.08	0.00	0.00	0.0	0.00
F	na	na	1.91	na	2.2	na	2.1	na
otal	83. 3	80.83	80. 3	81. 8	81. 9	80.8	81.2	81. 0

tructural Formula on the asis of 21 H F

i	8.00	.8	.98
Al	0.1	0.26	0.13
Fe3	0.02	0.01	0.02
g	0.00	0.00	0.00
Ca	3.91	3.92	3.89
a	0.12	0.10	0.06
	0.6	0.69	0. 2
r	0.00	0.00	0.00
a	0.00	0.00	0.00
F	0.9	1.10	1.0
otal Cat	12.8	12.8	12.80

ample	8 z a2	8 z a3	8 z6a3	8 z6a	8 z a1	8 z a2	8 z9a1	8 z11a1
i 2	1.12	0.90	2.0	1.10	2.62	0.81	3.10	2. 3
Al2 3	0.83	1.0	0.93	0. 0	0.88	0.	0.8	0.9
Fe2 3	0.09	0.0	0.26	0.09	0.22	0.19	0.2	0.1
g	0.00	0.00	0.00	0.00	0.00	0.00	0.00	0.00
Ca	2 .06	23.83	23.1	23.96	23.18	23.08	23.19	23.6
a2	0.2	0.28	0.	0.32	0.28	0.2	0.	0.2
2	3.66	3. 2	3.88	3.63	3.9	3.	3.9	.2
r	0.00	0.00	0.03	0.00	0.00	0.00	0.00	0.0
a	0.0	0.00	0.03	0.00	0.0	0.00	0.00	0.00
F	1.90	2.10	na	1.98	na	2.23	na	na
otal	81.98	81.9	80. 9	81.	81.19	80.	81. 9	82.0

tructural Formula on the asis of 21 H F

i	.9	.90	.9	.9
Al	0.1	0.19	0.13	0.1
Fe3	0.01	0.01	0.01	0.02
g	0.00	0.00	0.00	0.00
Ca	.00	3.96	3.99	3.88
a	0.08	0.08	0.10	0.08
	0. 3	0.	0. 2	0.69
r	0.00	0.00	0.00	0.00
a	0.00	0.00	0.00	0.00
F	0.93	1.03	0.9	1.10
otal Cat	12.91	12.89	12.90	12. 8

ample num er indicates depth of sample and mineral grain analyzed e.g. 8 z1a1 sample depth is 8 meters z1 is mineral grain 1 from this sample a1 is analysis 1 of this mineral grain

xide analyses in weight percent

na not analyzed for this constituent

eolite-like mineral micropro e data

2-2A zeolite-like mineral analyses

ample	lm 8 z3	lm 8 z3	lm 8 z3	lm 8 z10	lm 8 z10	lm 8 z10	lm 8 z12	lm 8 z13
i 2	6 .28	6 . 3	1.08	3.8	6 . 3	66.83	63.8	66.3
Al2 3	18. 6	19. 1	20.01	20.89	18.82	19.08	1 .63	18. 3
Fe2 3	0.13	0.09	0.0	0.11	0.13	0.11	0.08	0.0
g	0	0.02	0.02	0	0	0	0.02	0
Ca	3. 6	2.32	2.16	2.8	3.2	3.9	1.9	2.2
a2	3.28	.88	3.62	3.98	.36	2.88	.6	.
2	3. 8	.29	3.1	1.0	3.62	3.21	.8	.
r	0.01	0	0	0.02	0.02	0	0	0.03
a	0.12	0.12	0	0.06	0	0.03	0	0
H2	.9	2. 8	1. 2	-2.13	. 9	3.08	3.1	.
otal	101.8	101.6	101.62	100. 1	100.3	99.1	96.12	100. 6
tructural Formula 8 oxygens								
i	3.03	3.01	3.0	3.0	3.00	3.03	3.03	3.03
Al	1.00	1.02	1.02	1.02	1.03	1.02	0.99	1.01
Fe3	0.00	0.003	0.002	0.003	0.00	0.00	0.003	0.002
g	0	0.002	0.001	0	0	0	0.002	0
Ca	0.18	0.11	0.10	0.13	0.16	0.19	0.10	0.11
a	0.29	0. 2	0.30	0.32	0.39	0.2	0. 3	0.39
	0.21	0.2	0.1	0.06	0.21	0.19	0.29	0.26
r	0	0	0	0	0	0	0	0.001
a	0.002	0.002	0	0.001	0	0.001	0	0
otal Cat	. 1	.81	.66	.60	. 9	.68	.8	.80

ample num er indicates depth of sample and mineral grain analyzed e.g. 8 z3 sample depth is 8 meters z3 is mineral grain 3 from this sample

xide analyses in weight percent

H2 calculated from oxygen remaining after assigning oxygens to oxides

ilica micropro e data

ells CH1 and C1A silica analyses

ample	CH1- 0 z1	CH1- 0 z1	CH1- 0 z1	CH1- 0 z2	CH1- 0 z2
i 2	100.66	101.06	101. 1	101.29	101.33
Al2 3	0. 9	0.63	0. 9	0.66	0.63
Fe2 3	0.6	0. 8	0.6	0.60	0.
g	0.01	0.00	0.00	0.01	0.01
a	0.00	0.00	0.00	0.00	0.00
r	0.00	0.00	0.02	0.00	0.00
Ca	0.02	0.02	0.02	0.00	0.03
a2	0.32	0.3	0.29	0.3	0.30
2	0.09	0.0	0.06	0.12	0.0
otal	102.32	102.61	102.9	103.03	102.92

ample	C1A- 1op3	C1A- 1min1	C1A- 1min1	C1A- 1min2
i 2	92.6	9 . 9	93.91	92.12
Al2 3	0.01	0.03	0.01	0.00
Fe2 3	0.0	0.0	0.00	0.02
g	0.2	0.00	0.00	0.00
a	0.00	0.08	0.00	0.02
r	0.00	0.02	0.02	0.0
Ca	0. 3	0.31	0.32	0. 6
a2	0.03	0.01	0.01	0.01
2	0.00	0.00	0.00	0.01
otal	93. 1	9 .09	9 .2	92.69

ample num er indicates well depth of sample and mineral grain analyzed e.g. CH1- 0 z1 well CH1 sample depth is 0 meters z1 is mineral grain 1 from this sample

xide analyses in weight percent

Car onate micropro e data

ells CH-1 and 2-2A car onate minerals

ample	CH1- 0 -cal1	CH1- 0 -cal1	CH1- 0 -cal2	CH1- 0 -cal3	CH1- 0 -cal
ineral	iderite	iderite	iderite	Calcite	Calcite
i 2	0.00	0.01	0.00	0.00	0.01
Al2 3	0.00	0.00	0.00	0.00	0.00
Fe	9.69	0.02	1.11	.83	2.68
g	0.26	0.2	0. 2	6. 9	1. 9
Ca	. 8	. 0	3.6	6. 1	.19
a2	0.01	0.0	0.03	0.01	0.02
2	0.00	0.00	0.00	0.00	0.00
r	0.00	0.00	0.00	0.00	0.06
a	0.00	0.00	0.01	0.00	0.00
otal	.	.8	.3	8.3	61.

ample	CH1- 0 -cal	CH1- 0 -cal6	2-2A-691-arag1	2-2A-691-arag2
ineral	Calcite	Calcite	Aragonite	Aragonite
i 2	0.00	0.00	0.01	0.0
Al2 3	0.00	0.02	0.02	0.00
Fe	6.89	6.	0.0	0.01
g	6.02	6.21	0.00	0.00
Ca	36.	3.61	33. 8	38.81
a2	0.0	0.02	0.01	0.0
2	0.00	0.00	0.00	0.01
r	0.01	0.01	0. 9	0.6
a	0.00	0.01	0.12	0.02
otal	9. 0	6. 2	3 .29	39.60

ample num er indicates well depth of sample and mineral grain analyzed e.g. CH1- 0 -cal1 well CH1 sample depth is 0 meters cal1 is mineral grain 1 from this sample

xide analyses in weight percent

Feldspar micropro e data

ell 2-2A feldspar analyses

ample	16pl1c	16pl1r	16pl2c	16pl2r	16pl3c	16pl3r	16px2	91pl1c
ineral	P	P	P	P	P	P	P	P
i 2	2.	3.62	2.12	2.08	2.92	3.09	2.21	0. 8
Al2 3	30.1	29. 0	30.28	29. 6	30.19	29.	29.30	29. 0
Fe2 3	0. 6	0. 8	0. 1	0.89	0.81	0.8	0.	0.
g	0.08	0.0	0.11	0.0	0.13	0.06	0.0	0.11
Ca	13. 2	13.18	13.9	13. 3	13.9	13. 9	12.60	13.98
a2	3. 0	.00	3.	3.	3. 8	3. 8	.31	3.3
2	0.22	0.2	0.1	0.2	0.19	0.26	0.28	0.1
r	0.0	0.01	0.10	0.01	0.10	0.08		0.06
a	0.00	0.00	0.00	0.00	0.00	0.00		0.00
otal	101. 1	101. 9	100.99	100.10	101.8	101.3	99. 1	98.88
tructural formula calculated on the asis of 8 oxygens								
i	2.3	2. 0	2.3	2.3	2.3	2.38	2.38	2.3
Al	1.60	1.	1.61	1. 9	1. 9	1.	1. 8	1.62
Fe3	0.03	0.03	0.02	0.03	0.03	0.03	0.03	0.03
g	0.01	0.00	0.01	0.00	0.01	0.00	0.00	0.01
Ca	0.66	0.63	0.6	0.66	0.6	0.6	0.62	0.69
a	0.32	0.3	0.31	0.33	0.31	0.33	0.38	0.30
	0.01	0.01	0.01	0.01	0.01	0.02	0.02	0.01
a	0.00	0.00	0.00	0.00	0.00	0.00	0.00	0.00
otal Cat	.99	.99	.99	.99	.99	.99	.01	.99
Al ite	32.3	3 .91	31.39	32.92	31.39	33.1	3 .61	29.93
Anorthite	66.3	63.66	6 . 2	6 . 1	6 . 2	6 .3	60. 9	69.23
rthoclase	1.28	1. 3	0.89	1.3	1.09	1. 8	1.61	0.8

ell 2-2A feldspar analyses

ample	91pl1r	91pl2c	91pl2r	91pl3c	91pl3r	120pl1c	120pl1r	120pl2c
ineral	P	P	P	P	P	P	P	P
i 2	1.	1. 3	1.80	2.02	3.90	2.3	2.	1.
Al2 3	29. 2	29.9	29.8	30.12	29.22	29.26	29.39	30.03
Fe2 3	0. 3	0. 6	0.80	0.68	0.80	1.0	0. 6	0.63
g	0.10	0.08	0.08	0.10	0.13	0.3	0.1	0.1
Ca	13. 0	1 .06	13. 8	1 .09	12.9	13.8	13. 3	1 .12
a2	3.60	3.	3.60	3.	.2	3. 3	3.6	3.39
2	0.19	0.1	0.19	0.1	0.22	0.31	0.18	0.1
r	0.02	0.09	0.0	0.0	0.08	0.08	0.03	0.0
a	0.00	0.00	0.00	0.00	0.00	0.00	0.00	0.22
otal	99.00	100.0	100.1	100. 3	101. 3	100.69	100.2	100. 0
tructural formula calculated on the asis of 8 oxygens								
i	2.3	2.3	2.36	2.3	2. 1	2.3	2.38	2.3
Al	1. 9	1.61	1.60	1.61	1.	1. 6	1.	1.61
Fe3	0.03	0.03	0.03	0.02	0.03	0.0	0.03	0.02
g	0.01	0.01	0.01	0.01	0.01	0.02	0.01	0.01
Ca	0.66	0.69	0.6	0.68	0.62	0.6	0.66	0.69
a	0.32	0.30	0.32	0.31	0.3	0.30	0.32	0.30
	0.01	0.01	0.01	0.01	0.01	0.02	0.01	0.01
a	0.00	0.00	0.00	0.00	0.00	0.00	0.00	0.00
otal Cat	.99	.99	.99	.99	.99	.99	.98	.99
Al ite	32.3	30.36	31.	31.02	36. 6	30. 0	32.61	30.03
Anorthite	66. 0	68.68	6 .1	68.16	62.00	6 .	66.3	69.1
rthoclase	1.13	0.9	1.11	0.83	1.2	1.83	1.0	0.8

ample num er indicates depth of sample and mineral grain analyzed e.g. 16pl1c sample depth is 16 meters pl1 is mineral grain 1 from this sample c denotes analysis of mineral grain core

xide analyses in weight percent P Plagioclase r rim of mineral grain c core of mineral grain

Feldspar micropro e data

ell 2-2A feldspar analyses

ample	120pl2r	120pl3c	120pl3r	129pl1c	129pl1r	129pl2c	129pl2r	129pl3c
ineral	P	P	P	P	P	P	P	P
i 2	1. 9	2. 1	.31	3.9	.2	.0	.2	3.6
Al2 3	29.81	30.03	28.	28. 3	26.82	29.3	29.13	29.
Fe2 3	0. 9	0.61	0.8	0. 1	0.8	0.6	0.6	0. 6
g	0.1	0.13	0.18	0.1	0.0	0.11	0.10	0.06
Ca	1 .1	1 .03	12. 9	12.60	10.16	13.01	12.	13.1
a2	3.38	3.	.26	.3	.	.21	.6	.0
2	0.12	0.13	0.20	0.23	0.	0.2	0.2	0.22
r	0.02	0.0	0.03	0.03	0.08	0.08	0.02	0.10
a	0.03	0.00	0.0	0.00	0.00	0.1	0.02	0.00
otal	99.83	101.0	101.23	100. 6	101.18	101.89	102.6	101. 2
tructural formula calculated on the asis of 8 oxygens								
i	2.3	2.3	2. 3	2. 3	2.	2. 1	2.	2. 0
Al	1.60	1. 9	1. 2	1. 3	1. 1	1.	1. 2	1. 6
Fe3	0.02	0.02	0.03	0.02	0.03	0.02	0.02	0.03
g	0.01	0.01	0.01	0.01	0.01	0.01	0.01	0.00
Ca	0.69	0.68	0.61	0.61	0. 9	0.62	0. 9	0.63
a	0.30	0.31	0.3	0.38	0.	0.3	0. 0	0.3
	0.01	0.01	0.01	0.01	0.03	0.01	0.02	0.01
a	0.00	0.00	0.00	0.00	0.00	0.00	0.00	0.00
otal Cat	.99	.99	.98	.99	.98	.99	.00	.99
Al ite	29.98	31.28	3 . 1	3 .93	.99	36. 3	39. 6	3 .30
Anorthite	69.32	6 .99	61.33	60. 3	9.32	62.19	8.92	63.
rthoclase	0. 1	0.	1.16	1.33	2.69	1.38	1. 2	1.26

ell 2-2A feldspar analyses

ample	129pl3r	1 pl1c	1 pl1r	1 pl2c	1 pl2r	1 pl3c	1 pl3r	219pl1c
ineral	P	P	P	P	P	P	P	P
i 2	. 3	2.8	. 1	2. 9	2.0	2. 0	3.69	3. 0
Al2 3	26. 1	28.91	2 .88	29.21	29.20	28.8	28.18	2 .92
Fe2 3	0. 1	0.60	0. 3	0.63	0.8	0. 3	0.83	0.92
g	0.09	0.00	0.00	0.00	0.00	0.00	0.00	0.00
Ca	10.13	12.23	11.3	12.	12. 2	12.33	11. 9	10.86
a2	.61	.02	.6	3.90	3. 6	.0	. 8	.81
2	0. 8	0.21	0.2	0.20	0.18	0.20	0.28	0.26
r	0.0	0.09	0.09	0.11	0.0	0.0	0.11	0.0
a	0.00				0.09			
otal	101. 0	98.91	99.3	98.99	98. 0	98.61	99.36	98.
tructural formula calculated on the asis of 8 oxygens								
i	2. 6	2. 2	2. 8	2. 0	2.39	2. 1	2.	2.
Al	1. 0	1. 6	1. 0	1. 8	1. 8	1. 6	1. 2	1. 1
Fe3	0.02	0.02	0.03	0.02	0.03	0.03	0.03	0.03
g	0.01	0.00	0.00	0.00	0.00	0.00	0.00	0.00
Ca	0. 8	0.60	0.	0.61	0.62	0.61	0. 8	0. 3
a	0. 8	0.36	0. 1	0.3	0.3	0.36	0. 0	0. 3
	0.03	0.01	0.02	0.01	0.01	0.01	0.02	0.02
a	0.00	0.00	0.00	0.00	0.00	0.00	0.00	0.00
otal Cat	.98	.9	.98	.98	.9	.98	.99	.99
Al ite	8.6	36.8	1.9	3 .	3 .81	36. 6	0.09	3.80
Anorthite	8. 8	61.90	6.	63.0	6 .10	62.06	8.2	.6
rthoclase	2.	1.26	1.60	1.20	1.09	1.18	1.6	1.

ample num er indicates depth of sample and mineral grain analyzed e.g. 16pl1c sample depth is 16 meters pl1 is mineral grain 1 from this sample c denotes analysis of mineral grain core

xide analyses in weight percent P Plagioclase r rim of mineral grain c core of mineral grain

Feldspar micropro e data

ell 2-2A feldspar analyses

ample	219pl1r	219pl2c	219pl2r	219pl3c	219pl3r	8 pl1	8 pl2	8 pl1c
ineral	P	P	P	P	P	P	P	P
i 2	3. 2	0.	6.12	1.16	2.08	3.2	.12	1. 9
Al2 3	28.20	30. 2	26. 3	29.69	29.01	29.12	28.39	29.21
Fe2 3	0.9	0.8	0.81	0.	0.81	0. 8	1.01	0.8
g	0.00	0.00	0.00	0.00	0.00	0.09	0.11	0.00
Ca	11.31	13.88	9.66	12.80	12. 0	13.06	11.93	13.20
a2	. 8	3.1	. 0	3.38	3.86	.03	.8	3.
2	0.20	0.10	0.33	0.11	0.1	0.16	0.21	0.1
r	0.09	0.06	0.0	0.0	0.06	0.08	0.12	0.1
a						0.00	0.00	
otal	98.8	99.03	99.20	9 .9	98.	100. 9	101. 6	98.89
tructural formula calculated on the asis of 8 oxygens								
i	2.	2.33	2.	2.3	2. 0	2. 1	2. 6	2.38
Al	1. 2	1.6	1. 3	1.62	1. 8	1.	1. 9	1. 9
Fe3	0.03	0.03	0.03	0.03	0.03	0.03	0.03	0.03
g	0.00	0.00	0.00	0.00	0.00	0.01	0.01	0.00
Ca	0. 6	0.68	0.	0.6	0.62	0.63	0.	0.6
a	0. 1	0.28	0. 8	0.30	0.3	0.3	0. 2	0.3
	0.01	0.01	0.02	0.01	0.01	0.01	0.01	0.01
a	0.00	0.00	0.00	0.00	0.00	0.00	0.00	0.00
otal Cat	.98	.98	.98	.96	.98	.99	.00	.99
Al ite	1.	28.9	9.	32.09	3 .	3 . 2	1.9	33.6
Anorthite	.01	0.	8.2	6 .23	63.	63.	6.83	6 .
rthoclase	1.23	0.60	1.9	0.69	0.92	0.9	1.22	0.88

ell 2-2A feldspar analyses

ample	8 pl1r	8 pl2c	8 pl2r	8 pl3c	8 pl3r	61 pl1c	61 pl1r	61 pl2c
ineral	P	P	P	P	P	P	P	P
i 2	3. 2	2.82	6.16	2. 6	3.60	2.2	.	.3
Al2 3	2 . 3	29.0	26. 8	29.	28.82	29.18	2 . 0	26.81
Fe2 3	1. 3	0.80	1.0	0. 6	0. 6	0. 6	0. 3	0.8
g	0.00	0.00	0.00	0.00	0.00	0.00	0.00	0.00
Ca	10.	12. 9	9.9	12.6	11.92	13.01	8. 9	10. 2
a2	.60	.12	.63	3.89	.38	.10	6.33	.38
2	0.23	0.1	0.36	0.1	0.19	0.2	0.	0.3
r	0.06	0.03	0.08	0.06	0.0	0.03	0.06	0.0
a							0.08	
otal	98.22	99. 6	99. 9	99. 1	99. 1	99.	99. 1	99.33
tructural formula calculated on the asis of 8 oxygens								
i	2.	2. 1	2.	2.39	2. 3	2.39	2.60	2. 2
Al	1. 0	1. 6	1. 2	1. 8	1.	1.	1.36	1.
Fe3	0.0	0.03	0.0	0.03	0.03	0.03	0.03	0.03
g	0.00	0.00	0.00	0.00	0.00	0.00	0.00	0.00
Ca	0. 3	0.61	0. 8	0.62	0. 8	0.6	0. 3	0. 1
a	0. 1	0.36	0. 9	0.3	0.39	0.36	0. 6	0. 8
	0.01	0.01	0.02	0.01	0.01	0.01	0.03	0.02
a	0.00	0.00	0.00	0.00	0.00	0.00	0.00	0.00
otal Cat	.9	.98	.99	.98	.98	.00	.00	.00
Al ite	3.00	3 .02	9.	3 .	39. 1	3 .82	.	.03
Anorthite	. 9	62.0	8.36	63.6	9.38	62.81	2.00	0.83
rthoclase	1. 0	0.91	2.0	0.88	1.11	1.3	3.26	2.13

ample num er indicates depth of sample and mineral grain analyzed e.g. 16pl1c sample depth is 16 meters pl1 is mineral grain 1 from this sample c denotes analysis of mineral grain core

xide analyses in weight percent P Plagioclase r rim of mineral grain c core of mineral grain

Feldspar micropro e data

ell 2-2A feldspars analyses

ample	61 pl2r	61 pl3c	61 pl3r	16pl1	16pl2	16pl3	16pl
ineral	P	P	P	P	P	P	P
i 2	2.8	2. 6	2.2	0.39	3.6	9.22	9.36
Al2 3	28.29	2 .32	28.31	28.	2 .19	30.00	30.
Fe2 3	1.00	0.91	1.0	1.23	0.9	1.00	0.90
g	0.00	0.00	0.00	0.00	0.00	0.00	0.00
Ca	12.1	11.	12. 3	1 .00	11.36	1 .81	1 .8
a2	. 9	. 6	.23	3. 6	.9	3.0	2.99
2	0.29	0.2	0.23	0.1	0.2	0.11	0.09
r	0.11	0.02	0.06	0.03			
a							
otal	99.32	9 . 1	98.8	98.00	98.36	98.19	98.6
tructural formula calculated on the asis of 8 oxygens							
i	2. 2	2. 6	2. 1	2.3	2.	2.30	2.29
Al	1. 3	1. 0	1.	1. 8	1. 8	1.6	1.6
Fe3	0.0	0.03	0.0	0.0	0.03	0.0	0.03
g	0.00	0.00	0.00	0.00	0.00	0.00	0.00
Ca	0.60	0. 9	0.63	0. 0	0. 6	0.	0.
a	0. 1	0. 0	0.38	0.31	0.	0.28	0.2
	0.02	0.02	0.01	0.01	0.02	0.01	0.01
a	0.00	0.00	0.00	0.00	0.00	0.00	0.00
otal Cat	.01	.99	.00	.00	.00	.00	.00
Al ite	39.8	0.0	3 .0	30.6	3.3	26.96	26. 8
Anorthite	8. 6	8.33	61.6	68. 0	.10	2. 1	2.89
rthoclase	1.6	1.62	1.32	0.83	1.	0.62	0. 3

ell CH-1 feldspar analyses

ample	369f1c	369f1m	369f1r	369f1r	369f1	369f2c	369f2r	369f3c
ineral	AF	AF	AF	AF	AF	AF	AF	AF
i 2	68. 8	68.	68.69	68.	68.38	68.01	6 .9	68.31
Al2 3	18. 9	18. 6	18.	18.68	18.63	18.6	18. 8	18.
Fe2 3	0.13	0.13	0.1	0.2	0.2	0.1	0.1	0.1
Ca	0.32	0.32	0.2	0.2	0.29	0.31	0.22	0.
a2	6.3	6.32	6.	6.61	6.2	6.2	6.68	6.8
2	.08	6.9	6.92	6.82	.06	6.96	6. 9	6.38
r	0	0	0	0	0	0	0	0
a	0.11	0.01	0	0	0.0	0.03	0.11	0.08
otal	101.	101.06	101.33	101.08	100.9	100. 2	100.	101.21
tructural formula calculated on the asis of 8 oxygens								
i	3.02	3.02	3.02	3.02	3.03	3.02	3.02	3.01
Al	0.9	0.98	0.9	0.9	0.9	0.98	0.9	0.9
Fe3	0.00	0.00	0.01	0.01	0.01	0.01	0.01	0.01
Ca	0.02	0.02	0.01	0.01	0.01	0.02	0.01	0.0
a	0.	0.	0. 6	0.	0.	0.	0. 8	0. 9
	0. 0	0.39	0.39	0.38	0. 0	0.39	0.39	0.36
a	0.002	0	0	0	0.001	0.001	0.002	0.001
otal Cat	.96	.9	.96	.96	.9	.9	.9	.9
Al ite	6. 3	.02	8.28	8.	6.61	6.89	9.28	9. 3
Anorthite	1. 8	1.60	1.32	1.33	1.	1.	1.08	3.62
rthoclase	1.69	1.38	0.39	39.90	1.9	1.	39.6	36.66

ample num er indicates depth of sample and mineral grain analyzed e.g. 16pl1c sample depth is 16 meters pl1 is mineral grain 1 from this sample c denotes analysis of mineral grain core

xide analyses in weight percent P Plagioclase AF Alkali Feldspar r rim of mineral grain c core of mineral grain

ell CH-1 feldspar analyses

ample	09f2c	09f2r	09f3c	09f3r	26f2c	26f2r

Feldspar micropro e data

ell CH-1 feldspar analyses

ample	369f3r	369f c	369f r	369f m	f1c	f1c	f1r	f1r
ineral	AF	P	P	P	AF	AF	AF	AF
i 2	68.66	6 .99	66.61	66.1	6 .29	6 . 3	6 .8	6 .83
Al2 3	18. 2	22.3	21. 6	21. 3	18.	18.8	18. 6	18.68
Fe2 3	0.18	0.2	0.2	0.22	0.1	0.16	0.21	0.16
Ca	0.2	3.68	2. 1	2.	0.3	0.33	0.36	0.3
a2	6.	8.	8.66	8.66	.	.	.82	. 3
2	6.91	1.11	2.11	2.09	8.2	8.0	8.03	8.09
r	0	0	0	0	0	0	0	0
a	0	0	0.01	0.18	0	0.0	0.03	0.0
otal	101.26	101.11	101.91	101. 6	100.21	100. 2	101.06	100.88
tructural formula calculated on the asis of 8 oxygens								
i	3.02	2.8	2.89	2.89	3.01	3.01	3.01	3.02
Al	0.9	1.1	1.10	1.10	0.98	0.99	0.98	0.98
Fe3	0.01	0.01	0.01	0.01	0.01	0.01	0.01	0.01
Ca	0.01	0.1	0.13	0.13	0.01	0.02	0.02	0.02
a	0. 6	0.	0. 3	0. 3	0. 0	0. 0	0. 0	0. 9
	0.39	0.06	0.12	0.12	0.	0. 6	0. 6	0. 6
a	0	0	0	0.003	0	0.001	0.001	0.001
otal Cat	.96	.98	.98	.98	.98	.9	.9	.9
Al ite	8.33	.9	.01	.98	0. 1	1.10	1. 9	0.9
Anorthite	1.18	1 .68	12.9	13.11	1.	1.62	1. 6	1.6
rthoclase	0. 9	6.3	12.03	11.91	8.12	.2	6.	.3

ell CH-1 feldspar analyses

ample	f co	f r	f r	f c	f c	f r	f r	f r
ineral	P	P	P	AF	AF	P	P	P
i 2	2.62	.	3. 1	6 .6	6 .81	68.39	68.81	68.82
Al2 3	29.2	2 . 8	2 .99	18. 3	18.	19.	18.	18.2
Fe2 3	0. 9	0.	0.88	0.2	0.18	0.	0.92	1.03
Ca	12. 9	.	12.01	0.36	0.31	2.38	2.9	2.9
a2	3.8	. 9	.3	. 8	.66	8.	. 2	.26
2	0.22	0.26	0.3	8.2	8.23	1.6	1. 3	1.
r	0	0	0	0	0	0	0	0
a	0	0	0	0.0	0	0.06	0	0.03
otal	99.19	96.	99.2	100. 1	100.69	100.9	100.	99.89
tructural formula calculated on the asis of 8 oxygens								
i	2. 0	2. 6	2.	3.02	3.02	2.98	3.01	3.02
Al	1. 8	1. 9	1. 1	0.9	0.9	1.00	0.9	0.9
Fe3	0.03	0.03	0.03	0.01	0.01	0.02	0.03	0.03
Ca	0.61	0.38	0. 9	0.02	0.02	0.11	0.1	0.1
a	0.3	0. 3	0.39	0. 8	0. 9	0. 1	0.6	0.62
	0.01	0.02	0.02	0.	0.	0.09	0.08	0.09
a	0	0	0	0.001	0	0.001	0	0.001
otal Cat	.9	.90	.98	.96	.9	.91	.86	.8
Al ite	3 .03	1. 6	38.89	9.3	0.33	.90	.	3.3
Anorthite	63.63	6. 0	9.3	1. 9	1. 2	12.1	16.2	16. 1
rthoclase	1.3	1.8	1.	8.8	8.1	9.96	9.31	10.2

ample num er indicates depth of sample and mineral grain analyzed e.g. 16pl1c sample depth is 16 meters pl1 is mineral grain 1 from this sample c denotes analysis of mineral grain core

xide analyses in weight percent P Plagioclase AF Alkali Feldspar r rim of mineral grain c core of mineral grain

Feldspar micropro e data

ell CH-1 feldspar analyses

ample	f r	f i	f6c	f6r	86f1c	86f1r	86f1r	86f1c
ineral	P	AF	P	P	P	P	P	P
i 2	69.62	6 .	.01	.0	.68	6.01	.62	. 2
Al2 3	1 .89	18. 8	28.	28.61	2 .91	2 . 2	2 .6	2 .8
Fe2 3	1	0.16	0.83	0.83	0.81	0. 1	0. 2	0. 2
Ca	2.28	0.3	12.3	12.2	11.6	10.6	11.01	11.36
a2	. 3	.6	.1	.23	.6	.11	.06	.9
2	1.	8.1	0.2	0.2	0.28	0.3	0.33	0.32
r	0	0	0	0	0	0	0	0
a	0	0	0	0.0	0	0.1	0	0
otal	100.06	100.1	100.1	100.2	99.92	100. 1	100.38	100. 6
tructural formula calculated on the			8	8				
i	3.0	3.02	2.	2.	2. 8	2. 2	2. 0	2. 9
Al	0.92	0.98	1. 2	1. 3	1. 9	1. 6	1.	1. 8
Fe3	0.03	0.01	0.03	0.03	0.03	0.02	0.02	0.02
Ca	0.11	0.01	0.60	0. 9	0. 6	0. 1	0. 3	0.
a	0.6	0. 9	0.36	0.3	0. 1	0.	0.	0. 3
	0.10	0. 6	0.02	0.01	0.02	0.02	0.02	0.02
a	0	0	0	0.001	0	0.002	0	0
otal Cat	.8	.9	.9	.9	.98	.98	.98	.98
Al ite	. 9	0.69	3 .16	3 .98	1.30	.	.	3.03
Anorthite	12.68	1. 9	61.2	60.	.06	2.3	3.	.12
rthoclase	11. 2	.82	1. 9	1. 8	1.6	2.1	1.91	1.8

ell CH-1 feldspar analyses

ample	86f2c	86f2r	86f3c	86f3m	86f3r	86f3r	09f1c	09f1r
ineral	P	P	AF	AF	AF	AF	P	P
i 2	3.22	6.02	6 .8	68.1	6 .3	68. 9	2.69	3.01
Al2 3	29.2	2 .	18. 9	18. 2	18.96	18.12	29.26	28. 1
Fe2 3	0. 8	0.8	0.09	0.08	0. 6	0.9	0.68	0.8
Ca	12.8	10.93	0. 9	0.	0.98	1. 2	12.9	12.68
a2	3.89	.9	.3	.2	6.38	.	3.91	.0
2	0.22	0.33	8.12	8.08	6.36	6.2	0.2	0.2
r	0	0	0	0	0	0	0	0
a	0.01	0.01	0.0	0.1	0	0	0.03	0
otal	100.2	100.8	100.62	100.9	100.	100.9	99. 6	99. 2
tructural formula calculated on the asis of 8 oxygens								
i	2. 1	2. 1	3.02	3.02	2.99	3.03	2. 0	2. 2
Al	1. 6	1. 6	0.98	0.98	0.99	0.9	1.	1.
Fe3	0.03	0.03	0.00	0.00	0.02	0.03	0.02	0.03
Ca	0.62	0. 2	0.03	0.03	0.0	0.0	0.63	0.62
a	0.3	0. 3	0. 6	0.	0.	0.	0.3	0.36
	0.01	0.02	0. 6	0. 6	0.36	0.3	0.01	0.02
a	0	0	0.001	0.002	0	0	0.001	0
otal Cat	.9	.9	.9	.9	.96	.90	.98	.98
Al ite	3 .9	.2	8. 1	8.3	.	2. 8	3 .8	36.0
Anorthite	63.	3.80	2.96	2.89	.88	8.06	63. 6	62.3
rthoclase	1.30	1.93	8. 3	8.	3 .68	39. 6	1. 1	1. 8

ample num er indicates depth of sample and mineral grain analyzed e.g. 16pl1c sample depth is 16 meters pl1 is mineral grain 1 from this sample c denotes analysis of mineral grain core

xide analyses in weight percent P Plagioclase AF Alkali Feldspar r rim of mineral grain c core of mineral grain

Feldspar micropro e data

ineral	P	P	P	P	P	P
i 2	3.18	2.98	3.0	2.66	3.66	3.8
Al2 3	28.33	28. 9	29. 2	29.61	29. 2	29.
Fe2 3	0.6	0.8	0. 3	0.8	0.8	0.83
Ca	12. 6	12. 2	12.98	13.2	12.	12.
a2	.2	.2	3.8	3.8	3.98	.0
2	0.2	0.2	0.23	0.2	0.26	0.28
r	0	0	0	0	0	0
a	0	0	0	0	0.01	0.01
otal	99.1	99.16	100.38	100. 9	100.91	100.96
tructural formula calculated on the asis of 8 oxygens						
i	2. 3	2. 3	2. 0	2.38	2. 1	2. 2
Al	1. 3	1.	1.	1. 8	1. 6	1. 6
Fe3	0.02	0.03	0.03	0.03	0.03	0.03
Ca	0.62	0.61	0.63	0.6	0.61	0.60
a	0.3	0.3	0.3	0.3	0.3	0.3
	0.01	0.02	0.01	0.01	0.02	0.02
a	0	0	0	0	0	0
otal Cat	.99	.99	.98	.99	.98	.9
Al ite	3 .1	3 .36	3 . 6	33.89	3 . 6	36.28
Anorthite	61. 3	61.06	6 .19	6 . 2	62.91	62.0
rthoclase	1. 0	1. 8	1.3	1.39	1. 3	1.6

ample num er indicates depth of sample and mineral grain analyzed e.g. 16pl1c sample depth is 16 meters pl1 is mineral grain 1 from this sample c denotes analysis of mineral grain core

xide analyses in weight percent P Plagioclase AF Alkali Feldspar r rim of mineral grain c core of mineral grain

livine micropro e data

ell 2-2A olivine analyses

ample	16px1c	16ol1c	16ol1r	16ol2c	16ol2r	16ol3c	16ol3r	91px1
i 2	3 . 8	3 . 9	38.00	38.38	3 .91	3 .8	36. 0	3 .9
i 2	0.03	0.02	0.03	0.01	0.06	0.03	0.0	0.0
Al2 3	2. 0	1. 3	1.32	1. 9	1. 3	1.80	1.18	0. 1
Fe	29.	28.38	2 .	23.9	36. 1	26. 9	3 .92	33.0
n	0.38	0.39	0. 3	0.3	0.63	0.39	0. 1	0. 1
g	32.	33.62	3 .30	3 .33	2 .2	3 .22	28.	29.6
Ca	0.22	0.2	0.28	0.2	0.2	0.22	0.2	0.3
a2	0.0	0.00	0.01	0.02	0.01	0.02	0.01	0.00
2	0.00	0.00	0.01	0.00	0.00	0.00	0.00	0.01
Cr2 3	0.01							0.02
Calc otal	102.	102.16	102.12	101.8	102.03	102.0	102.0	99.9
tructural formula calculated on the asis of oxygens								
i	0.98	0.99	0.99	0.99	0.98	0.98	0.99	0.99
Al	0.0	0.0	0.0	0.0	0.0	0.06	0.0	0.01
Fe2	0.6	0.62	0.61	0. 2	0.83	0. 8	0. 9	0. 6
g	1.26	1.31	1.33	1. 3	1.11	1.36	1.16	1.22
Ca	0.01	0.01	0.01	0.01	0.01	0.01	0.01	0.01
a	0.00	0.00	0.00	0.00	0.00	0.00	0.00	0.00
	0.00	0.00	0.00	0.00	0.00	0.00	0.00	0.00
i	0.00	0.00	0.00	0.00	0.00	0.00	0.00	0.00
n	0.01	0.01	0.01	0.01	0.02	0.01	0.01	0.01
mg	66.03	6 .8	68. 9	3. 2	.09	0.33	9. 8	61. 3
otal Cat	2.98	2.99	2.99	2.99	3.00	2.99	3.00	3.00

ell 2-2A olivine analyses

ample	91ol1c	91ol1r	91ol2c	91ol2r	91ol3c	91ol3r	120ol1c	120ol1r
i 2	3 . 1	3 .62	3 .9	3 .16	3 .90	3 .31	38.36	38.0
i 2	0.0	0.08	0.03	0.10	0.02	0.03	0.01	0.03
Al2 3	2.00	1.36	1.0	1.08	1.02	1.00	0. 0	0.93
Fe	36.	0.8	2 .	1.9	22.88	2 .99	23.2	2 .00
n	0.	0.66	0.33	0.68	0.33	0.3	0.33	0. 1
g	2 .29	22.88	3 .0	22.30	38.02	3 . 8	3 .6	36.20
Ca	0.36	0.38	0.2	0. 1	0.26	0.3	0.32	0. 0
a2	0.01	0.01	0.00	0.02	0.00	0.02	0.00	0.03
2	0.00	0.02	0.00	0.02	0.00	0.00	0.00	0.00
Cr2 3								
Calc otal	102.2	100.8	101.1	100. 1	100.	99.	100.6	100.06
tructural formula calculated on the asis of oxygens								
i	0.9	0.98	0.99	0.98	0.98	0.99	1.00	1.00
Al	0.06	0.0	0.03	0.0	0.03	0.03	0.02	0.03
Fe2	0.83	0.9	0. 3	1.00	0. 0	0.	0. 1	0. 3
g	1.11	0.9	1. 3	0.9	1.	1. 0	1. 6	1. 1
Ca	0.01	0.01	0.01	0.01	0.01	0.01	0.01	0.01
a	0.00	0.00	0.00	0.00	0.00	0.00	0.00	0.00
	0.00	0.00	0.00	0.00	0.00	0.00	0.00	0.00
i	0.00	0.00	0.00	0.00	0.00	0.00	0.00	0.00
n	0.01	0.02	0.01	0.02	0.01	0.01	0.01	0.01
mg	.11	9.9	2.98	8.6	. 6	1.68	.2	2.89
otal Cat	3.00	2.99	3.00	3.00	3.00	3.00	2.99	2.99

ample num er indicates depth of sample and mineral grain analyzed e.g. 16ol1c sample depth is 16 meters ol1 is mineral grain 1 from this sample c denotes analysis of mineral grain core

xide analyses in weight percent r rim of mineral grain c core of mineral grain

livine micropro e data

ell 2-2A olivine analyses

ample	120ol2c	120ol2r	120ol3c	120ol3r	120px1	120px3	120px	129ol1c
i 2	39. 1	38.0	38.	38. 2	3 .82	36.0	3 .	3 .32
i 2	0.02	0.0	0.0	0.01	0.06	0.06	0.12	0.0
Al2 3	0. 3	0. 9	0.	1.3	0.6	0.36	0.6	1.66
Fe	1 . 0	23.00	20.8	22.	2 .2	31.	33.32	39.93
n	0.2	0.32	0.36	0.31	0.3	0. 3	0. 8	0.60
g	2.16	3 .09	38.98	38.0	36. 2	30.	28. 8	23.9
Ca	0.2	0.36	0.3	0.31	0.38	0. 2	0. 1	0.2
a2	0.00	0.00	0.02	0.01	0.02	0.00	0.02	0.00
2	0.00	0.01	0	0	0.01	0.00	0.00	0.01
Cr2 3					0.0	0.03	0.03	
Calc otal	100. 2	99.66	100.02	101.2	100.29	99.2	99.69	101. 8
tructural formula calculated on the asis of oxygens								
i	1.00	1.00	1	0.99	0.99	0.99	0.99	0.98
Al	0.02	0.02	0.02	0.0	0.02	0.01	0.02	0.0
Fe2	0.3	0. 0	0.	0. 9	0. 3	0. 2	0.	0.93
g	1. 9	1.	1.	1. 6	1. 3	1.2	1.19	1.00
Ca	0.01	0.01	0.01	0.01	0.01	0.01	0.02	0.01
a	0.00	0.00	0	0	0.00	0.00	0.00	0.00
	0.00	0.00	0	0	0.00	0.00	0.00	0.00
i	0.00	0.00	0	0	0.00	0.00	0.00	0.00
n	0.01	0.01	0.01	0.01	0.01	0.01	0.01	0.01
mg	80.9	.19	6.93	.93	2.9	63.32	60.63	1.6
otal Cat	2.99	2.99	2.99	2.99	3.00	3.00	3.00	2.99

ell 2-2A olivine analyses

ample	129ol1r	129ol3c	129ol3r	1 ol1c	1 ol1r	1 ol2c	1 ol2r	1 ol3c
i 2	3 .3	36. 2	3 . 8	3 .60	3 .2	38.0	36.60	3 .69
i 2	0.06	0.0	0.06	0.0	0.03	0.01	0.02	0.0
Al2 3	1.	1.3	1. 0	1. 6	1.63	1.06	1.23	1.0
Fe	39. 6	30.	36.92	2 .38	29. 8	2 .11	31.21	2 . 8
n	0.63	0. 1	0.62	0.	0.38	0.33	0.	0.3
g	23.81	31.12	26. 9	31.	28.3	36. 6	31.36	3 .3
Ca	0.3	0.31	0.3	0. 2	0. 9	0.2	0.29	0.29
a2	0.02	0.00	0.02	0.0	0.02	0.03	0.02	0.02
2	0.00	0.00	0.01	0.00	0.00	0.01	0.00	0.00
Cr2 3								
Calc otal	101. 2	100.62	101.6	99.	9 .63	101.	101.19	100.61
tructural formula calculated on the asis of oxygens								
i	0.99	0.99	0.98	1.01	1.03	0.99	0.98	0.99
Al	0.06	0.0	0.0	0.06	0.0	0.03	0.0	0.03
Fe2	0.92	0.69	0.8	0.61	0.68	0.	0. 0	0.
g	0.99	1.2	1.09	1.2	1.16	1. 2	1.26	1.39
Ca	0.01	0.01	0.01	0.01	0.01	0.01	0.01	0.01
a	0.00	0.00	0.00	0.00	0.00	0.00	0.00	0.00
	0.00	0.00	0.00	0.00	0.00	0.00	0.00	0.00
i	0.00	0.00	0.00	0.00	0.00	0.00	0.00	0.00
n	0.02	0.01	0.01	0.01	0.01	0.01	0.01	0.01
mg	1. 6	6 . 9	6.12	6 . 1	63.1	2.18	6 .1	0.98
otal Cat	2.98	2.99	2.99	2.9	2.9	3.00	3.00	2.99

ample num er indicates depth of sample and mineral grain analyzed e.g. 16ol1c sample depth is 16 meters ol1 is mineral grain 1 from this sample c denotes analysis of mineral grain core

xide analyses in weight percent r rim of mineral grain c core of mineral grain

livine micropro e data

ell 2-2A olivine analyses

ample	1 ol3r	219ol1c	219ol1r	219ol2c	219ol2r	219ol3c	219ol3c	219ol3r
i 2	36. 3	3 .89	3 .68	36. 1	3 .68	39.83	39.9	39.1
i 2	0.03	0.02	0.0	0.0	0.08	0.02	0.01	0.0
Al2 3	1.21	1.26	1.29	1.22	1.0	1.19	1.08	0.99
Fe	2 .9	2 .	2 .8	33.99	2.66	16.3	1 .96	19.98
n	0.	0.3	0.36	0. 6	0.62	0.2	0.2	0.33
g	29.32	36. 3	3 .31	28.	22.0	3.2	3.	39.96
Ca	0.	0.30	0.33	0.	0.36	0.2	0.2	0.31
a2	0.0	0.02	0.00	0.0	0.00	0.00	0.02	0.01
2	0.00	0.01	0.00	0.01	0.01	0.00	0.00	0.00
Cr2 3								
Calc otal	96.21	101.03	100.88	101.	101. 3	101.13	100.9	100.
tructural formula calculated on the asis of oxygens								
i	1.02	0.99	0.99	0.99	0.99	0.99	1.00	1.00
Al	0.0	0.0	0.0	0.0	0.0	0.0	0.03	0.03
Fe2	0.6	0. 3	0.	0.	1.01	0.3	0.33	0. 3
g	1.22	1. 2	1.38	1.1	0.9	1.61	1.62	1. 2
Ca	0.01	0.01	0.01	0.01	0.01	0.01	0.01	0.01
a	0.00	0.00	0.00	0.00	0.00	0.00	0.00	0.00
	0.00	0.00	0.00	0.00	0.00	0.00	0.00	0.00
i	0.00	0.00	0.00	0.00	0.00	0.00	0.00	0.00
n	0.01	0.01	0.01	0.01	0.02	0.01	0.01	0.01
mg	6 .1	2.81	0.8	60.1	.98	82. 2	82.91	8.09
otal Cat	2.96	3.00	2.99	2.99	3.00	2.99	2.99	2.99

ell 2-2A olivine analyses

ample	219ol3r	8 ol1alt	8 ol2c	8 ol2nr	8 ol3alt	61 ol1	61 ol2	61 ol3
i 2	38.18	3 .	38.0	3 .	3 .2	3 . 8	3 .18	3 . 0
i 2	0.0	0.0	0.02	0.03	0.0	0.08	0.06	0.09
Al2 3	1.0	0.68	0.81	1.0	1.2	0.29	0.20	0.69
Fe	2 .22	28.09	2 .16	31.29	31. 0	2. 0	.8	3. 8
n	0.3	0. 1	0.32	0.	0. 8	0.	0. 1	0.
g	36.33	3 .22	3 . 2	32.01	31.61	22.1	20. 2	20.89
Ca	0.3	0.32	0.29	0.29	0.2	0.30	0.28	0.29
a2	0.00	0.00	0.00	0.03	0.03	0.00	0.02	0.00
2	0.00	0.00	0.00	0.00	0.00	0.01	0.00	0.00
Cr2 3								
Calc otal	101. 9	101.30	101.3	102.61	102.3	100. 8	100.82	100.92
tructural formula calculated on the asis of oxygens								
i	0.99	0.99	1.00	0.99	0.99	1.00	0.99	0.99
Al	0.03	0.02	0.03	0.03	0.0	0.01	0.01	0.02
Fe2	0.	0.62	0.60	0.69	0. 0	1.02	1.09	1.0
g	1. 1	1.3	1.36	1.26	1.2	0.9	0.89	0.90
Ca	0.01	0.01	0.01	0.01	0.01	0.01	0.01	0.01
a	0.00	0.00	0.00	0.00	0.00	0.00	0.00	0.00
	0.00	0.00	0.00	0.00	0.00	0.00	0.00	0.00
i	0.00	0.00	0.00	0.00	0.00	0.00	0.00	0.00
n	0.01	0.01	0.01	0.01	0.01	0.02	0.02	0.02
mg	1.9	68.	69. 0	6 . 9	6 .21	8.21	.92	.9
otal Cat	2.99	3.00	2.99	3.00	2.99	3.00	3.00	3.00

ample num er indicates depth of sample and mineral grain analyzed e.g. 16ol1c sample depth is 16 meters ol1 is mineral grain 1 from this sample c denotes analysis of mineral grain core

xide analyses in weight percent r rim of mineral grain c core of mineral grain

livine micropro e data

ell 2-2A olivine analyses

ample	61 ol c	61 ol r	61 ol c
i 2	3 .02	3 . 3	3 .2
i 2	0.0	0.1	0.0
Al2 3	0.3	0. 2	0. 6
Fe	39.91	1. 8	1.03
n	0. 1	0. 2	0. 2
g	2 .3	22.19	23.33
Ca	0.29	0.2	0.29
a2	0.00	0.01	0.03
2	0.00	0.00	0.00
Cr2 3			
Calc otal	100. 0	99.93	101.

tructural formula calculated on the asis of oxygens

i	0.99	0.99	0.99
Al	0.01	0.02	0.03
Fe2	0.9	1.00	0.9
g	1.03	0.9	0.98
Ca	0.01	0.01	0.01
a	0.00	0.00	0.00
	0.00	0.00	0.00
i	0.00	0.00	0.00
n	0.02	0.02	0.02
mg	2.10	8.	0.3
otal Cat	3.00	2.99	2.99

ample num er indicates depth of sample and mineral grain analyzed e.g. 16ol1c sample depth is 16 meters ol1 is mineral grain 1 from this sample c denotes analysis of mineral grain core

xide analyses in weight percent r rim of mineral grain c core of mineral grain

Pyroxene micropro e data

ell 2-2A pyroxene analyses

ample	16px3c	16px3r	91px2	91px3	91px	120px2
i 2	9.31	0. 3	.36	6.82	6.90	3. 8
i 2	1.88	1.36	2.06	3.12	3.0	.06
Al2 3	3. 2	2.93	3.21	.11	.03	.6
Fe	10. 9	12. 8	16.3	11. 1	11.10	1 .
n	0.2	0.33	0.28	0.23	0.2	0.28
g	13.83	13.9	1 . 0	11.98	12.09	8.66
Ca	19. 0	18.	16.3	20.22	20.	19. 6
a2	0.3	0.33	0.3	0.	0.39	0. 6
2	0.00	0.00	0.00	0.00	0.00	0.00
Cr2 3	0.11	0.0	0.00	0.03	0.0	0.19
otal	99.12	100.69	99.	98.66	99.30	98.88
tructural formula calculated on the asis of 6 oxygens						
i	1.86	1.89	1. 1	1. 9	1. 8	1. 0
Al	0.1	0.13	0.1	0.19	0.23	0.26
Fe3	0.0	0.03	0.3	0.08	0.0	0.08
Fe2	0.29	0.36	0.18	0.30	0.29	0. 3
g	0. 8	0. 8	0.8	0.68	0.68	0. 1
Ca	0. 9	0.	0.66	0.83	0.83	0.82
a	0.03	0.02	0.03	0.03	0.03	0.0
	0.00	0.00	0.00	0.00	0.00	0.00
i	0.0	0.0	0.06	0.09	0.09	0.1
n	0.01	0.01	0.01	0.01	0.01	0.01
Cr	0.00	0.00	0.00	0.00	0.00	0.01
mg	2.6	68.32	83.10	69.8	0. 3	.02
otal Cat	.00	.00	.00	.00	.00	.00
ew Fe2 3	1.	1.18	11.92	2.	2.28	2.
ew Fe	9.29	11. 2	.62	9.22	9.0	13.1
ew Calc otal	99.2	100.81	100.6	98.9	99. 3	99.16
nstatite	1.93	1. 0	0.99	3 .80	3 .9	28. 8
Ferrosilite	1 . 9	19.20	10.3	16.33	1 .93	2 . 0
ollastonite	2.28	39. 0	38.6	.8	6.13	6. 2

ample num er indicates depth of sample and mineral grain analyzed e.g. 16px3c sample depth is 16 meters px3 is mineral grain 3 from this sample c denotes analysis of mineral grain core

xide analyses in weight percent r rim of mineral grain c core of mineral grain

ell CH-1 pyroxene analyses

Pyroxene micropro e data

ell 2-2A pyroxene analyses

ample	120px	120px	129px1	129px1	129px2c	129px2r
i 2	.66	.31	8.6	8.	9.1	8.88
i 2	3.61	3.92	1.6	1. 6	1.69	1.
Al2 3	3.8	.91	3.1	3.8	3.8	3.18
Fe	20.16	1 .6	16.22	19.06	13. 6	1 . 6
n	0. 8	0.31	0. 2	0. 9	0.3	0.38
g	9. 3	. 3	12.60	11.03	12.8	12.1
Ca	16.86	19.00	16.29	1 .82	1 .9	1 .91
a2	0. 6	0.69	0.23	0.29	0.2	0.29
2	0.03	0.08	0.01	0.01	0.00	0.01
Cr2 3	0.06	0.0	0.02	0.00	0.00	0.01
otal	99.92	99.3	99.30	100. 8	99.86	99. 0
tructural formula calculated on the asis of 6 oxygens						
i	1.	1. 8	1.8	1.86	1.86	1.8
Al	0.18	0.23	0.1	0.1	0.1	0.1
Fe3	0.1	0.0	0.0	0.0	0.03	0.0
Fe2	0. 9	0.	0. 8	0. 6	0. 1	0. 1
g	0.	0. 3	0. 2	0.63	0. 3	0.69
Ca	0. 0	0.80	0.6	0.6	0. 3	0.6
a	0.0	0.0	0.02	0.02	0.02	0.02
	0.00	0.00	0.00	0.00	0.00	0.00
i	0.11	0.12	0.0	0.0	0.0	0.0
n	0.02	0.01	0.01	0.02	0.01	0.01
Cr	0.00	0.00	0.00	0.00	0.00	0.00
mg	3.61	. 2	60.21	2.96	6 .1	. 6
otal Cat	.00	.00	.00	.00	.00	.00
ew Fe2 3	.	1. 1	1. 3	1.	1.06	1.6
ew Fe	1 .00	16.38	1 .8	1 .	12.80	1 .96
ew Calc otal	100. 0	99. 2	99.	100.6	99.96	99.86
nstatite	32.1	2 .	38.61	3 .26	39.01	3 .33
Ferrosilite	2 .81	30.3	2 . 1	30. 3	21.82	2 . 2
ollastonite	0.0	.10	3 .88	3 .31	39.1	3 .1

ample num er indicates depth of sample and mineral grain analyzed e.g. 16px3c sample depth is 16 meters px3 is mineral grain 3 from this sample c denotes analysis of mineral grain core

xide analyses in weight percent r rim of mineral grain c core of mineral grain

ell CH-1 pyroxene analyses

Pyroxene micropro e data

ell 2-2A pyroxene analyses

ample	129px3c	129px3r	682px1r	682px1c
i 2	.38	8.09	. 1	9.1
i 2	2.21	2.20	1. 9	0.9
Al2 3	. 0	.0	.30	2.
Fe	13. 9	12.19	8. 1	8.
n	0.29	0.31	0.1	0.2
g	13.06	12.6	13.39	1 .92
Ca	18.0	19. 6	18.9	18.1
a2	0.3	0.3	0.39	0.2
2	0.00	0.00	0.00	0.00
Cr2 3	0.01	0.0	0.2	0.22
otal	99.2	99.31	9 .03	9 .88
tructural formula calculated on the asis of 6 oxygens				
i	1.80	1.83	1.86	1.92
Al	0.20	0.18	0.20	0.12
Fe3	0.10	0.0	0.01	0.00
Fe2	0.33	0.32	0.2	0.2
g	0.	0. 2	0. 8	0.8
Ca	0.	0. 9	0.80	0. 6
a	0.03	0.03	0.03	0.02
	0.00	0.00	0.00	0.00
i	0.06	0.06	0.0	0.03
n	0.01	0.01	0.01	0.01
Cr	0.00	0.00	0.01	0.01
mg	69.2	69.01	.66	6.1
otal Cat	.00	.00	.00	.00
ew Fe2 3	3. 1	2.30	0. 6	0.12
ew Fe	10.33	10.12	8.10	8.33
ew Calc otal	99.61	99.	9 .09	9 .89
nstatite	1.02	39.13	2. 3	. 0
Ferrosilite	18.20	1 .	1 . 0	1 .32
ollastonite	0. 8	3.30	3.1	39.9

ample num er indicates depth of sample and mineral grain analyzed e.g. 16px3c sample depth is 16 meters px3 is mineral grain 3 from this sample c denotes analysis of mineral grain core
xide analyses in weight percent r rim of mineral grain c core of mineral grain

ell CH-1 pyroxene analyses

Pyroxene micropro e data

ell CH-1 pyroxene analyses

ample	369maf1	369maf2	369maf2	369maf2	369maf2r	369maf2r
i 2	0.6	0. 6	0.86	1. 8	1.0	0.9
i 2	0.81	0. 3	0.86	0. 2	0.38	0. 3
Al2 3	1.99	1. 3	2.0	1. 3	0.91	1.
Fe	12.0	13.10	10.81	11.30	16.29	1 .2
n	0.3	0. 1	0.29	0.33	0. 2	0.
g	1 .83	1 .19	1 .	1 .16	11.8	12.93
Ca	18.91	18. 2	18.	18.9	18.2	18.2
a2	0.2	0.26	0.2	0.26	0.23	0.30
2	0.00	0.01	0.00	0.00	0.01	0.03
otal	99.8	99.91	99. 8	100.03	99.	99.2
tructural formula calculated on the asis of 6 oxygens						
i	1.90	1.91	1.90	1.92	1.96	1.9
Al	0.09	0.08	0.09	0.08	0.0	0.0
Fe3	0.09	0.08	0.08	0.06	0.03	0.0
Fe2	0.29	0.33	0.2	0.30	0. 9	0. 2
g	0.83	0.80	0.88	0.8	0.68	0.
Ca	0. 6	0.	0.	0. 6	0.	0.
a	0.02	0.02	0.02	0.02	0.02	0.02
	0.00	0.00	0.00	0.00	0.00	0.00
i	0.02	0.02	0.02	0.02	0.01	0.02
n	0.01	0.01	0.01	0.01	0.02	0.02
mg	.29	0.82	.	.03	8.06	63.92
otal Cat	.00	.00	.00	.00	.00	.00
ew Fe2 3	3.2	2.98	2.9	2.02	1.1	1. 0
ew Fe	9.1	10. 2	8.1	9. 8	1 .26	13.01
ew Calc otal	100.19	100.21	99. 8	100.23	99. 9	99.38
nstatite	.20	2.3	6.82	. 6	3 .36	38. 6
Ferrosilite	1 .30	1 . 6	13. 6	1 .60	2 . 3	21.88
ollastonite	0. 0	0.1	39.62	39.9	39.11	39.36

ample num er indicates depth of sample and mineral grain analyzed e.g. 16px3c sample depth is 16 meters px3 is mineral grain 3 from this sample c denotes analysis of mineral grain core
xide analyses in weight percent r rim of mineral grain c core of mineral grain

ell CH-1 pyroxene analyses

Pyroxene micropro e data

ample	369maf3	369maf3	px1c	px1c	px1r	px1r
i 2	1.18	1.06	3.8	3.68	2.30	2. 0
i 2	0. 1	0.	0.	0. 0	0.	0.92
Al2 3	1.60	1.6	1.29	2.02	1.1	2.2
Fe	12.21	13.83	1 .69	16.11	21. 9	18.99
n	0.3	0.	0.3	0.32	0. 8	0.38
g	1 .9	13.61	2 .	26.	22.33	23. 6
Ca	18. 9	18.83	1. 2	1.96	1.9	2.2
a2	0.26	0.29	0.02	0.03	0.02	0.1
2	0.00	0.00	0.01	0.00	0.02	0.03
otal	100.0	100.2	100.9	101.1	100.28	101.2
tructural formula calculated on the asis of 6 oxygens						
i	1.91	1.92	1.9	1.92	1.9	1.91
Al	0.0	0.0	0.06	0.09	0.0	0.10
Fe3	0.08	0.08	0.0	0.0	0.0	0.0
Fe2	0.30	0.36	0. 0	0. 3	0.62	0. 2
g	0.83	0. 6	1.38	1. 2	1.23	1.29
Ca	0.	0. 6	0.0	0.08	0.08	0.09
a	0.02	0.02	0.00	0.00	0.00	0.01
	0.00	0.00	0.00	0.00	0.00	0.00
i	0.02	0.02	0.01	0.01	0.01	0.03
n	0.01	0.01	0.01	0.01	0.02	0.01
mg	3.61	68.12	3. 1	6.	66.	1.0
otal Cat	.00	.00	.00	.00	.00	.00
ew Fe2 3	2.9	2.	1.31	1.9	1. 6	1.9
ew Fe	9.	11.3	16. 1	1 .3	20.01	1 .2
ew Calc otal	100.3	100. 3	101.10	101.3	100. 6	101. 3
nstatite	.21	0.61	0.89	3.	63.89	6 . 9
Ferrosilite	1 .8	19.01	2 .68	22.3	32.12	2 .60
ollastonite	39.9	0.38	3. 3	3.91	3.99	.61

ample num er indicates depth of sample and mineral grain analyzed e.g. 16px3c sample depth is 16 meters px3 is mineral grain 3 from this sample c denotes analysis of mineral grain core
xide analyses in weight percent r rim of mineral grain c core of mineral grain

ell CH-1 pyroxene analyses

ample	86maf c	86maf c	maf6c	86maf6r	09maf1	09maf2c

Pyroxene micropro e data

ample	px2c	px2r	px3r	px3r	px	px c
i 2	1.29	1. 6	1. 3	1.61	1.20	3.26
i 2	0.9	0.6	0.81	0. 3	0.	0.
Al2 3	2.32	1.8	2.02	1.92	2.10	1.9
Fe	11.1	11.99	11.1	11.	12.13	1 .6
n	0.26	0.33	0.32	0.33	0.31	0.39
g	1 .83	1 .	1 .6	1 .2	1 .0	2 .98
Ca	18. 6	18.99	19.0	19.12	18.60	2.09
a2	0.2	0.29	0.32	0.29	0.28	0.0
2	0.02	0.01	0.01	0.02	0.01	0.00
otal	100.8	100. 2	101.06	101.00	100.	100.9
tructural formula calculated on the asis of 6 oxygens						
i	1.89	1.92	1.90	1.91	1.90	1.93
Al	0.10	0.08	0.09	0.08	0.09	0.08
Fe3	0.09	0.0	0.08	0.09	0.08	0.0
Fe2	0.26	0.31	0.26	0.28	0.30	0. 0
g	0.8	0.82	0.86	0.8	0.83	1.3
Ca	0.	0. 6	0.	0. 6	0.	0.08
a	0.02	0.02	0.02	0.02	0.02	0.00
	0.00	0.00	0.00	0.00	0.00	0.00
i	0.03	0.02	0.02	0.02	0.02	0.02
n	0.01	0.01	0.01	0.01	0.01	0.01
mg	.16	2.6	6. 8	.19	3.62	3.0
otal Cat	.00	.00	.00	.00	.00	.00
ew Fe2 3	3.10	2.32	3.01	3.08	2.80	1. 0
ew Fe	8.3	9.91	8. 3	8.9	9.61	16. 1
ew Calc otal	101.1	100.6	101.36	101.31	100. 3	101.08
nstatite	6. 6	3.	.90	.81	. 1	0.00
Ferrosilite	13. 8	16.36	13.88	1 . 9	1 .9	2 .80
ollastonite	39.66	0.20	0.22	0. 0	39.	.21

ample num er indicates depth of sample and mineral grain analyzed e.g. 16px3c sample depth is 16 meters px3 is mineral grain 3 from this sample c denotes analysis of mineral grain core
xide analyses in weight percent r rim of mineral grain c core of mineral grain

ell CH-1 pyroxene analyses

ample	09maf2r	09maf3c	09maf3r	26maf1c	26maf1r	26maf2c

Pyroxene micropro e data

ample	px c	px r	px6c	px6r	86maf1c	86maf1r
i 2	3.11	3.81	3.09	3. 0	3. 6	3.26
i 2	0. 9	0. 2	0. 3	0. 3	0. 1	0. 9
Al2 3	2.11	1.61	1.3	2.09	1.9	1. 8
Fe	1 .28	16.63	19.3	1 .13	1 .21	1 . 8
n	0.3	0.33	0.	0.3	0.29	0. 0
g	2 .32	26.11	2 .38	2 .0	2 .2	2 .
Ca	2.11	2.18	1.90	1.98	1.93	2.00
a2	0.03	0.0	0.02	0.03	0.0	0.0
2	0.00	0.01	0.00	0.00	0.01	0.00
otal	100.92	101.2	100.9	100.6	100.6	100. 2
tructural formula calculated on the asis of 6 oxygens						
i	1.92	1.93	1.93	1.91	1.91	1.93
Al	0.09	0.0	0.06	0.09	0.08	0.0
Fe3	0.0	0.0	0.06	0.06	0.0	0.06
Fe2	0.	0.	0. 3	0. 0	0.38	0.
g	1.36	1. 0	1.32	1.	1.	1.3
Ca	0.08	0.08	0.0	0.08	0.0	0.08
a	0.00	0.00	0.00	0.00	0.00	0.00
	0.00	0.00	0.00	0.00	0.00	0.00
i	0.02	0.01	0.01	0.01	0.01	0.01
n	0.01	0.01	0.01	0.01	0.01	0.01
mg	.21	. 2	1.38	8. 1	9.11	. 6
otal Cat	.00	.00	.00	.00	.00	.00
ew Fe2 3	1.	1.90	2.1	2.1	2.6	2.12
ew Fe	1 .68	1 .92	1 . 3	13.20	12.83	1 .
ew Calc otal	101.10	101. 3	101.18	100.89	100.92	100.93
nstatite	1.0	2. 3	68.6	.39	6.0	1. 6
Ferrosilite	2 .69	23.22	2 . 2	20.6	20.08	2 . 1
ollastonite	.26	.3	3.8	3.9	3.8	.03

ample num er indicates depth of sample and mineral grain analyzed e.g. 16px3c sample depth is 16 meters px3 is mineral grain 3 from this sample c denotes analysis of mineral grain core
xide analyses in weight percent r rim of mineral grain c core of mineral grain

Pyroxene micropro e data

ample	86maf2c	86maf2r	86maf3c	86maf3r	86maf3r	86maf3m
i 2	3. 3	3. 0	0.36	1. 8	0.90	1.02
i 2	0. 9	0. 9	1.03	0.6	0.9	1.01
Al2 3	1.29	2.11	2.8	1. 6	2. 1	2.3
Fe	16. 3	16.0	10.38	11.66	11.0	10.0
n	0.32	0.3	0.26	0.36	0.32	0.26
g	26.08	26. 9	16.20	1 .90	1 . 3	16.11
Ca	2.36	1.8	18.18	19.21	18.3	18. 0
a2	0.0	0.0	0.33	0.26	0.30	0.2
2	0.00	0.00	0.00	0.01	0.00	0.00
otal	101.0	100.9	99.61	100.09	100.01	99. 9
tructural formula calculated on the asis of 6 oxygens						
i	1.93	1.92	1.8	1.92	1.89	1.90
Al	0.06	0.09	0.13	0.0	0.11	0.10
Fe3	0.06	0.06	0.10	0.0	0.08	0.0
Fe2	0.	0. 2	0.22	0.29	0.26	0.2
g	1. 0	1. 2	0.90	0.83	0.8	0.89
Ca	0.09	0.0	0. 2	0.	0. 3	0.
a	0.00	0.00	0.02	0.02	0.02	0.02
	0.00	0.00	0.00	0.00	0.00	0.00
i	0.01	0.01	0.03	0.02	0.03	0.03
n	0.01	0.01	0.01	0.01	0.01	0.01
mg	6.08	.0	80.09	3.93	6.83	8.2
otal Cat	.00	.00	.00	.00	.00	.00
ew Fe2 3	2.3	2.1	3. 6	2.	2.90	2.32
ew Fe	1 .62	1 .10	.18	9.3	8. 6	.98
ew Calc otal	101.29	101.19	99.9	100.3	100.30	99.82
nstatite	2. 9	.21	8.66	3.8	6.	.
Ferrosilite	22. 9	22.08	12.10	1 . 8	1 .10	13.21
ollastonite	. 2	3. 1	39.2	0.6	39.1	39.2

ample num er indicates depth of sample and mineral grain analyzed e.g. 16px3c sample depth is 16 meters px3 is mineral grain 3 from this sample c denotes analysis of mineral grain core
xide analyses in weight percent r rim of mineral grain c core of mineral grain

Pyroxene micropro e data

i 2	.23	3.9	1.1	1.	0.80	1.2
i 2	0.3	0.3	0.9	0.80	0.92	0.98
Al2 3	1.12	1.18	2.3	1.	1.9	2.28
Fe	1 .2	16.0	9.83	10.63	11.32	10.21
n	0.33	0.3	0.2	0.29	0.33	0.2
g	2 . 9	26.62	16.08	1 . 3	1 .03	16.12
Ca	1.89	2.06	18.86	19.03	18.93	18.
a2	0.03	0.02	0.2	0.26	0.26	0.2
2	0.00	0.00	0.00	0.01	0.01	0.00
otal	100. 8	100.61	99.	100.2	99.	100.08
tructural formula calculated on the asis of 6 oxygens						
i	1.9	1.9	1.90	1.92	1.90	1.90
Al	0.0	0.0	0.10	0.08	0.09	0.10
Fe3	0.06	0.0	0.0	0.06	0.0	0.0
Fe2	0.39	0. 3	0.2	0.2	0.28	0.2
g	1.	1. 3	0.89	0.8	0.8	0.89
Ca	0.0	0.08	0.	0. 6	0. 6	0.
a	0.00	0.00	0.02	0.02	0.02	0.02
	0.00	0.00	0.00	0.00	0.00	0.00
i	0.01	0.01	0.03	0.02	0.03	0.03
n	0.01	0.01	0.01	0.01	0.01	0.01
mg	8.99	6.83	8.83	6. 3	.9	8.21
otal Cat	.00	.00	.00	.00	.00	.00
ew Fe2 3	2. 0	1.9	2.3	2.20	2.63	2.
ew Fe	13.08	1 .31	. 0	8.6	8.96	8.01
ew Calc otal	101.02	100.81	99.99	100. 6	99.81	100.33
nstatite	6.03	3.68	.36	.92	.6	.30
Ferrosilite	20.23	22.22	12. 2	1 .16	1 .93	13.18
ollastonite	3.	.10	39.92	39.92	0. 2	39. 2

ample num er indicates depth of sample and mineral grain analyzed e.g. 16px3c sample depth is 16 meters px3 is mineral grain 3 from this sample c denotes analysis of mineral grain core
xide analyses in weight percent r rim of mineral grain c core of mineral grain

Pyroxene micropro e data

i 2	0.6	3.99	3.01	1.	1. 6	3.88
i 2	1.03	0.36	0.	0.9	1.0	0.
Al2 3	2.28	0.89	1.	2.33	2.16	1.92
Fe	10.63	16.03	1 .88	9.99	10.3	1 .63
n	0.30	0.3	0. 0	0.21	0.29	0.3
g	1 . 2	26.81	26.33	16.26	1 .	26.86
Ca	19.1	2.06	2.20	18.93	18.9	1.99
a2	0.2	0.0	0.03	0.26	0.23	0.0
2	0.01	0.00	0.01	0.01	0.00	0.00
otal	99.83	100. 3	100.1	100. 3	100.13	101.21
tructural formula calculated on the asis of 6 oxygens						
i	1.89	1.9	1.91	1.90	1.92	1.92
Al	0.10	0.0	0.0	0.10	0.10	0.08
Fe3	0.09	0.06	0.0	0.0	0.0	0.0
Fe2	0.2	0. 2	0. 1	0.2	0.29	0. 2
g	0.86	1.	1. 2	0.89	0.86	1. 3
Ca	0.	0.08	0.09	0.	0. 6	0.08
a	0.02	0.00	0.00	0.02	0.02	0.00
	0.00	0.00	0.00	0.00	0.00	0.00
i	0.03	0.01	0.02	0.03	0.03	0.02
n	0.01	0.01	0.01	0.01	0.01	0.01
mg	.9	. 6	.60	8.9	.02	. 3
otal Cat	.00	.00	.00	.00	.00	.00
ew Fe2 3	3.13	2.36	2. 9	2. 1	1.2	1.86
ew Fe	.82	13.91	13.	. 3	9.22	13.96
ew Calc otal	100.1	100.	100. 1	100.68	100.2	101. 0
nstatite	6.08	.28	.1	.	.2	.36
Ferrosilite	13.02	21.62	21. 1	12.68	1 .06	21.68
ollastonite	0.90	.10	.	39. 8	39.69	3.96

ample num er indicates depth of sample and mineral grain analyzed e.g. 16px3c sample depth is 16 meters px3 is mineral grain 3 from this sample c denotes analysis of mineral grain core
xide analyses in weight percent r rim of mineral grain c core of mineral grain

Fe- i oxide micropro e data

ell CH-1 spinel and rhom ohedral series Fe- i oxides

ample	369ox2	369ox2	369ox2c	369ox2r	369ox1	mglass
ineral	Fe- i oxide	Fe- i oxide	Fe- i oxide	Fe- i oxide	Fe- i oxide	Fe- i oxide
i 2	0.16	0.03	0.0	0.03	0.0	0.06
i 2	1 .3	26.99	0.22	0. 9	.62	18.16
Al2 3	0.0	0.09	0.00	0.00	0.00	2.0
Fe	68.6	63.16	3. 6	2.06	8. 3	3.20
n	0.18	2.2	0.63	0. 0	1.26	0. 0
g	0.01	0.33	0.00	0.00	0. 2	1. 0
Ca	0.38	0.0	0.03	0.02	0.3	0.00
a2	0.00	0.02	0.00	0.03	0.00	0.01
2	0.0	0.02	0.02	0.03	0.00	0.00
otal	86.83	92.92	9 . 0	93. 6	98.12	9 . 0
tructural formula on asis of 32 oxygens						
i	0.0	0.010	0.011	0.009	0.01	0.018
Al	0.028	0.03	0.000	0.000	0.000	0. 31
Fe3	.100	3.106				.0 0
Fe2	12.21	13.629	10.3 1	10.039	11.3 1	11.303
g	0.00	0.1 6	0.000	0.000	0.1	0.6 0
Ca	0.13	0.01	0.009	0.006	0.102	0.000
a	0.000	0.012	0.000	0.01	0.000	0.006
	0.01	0.008	0.00	0.011	0.000	0.000
i	.391	6. 31	10. 31	10.901	10.02	.09
n	0.0 1	0.601	0.1 2	0.121	0.299	0.12
mg	0.0 1	1.131	0.000	0.000	1. 22	. 99
otal Cat	2 .000	2 .000	21.261	21.10	21.9 9	2 .000
ew Fe2 3	28.0	13.03				31.2
ew Fe	3. 1	1.				.08
ew otal	89.6	9 .22				98.63

ample num er indicates depth of sample and mineral grain analyzed e.g. 369ox2c sample depth is 369 meters ox2 is mineral grain 2 from this sample c denotes analysis of mineral grain core

xide analyses in weight percent r rim of mineral grain c core of mineral grain

Fe- i oxide micropro e data

ell CH-1 spinel and rhom ohedral series Fe- i oxides

ample	ox1	ox1r	ox1	ox1	ox2	ox3
ineral	Fe- i oxide	Fe- i oxide	Fe- i oxide	Fe- i oxide	Fe- i oxide	Fe- i oxide
i 2	0.18	0.0	0.08	0.10	0.09	0.21
i 2	1 .61	18.0	18.26	18.0	18.12	1 .93
Al2 3	2.10	2.00	2.08	2.06	1.82	1.
Fe	2. 1	3. 3	3. 1	3.	.19	.0
n	0. 1	0. 2	0.	0. 3	0. 2	0.6
g	1.66	1.	1. 3	1. 1	0.98	0.8
Ca	0.01	0.02	0.00	0.01	0.03	0.1
a2	0.01	0.00	0.00	0.00	0.00	0.02
2	0.00	0.02	0.00	0.01	0.01	0.02
otal	9 .69	9 .	96.10	96.03	9 . 6	96.3
tructural formula on asis of 32 oxygens						
i	0.0	0.021	0.02	0.030	0.02	0.063
Al	0.	0. 0	0. 30	0. 2	0.6	0. 11
Fe3	.161	.112	.0 0	.132	.11	.316
Fe2	11.183	11.29	11.32	11.2 8	11. 3	11.
g	0.	0.6	0.680	0.6 1	0. 39	0.388
Ca	0.003	0.006	0.000	0.003	0.010	0.0 8
a	0.006	0.000	0.000	0.000	0.000	0.012
	0.000	0.008	0.000	0.00	0.00	0.008
i	3.99	.0	.091	.0	.09	.033
n	0.10	0.132	0.111	0.13	0.132	0.16
mg	6.2 8	.389	.661	.62	3.66	3.2
otal Cat	2 .000	2 .000	2 .000	2 .000	2 .000	2 .000
ew Fe2 3	31.	31. 3	31. 0	31. 9	31.	32. 1
ew Fe	.33	.06	.	.16	.89	.80
ew otal	9 .8	98. 3	99.2	99.21	98.91	99.61

ample num er indicates depth of sample and mineral grain analyzed e.g. 369ox2c sample depth is 369 meters ox2 is mineral grain 2 from this sample c denotes analysis of mineral grain core

xide analyses in weight percent r rim of mineral grain c core of mineral grain

Fe- i oxide micropro e data

ell CH-1 spinel and rhom ohedral series Fe- i oxides

ample	ox	ox3	ox	ox	ox6	86ox1
ineral	Fe- i oxide	Fe- i oxide	Fe- i oxide	Fe- i oxide	Fe- i oxide	Fe- i oxide
i 2	0.10	0.18	2.86	0.21	0. 8	0.
i 2	18.3	23.3	1 . 9	18. 1	16.	21. 8
Al2 3	1. 2	1.	1.	1.63	1.93	0.86
Fe	3.9	6 .6	0. 0	3.38	3.02	6 . 8
n	0.68	0.63	0.63	0.	0.60	0. 1
g	0.92	0.9	1.08	1.01	1.08	0.26
Ca	0.10	0.10	0.13	0.02	0.08	0.08
a2	0.00	0.00	0.06	0.00	0.00	0.01
2	0.02	0.01	0.0	0.01	0.0	0.02
otal	9 .63	9 .3	9 .	9 .22	9 .00	91.
tructural formula on asis of 32 oxygens						
i	0.030	0.0	0.863	0.06	0.1 6	0.1
Al	0. 0	0. 2	0.623	0. 81	0.69	0.323
Fe3	.091	. 68	. 63	6.921	.336	.90
Fe2	11. 3	12.820	12.036	11.6 0	11.290	13.10
g	0. 13	0. 31	0. 86	0.	0. 91	0.123
Ca	0.032	0.033	0.0 2	0.006	0.026	0.02
a	0.000	0.000	0.03	0.000	0.000	0.006
	0.008	0.00	0.019	0.00	0.016	0.008
i	.1 8	. 00	3.9 1	.18	3.8 6	.219
n	0.1	0.16	0.161	0.1 1	0.1	0.111
mg	3.	3.2 9	3.882	3. 6	.168	0.93
otal Cat	2 .000	2 .000	2 .000	2 .000	2 .000	2 .000
ew Fe2 3	31.26	19. 6	2 .3	30. 1	31.96	20.
ew Fe	.82	9.89	.6	6.02	.26	9.18
ew otal	98. 6	96.33	9 .09	98.2	9 .20	93.60

ample num er indicates depth of sample and mineral grain analyzed e.g. 369ox2c sample depth is 369 meters ox2 is mineral grain 2 from this sample c denotes analysis of mineral grain core

xide analyses in weight percent r rim of mineral grain c core of mineral grain

Fe- i oxide micropro e data

ell CH-1 spinel and rhom ohedral series Fe- i oxides

ample	86ox1	86ox2	86ox3	86ox c	86ox r	09ox1
ineral	Fe- i oxide	Fe- i oxide	Fe- i oxide	Fe- i oxide	Fe- i oxide	Fe- i oxide
i 2	0.11	0.09	0.1	0.1	0.0	0.18
i 2	21.	20.03	20.20	9.6	1 .82	21.68
Al2 3	0. 9	0.6	0.6	1.0	0.8	1.06
Fe	68. 3	6 .80	69.18	9.28	3.60	6 .9
n	0.33	2.01	0.9	0. 1	0. 2	0. 1
g	0.22	0.06	0.0	0.10	0.	0.16
Ca	0.0	0.12	0.11	0.0	0.08	0.20
a2	0.03	0.00	0.00	0.00	0.00	0.00
2	0.03	0.02	0.01	0.01	0.01	0.03
otal	91.8	90. 8	91.33	90.81	91.62	91.9
tructural formula on asis of 32 oxygens						
i	0.03	0.029	0.0 8	0.0 8	0.022	0.0
Al	0.296	0.2	0.2 3	0. 00	0.32	0.396
Fe3	.3 0	6.00	.936	10.901	8.11	.1
Fe2	12.92	12.2 3	12.	10.1	11.3 3	12.8 1
g	0.10	0.029	0.033	0.0	0.212	0.0 6
Ca	0.01	0.0 1	0.038	0.01	0.02	0.068
a	0.018	0.000	0.000	0.000	0.000	0.000
	0.012	0.008	0.00	0.00	0.00	0.012
i	.1	.8 8	.860	2.30	3. 61	.1 2
n	0.089	0. 8	0.2	0.13	0.193	0.191
mg	0.800	0.23	0.26	0. 6	1.83	0. 8
otal Cat	2 .000	2 .000	2 .000	2 .000	2 .000	2 .000
ew Fe2 3	22.36	2 .80	2 .6	.6	3 .11	21.60
ew Fe	8.61	. 8	.00	38.22	2.91	8. 1
ew otal	9 .09	93.26	93.80	9 .38	9 .0	9 .13

ample num er indicates depth of sample and mineral grain analyzed e.g. 369ox2c sample depth is 369 meters ox2 is mineral grain 2 from this sample c denotes analysis of mineral grain core

xide analyses in weight percent r rim of mineral grain c core of mineral grain

Cha azite -ray powder diffraction data

ample 2-2A- 8

2θ	d	o	hkl
9. 2	9.28	30	101
12. 8	.09		
12.99	6.81	9	110
1 .01	6.32		
16.03	. 2	10	201
16.69	.31	3	
1 . 8	.98	21	003
19.00	.6		202
19.18	.62	3	
20. 8	.31	100	211
21. 0	.09		
22. 1	3.96		300
23.01	3.86	22	212
2 .8	3. 8	3	10
2 .90	3.	2	220
2 . 0	3.2		311
28.01	3.18	18	20
28. 3	3.1		
30.	2.92	93	01
30.9	2.88	28	21
31.60	2.83	3	223
32.38	2. 6		02
33. 0	2.68	26	20
3 . 1	2.60	1	10
3 .00	2. 6	3	
3 .92	2. 0	18	21
39.19	2.30		330
1.92	2.1		
3. 9	2.08	11	333

hkl data from Hauff and Phillips 1982

Clay -ray powder diffraction data

ell 2-2A clay x-ray powder diffraction analyses

ample 2-2A- 8

2θ	d	o	ineral	hkl
Air ried				
6.69	13.20	100		001
31. 1	2.8	23		
lycolated				
.32	16.60	100		001
10.66	8.29	1		002
26. 9	3.32	1		00
300°C				
9.03	9. 8	100		001
2 .99	3.18	9		003
31. 1	2.82			
0°C				
9.20	9.60	100		001
28.12	3.1	88		003
29. 0	3.03	3	C	10
31. 2	2.82	3		

ample 2-2A- 8

2θ	d	o	ineral	hkl
Air ried				
6.06	1 .	100		001
2 .08	3.69	1		00
2 .88	3.20	12	P	0 0
28.08	3.1	16	P	002
29.98	2.98	22		00
lycolated				
. 0	16.3	100		001
10. 3	8.2	16		002
26.8	3.32	2		00
2 .8	3.20	11	P	0 0
28.0	3.18	10	P	002
32. 3	2. 6	8		006
300°C				
9.11	9. 0	6		001
28.12	3.1	100		003
0°C				
9.3	9.	2		001
28.32	3.1	100		003

ample num er indicates well and depth of sample e.g. C1A-363 C1A well C1A clay from rock matrix 363 depth in meters

smectite kaolinite P calcic plagioclase C calcite uartz plagioclase peaks o scured y smectite peak

2θ corrected to 2 .606 corundum peak Cu α x-ray source hkl data from ac iff version .03

Clay -ray powder diffraction data

ell 2-2A clay x-ray powder diffraction analyses

ample 2-2A-682

2θ	d	o	ineral	hkl
Air ried				
6.0	1 .60	100		001
2 . 2	3.6	1		002
2 .81	3.21	29	P	0 0
28.03	3.18	29	P	002
lycolated				
.31	16.63	100		001
10. 8	8.3	16		002
26.89	3.31	32		00
2 .86	3.20	32	P	0 0
28.00	3.18	1	P	002
300°C				
8.93	9.89	38		001
2 .83	3.20	100	P	0 0
28.0	3.18	9	P	002
0°C				
9.31	9. 9	9		001
28.01	3.18	100		003

ample 2-2A-691

2θ	d	o	ineral	hkl
Air ried				
6.8	12.86	93		001
8.80	10.0	9		
28.13	3.1	100		00
lycolated				
.31	16.63	100		001
10.	8.38	20		002
1 .8	. 8	8		003
26. 0	3.36	3		00
31.8	2.81	11		006
300°C				
9.11	9. 0	8		001
18.6	.	2		002
19. 1	.	2		
28.1	3.1	100		003
0°C				
9.20	9.60	93		001
28.31	3.1	100		003

ample num er indicates well and depth of sample e.g. C1A-363 C1A well C1A clay from rock matrix 363 depth in meters

smectite kaolinite P calcic plagioclase C calcite uartz plagioclase peaks

o scured y smectite peak

2θ corrected to 2 .606 corundum peak Cu α x-ray source hkl data from ac iff version .03

Clay -ray powder diffraction data

ells 2-2A and 2 clay x-ray powder diffraction analyses

ample 2-2A-691

2θ	d	o	ineral	hkl
Air ried				
6.20	1 .2	96		001
12.28	.20			001
18. 6	.80			003
21.99	.0		P	20-1
2 .	3.60	100		002
2 .88	3.20	89	P	0 0
28.02	3.18	0	P	002
28. 3	3.1	0	P	220
lycolated				
.3	16. 0	100		001
6.03	1 .6	39		
12.20	.2			001
18. 9	. 9	29		
22.0	.02	31	P	20-1
2 . 3	3.60	6		002
26. 2	3.36	8		00
2 .82	3.20	9	P	0 0
28.03	3.18	9	P	002
300°C				
6.23	1 .1	23		
9.0	9. 6	1		001
12.31	.18			001
18.	. 8	28		
19. 1	.	29		
21.99	.0	23	P	20-1
2 .92	3.			002
2 .88	3.20	100	P	0 0
28.08	3.1	9	P	002
0°C				
6. 0	13.80	8		
9.08	9. 3	3		001
21.98	.0	3	P	20-1
23. 3	3.		P	111
2 .	3.62			
2 .88	3.20	100	P	0 0
28.08	3.1	86	P	002
28. 3	3.13	21	P	220

ample 2- 22

2θ	d	o	ineral	hkl
Air ried				
6.60	13.38	100		001
12. 1	.0	21		002
19.91	. 6	1		003
2 .01	3. 6	2		
26.	3.33	86		101
lycolated				
.29	16.69	6		001
10.66	8.29	1		002
26.8	3.32	100		101
300°C				
8.93	9.89	38		001
20.99	.23	30		100
2 .92	3.	36		
26.80	3.32	100		101
2 .91	3.19	1		003
0°C				
9.03	9. 8	2		001
26.63	3.3	100		101
2 .82	3.20	90		003

ample num er indicates well and depth of sample e.g. C1A-363 C1A well C1A clay from rock matrix 363 depth in meters

smectite kaolinite P calcic plagioclase C calcite uartz plagioclase peaks

o scured y smectite peak

2θ corrected to 2 .606 corundum peak Cu α x-ray source hkl data from ac iff version .03

Clay -ray powder diffraction data

ell 2 clay x-ray powder diffraction analyses

ample 2- 2

2θ	d	o	ineral	hkl
Air ried				
6.8	12.91	100		001
lycolated				
.31	16.63	100		001
10. 3	8.39	9		002
26.	3.36	30		00
31.9	2.80	13		006
300°C				
8.86	9.9	100		001
28.16	3.1	96		003
0°C				
9.19	9.61	100		001
28. 1	3.1	91		003

ample 2- 2

2θ	d	o	ineral	hkl
Air ried				
6.16	1 .3	100		001
lycolated				
.28	16. 2	100		001
10. 6	8.3	1		002
26. 3	3.36	26		00
31. 0	2.82	1		006
300°C				
9.0	9. 6	8		001
28.01	3.18	100		003
0°C				
9.1	9.6	100		001
28.21	3.16	89		003

ample 2-601

2θ	d	o	ineral	hkl
Air ried				
6.0	1 .60	81		001
2 .80	3.21	100	P	0 0
28.02	3.18		P	002
lycolated				
.28	16. 2	100		001
10.61	8.33	2		002
26. 1	3.36	3		00
2 .88	3.20	3	P	0 0
28.08	3.1	6	P	002
300°C				
8.9	9.88	33		001
2 .60	3.23	60	P	2-20
2 .8	3.20	100	P	0 0
28.06	3.18	90	P	002
28. 2	3.1	39	P	220
0°C				
9.2	9. 6	3		001
2 .89	3.20	8	P	0 0
28.09	3.1	100	P	002
28. 3	3.1		P	220

ample 2-103

2θ	d	o	ineral	hkl
Air ried				
6.8	12.89	100		001
28.23	3.16	19		00
lycolated				
.38	16. 1	100		001
10. 1	8.2	18		002
16.18	.	2		003
26.90	3.31	23		00
32. 6	2. 6	6		006
300°C				
8.91	9.92	60		001
28.26	3.16	100		003
0°C				
9.21	9. 9	91		001
28. 0	3.13	100		003

ample num er indicates well and depth of sample e.g. C1A-363 C1A well C1A
clay from rock matrix 363 depth in meters
smectite kaolinite P calcic plagioclase C calcite uartz plagioclase peaks
o scured y smectite peak
2θ corrected to 2 .606 corundum peak Cu α x-ray source hkl data from ac iff version .03

Clay -ray powder diffraction data

ell 2 clay x-ray powder diffraction analyses

ample 2-1063					ample 2-106				
2θ	d	o	ineral	hkl	2θ	d	o	ineral	hkl
Air ried					Air ried				
6. 1	13.16	8		001	6.92	12. 6	100		001
2 .8	3.20	62	P	0 0	28.18	3.16	62		00
28.0	3.18	2	P	002					
29.	3.03	100	C	10					
lycolated					lycolated				
.	16.20	100		001	.32	16.60	100		001
10. 2	8.2	23		002	10.6	8.31	20		002
26.8	3.32	38		00	26.63	3.3			00
2 .92	3.19	19	P	0 0	32.06	2. 9	1		006
28.10	3.1	28	P	002					
29. 8	3.02	1	C	10					
300°C					300°C				
8.90	9.93	38		001	9.0	9.	6		001
2 .83	3.20	8	P	0 0	18. 0	.	23		002
28.08	3.1		P	002	28.23	3.16	100		003
29.	3.02	100	C	10					
0°C					0°C				
9.3	9.	3		001	9.36	9.	6		001
28.03	3.18	100		003	28.39	3.1	100		003
28. 3	3.1	66	P	220					
29.	3.03	91	C	10					

ample num er indicates well and depth of sample e.g. C1A-363 C1A well C1A
clay from rock matrix 363 depth in meters
smectite kaolinite P calcic plagioclase C calcite uartz plagioclase peaks
o scured y smectite peak
2θ corrected to 2 .606 corundum peak Cu α x-ray source hkl data from ac iff version .03

Clay -ray powder diffraction data

ells 2 and C1A clay x-ray powder diffraction analyses

ample 2-106					ample C1A-363				
2θ	d	o	ineral	hkl	2θ	d	o	ineral	hkl
Air ried					Air ried				
6.09	1 . 0	100		001	6.39	13.82	100		001
12.13	.29	11		002	2 .92	3.19		P	0 0
18.22	.86	1		003	28.1	3.1	60	P	002
2 . 1	3.63	2		00	28. 3	3.1		P	220
30.36	2.9	2		00					
lycolated					lycolated				
. 0	16.3	100		001	.32	16.60	100		001
10.	8.22	18		002	10.63	8.32	18		002
26.68	3.3	33		00	26. 1	3.36	21		00
32.0	2. 9	9		006	2 .83	3.20	16	P	0 0
					28.03	3.18	1	P	002
					31.99	2.80	1		006
					32.39	2. 6	1		
300°C					300°C				
9.09	9. 2	6		001	9.13	9.68	83		001
18.68	.	22		002	28.10	3.1	100		003
28.21	3.16	100		003					
0°C					0°C				
9.30	9. 0	90		001	9.21	9. 9	82		001
28.39	3.1	100		003	28.06	3.18	100		003
					28. 2	3.1	3	P	220

ample num er indicates well and depth of sample e.g. C1A-363 C1A well C1A
clay from rock matrix 363 depth in meters
smectite kaolinite P calcic plagioclase C calcite uartz plagioclase peaks
o scured y smectite peak
2θ corrected to 2 .606 corundum peak Cu α x-ray source hkl data from ac iff version .03

Clay -ray powder diffraction data

ell C1A clay x-ray powder diffraction analyses

ample C1A- 93

2θ	d	o	ineral	hkl
Air ried				
6.12	1 . 3	68		001
23. 1	3.	0	P	111
2 . 8	3.21	100	P	0 0
2 .96	3.19	1	P	002
28. 3	3.1	2	P	220
lycolated				
.3	16.	100		001
10.69	8.2	23		002
23. 2	3.	2	P	111
26. 9	3.3	9		00
2 .8	3.20	82	P	0 0
28.03	3.18	63	P	002
300°C				
9.01	9.81	21		001
22.03	.03	32	P	20-1
23.	3.	36	P	111
2 .8	3.20	98	P	0 0
28.03	3.18	100	P	002
0°C				
9.28	9. 2	36		001
23. 8	3.	28	P	111
2 .81	3.21	9	P	0 0
28.02	3.18	100	P	002
28. 0	3.13	66	P	220
33.1	2. 0	3		

ample C1A- 2

2θ	d	o	ineral	hkl
Air ried				
23.	3.	38	P	111
2 . 8	3.21	100	P	0 0
2 .98	3.19	82	P	002
31.88	2.80	3		
lycolated				
21.92	.0	1	P	20-1
23.66	3. 6		P	111
2 . 9	3.21	100	P	0 0
28.03	3.18	93	P	002
31.9	2.80	9		
300°C				
21.9	.0	8	P	20-1
23.66	3. 6	3	P	111
2 .81	3.21	100	P	0 0
28.0	3.18	8	P	002
32.01	2. 9	36		
0°C				
21.9	.0	33	P	20-1
23.6	3. 6	2	P	111
2 .80	3.21	100	P	0 0
28.02	3.18	61	P	002
31.91	2.80	20		

ample num er indicates well and depth of sample e.g. C1A-363 C1A well C1A clay from rock matrix 363 depth in meters

smectite kaolinite P calcic plagioclase C calcite uartz plagioclase peaks o scured y smectite peak

2θ corrected to 2 .606 corundum peak Cu α x-ray source hkl data from ac iff version .03

Clay -ray powder diffraction data

ell CH-1 clay x-ray powder diffraction analyses

ample CH1-					ample CH1- 96				
	2θ	d	o	ineral	hkl		2θ	d	o	ineral	hkl
Air ried						Air ried					
	6. 8	13. 2			001		6.	13.08	100		001
	29. 9	3.03	100	C	10						
lycolated						lycolated					
	.23	16.88	100		001		.32	16.60	100		001
	26. 9	3.3	36		00						
300°C						300°C					
	8.99	9.83	98		001		8.8	9.99	100		001
	28.01	3.18	100		003						
0°C						0°C					
	9.22	9. 8	6		001		9.20	9.60	100		001
	2 . 6	3.21	100		003		2 .82	3.20	63		003

ample num er indicates well and depth of sample e.g. C1A-363 C1A well C1A
clay from rock matrix 363 depth in meters
smectite kaolinite P calcic plagioclase C calcite uartz plagioclase peaks
o scured y smectite peak
2θ corrected to 2 .606 corundum peak Cu α x-ray source hkl data from ac iff version .03

hermodynamic modeling water chemistry

ell	ater upply	ell	-1	-1	-1	-1
epth nterval feet	39 - 9	1 11 - 2206	3 9 - 3 13	3 9 - 8 8	210 - 1036	
Alkalinity mg	160	210	20	6 0	0	
As ug	1	20	2	3		
icar onate mg	190	220	80	820	900	
ug	280	900	80	30	60	
Ca mg	6	10	8.1	8.9	.3	
Cl mg		1	1	13	12	
Cr - total ug	20	20	10	10	0	
F mg	0.2	1.1	12	13	13	
Fe ug	0	0	0	1200	1100	
P ug	0	0	0	0		
i ug		0	290	280		
g mg	28	2	1.1	1.1	0.	
n ug	0	20	110	60	0	
mg	3	10	9.2	8.1	.	
e ug	2	1	0	0		
i mg	2	60	33	39		
a mg	12	92	330	3 0	390	
r ug	3 0	100	120	1 0	1 0	
mg	0	32	69	9	99	
pH	.8	8.2	8.2	8.3	.9	
C	12	3	38	0		

ata from ann 1986

hermodynamic modeling water chemistry

ample ocation	CPP-1	CPP-1	CPP-2	CPP-3
ample ate	ec- 0	ep-	ep- 1	ep- 1
ample ethod	Pump	ap	Pump	ailer
ample epth	0- 86	0- 86	3-60	3- 98
Analyte				
i 2 mg	2	21	22	16
issolved Fe mg	0.03	0	0.02	0.21
otal Fe mg	0.06			
Ca mg	3	8		39
g mg	13	12	13	12
a mg	.9	8.3	.8	8
mg	3.	2.	1.2	.
HC 3 mg	1	18	1 6	160
mg	20	22	21	21
Cl mg	10	9	10	9.8
F mg	0.2	0.1	0.2	0.2
3 mg	0.9	1.	1	1.2
mg	0.01	0.1		
in C	12	12	12	13
pH	.8	.8	.9	8

ata from Fromm 199

Analyte	ean Analytical esults
mg	2.
a mg	20
g mg	1
Ca mg	
H i mg	3
HC 3 mg	1
mg	23
Cl mg	2
F mg	0.2
pH	8.2
C	13

ata from c ing 199

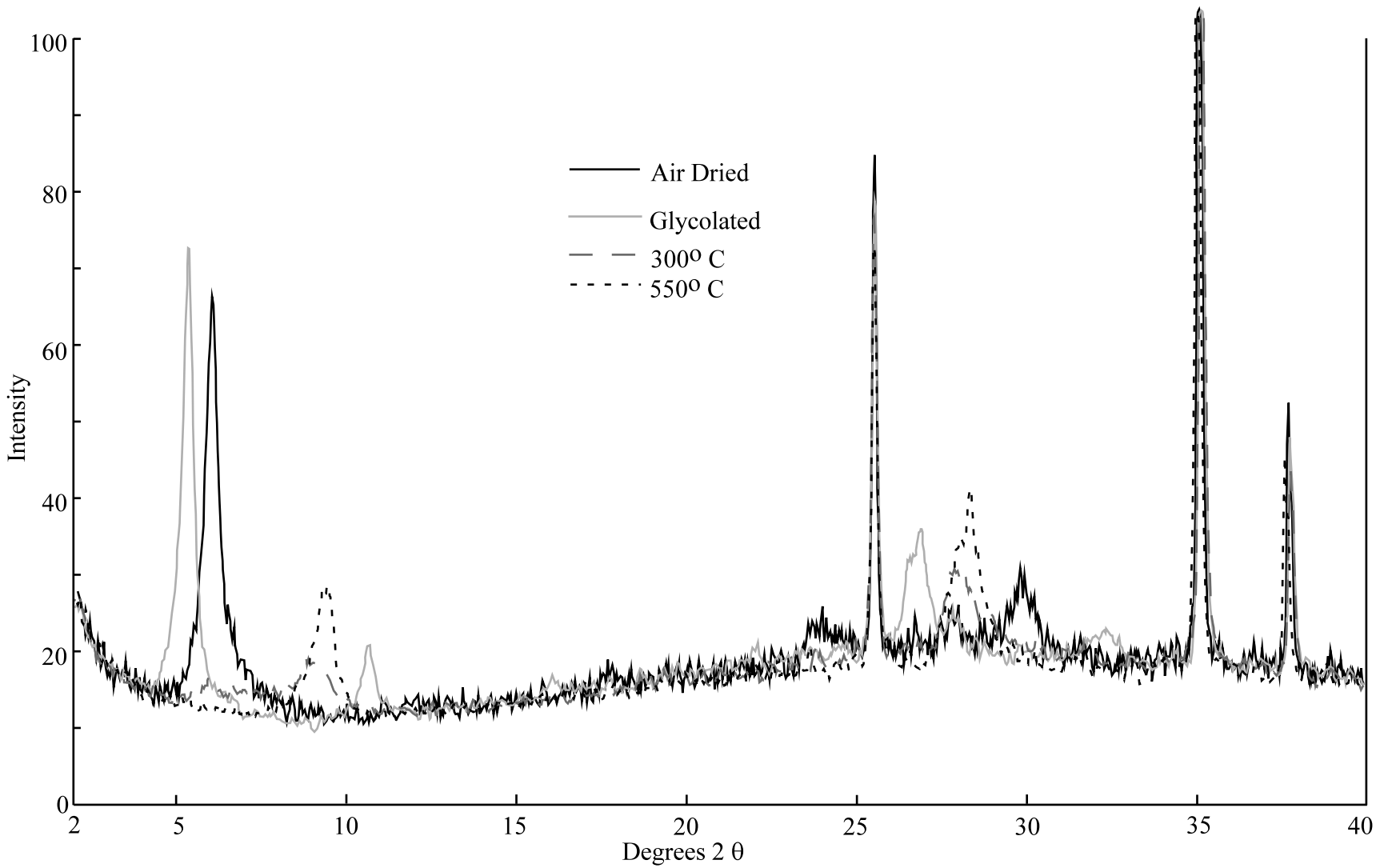

X-ray powder diffraction pattern of smectite clay from the rock matirx of well 2-2A from a depth of 485.0 meters.

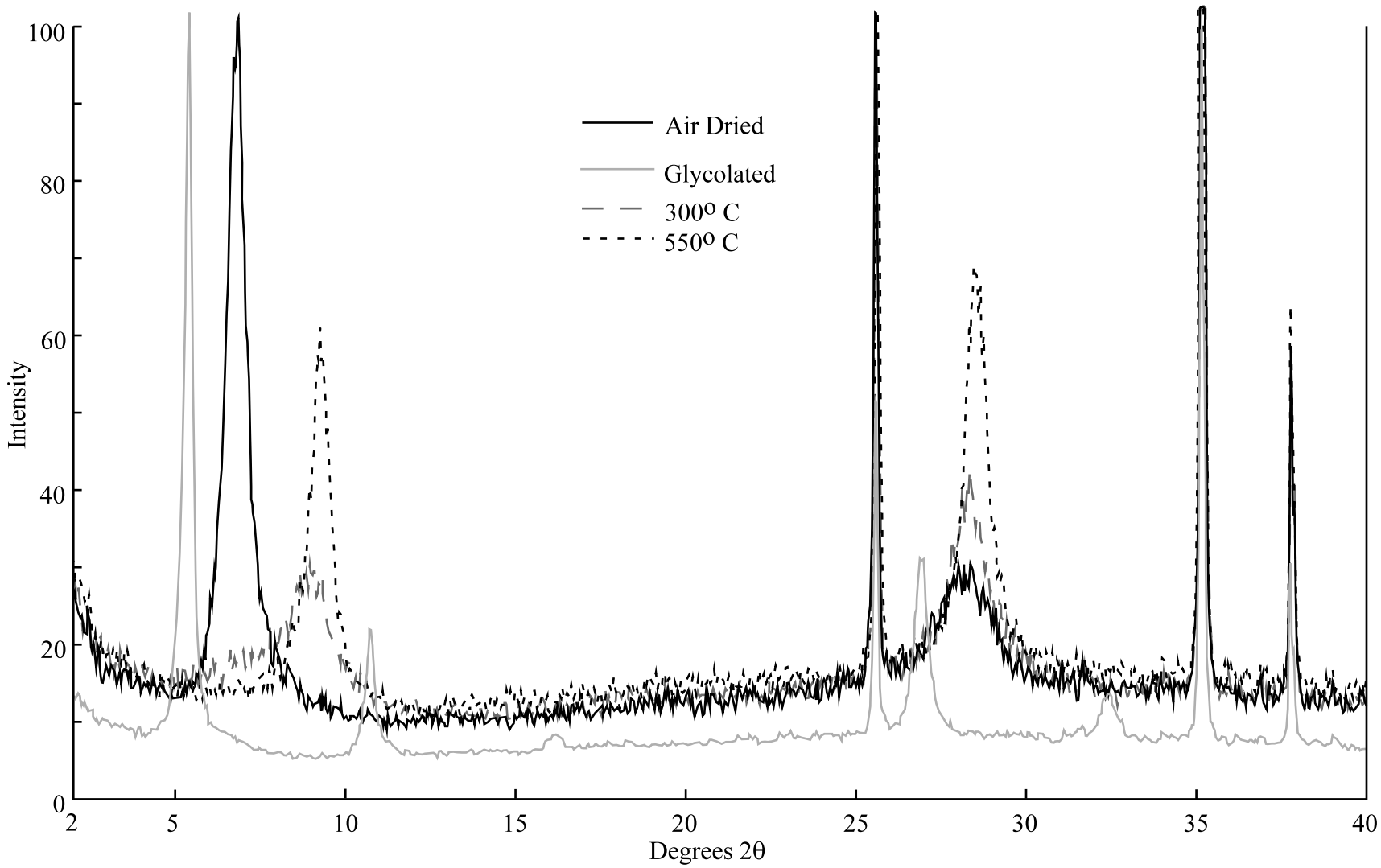

X-ray powder diffraction pattern of smectite clay from a fracture of well WO2 from a depth of 1,034.8 meters.

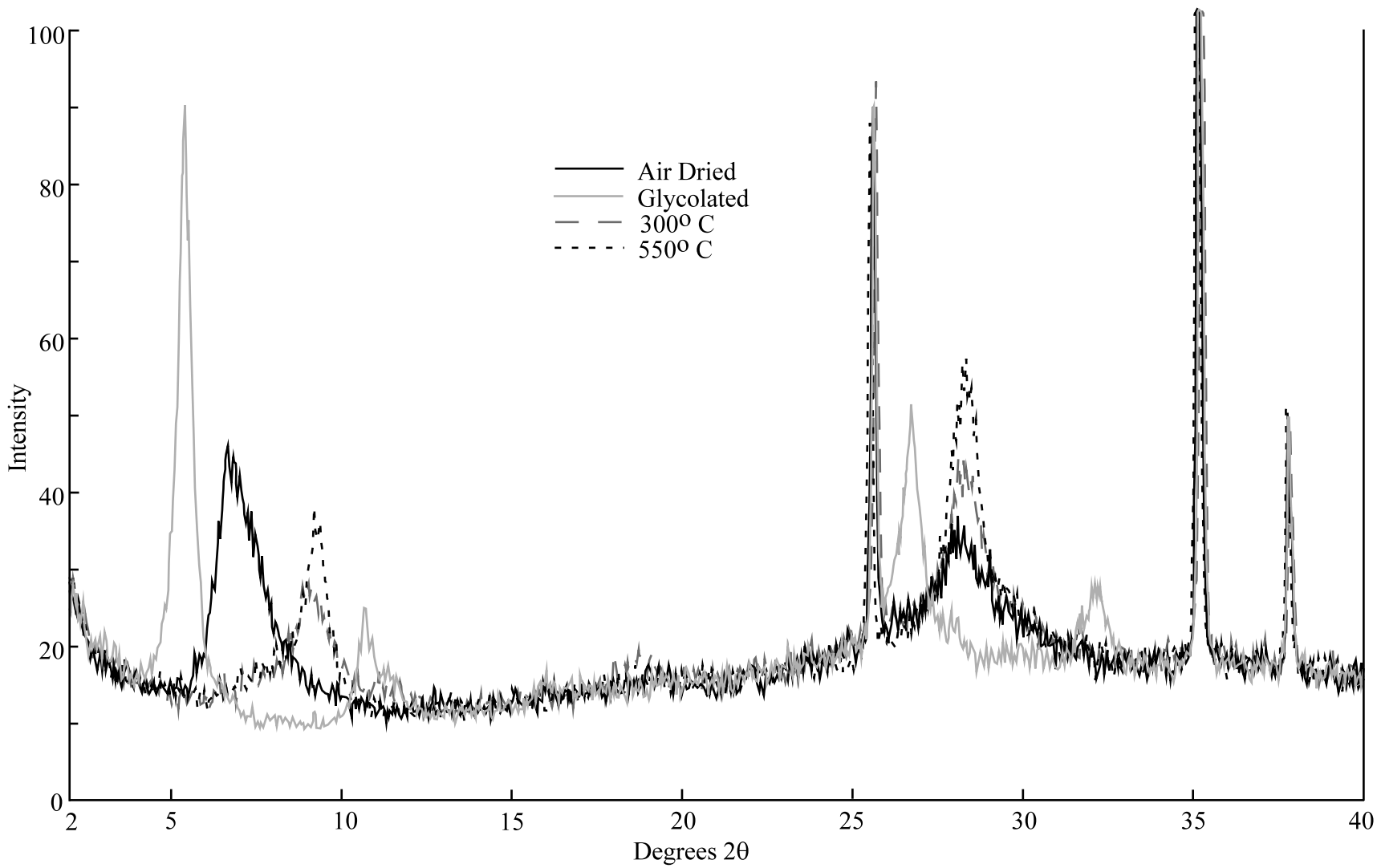

X-ray powder diffraction pattern of smectite clay from a vug of well WO2 from a depth of 1,064.8 meters.